DEPARTMENT OF BIOTECHNOLOGY

Ph.D. Thesis

Characterization of Tumor Cells and Immune Microenvironment Interactions in Non-Small Cell Lung Cancer. Translational implications

Susana Torres Martínez

Supervisors:

Dr. Carlos Camps Herrero

Dr. Eloisa Jantus Lewintre

February 2024

CARLOS CAMPS HERRERO, Dr. por la Universitat de València, Catedrático del Departamento de Medicina de la Universitat de València y jefe del Servicio de Oncología del Hospital General Universitari de València.

CERTIFICA:

Que Dña. Susana Torres Martínez, Graduada en Biotecnología, ha realizado bajo mi dirección la Tesis Doctoral que lleva por título "Characterization of Tumor Cells and Immune Microenvironment Interactions in Non-Small Cell Lung Cancer. Translational implications". Dicha tesis reúne todos los requisitos necesarios para su juicio y calificación.

Fdo.: Carlos Camps
Profesor Titular de Medicina
Facultad de Medicina
Universitat de València

Prof. Carlos Camps Herrero
D.N.I: 22517012N

ELOISA JANTUS LEWINTRE, Dra. por la Universitat de València, jefa del Laboratorio de Oncología Molecular de la Fundación del Hospital General Universitari de València y Profesora Titular del Departamento de Biotecnología de la Universitat Politècnica de València.

CERTIFICA:

Que Dña. Susana Torres Martínez, Graduada en Biotecnología, ha realizado bajo mi dirección la Tesis Doctoral que lleva por título "Characterization of Tumor Cells and Immune Microenvironment Interactions in Non-Small Cell Lung Cancer. Translational implications". Dicha tesis reúne todos los requisitos necesarios para su juicio y calificación.

Dra. Eloisa Jantus Lewintre
D.N.I: 24474835Y

‚‚If they want to have fun for life, they should be a scientist.''

Katarine Karikó

AGRADECIMIENTOS

Y llego el día,

Después de 5 años ha llegado el día en el que todo el esfuerzo, todos los obstáculos, la distancia, la soledad, la frustración, los lloros, las emociones y la desesperación han valido la pena. El día que decidí estudiar el máster en Valencia y poner 180 km de por medio no imaginé que llegaría hasta aquí. No ha sido fácil, pero de lo que sí estoy segura es que esta etapa ha supuesto un gran aprendizaje en mi vida, y todo gracias a esa gente que lo ha hecho posible.

2018. Época pre-pandemia. Clase de inglés. Cuando la profesora pregunta: ¿Who do you have as a mentor or guide to follow? Mi cabeza rápidamente contestó Eloisa, mi jefa. La Dra. Eloisa ha sido siempre un ejemplo a seguir en este mundo científico tan sacrificado. Esa pasión, ese poder con todo, ese sacrificio, esa sabiduría, es lo que cualquier científico quisiera llegar a conseguir. Gracias por tu ayuda en esta andadura, por tu sabiduría, por tu apoyo, por tus sabios consejos siempre y sobre todo por tu confianza. Nunca dejaré de estar agradecida.

Del mismo modo, me gustaría agradecer al Dr. Carlos Camps, mi director, al que le agradezco la confianza depositada en mí. Gracias por brindarme la oportunidad de formar parte de este gran equipo multidisciplinar y permitirme crecer cada día en el mundo de la investigación.

Y por supuesto, a la Dra. Silvia Calabuig, que, siendo sincera, sin ella no hubiera podido llegar hasta aquí. Eres un gran ejemplo de sacrificio, dedicación y trabajo. No sólo has estado ahí para lo profesional, sino que siempre he sentido un apoyo para lo personal. Gracias, gracias y gracias por estar ahí siempre, por regañarnos cuando hacía falta, por animarnos cuando era necesario, por dar sin esperar recibir. Porque al fin y al cabo siempre has sido la pieza fundamental, aquella que, si falta, hace que no se pueda formar el puzle. Porque si algo se sabe es que, Silvia, siempre está al pie del cañón.

Expresar también mi agradecimiento al Dr. Rafael Sirera por apoyarme, ayudarme y animarme a convertirme en una gran científica.

Dar las gracias a los compañeros del Hospital General de Valencia, por toda su importante labor asistencial, ayuda y colaboración. Y también me gustaría extender el agradecimiento a los servicios de Cirugía Torácica y al de Anatomía Patológica. Y por supuesto, a todos los pacientes por sus donaciones desinteresadas para la investigación contra el cáncer y a sus familiares.

I would also like to thank Dr. Luca Roz and Dra. Giulia Bertolini, who, despite the pandemic, opened their laboratory at Istituto Nazionale dei Tumori for me, not only for their scientific support during my internship, but also for their concern about my well-being.

Y cómo no, a mi gran familia valenciana de onco lab, más conocidos como eOM. Gracias a cada uno por su aportación en este trabajo. Elena, que fuiste mi pupila y te has convertido en un gran técnico, te deseo lo mejor en esta nueva etapa que está por venir, te lo mereces. MariLuz, que bien tu nombre lo indica, das luz y creas paz para los que trabajamos a tu lado. Sandra, que desde el principi estigueres ahí y sempre has tingut bons consells. Eva, muchas gracias por tu apoyo siempre, por tu ayuda y por haberme enseñado tanto. Alejandro, gracias por toda la ayuda que desde el principio me ofreciste, no cambies nunca. Y otros muchos han sido los que han creado un ambiente genial de trabajo y compañerismo y que han aportado su granito a esta tesis: Maria José, Eva PD-L1, Frank, Héctor, Bruno, Clara, Álvaro, Nora, Maca🌸 y estudiantes. Y a ti Ester (Esther lab antes en mis contactos), que llegaste en mi último empujón, para impulsarme, para estar ahí, para ser mi mano izquierda, para aconsejarme, para darme tus achuchones y sobre todo para convertirte en una AMIGA, ya no hay vuelta atrás.

No és fácil estar lejos de los tuyos y aquí tengo que dar especialmente las gracias a las pupis y nuestra mami, por haber hecho de Valencia un hogar para mí. Me enseñaste y sigo aprendiendo de ti, me cuidaste y lo sigues haciendo, me trataste y lo haces como si fuera de tu familia. Gracias por apoyarme y estar siempre pendiente de mí. Gracias por ese whastapp cada mañana de buenos días. Sin ti este camino no hubiera sido posible, Marais. Y a mis dos pupis, que dejasteis de ser compañeras para ser AMIGAS. Mi

oriolana, mi hermana mayor, siempre has estado ahí, para todo. Te has convertido en un gran apoyo en mi vida y esta tesis tiene un pedacito de ti, Elena. Andrea, nuestra bioinformática, nunca dejaré de aprender de ti, gracias por todos estos 6 años de apoyo. Gracias por abrirme las puertas, y junto a Pablo, hacer que me sintiera como en casa. Chicas, estas tesis nos han quitado mucho, pero indudablemente nos han enseñado también mucho y nos ha hecho más fuertes, estoy segura de que sólo nos esperan cosas buenas.

A mis amigas Santa Poleras, Sofia, Henar y María, y a mi familia biotech, Carol, Ana, AnnaQu, Adela y Clara, porque sé que no importa el tiempo ni la distancia, siempre podré contar con ellas.

Pero si a alguien va dedicada esta tesis, es a mi familia, lo más importante en mi vida. Quienes me conocen saben lo familiar que soy (que se lo digan a mi coche de tantos viajes de Ida y Vuelta). Agradecer a mis padres todo lo que han hecho por mí y por haber hecho posible que yo hoy esté dónde estoy. También a mi hermano, Carmen y mi pequeña por su apoyo.

Y a Andrés, agradecerte todos estos años a mi lado, por ayudarme en todo (Photoshop incluido 😉), por apoyarme, por seguir al pie del cañón y por soportar mis altibajos. Sin ti a mi lado, no hubiera podido llegar hasta el final de este camino. Ahora te toca a ti.

No sé qué me deparará el futuro, pero de lo que sí estoy segura es de que todos vosotros marcasteis un gratificante viaje en mi camino.

Gracias a todos,

ABSTRACT

It is widely recognized that the immune system actively contributes to the process of oncogenesis. Nonetheless, the complex field of immuno-oncology is constantly evolving, driven by cancer heterogeneity and the exceptional plasticity of the immune cells participating in this process. There is a significant amount of evidence indicating that tumor cells can create an immunosuppressive microenvironment that favors tumor development and spreading. In this study we aim to delve deeper into the study of immune tumor microenvironment (TME), which will result in an improved characterization of patient`s immune contexture and the search for new biomarkers in lung cancer.

In this thesis, long term patient derived lung cancer cell (PDLCC) cultures from early-stage non-small cell lung cancer (NSCLC) patients and commercial cell lines were employed for sphere-forming assays for cancer stem cells enrichment and adherent conditions for the control counterparts. Using RT-qPCR, gene expression profiles of immune-mediators were analyzed showing that expression levels of most selected genes were higher in tumorspheres compared with the adherent cells counterparts. Together with secretion profiles, Galectin-3 (GAL3 or *LGALS3* when protein or gene are referenced, respectively) was selected as the molecule that could have a strong implication in the modulation of TME. Immunoblot, flow cytometry and immunofluorescence analyses confirmed that GAL3 was consistently increased in tumorspheres from lung adenocarcinoma (LUAD) cultures and showed differential localization and expression patterns. Extracelullar vesicles from tumorspheres also exhibited high levels of *LGALS3*. Next, we revealed that GAL3 could play a crucial role as an immunomodulatory molecule expressed and secreted in the TME, modulating immunosuppression through regulatory T cells (T_{REGS}). This was confirmed in patient's tumor samples, where higher levels of LGALS3 correlated with increased T_{REGS}, suggesting that tumors may be recruiting this population through GAL3. The prognostic and diagnostic roles of soluble GAL3 (sGAL3) and other immune-mediators (sICOSL, sFGL1, sGAL1, sMICA, sMICB, sCD276) were evaluated in a cohort of 94 early-stage NSCLC patients from *Consorcio Hospital General Universitario de Valencia* (*CHGUV*) (test cohort). Based on Receiver Operating Characteristic (ROC) curve analysis, sFGL1, sGAL3 and its combination yielded optimal

diagnostic efficacy in our patient's cohort. A Cox regression analysis revealed an association between sGAL3 and prognosis. Kaplan-Meier plots show that, in the early-stage LUAD subcohort, patients with high levels of sGAL3 experienced shorter relapse-free survival (RFS) (29.70 vs. 125.47 months, p=0.048) and overall survival (OS) (29.70 vs. not reached (NR) months, p=0.021), while no such association was observed in the lung squamous cell carcinoma (LUSC) subcohort. Multivariate analysis indicated that sGAL3 could be an independent biomarker of prognosis for OS and RFS. Gene expression of our panel of immunoregulatory factors was also analyzed in an independent group of 661 patients from TCGA (validation cohort), confirming the independent prognostic value of *LGALS3* in the LUAD subcohort for RFS [23.74 vs. 37.6 months, p=0.021] and OS [40.49 vs. 103.90 months, p=0.004].

The diagnostic, predictive and prognostic role of these immune-mediators was also evaluated in plasma samples at baseline (PRE) and at first response assessment (FR) in a cohort of 52 advanced-stage NSCLC patients from *CHGUV* treated in first-line with pembrolizumab. Based on ROC analysis, sFGL1, sGAL3 and its combination were also found to have a diagnostic value in this clinical setting. The Mann-Whitney test revealed that sGAL3 at FR and sMICB at PRE and FR were associated with clinical benefit in the entire cohort and in the LUAD subcohort. sCD276 was also associated with objective response in the entire cohort and in the LUAD subcohort. A Cox regression analysis identified sMICB at FR as an independent biomarker for progression-free survival (PFS) in the entire cohort and for PFS and OS in the LUAD subcohort. Furthermore, sGAL3 at PRE was found to be an independent biomarker for PFS and OS in the entire cohort, and sGAL3 at FR was identified as an independent biomarker for OS in the LUAD subcohort. A decreased in the levels of sGAL3 on treatment was associated with reduction of OS in our patient's entire cohort. In conclusion, our findings provide relevant prognostic and predictive information on the role of GAL3 and other immune-mediators for lung cancer patients and served as the basis for developing new biomarkers and therapies.

RESUMEN

El sistema inmunológico contribuye activamente al proceso de oncogénesis. No obstante, el campo de la inmuno-oncología está en constante evolución, debido a la heterogeneidad tumoral y la plasticidad de las células inmunitarias que participan en este proceso. Existen evidencias que indican que las células tumorales pueden crear un microambiente inmunosupresor favoreciendo el desarrollo y la propagación del tumor. En esta tesis, buscamos profundizar en el estudio del microambiente inmunitario del tumor (TME), lo que resultaría en una mejor caracterización del contexto inmunológico de los pacientes y la búsqueda de nuevos biomarcadores en el cáncer de pulmón.

En esta tesis, se emplearon cultivos derivados de pacientes con cáncer de pulmón de células no pequeñas (CPNM) en etapa temprana, y líneas celulares comerciales para ensayos de formación de tumoresferas para enriquecimiento de células madre cancerosas y condiciones adherentes como control. Utilizando la técnica de RT-qPCR, se analizaron los perfiles de expresión génica de diversos factores inmunorreguladores, observándose una mayor expresión de la mayoría de ellos en las tumoresferas en comparación con las células adherentes. Junto con los perfiles de secreción, la Galectina-3 (GAL3 o *LGALS3* cuando se referencian la proteína o el gen, respectivamente) se seleccionó como la molécula que podría tener una fuerte implicación en la modulación del TME. El análisis de electrotransferencia, citometría de flujo y de inmunofluorescencia confirmaron que la GAL3 aumentaba consistentemente en las tumoresferas de cultivos de adenocarcinoma (ADC) y mostraba patrones de localización y expresión diferencial. Las vesículas extracelulares procedentes de tumoresferas también exhibieron niveles altos de *LGALS3*. Además, revelamos que la GAL3 podría desempeñar un papel crucial como molécula inmunomoduladora expresada y secretada en el TME, modulando la inmunosupresión a través de las células T reguladoras (T$_{REGS}$). Esto se confirmó en muestras tumorales de pacientes, dónde los niveles de expresión altos de *LGALS3*, se correlacionaron con mayores niveles de T$_{REGS}$, lo que sugiere que los tumores pueden reclutar esta población a través de la GAL3. Posteriormente, se evaluaron los roles pronósticos y diagnósticos de la GAL3 soluble (sGAL3) y otros factores inmunorreguladores (sICOSL, sFGL1, sGAL1, sMICA, sMICB, sCD276) en una cohorte de 94 pacientes con CPNM en estadios tempranos resecables procedente del Consorcio

Hospital General Universitario de Valencia (CHGUV) (cohorte test). En el análisis de curva ROC, sFGL1, sGAL3 y su combinación mostraron una eficacia diagnóstica óptima para los pacientes con CPNM. El análisis de regresión de Cox reveló una asociación entre sGAL3 y el pronóstico. Además, el análisis de supervivencia de Kaplan-Meier demostró que, en la sub-cohorte de ADC en estadio temprano, los pacientes con niveles altos de sGAL3 experimentaron una supervivencia libre de recaída (SLR) [29,70 vs. 125,47 meses, *p*=0,048] y una supervivencia global (SG) más corta [29,70 vs. no alcanzada (NA) meses, *p*=0,021], mientras que no se observó ninguna asociación en la sub-cohorte de pacientes con carcinoma de células escamosas (CCE). El análisis multivariante indicó que sGAL3 podría ser un biomarcador pronóstico independiente para SLR y SG. La expresión génica de nuestro panel de factores inmunoreguladores también se analizó en un grupo independiente de 661 pacientes de TCGA (cohorte de validación), confirmando el valor pronóstico independiente de *LGALS3* en la sub-cohorte de ADC para SLR [23,74 vs. 37,6 meses, *p*=0,021] y SG [40,49 vs. 103,90 meses, *p*=0,004].

El papel diagnóstico, predictivo y pronóstico de estos factores también se evaluó en muestras de plasma en el momento basal (PRE) y en la evaluación de la primera respuesta (FR) en una cohorte de 52 pacientes con CPNM en estadio avanzado procedente del CHGUV tratados en primera línea con pembrolizumab. En el análisis de curva ROC, sFGL1, sGAL3 y su combinación se nuevo ofrecieron una eficacia diagnóstica óptima para esta cohorte de pacientes. La prueba de Mann-Whitney reveló que sGAL3 en FR y sMICB en PRE y FR estaban asociados con un beneficio clínico en toda la cohorte y en la subcohorte de ADC. sCD276 también se asoció con la respuesta global en toda la cohorte y en la sub-cohorte de ADC. Un análisis de regresión de Cox identificó a sMICB en FR como un biomarcador independiente para la supervivencia libre de progresión (SLP) en toda la cohorte y para SLP y SG en la sub-cohorte de ADC. Además, sGAL3 en PRE se encontró como un biomarcador independiente para SLP y SG en toda la cohorte y en FR se identificó como biomarcador independiente para SG en la sub-cohorte ADC. Una disminución en los niveles de sGAL3 en los pacientes en tratamiento se asoció con una reducción en la SG en toda la cohorte. En conclusión, nuestros hallazgos proporcionan información diagnóstica, pronóstica y predictiva relevante del rol de la GAL3 y otros factores inmunoreguladores para los pacientes con cáncer de pulmón y sirven como base para el desarrollo de nuevos biomarcadores y terapias.

RESUM

El sistema immunològic contribuïx activament en el procés d'oncogènesi. No obstant això, el complex camp de la immunooncologia està en constant evolució, a causa de la heterogeneïtat tumoral i l'excepcional plasticitat de les cèl·lules immunològiques que participen en aquest procés. Existeixen evidències que indiquen que les cèl·lules tumorals poden crear un microambient immunosupressor que afavorix el desenvolupament i la propagació del tumor. En aquest estudi, busquem profunditzar en l'estudi del microambient immunològic del tumor (TME), el que resultaria en una millor caracterització del context immunològic dels pacients i la recerca de nous biomarcadors en el càncer de pulmó.

En aquesta tesi, s'utilitzaren cultius de llarg termini establits a partir de pacients amb càncer de pulmó de cèl·lules no petites en etapa primerenca, i línies cel·lulars comercials per a assajos de formació de tumorsferes per a l'enriquiment de cèl·lules mares canceroses i condicions adherents com a control. Utilitzant la tècnica de RT-qPCR, s'analitzaren els perfils d'expressió gènica de diversos factors immunoreguladors, i es va observar una major expressió de la majoria d'ells en les tumorsferes en comparació amb les cèl·lules adherents. Juntament amb els perfils de secreció, la Galectina-3 (GAL3 o *LGALS3* quan es fa referència a la proteïna o al gen, respectivament) es va seleccionar com la molècula que podria tindre una forta implicació en la modulación del TME. L'anàlisi d'electrotransferència, citometria de flux i d'immunofluorescència va confirmar que la GAL3 augmentava consistentment en les tumorsferes de cultius d'adenocarcinoma de pulmó (ADC) i mostrava patrons de localització i expressió diferencial. Les vesícules extracel·lulars precedents de les tumorspheres també van exhibir nivells alts de *LGALS3*. A més, vam revelar que la GAL3 podria jugar un paper crucial com a molècula immunomoduladora expressada i secreta en el TME, modulant la immunosupressió a través de les cèl·lules T reguladores (T_{REGS}). Això es va confirmar en mostres tumorals de pacients amb nivells d'expressió elevats de GAL3, que a més tenien majors nivells de T_{REGS}, el que suggereix que els tumors poden reclutar aquesta població a través de la GAL3. Posteriorment, es van avaluar els rols pronòstics i diagnòstics de la GAL3 soluble (sGAL3) i altres factors immunoreguladors (sICOSL, sFGL1, sGAL1, sMICA, sMICB, sCD276) en una cohort de 94 pacients amb càncer de pulmó de cèl·lules no microcítiques (CPNM)

en estadi primerenc procedent del Consorci Hospital General Universitari de València (CHGUV) (cohort de test). L'anàlisi de la corba ROC, sFGL1, sGAL3 i la seua combinació van mostrar una eficàcia diagnòstica òptima en la nostra cohort. L'anàlisi de regressió de Cox va revelar una associació entre sGAL3 i el pronòstic. A més, l'anàlisi de supervivència de Kaplan-Meier va demostrar en la subcohort de ADC en estadi primerenc, que els pacients amb nivells alts de sGAL3 van experimentar una supervivència lliure de recaiguda (SLR) [29,70 vs. 125,47 mesos, p=0,048] i una supervivència global (SG) més curta [29,70 vs. no assolida (NR) mesos, p=0,021], però no en la de carcinoma de cèl·lules escamoses (CCE). L'anàlisi multivariant va indicar que sGAL3 podria ser un biomarcador independent del pronòstic per a SG i SLR. L'expressió gènica de tots aquests factors immunoreguladors també es va analitzar en un grup independent de 661 pacients de TCGA (cohort de validació), confirmant el valor pronòstic independent de *LGALS3* en la subcohort de ADC per a SLR [23,74 vs. 37,6 mesos, p=0,021] i SG [40,49 vs. 103,90 mesos, p=0,004].

El paper diagnòstic, predictiu i pronòstic d'aquests factors immunoreguladors també es va avaluar en el moment basal (PRE) i en l'avaluació de la primera resposta (FR) en una cohort de 52 pacients amb CPNM en estadi avançat procedent del CHGUV tractats en primera línia amb pembrolizumab. Segons l'anàlisi de la corba ROC, sFGL1, sGAL3 i la seua combinació de nou van oferir una eficàcia diagnòstica òptima per als pacients d'aquesta cohort. La prova de Mann-Whitney va revelar que sGAL3 en FR i sMICB en PRE i FR estaven associats amb un benefici clínic durador en tota la cohort i en la subcohort de LUAD. sCD276 també es va associar amb la resposta global en tota la cohort i en la subcohort de ADC. Un anàlisi de regressió de Cox va identificar sMICB en FR com a biomarcador independent per a la supervivència lliure de progressió (SLP) en tota la cohort i per a SLP i SG en la subcohort de ADC. A més, sGAL3 en PRE es va trobar com a biomarcador independent per a SLP i SG en tota la cohort, i sGAL3 en FR es va identificar com a biomarcador independent per a SG en la subcohort de ADC. Una disminució en FR dels nivells de sGAL3 es va associar amb una reducció en la SG en tota la cohort. En conclusió, els nostres descobriments proporcionen informació rellevant sobre el rol diagnòstic y el pronòstic de la GAL3 y altres factor inmunoreguladors per als pacients amb càncer de pulmó i serveixen com a base per al desenvolupament de nous biomarcadors i teràpies.

INDEX

LIST OF ABBREVIATIONS

7AAD: 7-aminoactinomicina D

ACTB: Actin beta

ADH: Adherent-cultures cells

AIDs: Acquired immunodeficiency syndrome

AKT1: AKT Serine/Threonine Kinase 1

ALK: Anaplastic lymphoma kinase

APC: Allophycocyanin

APCs: Antigen-presenting cells

ARG2: Arginase 2

ARN: Ribonucleic acid

ASC: Adenosquamous carcinoma

ATCC: American type culture collection

AUC: Area under the ROC curve

B2M: Beta-2-microglobulin

BCA: Bicinchoninic acid

bFGF: Basic fibroblast growth factor

BRAF: B-Raf proto-oncogene

BSA: Bovine serum albumin

BTLA: B and T lymphocyte attenuator

BV: Brilliant violet

CAFs: Cancer associated fibroblasts

cAMP: cyclic adenosine phosphate

CBR: Clinical benefit rate

CD: Cluster of differentiation

CD137L: TNF superfamily member 9

CD206: Mannose receptor, C type 1

CDKN1B: Cyclin dependent kinase inhibitor 1B

cDNA: Complementary DNA

cfRNA: Cell-free RNA

CHGUV: Consorcio Hospital General Universitario de Valencia

CI: Confidence interval

circRNA: Circular RNAs

CM: Conditioned media

CNVs: Copy number variation

CO2: Carbon dioxide

COPD: Obstructive pulmonary disease

Ct: Cycle threshold

CR: Complete response

CSCs: Cancer stem cells

CT: Chest computed tomography

CTCs: Circulating tumor cells

ctDNA: Circulating tumor DNA

CTECs: Circulating tumor vascular endothelial cells

CTLA4: Cytotoxic T-lymphocytes associated antigen 4

ctRNA: Circulating tumor RNA

CV: Coefficients of variation

DAPI: 4',6-diamidino-2-phenylindole

DC: Dendritic cell

DCB: Durable clinical benefit

DDR2: Discoidin domain receptor tyrosine kinase 2

DNA: Deoxyribonucleic acid

EBUS: Endobronchial ultrasound

ECM: Extracellular matrix

EDTA: Ethylene diamine tetra-acetic acid

EGF: Epidermal growth factor

EGFR: Epidermal growth factor receptor

ELISA: Enzyme-linked immunosorbent assays

EMA: European Medicines Agency

EML4: Echinoderm microtubule-associated protein-like 4

EMT: Epithelial-mesenchymal transition

ERK: Extracellular signal-regulated kinases

EUS: Endoscopic ultrasound

EVs: Extracellular vesicles

FASL: Fas ligand

FBM: Fibroblast medium

FBS: Fetal bovine serum

FDA: Food and Drug Administration

FFPE: Formalin-fixed paraffin-embedded

FGFR1: Fibroblast growth factor receptor 1

FGL1: Fibrinogen-like protein 1

FMOs: Fluorescence minus one

FR: First response assessment

GAL1: Galectin-1

GAL3: Galectin-3

GAL9: Galectin-9

GAPDH: Glyceraldehyde-3-phosphate dehydrogenase

GUSB: Beta-glucuronidase

HER2: Human epidermal growth factor receptor 2

HLA: Human leukocyte antigen

HLAE: Major histocompatibility complex class I antigen E

HLAF: Major histocompatibility complex class I antigen F

HLAG: Major histocompatibility complex class I antigen G

HPF: High-powered field

HR: Hazard ratio

ICGC: International Cancer Genome Consortium

ICIs: Immune checkpoints inhibitors

ICOSL: Inducible T cell costimulatory ligand

IDO1: Indoleamine 2,3-dioxygenase 1

IF: Immunofluorescence

IFNγ: Interferon-gamma

IHC: Immunohistochemistry

IL: Interleukin

ILT-2: Ig-like transcripts

IQR: Interquartile range

ITS: Insulin-Transferrin-Selenium

KEAP1: Kelch-like ECH-associated protein 1

KIF5B: Kinesin family member 5b

KIRs: Killer Ig-like receptors

KRAS: Kirsten rat sarcoma viral oncogene homolog

LAG3: Lymphocyte activation gene 3

LDCT: Low-dose computed tomography

LGALS3: Galectin 3 gene

LGALS3BP: Galectin 3 binding protein gene

LGALS9: Galectin 9 gene

L-glu: L-glutamine

LLCC: Lung large-cell carcinoma

LLOQ: Lower limit of quantification

LM22: Leukocyte 22 data matrix

LNs: Lymph nodes

LUAD: Lung adenocarcinoma

LUSC: Lung squamous cell carcinoma

M-CSF: Macrophage colony-stimulating factor

MDSCs: Myeloid-derived suppressor cells

MEK: Mitogen-activated protein kinase kinase

MET: Mesenchymal epithelial transition factor proto-oncogene

MHC: Major histocompatibility complex

MICA/B: Major histocompatibility complex class I polypeptide-related Seq A/B

miRNA: MicroRNA

ml: Mililiters

MSI: Microsatellite instability

NGS: Next-generation sequencing

NK: Natural killer cells

NKG2D: natural killer group 2D

NLR: Neutrophils-to-lymphocytes ratio

NOS2: Nitric oxide synthase 2

NPV: Negative predictive value

NRF2: Nuclear factor erythroid 2-related factor 2

NR: Not reached

NSCLC: Non-small cell lung cancer

NTCs: Non-template controls

NTRK: Neutrophil receptor tyrosine kinase

OCA-Plus: Oncomine™ Comprehensive Assay Plus

ORR: Objective response rate

OS: Overall survival

OX40L: TNF Receptor superfamily member 4

P/S: Penicillin-streptomycin

PBMCs: Peripheral blood mononuclear cells

PBS: Phosphate-buffered saline

PC: Patient Code

PCA: Principal component analysis

PD: Progression disease

PD1: Programmed cell death protein 1

PDGFRA: Platelet-derived growth factor receptor A

PDL1: Programmed cell death 1 ligand 1

PDL2: Programmed cell death 1 ligand 2

PDLCC: Patient derived lung cancer cell

PE: Phycoerythrin

PET: Positron emission tomography

PFS: Progression-free survival

PIK3CA: Phosphatidylinositol-4,5-bisphosphate 3-kinase catalytic subunit alpha

PPV: Positive predictive value

PR: Partial response

PRE: Baseline

PS: Performance status

PTEN: Phosphatase and tensin homolog

PVDF: Polyvinylidene difluoride

QC: Quality control

RECIST 1.1: Response evaluation criteria in solid tumors

RET: Ret proto-oncogene

RFS: Relapse-free survival

ROC: Receiving operation curve

ROCKi: Rho-kinase inhibitor

ROS1: Reactive oxygen species protooncogene 1, receptor tyrosine kinase.

RR: Response rate

RT: Reverse transcription

RT: Room temperature

RT-qPCR: Real time quantitative polymerase chain reaction

SCLC: Small cell lung carcinoma

SD: Stable disease

SDS-PAGE: Sulfate polyacrylamide gel electrophoresis

sGAL3: Soluble GAL3

SNVs: Single-nucleotide variants

SOX2: SRY-Box transcription factor 2

SPH: Tumorspheres

STAT3: Signal transducer and activator of transcription 3

STK11: Serine/Threonine kinase 11

STR: Short tandem repeat analysis

TAMs: Tumor-associated macrophages

TCGA: The Cancer Genome Atlas

TCR: T cell receptor

TEPs: tumor educated platelets

TFG: TRK-fused gene

TGFβ: Transforming Growth Factor Beta

Th1: T helper 1

TIICs: Tumor-infiltrating immune cell

TIM3: T cell membrane protein 3

TKIs: Tyrosine kinase inhibitors

TMB: Tumor mutational burden

TMB-H: High tumor mutational burden

TME: Tumor microenvironment

TMP: Tropomyosin 4

TNF: Tumor necrosis factor

TNM: Tumor node metastasis system classification

TP53: Tumor protein-53

TRAIL: Tumor necrosis factor-related apoptosis-inducing ligand

TREGS: Regulatory T cells

TTF-1: Thyroid transcription factor 1

VEGFA: Vascular endothelial growth factor A

X2: Chi-squared

2D: Two dimensions

3D: Three dimensions

μl: Microliters

Pg/ml: picogram/milliliters

mM: Millimolar

pH: Measure of acidity or alkalinity

cell/ml: Cells/ milliliters

LIST OF FIGURES

LIST OF TABLES

I. INTRODUCTION

1. CANCER

1.1. CONCEPT

Cancer is defined as a group of related diseases that can affect any part of the body. In cancer, abnormal cells can grow uncontrollably and spread to other tissues. However, a more intricate perspective on cancer emerges. First, tumors can recruit normal cell types and other types of cells, creating a complex ecosystem known as the tumor microenvironment (TME). This involves innumerable interactions among different components, which contribute to the enhanced proliferation and invasion of cancer cells (Hanahan & Weinberg, 2000). Second, defects affecting components of the DNA maintenance machinery, combined with the large number of cell division, lead to genome instability, a critical factor for the development of tumors (Marusyk et al., 2012).

1.2. MOLECULAR BASES OF CANCER

In the year 2000, Hanahan and Weinberg proposed that all tumors share six capabilities acquired during tumorigenesis (Hanahan & Weinberg, 2000). In 2011, theses authors added four new features emphasizing the significance of TME (Hanahan & Weinberg, 2011). A decade later, Hanahan revisited the hallmarks once again and introduced four additional emerging hallmarks recognizing the big progress performed in the study of cancer through big data (Hanahan, 2022) (Figure 1).

Thus, the fourteen hallmarks of cancer are the following:

1) **Sustaining proliferative signaling:** Cancer cells acquire mutations that can affect key oncoproteins, resulting in constitutive activation of proliferative signaling and the failure of normal negative feedback mechanisms. As a result, cancer cells acquired the ability to sustain uncontrolled cell proliferation without the need for mitogenic growth stimuli.

2) **Evading growth suppressor:** Signals from the TME can promote tumor growth by inactivating tumor suppressors. Consequently, cancer cells can disrupt tumor suppressor genes, rendering them insensitive to inhibitory growth signals and allowing for unchecked replication.

3) **Apoptosis evasion:** Programmed cell death through apoptosis serves as a natural barrier to cancer development. Tumors cells employ various strategies to evade apoptosis triggered by cell surface receptors, soluble factors, immune effector cells, and anticancer therapies, thus facilitating tumor progression. For instance, one of the most mechanisms used involves the loss of tumor protein-53 (*TP53)* tumor suppressor function, which cause apoptosis when DNA damage is detected.

4) **Enabling replicative immortality:** Normal cells have a limited number of successive cell growth and division cycles. Once this limit is reached, cells lose the protective function of telomeres and start a state of senescence, stopping further growth. In cancer cells, telomeres maintain their length due to increased telomerase enzyme activity, allowing for replicative immortality.

5) **Inducing angiogenesis:** Angiogenesis, the growth of new blood vessels from existing ones, is an essential requirement in cancer development and progression. The tumor-associated neovasculature sustains the supply of nutrients and oxygen to tumors while removing metabolic waste and carbon dioxide. Tumor cells produce inducer factors that continuously stimulate the sprouting of new vessels.

6) **Activating invasion and metastasis:** Metastasis involves the invasion of tumor cells to the adjacent tissue, intravasation, survival in the circulation, extravasation, and colonization of targeted organs. Cancer cells can escape from primary tumor and invade neighboring tissues or distant sites. Tumors develop various strategies to facilitate invasion and metastasis, such as downregulating the expression of E-cadherin, a key cell-to-cell adhesion molecule, in carcinoma cells.

7) **Acquiring genome instability and mutations:** Tumor cells can accumulate random mutations and chromosomal rearrangements that contribute to tumor development and progression. Tumor cells may increase mutation rates due to a breakdown in one or more components of the genomic maintenance machinery or other factors.

8) **Tumor-promoting inflammation:** Some tumors are infiltrated by immune cells, leading to inflammation that enhances tumorigenesis and progression.

Inflammation supplies the TME with bioactive molecules, including survival factors, pro-inflammatory cytokines, chemokines, growth factors, proangiogenic factors, and extracellular matrix-modifying enzymes. All these molecules facilitate the neovascularization, invasion, metastasis, and epithelial cell proliferation.

9) **Reprogramming energy metabolism:** During neoplastic process, altered energy metabolism are produced to prevent apoptosis and stimulate cell proliferation and division of neoplastic cells.

10) **Evading immune destruction:** Tumors employ many strategies to evade immune destruction. TME achieves immunosuppression through different mechanism, such as recruiting regulatory T cells (T_{REGS}) and myeloid-derived suppressor cells (MDSCs) that can suppress the function of cytotoxic lymphocytes.

11) **Unlocking phenotypic plasticity:** Malignant cells evade differentiation and unlock phenotypic plasticity to sustain growth. This happens in different ways, including the de-differentiation of cells approaching differentiation, blocking differentiation from progenitor cell stages, and transdifferentiating into different cell lineages.

12) **Non-mutational epigenetic reprogramming**: Many cancer cells acquired changes in the epigenetic landscape. Tumors can reprogram a big number or gene-regulation networks to alter gene expression.

13) **The microbiome**: Microorganisms, representing nearly 40 trillion cells that reside within us, can have either protective or deleterious effects on cancer development, progression, and responses to therapies. Multiple tissue microbiomes are implicated in modulating tumor phenotypes including growth, inflammation, immune evasion, genome instability and therapy resistance.

14) **Senescence**: Cancer cells can be induced to undergo senescence, an irreversible form of proliferative arrest. In some context, senescent cells stimulate tumor development and malignant progression. The main mechanism involved is thought to be the senescence-associated secretory phenotype, in which cells secrete high levels of inflammatory cytokines,

immune modulators, growth factors and proteases. Consequently, senescent cancer cells contribute to proliferative signaling, apoptosis evasion, invasion and metastasis, angiogenesis, and suppression of tumor immunity.
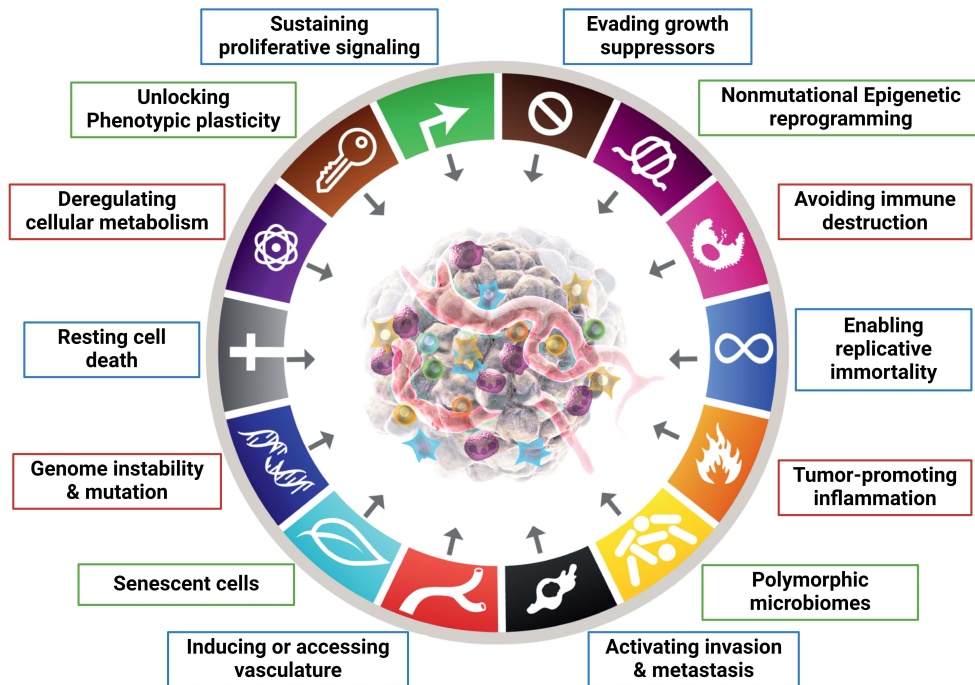
Figure 1. Hallmarks of cancer. Blue boxes, the six acquired capabilities - Hallmarks of cancer proposed in 2000. Red boxes, the four hallmarks introduced in 2011 "reprogramming cellular metabolism", "avoiding immune destruction", "tumor-promoting inflammation" and "genome instability and mutation". Green boxes, additional proposed emerging hallmarks and enabling characteristics involving "unlocking phenotypic plasticity," "nonmutational epigenetic reprogramming," "polymorphic microbiomes," and "senescent cells." Adapted from (Hanahan, 2022; Hanahan & Weinberg, 2000).

It is increasingly evident that the TME is crucial for the development and evolution of tumors. The dynamic interplay between cancer cells and their microenvironment, comprising stromal cells (cellular components) and extracellular matrix (ECM) elements (non-cellular), is crucial for inducing cancer cell heterogeneity, clonal evolution and to increase the multidrug resistance, ultimately leading to cancer cell progression and metastasis.

2. LUNG CANCER

2.1. EPIDEMIOLOGY

In 2020, an estimated 19.3 million new cancer cases were diagnosed and there were 9.9 million deaths worldwide. Among all cancers, lung is the second most diagnosed and the leading cause of cancer death with 2.2 million new lung cancer cases per year and an

estimate of 1.8 million deaths (Figure 2) (Sung et al., 2021). Trends in lung cancer mortality in Spain are like those observed in most developed countries. In 2023, lung cancer was the third most common cancer diagnosed in men, after prostate and colorectal cancers, and the fourth most common in women, after colorectal, prostate and breast cancers (information obtained from the Spanish Association against Cancer website), with a 5-year survival rates of 12.7% in women and 17.0% in men (Sociedad Española de Oncologia Médica., 2023).
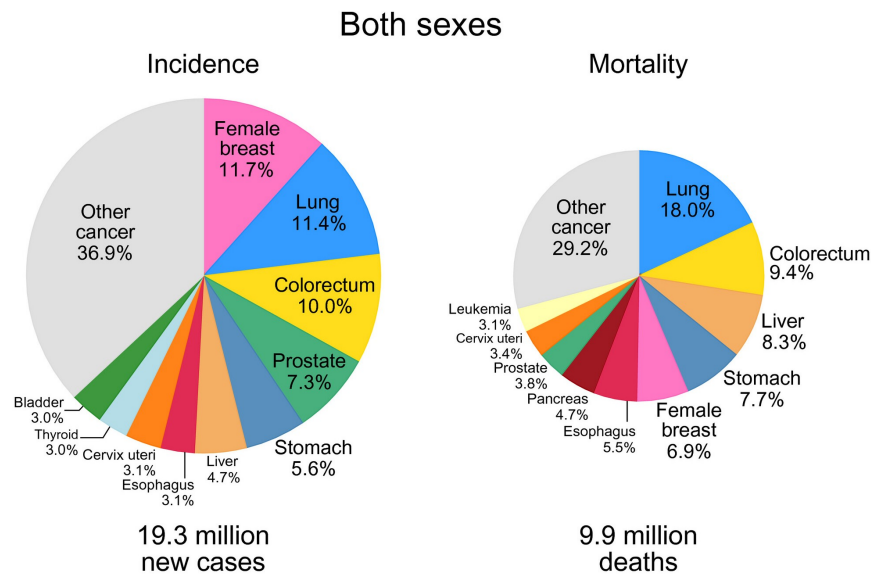
Figure 2. Distribution of cases and deaths for the top 10 most common cancers in 2020 for both sexes. Adapted from (Sung et al., 2021).

2.2. ETIOLOGY

Cigarette smoking is the leading cause of lung cancer, responsible for at least 80% of lung cancer deaths (Islami et al., 2015). Tobacco contains more than 50 carcinogens that trigger the accumulations of genetic mutations, in lines with molecular data indicating that lung cancer is among the tumors with the highest number of accumulated mutations per tumor (Alexandrov et al., 2014). The degree of risk for lung cancer in current smokers depends on number of years and packs smoked (Hecht, 2011). It has also been observed that around 30% of passive smokers develop lung cancer (C. H. Kim et al., 2014).

There are other factors linked with lung cancer development such as lifestyle, environmental or occupational exposures to contaminants like radon gas, arsenic and arsenic compounds, asbestos, beryllium and beryllium oxide and polycyclic aromatics

hydrocarbons (Spyratos et al., 2013). Personal or family history of lung cancer serves as a risk factor for an individual's likelihood of developing lung cancer (Kanwal et al., 2017). Additionally, alcohol consumption, some infectious agents, diet type and other diseases like diffuse cystic fibrosis are considered risk factors for lung cancer (Corrales et al., 2020).

2.3. DIAGNOSIS AND PROGNOSIS

Cough is the most common symptom, occurring in approximately half of patients with lung cancer, followed by chest pain, hemoptysis, weight loss and dyspnea (Kocher et al., 2015). Diagnosis requires a biopsy for histologic confirmation. About 70% of the patients are diagnosed at advanced stage of the disease, with distant metastasis in most cases and no curative surgical options (Reck & Rabe, 2017).

Nowadays, patients with known or suspected lung cancer should undergo clinical evaluation and a contrast-enhanced chest computed tomography (CT) scan (de Koning et al., 2020; Reck & Rabe, 2017). If any extrathoracic abnormalities are found, a fluorodeoxyglucose(18F-FDG)-positron emission tomography (PET) scan is recommended to evaluate the metastasis (Nasim et al., 2019). These methods are often complemented with endobronchial ultrasound (EBUS) and bronchoscopy techniques and endoscopic ultrasound (EUS) for diagnosis (Kazakov et al., 2017).

In addition, clinical staging is one of the most important prognostic factors that influences management options in lung cancer patients. Since the 1970s, the tumor-node-metastasis (TNM) staging system (T: size of primary tumor, N: number and location of affected lymph nodes (LNs), and M: presence of local or distant metastasis) has been constantly reviewed, with the latest, 8th edition. This edition was being effective internationally from 2018 (Lim et al., 2018) (Table 1)

Table 1. The T, N and M descriptors in the 8th edition of the TNM staging system for lung cancer. Adapted from (Goldstraw et al., 2016).

T: Primary tumor	
Tx	Primary tumor cannot be assessed, or tumor proven by the presence of malignant cells in sputum or bronchial washings but not visualized by imaging or bronchoscopy.
T0	No evidence of primary tumor.
Tis	Carcinoma in situ
T1	Tumor 3 cm or less in greatest dimension, surrounded by lung or visceral pleura, without bronchoscopic evidence of invasion more proximal than the lobar bronchus (i.e. not in the main bronchus)[1].
T1a(mi)	Minimally invasive adenocarcinoma[2].
T1a	Tumor ≤1 cm in greatest dimension[1].
T1b	Tumor >1 cm but ≤2 cm in greatest dimension[1].
T1c	Tumor >2 cm but ≤3 cm in greatest dimension[1].
T2	Tumor > 3cm but ≤5 cm; or tumor with any of the following features[3]: - Involves main bronchus regardless of distance from the carina, but without involvement of the carina. - Invades visceral pleura. - Associated with atelectasis or obstructive pneumonitis that extends to the hilar region, involving part or all of the lung.
T2a	Tumor >3 cm but not more than 4 cm in greatest dimension.
T2b	Tumor >4 cm but ≤5 cm in greatest dimension.
T3	Tumor >5 cm but ≤7 cm in greatest dimension, or directly invades any of the following structures: chest wall (including parietal pleura and superior sulcus tumors), phrenic nerve, parietal pericardium; or associated with separate tumor nodule(s) in the same lobe as the primary.
T4	Tumor >7 cm in greatest dimension, or invades any of the following structures: diaphragm, mediastinum, heart, great vessels, trachea, recurrent laryngeal nerve, oesophagus, vertebral body, carina; or associated with separate tumor nodule(s) in a different ipsilateral lobe to that of the primary.
N: Regional Lymph Node Involvement	
Nx	Regional lymph nodes cannot be assessed.
N0	No regional lymph node metastasis.
N1	Metastasis in ipsilateral peribronchial and/or ipsilateral hilar lymph nodes and intrapulmonary nodes, including involvement by direct extension.
N2	Metastasis in ipsilateral mediastinal and/or subcarinal lymph node(s).
N3	Metastasis in contralateral mediastinal, contralateral hilar, ipsilateral or contralateral scalene, or supraclavicular lymph node(s).
M: Distant Metastasis	
M0	No distant metastasis.
M1	Distant metastasis present.
M1a	Separate tumor nodule(s) in a contralateral lobe; tumor with pleural or pericardial nodule(s) or malignant pleural or pericardial effusion[4].
M1b	Single extrathoracic metastasis[5].
M1c	Multiple extrathoracic metastases in one or several organs.

[1]The uncommon superficial spreading tumor of any size with its invasive component limited to the bronchial wall, which may extend proximal to the main bronchus, is also classified as T1a.
[2]Solitary adenocarcinoma, ≤ 3 cm in size, with lepidic pattern and ≤ 5mm invasion in any one focus.
[3]T2 tumors with these features are classified T2a if 4 cm or less in greatest dimension or if size cannot be determined, and T2b if greater than 4 cm but not larger than 5 cm in greatest dimension.
[4]Most pleural (pericardial) effusions with lung cancer are due to tumor. In a few patients, however, multiple microscopic examinations of pleural (pericardial) fluid are negative for tumor, and the fluid is non-bloody and is not an exudate. Where these elements and clinical judgement dictate that the effusion is not related to the tumor, the effusion should be excluded as a staging descriptor.
[5]This includes involvement of a single distant (non-regional) lymph node.

Combining these parameters, the staging of lung tumors from IA1 to IVB is defined (Table 2). To make an adequate decision in terms of treatment, it is also needed the histological classification of the tumor, including the molecular characterization (Goldstraw et al., 2016).

Table 2. Staging criteria based on the 8th edition of the TNM staging system for lung cancer. Adapted from (Goldstraw et al., 2016).

TNM staging		N categories (Overall stage)		
T/M	N0	N1	N2	N3
T1a	IA1	IIB	IIIA	IIIB
T1b	IA2	IIB	IIIA	IIIB
T1c	IA3	IIB	IIIA	IIIB
T2a	IB	IIB	IIIA	IIIB
T2b	IIA	IIB	IIIA	IIIB
T3	IIB	IIIA	IIIB	IIIC
T4	IIIA	IIIA	IIIB	IIIC
M1a	IVA	IVA	IVA	IVA
M1b	IVA	IVA	IVA	IVA
M1c	IVB	IVB	IVB	IVB

N, node involvement; T, tumor size; M, metastasis.

2.4. HISTOLOGICAL CLASSIFICATION

The gold standard procedure for diagnosing lung cancer involves the use of histological and pathological techniques (Galli & Rossi, 2020). There are two main subtypes of lung cancer, small cell lung carcinoma (SCLC) representing 15% of the cases, and non-small cell lung carcinoma (NSCLC) accounting for the remaining 85%. NSCLC is further classified intro three types: squamous cell carcinoma (LUSC), adenocarcinoma (LUAD) and large-cell carcinoma (LLCC). These three subtypes are discussed as follows:

1) LUAD: It is the most common type of NSCLC, comprising around 40% of all lung cancer (Meza et al., 2015). It originates in the small airway epithelial, particularly the type II alveolar cells, which secrete mucus and other substance. LUAD tends to occur in the peripheral areas of the lung and is therefore more likely to the surgically resected (Zheng, 2016). LUAD exhibits different histological patterns such as lepidic, acinar, papillary, micropapillary, and solid patterns, being these last two the ones with a most aggressive behavior (Kuhn et al., 2018). Tumor cells tends to produce mucine and

express immunohistochemical markers such as the thyroid transcription factor 1 (TTF-1) and napsin A (Ye et al., 2011).

2) LUSC: It comprises the 30% of all lung carcinomas. It originates in one of the main airway branches in the center of the lungs (Socinski et al., 2016). These tumors typically exhibit keratinization and/or intercellular bridges. They express immunohistochemical markers associated with squamous cell differentiation, such as p40 or p63 and cytokeratin 5/6 (Gurda et al., 2015).

3) LLCC: It accounts for approximately 5% to 10% of all lung cancers. These tumors are poorly differentiated and do not exhibit histological or immunohistochemical evidence of squamous cell, glandular, or small-cell differentiation (Zheng, 2016).

2.5. MOLECULAR PROFILE

In recent decades, significant progress has been achieved in understanding the molecular and cellular processes driving cancer initiation, maintenance, and progression (Collisson et al., 2014). NSCLC is one of the most genetically diverse tumors, and therefore, there are a variety of molecularly defined subsets of patients characterized by specific sets of driver mutations. *EGFR* (epidermal growth factor receptor) and *KRAS* (Kirsten rat sarcoma 2 viral oncogene homolog) mutations, along with *EML4-ALK* fusions (echinoderm microtubule-associated protein-like 4 - anaplastic lymphoma kinase), are the three most frequent driver alterations in LUAD, occurring in approximately 35–40% of tumors. Recurrent alterations characteristic of LUSC include amplification of *SOX2* (SRY-Box Transcription Factor 2), *PIK3CA* (Phosphatidylinositol-4,5-Bisphosphate 3-Kinase Catalytic Subunit Alpha), *PDGFRA* (Platelet Derived Growth Factor Receptor Alpha) and *FGFR1* (Fibroblast Growth Factor Receptor 1) as well as mutation of *DDR2* (Discoidin Domain Receptor Tyrosine Kinase 2), *AKT1* (AKT Serine/Threonine Kinase 1) and *NRF2* (NFE2 Like BZIP Transcription Factor 2). Many alterations are observed at similar frequencies in both LUAD and LUSC, including *TP53*, *BRAF* (B-Raf Proto-Oncogene, Serine/Threonine Kinase), *PIK3CA*, *MET* (MET Proto-Oncogene, Receptor Tyrosine Kinase) and *STK11* (Serine/Threonine Kinase 11) mutations, loss of *PTEN* (Phosphatase and Tensin Homolog) and amplification of *MET*, with *BRAF*, *PIK3CA* (Figure 3) (Pikor et al., 2013).

Non-small Cell Lung Cancer
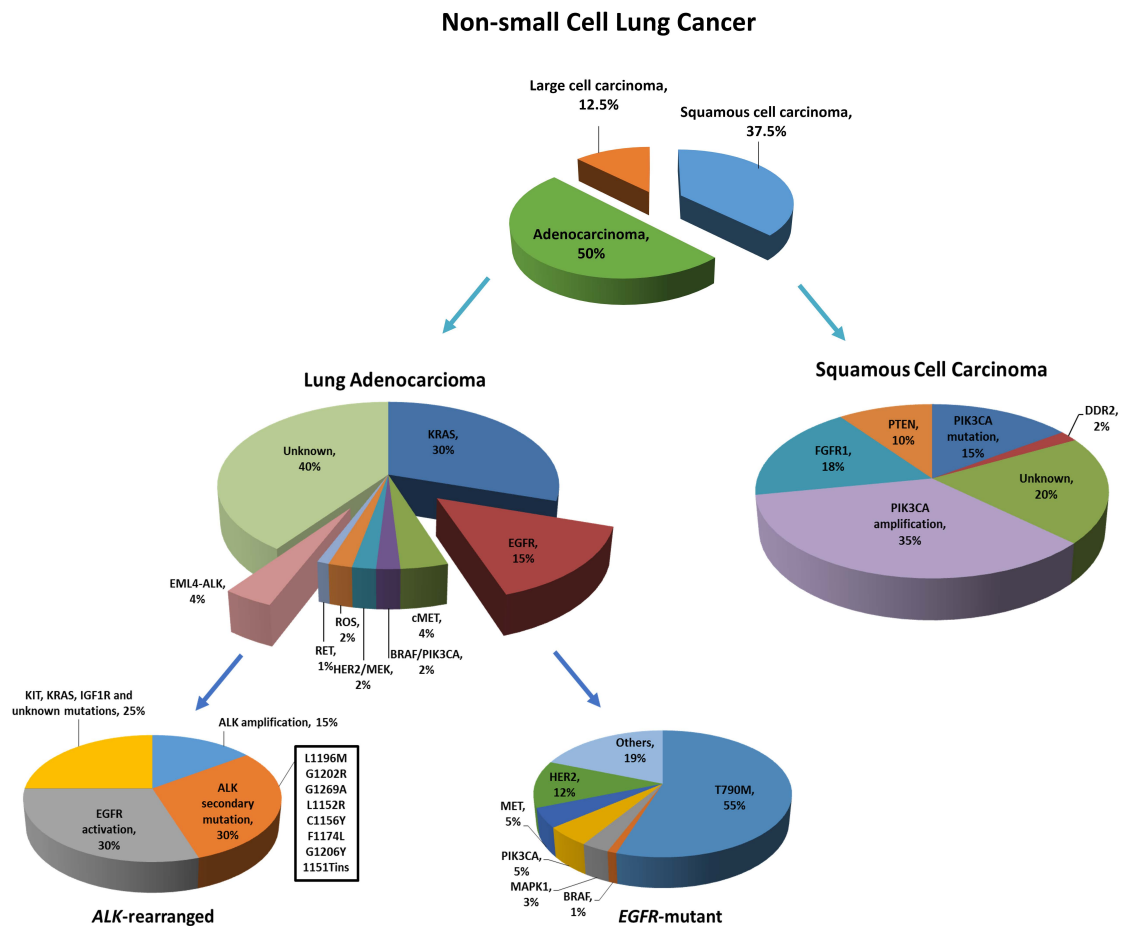
Figure 3. Mutational profiles in non-small cell lung cancer. ALK, anaplastic lymphoma kinase; BRAF, B-Raf proto-oncogene; DDR2, discoidin domain receptor tyrosine kinase 2; EGFR, epidermal growth factor receptor; EML4, echinoderm microtubule-associated protein-like 4; FGFR1, fibroblast growth factor receptor 1; HER2, human epidermal growth factor receptor 2; IGF1R, insulin-like growth factor 1 receptor; KIT, proto-oncogene c-Kit; KRAS, Kirsten rat sarcoma viral oncogene homolog; MAPK1, mitogen-activated protein kinase 1; MEK, mitogen-activated protein kinase kinase; MET, mesenchymal epithelial transition factor proto-oncogene, receptor tyrosine kinase; PI3KCA, phosphatidylinositol-4,5-bisphosphate 3-kinase catalytic subunit alpha; PTEN, phosphatase and tensin homolog; RET, ret proto-oncogene; ROS1, reactive oxygen species protooncogene 1, receptor tyrosine kinase. Adapted from (Chan & Hughes, 2015; Pikor et al., 2013).

2.6. MOLECULAR TARGETS AND TARGETED THERAPIES

EGFR alterations are present in 10-15 % of LUADs (Siegelin & Borczuk, 2014). *EGFR* belongs to a family of receptor tyrosine kinases that can activate a range of pathways associated with cell growth and proliferation when activated. Mutations in *EGFR* lead to uncontrolled cell division through constant activation. *EGFR* mutations commonly occur in exons 18-21 which confers sensitivity to *EGFR* tyrosine kinase inhibitors (EGFR-TKIs) (Torres et al., 2020). The two most common mutations are exon 19 deletions (60%) and L858R (a missense substitution of Leu for Pro at position 858 of the protein), leading to a constitutive activation of the tyrosine kinase of the receptor. These mutations are correlated with the response in patients receiving EGFR-TKIs (Inoue et al.,

2013; Pao et al., 2004; Thomas J Lynch et al., 2004). Less common mutations, including insertions in exon 20 or in-frame duplications, have also been identified (Helena A. Yu et al., 2014; Leonetti et al., 2019).

KRAS activating mutations lead to constitutive signaling and are present in about 25% of LUAD and 4% of LUSC (Dearden et al., 2013). *KRAS* encodes a G-protein that controls a range of signal transduction pathways regulating differentiation, cell proliferation and survival. The most common mutations are found in codons 12, 13, 59 and 61, being G12C and G12V the most frequent ones (Cook et al., 2021). To date, only irreversible small-molecule inhibitors targeting *KRAS* G12C have been approved and are used in clinical practice (Jänne et al., 2022; Rosell et al., 2023; Skoulidis et al., 2021). Other research approaches are focus on inhibiting downstream molecules in the RAS/RAF/MEK/extracellular signal-regulated kinases (ERK) and PI3K/AKT/mTOR pathways (Cox et al., 2014).

ALK rearrangements, resulting in fusions of the intracellular kinase domain with the amino terminal end of mainly *EML4*, promote malignant growth and proliferation (Soda et al., 2008). These rearrangements occur on chromosome 2p23 due to the fusion between the 5´end of the *EML4* gene and the 3´end of the *ALK* gene. More recently, different partner genes have been identified in a small subset of ALK rearrangements (less than 1% of cases) including *KIF5B* (kinesin family member 5b), *TFG* (TRK-fused gene) and *TPM4* (Tropomyosin 4) (W. Wu et al., 2017). *ALK* inhibition with specific TKIs leads to a good response (Shaw et al., 2013; Soda et al., 2007).

Other less common alterations (including single-nucleotide variants (SNVs), copy number variations (CNVs), and/or fusions) can be found in LUAD tumors in genes such as *RET* (ret proto-oncogene), *NTRAK* (neurotrophic tyrosine receptor kinase), *ROS1* (reactive oxygen species proto-oncogene 1, receptor tyrosine kinase), *BRAF*, *HER2* (human epidermal growth factor receptor 2), *MEK1* (mitogen-activated protein kinase 1) and *MET* (Gkolfinopoulos & Mountzios, 2018).

On the other side, LUSC tumors are characterized by genomic complexity and a high overall mutational load. *PIK3CA* is one of the gene most frequently altered in LUSC

(Yamamoto et al., 2010). Another gene amplified in 20% of LUSC cases is FGFR1 (Miao et al., 2016). *PTEN and DDR2* have been altered in LUSC with a frequency of 10% and 2%, respectively (Bong et al., 2011; Hammerman et al., 2012). In *EGFR* gene, only some alterations such as exon 19 deletions, L858R, exon 20 insertions and L861Q have been identified in LUSC (R. Jin et al., 2021).

2.7. CURRENT THERAPEUTIC APPROACHES IN NSCLC

Treatment in NSCLC is stage-specific. Whenever possible, patients with early-stage (stage I, II and some IIIA) should undergo a surgical resection. For non-surgical patients, stereotactic or conventional radiotherapy should be considered (Robinson & Bradley, 2010). Neo-adjuvant or adjuvant chemotherapy or radiotherapy can be recommended in resected cases to improve local control (Mcelnay & Lim, 2014; Postmus et al., 2017).

Management of unresectable NSCLC has undergone remarkable changes in the last years. Targeted therapies have emerged, increasing patient survival, and reducing the toxicity associated with conventional chemotherapy (C. Y. Yang et al., 2020). The most widely used targeted therapies are the EGFR TKIs (Chan & Hughes, 2015). The EGFR TKIs include the first-generation drugs as erlotinib and gefitinib, second-generation inhibitors such as afatinib and dacomitinib, and third-generation TKIs such as osimertinib and rociletinib (Rui et al., 2020; Sequist et al., 2015). The landscape in the treatment of EGFR mutant NSCLC has evolved substantially in recent years, with Osimertinib showing better progression-free survival (PFS) and less toxicity compared to first-generation EGFR-TKIs, moving Osimertinib to frontline therapy (Ramalingam et al., 2020). Despite high response rates achieved with EGFR TKI's, most patients develop resistance to the treatment (Ricordel et al., 2018; Westover et al., 2018). Currently, efforts are focused on understanding these mechanisms of resistance to select the best therapeutic strategy (Ricordel et al., 2018).

In patients with *ALK* and *ROS1* translocations, different generations of TKIs have been approved in first- and subsequent-lines (Cooper et al., 2022). The main mechanisms resulting in resistance to these therapies are secondary mutations in *ALK* (Okada et al., 2019). To address this issue, lorlatinib is a new-generation ALK inhibitor with activity

against all the known *ALK* inhibitor resistance mutations, and it was approved by the Food and Drud Administration (FDA) for ALK translocated or mutated NSCLC (Shaw et al., 2020; Solomon et al., 2018).

Recently, other new driver mutations in genes such as *HER2*, *RET*, *NTRK*, *MET*, *BRAF*, and *KRAS* have been identified in metastatic NSCLC with targetable therapeutic options. Therapies targeting these mutations include TKIs, monoclonal antibodies, and antibody-drug conjugates (Hendriks et al., 2023; Rosell et al., 2023) (Figure 4).

In the recent days, the landscape of treatment of NSCLC has dramatically changed due to immunotherapy. In a normal scenario, the immune system can recognize and destroy cancer cells through a highly regulated process involving an equilibrium of activating and inhibitory signals. Tumor cells can disrupt this equilibrium, evading immune surveillance. One of these pathways involved the axis programmed cell death protein 1 (PD1) and it ligands (PDL1 and PDL2). Tumors cells can overexpress *PDL1* and interact with PD1 on T cells leading to its inactivation. Fortunately, this interaction can be blocked with monoclonal antibodies against PD1 or PDL1. Current immune checkpoint inhibitors (ICIs) approved for NSCLC include the anti-PD1 antibodies nivolumab (human IgG4) and pembrolizumab (humanized IgG4), as well as the anti-PDL1 antibodies atezolizumab (human IgG1, with the Fc domain engineered to prevent antibody-directed cell cytotoxicity), durvalumab (human IgG1 engineered), and avelumab (human IgG1) (Qiu et al., 2019). ICIs have been approved as a second-line therapy for patients with advanced NSCLC whose tumors progress to platinum-based chemotherapy or targeted therapies as well as in the first-line NSCLC setting. While nivolumab and atezolizumab are used irrespective of *PDL1* tumor expression, pembrolizumab is used if *PDL1* expression is at least 1% (Raju et al., 2018). Pembrolizumab have been approved as a single agent for the first-line treatment of patients with metastatic NSCLC harboring high expression of *PDL1* (more than 50%) in the absence of *EGFR* mutations or *ALK* or *ROS1* fusions (Mok et al., 2019).

Advanced Non-squamous cell

YES ← **Targetable driver mutation present?** → NO

EGFR mutation	*ALK* translocations	*ROS1* translocations	Others	PS 0-2 and PD-L1 ≥ 50%	PS 0-1 and any expression of PD-L1	PS2 and PDL1 < 50%
First-line treatment				**First-line treatment**		
Osimertinib[1] (Gefitinib/ Erlotinib/Afatinib/ Dacomitinib/ Erlotinib + Ramucirumab or Bevacizumab/ Getifinib-carboplatin-pemetrexed)	Alectinib[1] (Brigatinib, Lorlatinib, Crizotinib, Ceritinib)	Crizotinib /Entrectinib /Repotrectinib	**NTRK fusion**→ Platinum doblet +ICI/Larotrectinib/ Entrectinib **BRAF mutation**→ dabrafenib+ Trametinib **MET Exon 14 Skipping**→Platinum doblet +ICI/ Tepotinib/Capmatinib **RET Translocation**→ Selpercatinib/Pralsetinib **HER2 mutation**→ Trastuzumab-deruxtecan. **EGFR ex20ins**→ Amivantamab/ Mobovertinib **KRAS G12C mutation**→ Sotorasib/ Adagrasib.	Pembrolizumab /Cemiplimab[5]	Pembrolizumab-ChT/ Atezolizumab-ChT-bevacizumab/ Durvalumab-tremelimuma-Platinium doublet/Nivolumab-ipilimumab[6]+2 cycles of Platinium doublet followed by nivolumab-ipilimumab Nivolumab-ipilimumab[6]	Platinium doublet with pemetrexed or Single agent ChT
				Second-line tratment		
				Platinium doublet with pemetrexed/ Carboplatin-paclitaxel-bevacizumab / Re-challenge ICI	Pemetrexed /Docetaxel/Nintedanib-docetaxel/Ramucirumab-docetaxel/Re-challenge ICI	Nivolumab,Atezolizumab, pembrolizumab[6] or atezolizumab.
Second-line treatment						
Osimertinib(T790M+)[2] Platinium doublet with pemetrexed + Atezolizumab-bevacizumab	Alectinib[3], Ceritinib[3], Brigatinib[3], Lorlatinib[4] or Platinium doublet with pemetrexed + Atezolizumab-bevacizumab	Platinium doublet with pemetrexed	Platinium doublet with pemetrexed + immunotherapy			

1. Preferred Option
2. Patients with disease progression to Gefitinib, Erlotinib o Afatinib
3. Patients with disease progression to Crizotinib
4. After at least 1 ALK TKI, other than crizotinib
5. For PS2
6. Only if PDL1 ≥ 1%

Advanced Squamous cell

YES ← **Targetable driver mutation present?** → NO

Molecular test		PS 0-2 and PD-L1 ≥ 50%	PS 0-1 and any expression of PD-L1	PS2 and PDL1 < 50%
EGFR/ALK/ROS1/MET/EGFRex20ins/KRASG12C/NTRK/HER2		**First-line treatment**		
Positive	**Negative**	Pembrolizumab /Atezolizumab /Cemiplimab[1]	Pembrolizumab-ChT/ Durvalumab-tremelimuma-Platinium doublet/Nivolumab-ipilimumab[2]+2 cycles of Platinium doublet followed by nivolumab-ipilimumab/Cemiplimab-Platinium doublet/Nivolumab-ipilimumab[2]	Platinium doublet with pemetrexed or Single agent ChT
Targeted Therapy	Follow recommended treatment in line of ECOG PS & PD-L1 expression level	**Second-line tratment**		
		Platinium doublet with pemetrexed/ Carboplatin-paclitaxel-bevacizumab / Re-challenge ICI	Pemetrexed /Docetaxel/Nintedanib-docetaxel/Ramucirumab-docetaxel/Re-challenge ICI	Nivolumab,Atezolizumab, pembrolizumab[1], docetaxel, Ramucirumab-docetaxel, Afatinib.

1. For PS2
2. Only if PDL1 ≥ 1%

Figure 4. Treatment algorithm for advanced-stages non-small cell lung cancer (Non-Squamous Cell and Squamous Cell). Own design created with PowerPoint.

Despite ICIs and targeted therapies having led to prolonged survival in selected patients, many patients still do not respond to treatments, leading to disease progression or relapse. Treatment resistance is generally due to the intrinsic complexity of the tumor. Tumors can be characterized as a complex ecosystem where different populations of non-tumor cells infiltrate the tumor, contributing to the creation of a microenvironment that sustains the growth of the tumor cells (Hanahan & Weinberg, 2011). Furthermore, cancer cells are heterogeneous displaying many phenotypic, genetic, and functional differences, which means that not all the subclones in the tumor are affected by treatments in the same way (Marusyk et al., 2012). In fact, there is strong evidence showing that treatment resistance is highly associated to populations of tumor cells with stem-like properties, called cancer stem-like cells (CSCs).

3. CANCER STEM CELLS

3.1. TUMOR HETEROGENEITY

Tumors are dynamics and continue to evolve, generating a molecularly heterogeneous bulk tumor consisting of cancer cells with different molecular features. This heterogeneity can derive from cell-intrinsic properties, including variability in the genetics, epigenetics, transcriptomics, and/or phenotypic changes, as well as cell-extrinsic properties arising from factors in the microenvironment, including the composition of the ECMs and factors that affect the tumor's ability to recruit a blood supply and to recruit stromal cell types that aid tumor growth (Marjanovic et al., 2013).

Different levels of heterogeneity have been described in cancer: intertumoral and intratumoral heterogeneity. Intertumoral heterogeneity refers to the variability between patients harboring the same tumor type, resulting from patient-specific factors such as germline genetic variations, differences in somatic mutation profile, and environmental factors. Intratumoral heterogeneity refers to heterogeneity among the population of tumor cells within a single patient (Lawson et al., 2018; Marusyk et al., 2012) (Figure 5). Two models have been historically proposed to explain cancer cell heterogeneity: clonal evolution theory and CSC theory.

The first model, the clonal evolution theory, also called stochastic model was described by Nowell in 1976. This model suggest that the tumor arise from a single cell immediately after the appearance of multiple driver mutations, resulting in a variety of cells with different genotype and phenotype. The mutant clones resulting from beneficial mutations in a Darwinian-like way, gain selective advantage and can contribute to sustaining tumor growth, progression, and resistance to therapy (Nowell, 1976). It is important to consider the selection pressure imposed by the TME on the selective outgrowth of clones with more malignant phenotypes. Therefore, the tumor mass is composed of distinct clones (all derived from the same cell of origin) with different stochastic mutations. In this model, the frequency of cancer cells with tumorigenic potential is high, the tumor organization is not necessarily hierarchical, and the rational approach to therapy has been to target most or all cells.
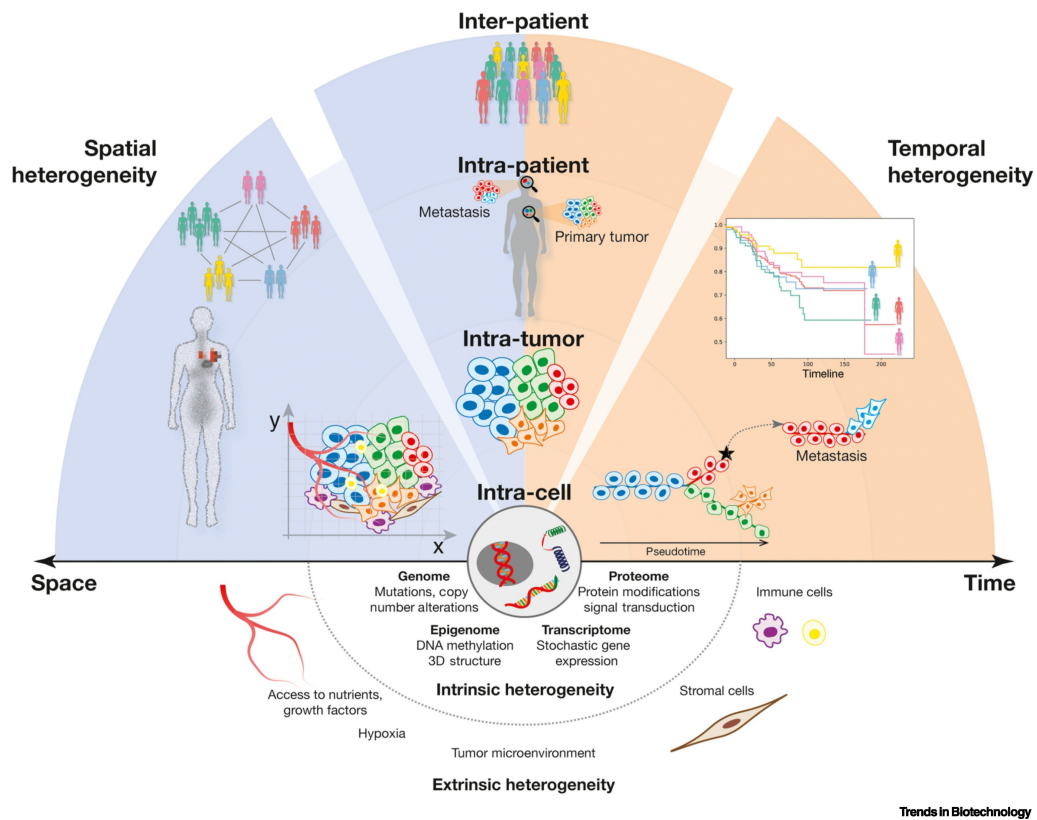
Figure 5. Tumor heterogeneity across scales and dimensions. Reproduced from (Kashyap et al., 2022).

The CSC model, also known as hierarchical model, proposes that the progression and growth of most of cancers, as well as the cell heterogeneity, are driven by small, phenotypically distinct subset of cells known as CSCs (Dick, 2008). It is suggested that CSCs undergo epigenetic changes like the differentiation of normal cells, giving rise to phenotypically diverse non-tumorigenic cancer cells that make up the bulk of cells in a tumor. In contrast to the stochastic model, in this model, the tumor bulk is established by a pool of CSCs capable of undergoing self-renewal to generate daughters that exhibit the CSC phenotype once again. They can also undergo asymmetric division to develop daughters (non-CSCs) with limited tumorigenic and metastatic potential. In this model the tumor is organized in a hierarchical manner, the frequency of cancer cells with tumorigenic potential is from rare to moderate, and the therapy approach enables to target only tumorigenic cells.

In more recent years, these two models are proposed as a unified model by some authors (Meacham & Morrison, 2013). Recently, a model of clonal evolution applied to CSCs was proposed by Kreso et al. In this model, called the plasticity model, CSCs can acquire mutations and generate new stem cell branches, while at the same time, tumor

cells in the non-CSC subpopulation can undergo epithelial-mesenchymal transition (EMT) and acquire CSC-like features contributing to tumor heterogeneity (Kreso & Dick, 2014; Rich, 2016) (Figure 6).
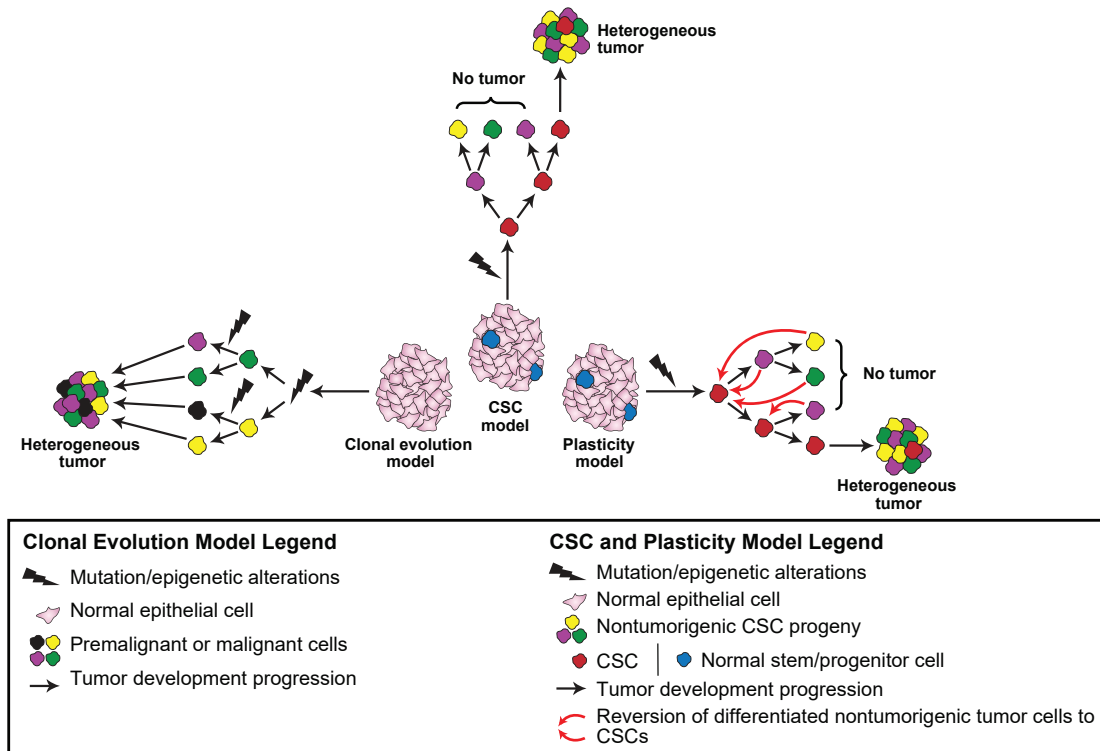
Figure 6. Model for tumor heterogeneity. **Stochastic vs. Cancer Stem Cell (CSCs) vs. plasticity models.** According to the clonal evolution model, mutations accumulate through time and any cell may have tumorigenic potential. Whereas in the CSC model, only stem cells possess tumorigenic potential while differentiated cells do not have tumorigenic capacity. Furthermore, plasticity model suggested that cells' differentiation is bidirectional; thus, a differentiated nontumorigenic cancer cell can revert back to CSC. Reproduced from (Rich, 2016).

Now, the question is, what is the precursor of CSCs, and how does a normal cell obtain the ability to infinitely self-renew? CSCs may originate from the malignant transformation of either tissue-specific stem cells, bone marrow stem cells, or even normal differentiated somatic cells that undergo a dedifferentiation process. The transition of these cells to CSC may include a set of molecular and cellular events, such as cell fusion, horizontal gene transfer, DNA mutation and aneuploidy, and/or microenvironmental factors. Stem cells are pluripotent and show self-renewal ability, so that CSCs could just use aberrantly stem cell pathways to support their self-renewal (Diwakar R Pattabiraman and Robert A. Weinberg, 2014).

4. LUNG TUMOR MICROENVIRONMENT (TME)

4.1. THE IMMUNOLOGY OF TME

During cancer initiation and progression cancer cells interact with a variety of resident and infiltrating host cells, secreted factors, and ECM proteins, all together known as the TME. The TME can either positively or negatively affect tumor development. In terms of stroma cells which contribute to the the immunescape, we can distinguish:

a) Dendritic cells (DCs): These are antigen-presenting cells (APCs) derived from bone marrow precursors. DCs are recognized as central orchestrators of antitumoral immunity due to their ability to cross-present tumor antigens to prime T lymphocytes in the draining LNs (Sánchez-Paulete et al., 2017). It has been reported that in patients with NSCLC, DCs upregulate the co-inhibitory molecule B7-H3 and therefore fail to stimulate T cells (Schneider et al., 2011). However, tumors can recruit immune-suppressive DCs and employ numerous strategies to suppress DC-based anti-tumor immunity. DCs also secreted transforming growth factor-β (TGF-β) inducing the differentiation of $CD4^+T$ cells into $CD4^+CD25^+$forkhead box P3 $(FOXP3)^+$ T_{REGS} cells that suppress T cell proliferation.

b) Myeloid-derived suppressor cells (MDSCs): They are a heterogeneous immunosuppressive cell population capable of suppressing T cell proliferation and cytokine production, attenuating both adaptive and innate immune responses. MDSCs play a key role in tumor evasion of immune surveillance (Z. Yang et al., 2020). As currently was revealed, MDSCs are involved in tumor progression by promoting tumor angiogenesis, tumor cell invasion and premetastatic niche formation (Myrna L. Ortiz, Lily Lu, Indu Ramachandran, 2014; Srivastava et al., 2012).

c) Tumor-associated macrophages (TAMs): TAMs are abundant components in the immune infiltrate of NSCLC and display a range of phenotypes, including

M1 (classically activated macrophages with pro-inflammatory and antitumor activity) and M2 (alternatively activated macrophages with proangiogenic and immunosuppressive protumor activity) (Q. Yang et al., 2020). The increase in TAMs is associated with low survival rates in many human malignant neoplasms. Nevertheless, the prognostic relevance of TAMs in NSCLC remains unclear. Recently, it has been revealed that M2 TAMs may induce tumor cell aggressiveness and proliferation, increasing the metastatic potential during NSCLC progression, which leads to a poor prognosis in patients with NSCLC (Sumitomo et al., 2019). Naïve macrophages also called resting-state macrophages M0, are usually considered precursors of polarized macrophages. Naïve macrophages display phagocytic functions, recognize pathogenic agents, and rapidly undergo polarization towards pro or anti-inflammatory macrophages to acquire their full panel of functions (Chaintreuil et al., 2023).

d) Neutrophils: Neutrophils constitute a group of white blood cells known as polymorphonuclear cells. Neutrophils infiltrating mouse tumors can either promote carcinogenesis by supporting tumor-related inflammation, angiogenesis and metastasis or restrict tumor growth through the expression of antitumor and cytotoxic mediators. It has been reported that tumor-infiltrating neutrophils expressing APCs markers can cross-present antigens and trigger antitumor T cell response in early-stages of human lung cancer (Singhal et al., 2016).

e) Natural killer cells (NK): NK are lymphocytes critical in the innate immune system playing a key role in antitumor immunity by directly recognizing tumor cells as targets (Zeng et al., 2006). However, NK cell population found in NSCLC has been reported as displaying alterations in the expression of relevant NK cell receptors, downregulation of activating (NKp30, NKp80, CD16, DNAM-1) and inhibitory (Ig-like transcripts (ILT-2) and Killer Ig-Like Receptors (KIRs)) receptors, as well as upregulation of NKG2A when compared to the normal counterpart (Platonova et al., 2011). Functionally, intratumoral

NK cells have shown impairments in the ability to both degranulate and produce IFNγ (Platonova et al., 2011) in response to classical NK cell targets, potentially acquiring a proangiogenic phenotype due to the signals provided by the TME (Carrega et al., 2008).

f) CD4$^+$ and CD8$^+$ T cells: T lymphocytes infiltrating tumors and their immunoregulatory cytokines can promote effectors functions in the TME and mediate the response to ICBs. CD8$^+$ T cells target tumor cells through different mechanisms such as production and release of interferon-gamma (IFN-γ), tumor necrosis factor (TNF) and granzyme B after T cell receptor (TCR) activation (M. St. Paul & Ohashi, 2020). Nevertheless, tumors employ a lot of mechanisms to inhibit CD8$^+$ T cells. For instance, T$_{REGS}$ can directly suppress the antitumor function of CD8$^+$ T cells (Ganesan et al., 2013). In NSCLC patients, disease progression is associated with increased expression of markers of T cells exhaustion, including PD1, T cell membrane protein 3 (TIM3), lymphocyte activation gene 3 (LAG3), cytotoxic T-lymphocyte associated antigen 4 (CTLA4) and B and T lymphocyte attenuator (BTLA) on CD8$^+$ T cells (Thommen et al., 2015). Regardless of the central role of CD8$^+$ T cells in antitumor immunity, an efficient antitumor immune response also requires the cooperation of CD4$^+$ T cells since it has been demonstrated that the efficacy of PD1 inhibition was only partially reversed by depletion of CD8$^+$ T cells but was completely removed by the additional depletion of CD4$^+$ T cells in *KRAS*-driven mouse model (Markowitz et al., 2018). Our group had reported that the presence of CD8$^+$ T cells in the tumor compartment of NSCLC patients was associated with better outcomes (Usó et al., 2016).

g) FOXP3$^+$T$_{REG}$ cells: regulatory T cells play a crucial role in the regulation of tumor immunity inhibiting the activation and differentiation of CD4$^+$ helper T cells and CD8$^+$ cytotoxic T cells to induce reactivity against autologous and tumor-expressed antigens (Ohue & Nishikawa, 2019). T$_{REGS}$ can impair the function of immune effector cells through a range of mechanisms and are key factors in tumor immune scape (C. Li et al., 2020). For instance, T$_{REGS}$ can

secrete transforming growth factor beta (TGFβ), interleukine 10 (IL10) and interleukine (IL35) leading to downregulation of antitumor immunity, suppression of antigen presentation by DCs and CD4$^+$ helper T cell function (Jarnicki et al., 2006; Wei et al., 2017). Furthermore, T$_{REGS}$ functions include direct destruction of other cells by secreting granzyme, perforin and cyclic adenosine phosphate (cAMP)(Cao et al., 2007; Sojka et al., 2008). Our group has previously reported that the presence of FOXP3+ cells in NSCLC patients was associated with worse overall survival (OS) (Usó et al., 2016).

h) Cancer associated fibroblast (CAFs): NSCLC tumors often exhibit desmoplasia, which is characterized by the presence of CAFs (Altorki et al., 2019). CAFs mediate cancer cell proliferation, invasion, angiogenesis, drug resistance and metastasis (Feng et al., 2022). Between all these functions, CAFs also modulate immune response in the TME. For instance, CAFs isolated from specimens from NSCLC patients expressing the ligands of PD1 receptor, PDL1 and PDL2 were able to suppress T cell function in co-culture experiments (Nazareth et al., 2007). In the same way, CAFs can cross-present antigens complexed with major histocompatibility complex class I (MHC I) molecules to antigen-specific CD8+ T cells, triggering to antigen-specific upregulation of PDL2 and Fas ligand (FASL) in these T cells leading to their elimination (Lakins et al., 2018).

As we have seen, the role of the immune system during tumorigenesis is also crucial.

4.2. TUMOR CELL-MEDIATED IMMUNOSUPPRESION

There is a lot of evidence showing that tumor cells acquire mechanisms to either evade immune cell detection or inhibit the anti-tumor immune response, which favors tumor development and spreading. Tumor cells employ different mechanism to regulate the immune microenvironment, including the release of a series of immunoregulatory and proapoptotic mediators (Rabinovich et al., 2007), alterations of components of the antigen presentation machinery (Marincola et al., 2000), defects in proximal TCR

signaling (Koneru et al., 2005), activation of negative regulatory pathways (also known as immune checkpoints) and induction or attraction of immunosuppressive cells such as MDSC, TAMs, DCs, and T_{REGS} (Elizabeth A. Vasievich and Leaf Huang, 2011).

4.2.1. IMMUNE CHECKPOINTS

The activation of T cells is a crucial factor in the immune response (Lenschow & Bluestone, 1993). The first signal for T-cell activation is when T cells recognize antigen peptides presented via the T-cell receptor by MHC on APCs. The second signal is a co-stimulatory signal from CD28 on T cells and CD80/CD86 on APCs (Lenschow et al., 1996). This activation requires of a third signal, such as cytokines like Interleukine 2 (IL2). To regulate this pathway, Leach and his colleagues validated that blockade of CTLA4 could downregulate T-cell response, enhancing antitumor response in immunocompetent mouse models (Leach et al., 1996). A few years later, Gordon J. Freeman revealed that CTLA4 could bind to PDL1 and lead to the inhibition of lymphocyte proliferation (Freeman et al., 2000). In addition to CTLA, which is probably the most extensively studied regulatory signal, other molecules and interactions with regulatory capacity have been investigated. For example, the binding of PD1 to PDL1 inhibiting T-cell responses; the binding of TIM3 to its ligand galectin-9 (GAL9) leading to the death of T helper 1 (Th1) cells (C. Zhu et al., 2005); the binding of LAG3 to a range of receptors (MHC-II molecules, galectin-3 (GAL3), fibrinogen-like protein 1 (FGL1), a-synuclein and LSECtin) with inhibitory effects on T cells (Kouo et al., 2015; Mao et al., 2016; Visan, 2019; Xu et al., 2014); or the binding of CD276 (also known as B7-H3) to its receptor (not yet identified) on CD4$^+$ and CD8$^+$ T cells, inhibiting T cell proliferation and downregulating cytokines production, among other mechanism (Vigdorovich et al., 2013). As their function in the balance of the immune system, costimulatory or coinhibitory proteins are defined as immune checkpoint proteins. These factors play a significant role in cancer immunotherapy (Pardoll, 2012). Tumors can disrupt the immune response by directly inhibiting the functions of T cells and NK cells and escaping from immunosurveillance by dysregulating these immune checkpoints signaling pathways. Tumor cells up-regulated the expression of ligands for T cell inhibitory and apoptotic receptors such as PDL1, PDL2, GAL9, FGL1, GAL3, CD200 and CD276 (Figure 7) (S. Dutta et al., 2023; Shao & Owens, 2023). Cancer cells are also able to express tolerogenic or immunosuppressive

molecules such as non-classical human leukocyte antigen (HLA) molecules HLAE, -F, -G, while also expressing lower levels of co-stimulatory molecules necessary for the proper activation of T cells such as CD40, CD80, or CD86. (Airoldi et al., 2003; Wischhusen et al., 2007). All these mechanisms are compiled in Figure 7.
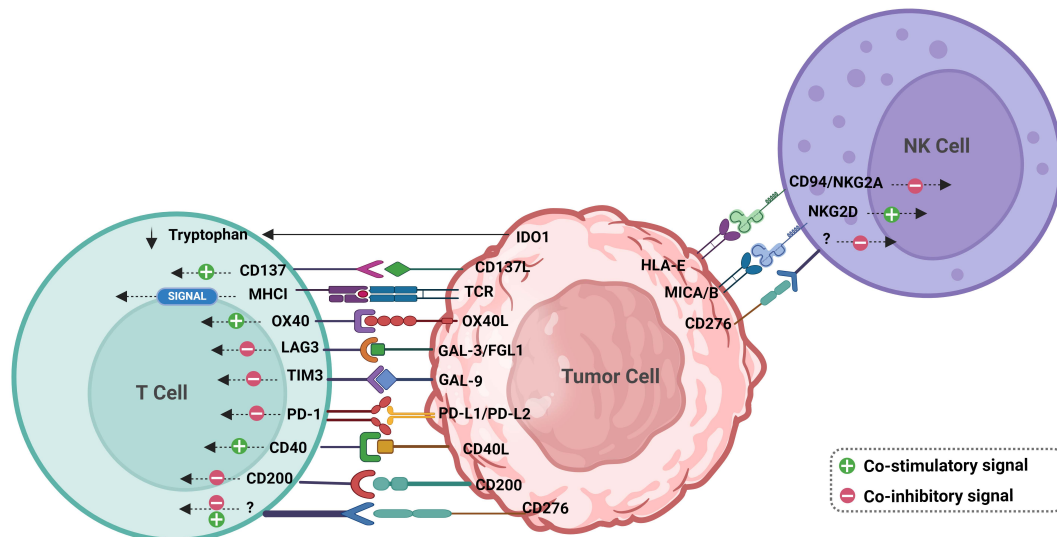
Figure 7. Immune checkpoint receptors and their ligands in the context of the tumor immune microenvironment (TME). The figure illustrates an overview of implicated receptor-ligand interactions and their general effects on the immune response. Co-stimulatory (green +) and co-inhibitory (red -) interactions involving tumor cells, T cells and NK cells. NK, natural killer. Own design created with BioRender.com.

4.2.2. IMMUNOSUPPRESSIVE FACTORS

Increasing evidence reveals that tumor cells employ post-translational mechanism such as the secretion of ligands as soluble forms, to suppress NK activating receptors, thus preventing the binding of activating ligands on their surfaces evading NK cell recognition (Molfetta et al., 2019). The major histocompatibility complex class I polypeptide-related seq A/B (MICA/B), which are natural killer group 2D (NKG2D) ligands, are transmembrane proteins with MHC-like extracellular domains. The cleavage of surface MICA/B proteins occurs through a series of steps, which includes the participation of MICA/B alpha-3 domain, ERp5, and proteases. The soluble variants of MICA/B proteins have the ability to attach to NKG2D receptors located on NK cells, leading to a prolonged suppression of these cells (Xing & Ferrari de Andrade, 2020).

Tumor cells can also produce different types of galectins (β-galactosidase-binding lectins) which contribute to carcinogenesis and cancer progression. Some studies have

demonstrated that galectin-1 (GAL1), GAL3, and GAL9 are associated with lung cancer initation, progression and poor survival (Chung et al., 2012, 2015; Kadowaki et al., 2012). One of the major functions of galectins is the regulation of the immune responses. GAL1/IL10 functional axis may be an important regulator in lung cancer-mediated immune suppression by mediating DC anergy (Kuo et al., 2011). GAL9 has also been showed to increase TIM3^{+} DCs, enhancing anticancer immunity through its interaction with TIM3 in MethA cell-bearing mice (Nagahara et al., 2008). GAL3 has a broad range of effects on T cell, NK, macrophages, neutrophils, etc. (Demotte et al., 2010; Stillman et al., 2006; Xue et al., 2013a). For instance, GAL3 can inhibit the cell function even induce apoptosis of T cells by binding to CD45 (Demetriou et al., 2001; Xue et al., 2013). Tumor cells can also produce Indoleamine 2,3-Dioxygenase 1 (IDO1), resulting in low levels of L-arginine and L-tryptophan in the TME, which are necessary for T cell proliferation and activity (Holmgaard et al., 2015). Some tumor cells also suppress immune cell functions through the expression of non-classical MHC class I molecules such as HLAE and HLAG (Contini et al., 2003). In addition, tumor cells secrete IL10 and TGFβ that inhibit immune cell functions through different mechanisms (Mirlekar, 2022).

5. TUMORSPHERES: A 3D MODEL TO STUDY TME

To study the TME, various 3D model systems have been suggested as innovative approaches, encompassing simple cell co-cultures within hydrogels to intricate multi-component microfluidic systems, each offering unique advantages and limitations (Figure 8). 3D models act as the perfect intermediary between basic 2D cultures and intricate *in vivo* systems. Common cancer models such as spheroids (also known as tumorspheres), have become essential tools for uncovering new biological knowledge and advance in therapeutics strategies, or complement complex time-consuming *in vivo* and clinical studies.

Tumorspheres represent one such 3D model, consisting in aggregations of cells with one or more cell types that can be cultured in suspension through spheres-forming assays. The initial use of sphere-forming assays was to culture cells from the adult brain (Reynolds & Weiss, 1992). These assays consist in growing cells under non-adherent conditions using serum-free medium with minimal growth requirements, employing

either fresh tumor tissue or commercial cell lines as a starting point. Cells directly extracted from surgical resection samples have been demonstrated to serve as superior models for tumor characterization when compared to cell lines. However, establishing primary cultures presents challenges and is time-consuming, primarily due to issues such as limited cell viability, extensive necrosis in some tumor specimens, and the proliferation of non-tumorigenic cell types in cultures. Consequently, most studies to date have been performed on commercial cell lines. Our group has established primary cultures using sphere-forming assays for CSC enrichment. These patient-derived tumorspheres showed self-renewal and unlimited exponential growth potentials, resistance against chemotherapeutic agents, invasion, and differentiation capacities *in vitro*, and superior tumorigenic potential *in vivo*. Moreover, lung tumorspheres exhibited increased expression of genes encoding for cytoprotective enzymes, pluripotency inducers, cell cycle regulators, metastasis-related genes, and components of Notch, and Wnt pathways (Herreros-Pomares et al., 2019).

	Description	Advantages	Disadvantages
Hydrogels	Crosslinked polymer structures sharing similarity to native matrix in which cell types can be embedded	Additional matrix proteins can be incorporated; Ability to tailor properties; High throughput	Batch to batch variation; Basic composition; Cell structures may not recapitulate physiology
Organotypic	Specialised hydrogel approach in which cancer cells are layered on top and submitted to a gradient	Compartmentalization of different cell types; Long term cellular crosstalk can be examined; Ability to introduce gradients	Time-consuming; Mostly restricted to end-point analysis
Spheroids	Cellular aggregated consisting of one or more cell types which can be cultured in suspension or embedded within a hydrogel	Establishment of hypoxia/nutrients gradients; Spatially distinct modelling of cancer-stromal crosstalk; Real time imaging possible	Dependent on cells' ability to form spheroids; Limited to short term culture
Organoids	Self-assembling multicellular structures which closely resemble organization of host tissue	Model innate heterogeneity; Can be embedded in hydrogels containing additional TME cells; Reproducible	High maintenance; Limited to specific cancer types
Explants	Isolated tissue segments, retaining physiological characteristics, capable of being cultured *ex vivo* as a functional unit	Native cell type interactions retained; Close recapitulation of tumour-TME interactions	Challenging to manipulate genetically; Access to tissue may be limited; Technically demanding
Microfluidis	Bespoke Bioengineered chips facilitating the study of compartmentalized cell types under fluid flow	Recapitulates circulation; Real time imaging possible; Flexibility in design of cellular compartments	Expensive manufacturing process; Highly specialised

Figure 8. Usual 3D approaches to modeling tumor microenvironment. Adapted from (Carter et al., 2021).

Comparing with traditional monolayer 2D cell cultures, 3D tumorspheres models provide an environment more closely resembles an actual tumor mass within the body. These models feature self-imposed nutrient gradients, enhanced immuno-modulatory capabilities, and hypoxic gradients, reflecting the fact that not all cancer cells are uniformly exposed to nutrients and oxygen (Fontana et al., 2021).

6. BIOMARKERS IN LUNG CANCER. ROLE OF LIQUID BIOPSY

6.1. THE STATUS IN EARLY STAGES

Despite extensive efforts to combat lung cancer, the 5-year survival rates remain below 17% (Hirsch et al., 2017). Early diagnosis and treatment of lung cancer significantly improves prognosis. Due to the absence of highly sensitive and specific screening techniques for early lung cancer detection, there is an urgent need for alternative, minimally invasive, or non-invasive biomarkers that can provide diagnostic and prognostic insights. Biomarkers have the potential to aid in risk assessment for asymptomatic individuals, as well as in nodule characterization and prognosis (Jantus-Lewintre et al., 2012).

Currently, lung cancer biopsy remains the preferred method for precise NSCLC diagnosis, although obtaining specimens can often be challenging. Nowadays studies have been focused on exploring new minimal invasive methodologies. Low-dose computed tomography (LDCT) screening is considered a standard method for early lung cancer detection. However, it is associated with a relatively high incidence of pulmonary nodules, radiation exposure, and a notable rate of false-positive diagnoses (Wait et al., 2022).

New liquid biopsy approaches, which represents a non-invasive method for testing tumor biomarkers in biological fluids, are emerging as promising techniques for diagnosis, prognosis, and predictive assessment in lung cancer patients across stages (Figure 9) (W. Li et al., 2022; Santarpia et al., 2018). It is possible to detect various types of tumor-derived material in a blood sample such as circulating tumor DNA (ctDNA),

circulating tumor RNA (ctRNA), circulating tumor cells (CTCs), extracellular vesicles (EVs), metabolites, proteins, tumor educated platelets (TEPs) (among other), which can be used as a source for biomarkers testing (Figure 10).
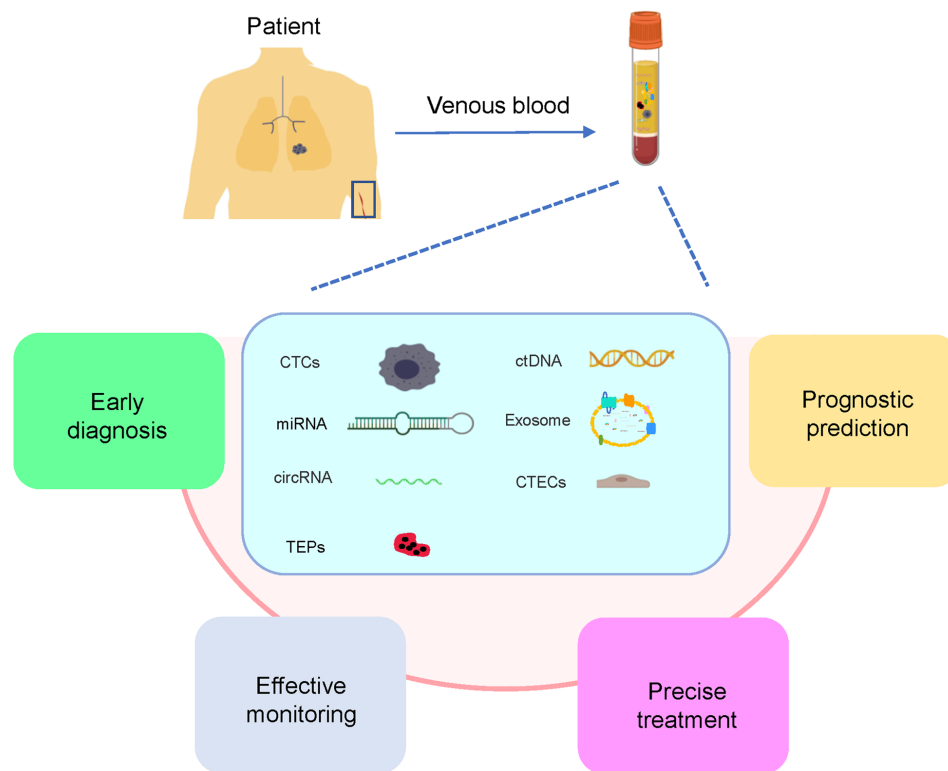
Figure 9. Clinical applications of liquid biopsy in early-stage NSCLC. CTCs, circulating tumor cells; miRNA, microRNAs; circRNA, circular RNAs; TEPs, tumor-educated blood platelets; ctDNA, circulating tumor DNA, CTECs, circulating tumor vascular endothelial cells. Reproduced from (W. Li et al., 2022).

Regarding prognostic biomarkers, some are being used in early lung cancer management. Accurate histopathological evaluation is crucial in NSCLC clinical management. Histology is a prognostic factor in early-stage NSCLC. Although studies are controversial, most of the results indicate that, except for stage 1, LUAD carries worse prognosis than LUSC (Bosch-Barrera et al., 2012; Hao et al., 2022; Yun et al., 2023). Further histopathological subtyping holds significant prognostic relevance (Kadota et al., 2014; Yoshizawa et al., 2011). Another prognostic factor widely studied in early-stage NSCLC is the immune cell infiltration of the TME (Hernández-Prieto et al., 2015; Usó et al., 2016, 2017). Several potential circulating biomarkers are currently under investigation. For instance, it has been reported that EpCAM/MUC1 mRNA-positive CTCs significantly decrease relapse-free survival (RFS) and OS in NSCLC patients (W. F. Zhu et al., 2014). Furthermore, high levels of CTCs from pulmonary veins have been associated with poor survival in early-stage NSCLC patients (Chemi et al., 2019). Regarding ctDNA,

few studies have been conducted to date, but it appears that high levels of ctDNA may be indicative of a worse prognosis (Abbosh et al., 2017). The potential of EVs to be a source of biomarkers for prognosis has also been proposed (Duréndez-Sáez et al., 2022). Overall, different markers have shown some degree of prognostic value in lung cancer, but their use in clinical practice is limited by the lack of reproducibility and independent validation.
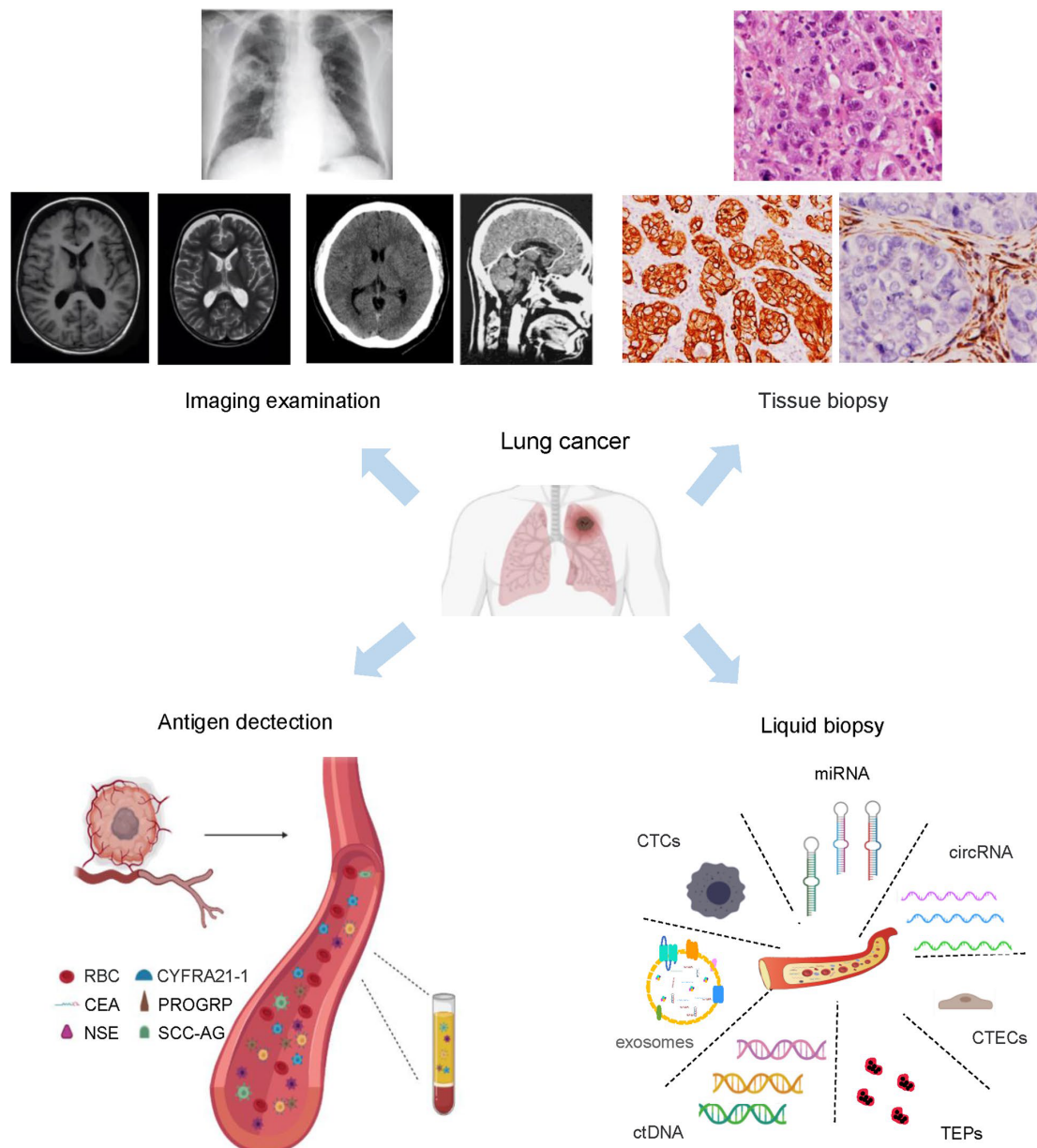
Figure 10. Pipilines for lung cancer clinical examination and diagnosis. Common imaging tests used for early examination and diagnosis of lung cancer include X-rays, magnetic resonance images, and low-dose spiral computed tomography. Methods for examining cancer tissue samples include hematoxylin and eosin staining, immunohistochemistry, and optical imaging techniques. Examination and diagnosis of peripheral blood with tumor antigens is routinely used in clinical examination. Liquid biopsy is becoming a promising approach for identifying high-risk patients' post-surgery and monitoring disease progression and treatment response over time. CTCs, circulating tumor cells; miRNA, microRNAs; circRNA, circular RNAs; TEPs, tumor-educated blood platelets; ctDNA, circulating tumor DNA, CTECs, circulating tumor vascular endothelial cells. Reproduced from (W. Li et al., 2022).

6.2. THE STATUS IN ADVANCED STAGES

Molecular biomarkers may provide important information on prognosis and allow the selection of patients for specific therapies in advanced-stages. Today, instead of non-selective chemotherapies, all patients with advanced NSCLC eligible for treatment require fast and comprehensive screening of biomarkers for first-line patient selection for targeted therapy, chemotherapy, or immunotherapy (with or without chemotherapy). To prevent unnecessary re-biopsies, the initial biomarker screening for first-line treatment should include markers that remain actionable for subsequent lines of treatment as well. Many molecular biomarkers are currently part of routine diagnosis for guiding the treatment with therapies targeting actionable mutations of patients with advanced NSCLC. Additionally, PDL1 and tumor mutational burden (TMB) can predict a favourable response to ICIs in advanced NSCLC. Although these last predictive biomarkers are clinically useful, many patients do not respond to ICIs. Accurately predicting the response to ICIs is essential for identifying patients who are likely to derive the greatest benefit from this costly treatment and for sparing those who won't benefit from ICIs from unnecessary side effects.

Thus, prioritizing the identification of patients who will benefit is crucial for treatment optimization. Nowadays, in NSCLC, the assessment of tumor PDL1 expression through immunohistochemistry (IHC) is regarded as the primary determinant approved by the FDA for responsiveness to ICIs. Currently, six FDA-approved monoclonal antibodies targeting the PD1/PDL1 interaction and linked to different PDL1 IHC expression testing are employed for the therapy of patients with NSCLC (Hendriks et al., 2023). There are many challenges regarding PDL1 as biomarker in NSCLC. PDL1 represents a flawed and ever-changing biomarker, with limitations stemming from both the testing methods and the inherent characteristics of the tumor (Mathew et al., 2017).

Two more FDA-approved companion diagnostic assays where successfully developed, microsatellite instability (MSI) and the last TMB, which are commonly employed for selecting patients who will benefit of ICIs treatment (Y. Wang et al., 2021). Firstly, MSI-high tumors exhibit strong immunogenicity, and this characteristic has been used as a predictive indicator for ICIs response. Clinical trials have consistently shown a

notably favorable response rate (RR) in various MSI-high cases, leading to the FDA's first agnostic therapeutic approval for patients with unresectable or metastatic MSI-High solid tumors, regardless of tumor location (Le et al., 2017; Overman et al., 2017). However, this condition is not frequent in lung cancer, accounting for less than 1% of cases (Warth et al., 2016). Secondly, TMB could be another predictor of ICIs efficacy. TMB is defined as the cumulative count of non-synonymous somatic mutations within the genomics coding region. These mutations have the potential to generate neoantigens and enhance the tumor's immunogenicity. TMB assessment can be conducted through various methods, each with different threshold, and can be performed using either tumor tissue (tTMB) or blood samples (bTMB). Both data regarding their predictive value can be contradictory. FDA granted approval to pembrolizumab for treating adult and pediatric patients with unresectable or metastatic solid tumors characterized by a high TMB (TMB-H; ≥10 mutations/megabase or mut/Mb) (Marcus et al., 2021). Data published after FDA approval raised concerns regarding specific aspects of the approval process, particularly concerning the approved disease types and the chosen cut-off point (McGrail et al., 2021). Despite the presence of uncertainties, the accelerated approval for pembrolizumab, will provide a treatment alternative for patients afflicted with rare TMB-H cancers.

Overall, all these current companion diagnostic assays require testing on tissue biopsy. Hence, considering the constraints of all these tumor biomarkers in predicting ICIs response, there is an urgent requirement for the improved the use of FDA-approved biomarkers and the discovery of more effective predictive biomarkers. In this regard, liquid biopsy offers many advantages over tissue biopsy. First, blood sample collection is non-invasive, more cost-effective, and easily accessible than a tissue biopsy. Second, blood collection allows multiple samplings, facilitating the continuous and real-time monitoring of ICIs response and resistance during treatment, whereas tissue biopsy is typically a one-time procedure performed before treatment. Finally, liquid biopsy has the potential to address the spatial and temporal heterogeneity often linked to tissue biopsy (Goh et al., 2023). Below are the different types of circulating biomarkers.

6.2.1. CIRCULATING BIOMARKERS

Circulating biomarkers in peripheral blood are currently the subject of extensive research. Peripheral blood contains various components, such as white blood cells, platelets, proteins, nucleid acids, and vesicles, which could potentially contribute to predict response to therapy, monitoring treatmet, detect mechanisms of resistance and for prognostic assessment (Figure 11).
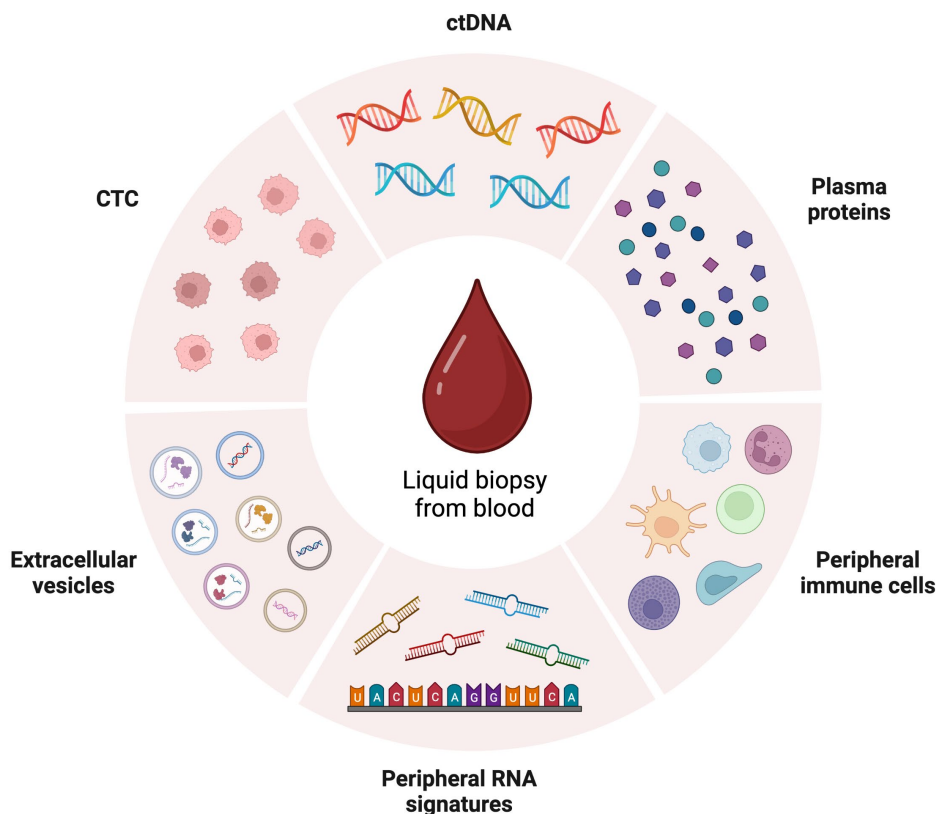
Figure 11. Multiple circulating biomarkers in the peripheral blood that are used in liquid biopsy. CTC, circulating tumor cell; ctDNA, circulating tumor DNA. Reproduced from (Goh et al., 2023)

- **Circulating tumor DNA (ctDNA)**

Among all the circulating biomarkers used to predict ICIs response, ctDNA is the most thoroughly investigated, particularly for analysis of tumor genetic alterations and more complex biomarkers like blood TMB. Many studies revealed that levels of ctDNA correlates with ICIs treatment response and resistance in NSCLC patients (Cabel et al., 2017; Goh et al., 2023; Goldberg et al., 2018; H. Wang et al., 2021; Weber et al., 2021). Moreover, in patients with insufficient tissue biopsy, ctDNA is used to analyze tumor-

specific molecular alterations such as somatic mutations and DNA methylation patterns (Cho et al., 2020; Duruisseaux et al., 2018; Pavan et al., 2021; H. Zhu et al., 2021).

- **Circulating Tumor Cells (CTCs)**

CTCs also contain valuable genetic, transcriptomic, and proteomic data that can assist in diagnosis, treatment, and prognosis. The correlation between the quantity of CTCs and the response to ICIs therapy has been investigated. A high count of CTCs before starting ICIs treatment was linked to a worse prognosis and an increased likelihood of disease progression in advanced-stage NSCLC (Guibert et al., 2018; Papadaki et al., 2020). Moreover, relationship between PDL1 expression on CTCs and response to ICIs therapy has also been explored (Guibert et al., 2018; Nicolazzo et al., 2016).

- **Peripheral immune cells**

The peripheral immune cells have also been a subject of study in the recent years. $CD8^+$ T and CD4+ T cells, T_{REGS} and the neutrophils-to-lymphocytes ratio (NLR) affect prognosis and ICIs response in advanced NSCLC (P. Li et al., 2021; Ottonello et al., 2020; Petrova et al., 2020). Moreover, our laboratory revealed that the analysis of circulating TCR-β repertoire may provide information about the immune response in anti-PD-1 treated NSCLC patients (Dong et al., 2021)

- **Extracellular vesicles (EVs)**

In terms of EVs, the studies have been focusing on exosomal PDL1 and miRNAs. Most available data shown that decrease in exosomal PDL1 protein expression has been associated with better response and prognosis (J. Chen et al., 2021; de Miguel-Perez et al., 2022; Shimada et al., 2021; Y. Wang et al., 2022).

- **Plasma cytokines**

Plasma cytokines and chemokines are soluble proteins found in bloodstream, produced by both immune cells (such as monocytes, macrophages, neutrophils, and lymphocytes) and non-immune cells (including endothelial cells, epidermal cells, and fibroblasts). These soluble molecules attach to their specific receptors on the surface membrane of target cells, initiating intracellular signaling and regulating the growth and

activity of these cells (Ramachandran et al., 2021; M. Wang et al., 2021). The relationship between many of these soluble molecules, particularly proinflammatory cytokines, have been explored in the recent years. Different studies agree that lower levels of cytokines such as IL6 or IL8 correlate with improved survival and a better response to immunotherapy in advanced-stage NSCLC patients (D. H. Kang et al., 2020; Keegan et al., 2020; Sanmamed et al., 2017; Schalper et al., 2020). Apart from these interleukins, other protein levels found in plasma have been related to ICIs response in NSCLC such as soluble PDL1 (sPDL1), soluble PDL2 (sPDL2), soluble Granzyme B (sGranzyme B) and soluble IFNγ (sIFNγ) (Costantini et al., 2018; D. Liu et al., 2017; Okuma et al., 2017; J. Zhao et al., 2017).

Despite the numerous studies focusing on the search for new circulating biomarkers, only ctDNA have reached clinical practice. Therefore, we must continue looking for robust biomarkers that can predict how a patient will fare in advanced stages and how they will respond to therapy.

II. OBJECTIVES

NSCLC remains one of the most lethal solid tumors worldwide. The immune evasion mechanisms promoted by the tumor are among the reasons explaining the high mortality rates in this type of tumor.

We hypothesize that cancer cells in NSCLC are poorly recognized targets by the immune surveillance system, promoting an immunosuppressive environment crucial during tumorigenesis. Consequently, the aim of this thesis work is to delve into the study of the interplay between lung tumor cells and their immune microenvironment, translating the findings into the search for biomarkers that can help improve prognosis.

The specific goals of this thesis are as follows:

Exploratory phase:

1. To analyze the gene expression of immune-mediators on adherent cultures and tumorspheres from lung cancer cell lines and patient derived lung cancer cells (PDLCC) cultures.

2. To investigate the presence of soluble immune-mediators in supernatants from adherent cultures and tumorspheres from lung cancer cell lines and PDLCC cultures.

3. To characterize the expression of selected immune-mediators that could have a strong impact on TME.

4. To study the influence of soluble immune-mediators produced by tumorspheres and co-cultures with CAFs on immune cells (macrophages and T_{REGS}).

Translational phase:

5. To translate the findings from the exploratory phase to the analysis of blood-based immune-mediator biomarkers in NSCLC patients

    5.A. In a cohort of surgically resected NSCLC patients (test cohort) validating the results obtained in an independent *in-silico* cohort from TCGA (validation cohort).

    5.B. In a cohort of advanced-stage NSCLC patients treated with ICI in the first-line (advanced-stage NSCLC cohort).

6. To integrate all the exploratory and translational results evaluating the contribution of immune-mediators as potential biomarkers in NSCLC.

III. MATERIALS & METHODS

1. STUDY DESIGN

This study comprises two different phases which are summary in Figure 12.
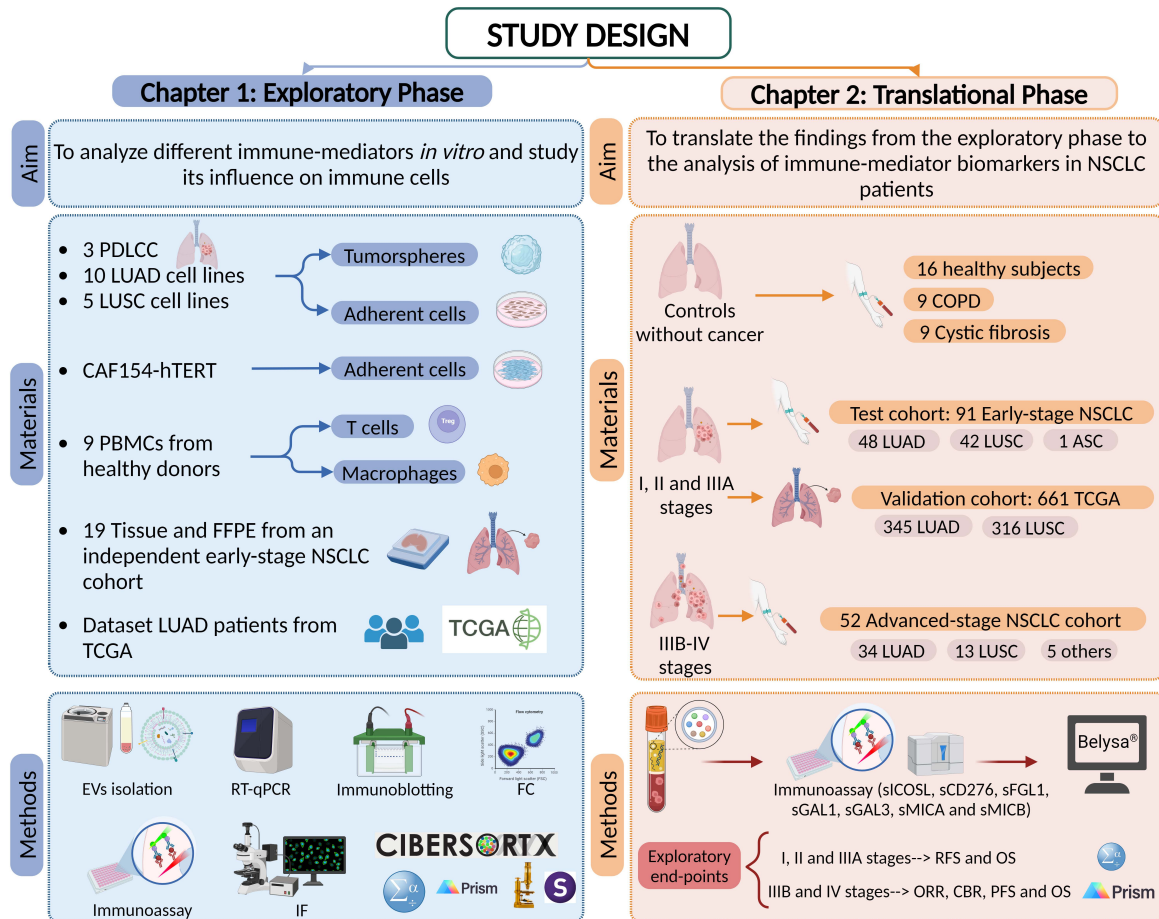
Figure 12. Study design of exploratory phase (Chapter I) and translational phase (Chapter II). In the **exploratory phase,** 3 patient derived lung cancer cell (PDLCC) cultures, 10 lung adenocarcinoma (LUAD) cell lines, 5 squamous cell carcinoma (LUSC) cell lines, 1 cancer-associated fibroblast cell line (CAF154-hTERT), 9 peripheral blood mononuclear cells (PBMCs), 19 tissue and formalin-fixed paraffin-embedded (FFPE) from an independent chort from early-stage NSCLC cohort and a data set of LUAD patients from The Cancer Genome Atlas (TCGA) were used. Methods used were ultracentrifugation for extracellular vesicles (EVs) isolation, real time quantitative polymerase chain reaction (RT-qPCR), immunoblotting, flow cytometry (FC), immunoassay, Immunofluorescence (IF) and statistical and images softwares such as CIBERSORTx tool, Statistical Package for the Social Sciences v.23 (SPSS), SIMCA-P software and GraphPad Prism. In the **translational phase**, 32 controls without cancer (16 healthy subjects, 9 with chronic obstructive pulmonary disease (COPD), and 9 with cystic fibrosis), 91 early-stage NSCLC test cohort (48 LUAD, 42 LUSC and 1 adenosquamous cancinoma (ASC)), a validation cohort of 661 patients from TCGA and 52 advanced-stage NSCLC cohort (34 LUAD, 13 LUSC and 5 with others histologies) were used. Methods used were immunoassay and statistical softwares such as Belysa, SPSS v.23 and GraphPad Prism. PDLCC, patient derived lung cancer cell; LUAD, lung adenocarcinoma; LUSC, lung squamous cell carcinoma; PBMCs, peripheral blood mononuclear cells; FFPE, formalin-fixed paraffin-embedded; TCGA, The Cancer Genome Atlas; RT-qPCR, real time quantitative polymerase chain reaction; FC, flow cytometry; IF, immunofluorescence; RFS, relapse-free survival; OS, overall survival; ORR, objective response rate; CBR,clinical benefit rate; PFS, progression-free survival; sICOSL, soluble inducible T Cell costimulatory ligand; sCD276, soluble cluster of diferentation 276; sFGL1, soluble fibrinogen-like protein 1; sGAL1, soluble Galectin-1; sGAL3, soluble Galectin-3; sMICA, soluble major histocompatibility complex class I polypeptide-related seq A; sMICB, soluble major histocompatibility complex class I polypeptide-related seq B. Own design created with BioRender.com.

2. MATERIALS

2.1. COHORTS AND SAMPLES INCLUDED IN THE STUDY

2.1.1. CONTROL GROUP

The control group comprised 34 anonymous controls without cancer, including 16 healthy subjects, 9 with chronic obstructive pulmonary disease (COPD) and 9 with cystic fibrosis, who were matched for age and gender. Control samples were collected at the same time points as the patient samples at the *Consorcio Hospital General Universitario de Valencia* (*CHGUV*).

2.1.2. BLOOD FROM EARLY-STAGE NON-SMALL CELL LUNG CARCINOMA TEST COHORT

The translational phase included an initial cohort of 91 early-stage NSCLC patients from *CHGUV*. This cohort comprised 48 patients with LUAD, 42 patients with LUSC and 1 patient with adenosquamous (ASC) histology collected from July 2004 to September 2019. A pathological report was accessible for all the samples, allowing their characterization. The selection of these patients was based on specific eligibility criteria: eligibility for surgical resection, no prior treatment, age 18 years or older, not pregnant, and confirmed diagnosis of NSCLC in stages I to IIIA (according to the American Joint Committee on Cancer staging manual). In all cases, peripheral blood samples were obtained through venipuncture by a qualified professional before surgery. These peripheral blood samples were collected in 2 tubes of 10mL with the anticoagulant ethylene diamine tetra-acetic acid (EDTA) (BD Vacuitaner®) and plasma was isolated by centrifugation (1600 g, 10 minutes, 4°C) and then stored at -80°C until analysis. For this study, plasma samples were mixed by vortexing before the immunoassay experiment. The study was conducted in accordance with the Declaration of Helsinki and the institutional ethical review board approved the protocol (see on Appendices). All individuals signed an informed consent for sample acquisition for research purposes before the beginning of this study.

2.1.3. VALIDATION COHORT FROM TCGA

A validation cohort from The Cancer Genome Atlas (TCGA) was also included in this study. This cohort consisted of 661 patients with histological diagnosis of LUAD or LUSC. Patients with post-surgical complications were excluded from analyses, and only those patients who had at least 1 month of follow-up were considered for inclusion.

2.1.4. TISSUE FROM EARLY-STAGE NON-SMALL CELL LUNG CARCINOMA PATIENTS

An independent cohort of cryopreserved tumor tissue samples from 19 patients were used in the exploratory phase. The selection of these patients was based on the same specific eligibility criteria than in the test cohort. These tissue samples were preserved in RNALater® (Applied Biosystems) to prevent RNA degradation and were fresh-frozen at -80°C until further analysis. Data of expression of *FOXP3*, *CD4*, and *CD8* in both tumor and stromal areas from formalin-fixed paraffin-embedded (FFPE) (via IHC and Real Time Quantitative Polymerase Chain Reaction (RT-qPCR)) from these patients were collected from Usó M et al (Usó et al., 2016).

2.1.5. BLOOD FROM ADVANCED-STAGE NSCLC COHORT

Advanced cohort included 52 patients treated with first-line pembrolizumab in monotherapy (200 mg every 21 days) (collected from February 2018 to July 2021) and fitted the following eligibility criteria: candidate for pembrolizumab treatment, non-pretreated, over 18 years, non-pregnant, irresectable stage IIIA-IV (according to the American Joint Committee on Cancer staging manual) and with a histological diagnosis of NSCLC. All cases were individuals with histologically confirmed NSCLC and those with autoimmune disease or acquired immunodeficiency syndrome (AIDs) were excluded from the present study. According to guidelines, all patients treated with pembrolizumab in monotherapy exhibited PDL1 expression ≥50% (assessed by tumor proportion scores, defined as the number of positive tumor cells divided by the total number of viable tumor cells multiplied by 100%) in their tumor samples. A total of 34 plasma samples were collected at baseline (PRE) before the initial pembrolizumab administration, and 25 plasma samples were collected at the first response assessment (FR) for the advanced

LUAD cohort. For the advanced LUSC cohort, 13 samples were collected at PRE before the first pembrolizumab administration and at FR. For other histologies, 5 samples were collected at PRE before the first pembrolizumab administration and at FR. All patients were followed up until May 2023. These peripheral blood samples were collected in 2 tubes of 10mL with the anticoagulant EDTA (BD Vacuitaner®) and plasma was isolated by centrifugation (1600 g, 10 minutes, 4°C) and then stored at -80°C until analysis. For this study, plasma samples were mixed by vortexing before the immunoassay experiment. The study was conducted in accordance with the Declaration of Helsinki and the institutional ethical review board approved the protocol (see on Appendices). All patients signed an informed consent for sample acquisition for research purposes before the beginning of this study.

2.1.6. EXPLORATORY ENDPOINTS AND PATIENTS EVALUATION

Clinical and follow-up information for patients was extracted from their medical records. For early-stage NSCLC test cohort, exploratory endpoints included were RFS and OS. RFS and OS were defined as the time from diagnosis to the occurrence of the endpoint (objective disease relapse and death, respectively) or the last follow-up.

For the advanced-stage NSCLC cohort, the relationship between plasma levels of biomarkers and tumor response and survival was to be explored. To this end, tumor response was evaluated every 21 days using the Response Evaluation Criteria in Solid Tumors version 1.1 (RECIST 1.1). The objective response rate (ORR) was evaluated and defined as the proportion of patients achieving complete (CR) or partial response (PR), stable disease (SD), or progressive disease (PD). Durable clinical benefit (DCB) (i.e., CR, PR, or SD, lasting 6 months or more after initiation of pembrolizumab treatment) and non-DCB (PD within 6 months after treatment start) were also analyzed. Clinical Benefit Rate (CBR) was also evaluated and defined as the proportion of patients who achieved CR, PR or SD for 6 months or more. PFS was described as the interval from the beginning of pembrolizumab treatment to the objective disease progression or last follow-up. OS was defined as the interval from the beginning of pembrolizumab treatment to death or last follow-up.

2.2. *IN VITRO* CELL CULTURES

2.2.1. PATIENT DERIVED LUNG CANCER CELL CULTURES

Following the tumor dissociation protocol previously described by our group, surgical tumor specimens from patients were established as both monolayers and tumorspheres (Herreros-Pomares et al., 2019). Notably, in this protocol, we introduced the use of the Rho-kinase inhibitor (ROCKi) (Tocris Bioscience), which has enabled the establishment of long-term primary cultures. For this study, we established and employed three long-term patient derived lung cancer cell (PDLCC) cultures (PC301, PC435, and PC471). Tumor profiling of each PDLCC cultures was determined by next-generation sequencing (NGS) using Oncomine Comprehensive Assay (Thermo Fisher Scientific) and Ion Gene Studio S5 System (Thermo Fisher Scientific) to obtain a complete tumor profiling of each patient. Detailed clinicopathological information for each of the PDLCC cultures included in this part of the study is summarized in Table 3. Fresh PDLCC cultures were cultured in Advanced DMEM/F12 (Gibco) medium supplemented with 10% fetal bovine serum (FBS) (Gibco), 200 µg/mL penicillin-streptomycin (P/S) (Gibco) and 2 mM of L-glutamine (L-glu) (Gibco). Spheres-forming assays were employed for obtaining tumorspheres enriched in CSCs. To obtain tumorspheres, monolayer cells were trypsinized using 0.05% trypsin-EDTA when they reached 80% confluence. Trypsinized cells were seeded at low density in ultra-low attachment plates with serum-free Advanced DMEM/F12 medium supplemented with 0.4% bovine serum albumin (BSA) (Sigma-Aldrich), 50 µg/ mL Epidermal Growth Factor (EGF) (Gibco), 20 µg/mL basic Fibroblast Growth Factor (bFGF) (Gibco), Insulin-Transferrin-Selenium (ITS) PREMIX (Gibco), 100 µg/mL P/S (Gibco) and 2% B27 (Gibco) and 2 mM of L-glu (Gibco). Cultures were expanded through enzymatic dissociation, followed by re-plating of both individual cells and any remaining small aggregates into fresh complete medium, which was refreshed twice a week. The following experiments took place after 5 days when the cells started to grow and form floating aggregates. In all cases, cells were maintained at 37°C within 5% CO_2 atmospheres.

Table 3. Clinicopathological characteristics of long-term patient derived lung cancer cell cultures included in this study.

Patient Code (PC)	Gender	Age	TNM Stage	Histology	Smoking Status	Progression /Exitus	RFS	Mutational Status
435	Male	73	IIB	LUAD	Former	No	24	KRAS p.G12C PIK3CA p.H1047R
471	Female	85	IIA	LUAD	Never	No	27	PIK3CA p.D538N
301	Male	71	IIB	LUSC	Former	No	75.50	PIK3CA p.G118D TP53 p.S261V*fs84

LUAD, lung adenocarcinoma; LUSC, lung squamous cell carcinoma; RFS, Relapse-free survival; PC, patients code; TNM, tumor-node-metastasis.

2.2.2. CELL LINES

Fifteen human NSCLC cell lines, LUAD cell lines (A549, NCI-H1395, NCI-H1650, NCI-H1975, NCI-H1993, NCI-H2228, NCI-H23, NCI-H358, HCC827, PC9) and LUSC cell lines (SW900, LUDLU-1, NCI-H520, NCI-H1703 and SK-MES-1) were used for *in vitro* experiments. LUAD cell lines were obtained from the American Type Culture Collection (ATCC), while LUSC cell lines were kindly provided by Dr. J. Carretero (University of Valencia, Spain), except for SW900, which was purchased from ATCC. The main characteristics of these lung cancer cell lines are detailed in Table 4. Cells lines were cultured in RPMI-1640 medium (Gibco), which was enriched with 10% FBS, 200µg/mL of P/S, and 0.001% non-essential amino acids. To generate tumorspheres, when the monolayer cells reached 80% of confluence, they were disaggregated using 0.05% trypsin-EDTA. These trypsinized cells were then seeded in ultra-low attachment plates, with serum free RPMI-1640 medium supplemented with 0.4% BSA, 50 µg/mL EGF, 20 µg/mL bFGF, 5 µg/mL ITS PREMIX, 2% B-27, 200 µg/mL P/S, and 0.001% non-essential amino acids at a low seeding density. Subsequently, cultures were expanded through enzymatic dissociation of tumorspheres, followed by the re-plating of both individual cells and any remaining small aggregates. This process was carried out in fresh complete medium, which was replaced twice a week. The immortalized patient-derived fibroblast cell line, CAF154-hTERT, originates from cancer-associated primary fibroblasts and was kindly provided by Dr. Luca Roz (*Istituto Nazionale dei Tumori*, Italy). The generation and the characteristics of this cell line have been previously described by the authors (Andriani et al., 2018). CAF154-hTERT cells were grown in Fibroblast Basal Medium (FBM) supplemented with the Fibroblast Growth Kit-Low serum (ATCC). All cells were maintained at 37°C in humidified atmosphere containing 5% CO_2.

Table 4. Clinicopathological characteristics of the commercial cell lines included in the study.

Patient Code (PC)	Gender	Age	Smoking Status	Histology	Mutational Status
A549	Male	58	NS	LUAD	*KRAS* p.G12S, *KEAP* p.G333C
NCI-H1395	Female	55	Current	LUAD	*BRAF* p.G469A
NCI-H1650	Male	27	Current	LUAD	*EGFR* p.E746_A750del
NCI-H1975	Female	NS	Never	LUAD	*EGFR* p.L858R+ p.T790M, *PIK3CA* p.G118D, *TP53* p.R273H
NCI-H1993	Female	47	Current	LUAD	*c-MET* amplification
NCI-H2228	Female	NS	Never	LUAD	*EML4-ALK* fusion, *TP53* p.Q331*, *RB1* p.E204fs*10
NCI-H23	Male	51	NS	LUAD	*KRAS* G12C; *TP53* M246I; *KEAP* p.Q193H
NCI-H358	Male	NS	NS	LUAD	*KRAS* p.G12C
HCC-827	Female	39	NS	LUAD	*EGFR* p. E746_A750del, *TP53* p.V218del
PC9	Male	NS	NS	LUAD	*EGFR* p.E746_A750del, *TP53* p.R248Q
SW900	Male	53	NS	LUSC	*KRAS* p.G12V, *TP53* p.Q167*
LUDLU-1	Male	72	NS	LUSC	*TP53* p.R248W
NCI-H520	Male	NS	NS	LUSC	*TP53* p.W146*
NCI-H1703	Male	54	NS	LUSC	-
SK-MES-1	Male	65	NS	LUSC	*TP53* p.E298*

LUAD, lung adenocarcinoma; LUSC, lung squamous cell carcinoma; NS; not specified; PC, patient code.

All cell cultures (both primary and commercial) underwent Mycoplasma testing prior to all experiments. Moreover, the authenticity of all human cell cultures was confirmed through short tandem repeat analysis (STR) using the AmpFLSTR™ Identifiler™ Plus PCR Amplification Kit (Thermo Fisher Scientific).

3. METHODS

3.1. ISOLATION OF EXTRACELULLAR VESICLES FROM CELL CULTURES

To isolated EVs derived from tumor cultures, cells were grown in T175 cm² flasks until they reached 70–80% confluence over a 72-hour period in 30 mL of media depleted of FBS (in the case of tumorspheres cultures). Following the 72-hour incubation, cellular debris was removed through differential centrifugation, first at 500 g for 5 minutes, and subsequently at 3000 g for 15 minutes. The resulting supernatant was then passed through a 0.2 μm filter (Corning) and ultra centrifuged at 110,000× g for 90 minutes using a CP-NX, P50AT2 Rotor (Hitachi). A second ultra-centrifugation step was performed, and the EVs were ultimately resuspended in 30 mL of phosphate-buffered saline (PBS) (Corning). All centrifugation steps were executed at 4 °C. Finally, the EVs were concentrated in a small volume (30–60 μL) of filtered PBS and stored at −80 °C until the analysis.

3.2. PBMCS CULTURE

Peripheral Blood Mononuclear Cells (PBMCs) from 9 healthy volunteers were plated at 1×10^6 cells/well in well plates and incubated at 37°C for 4 hours. After the incubation, non-adherent cells (T cells) were isolated and used for the experiments. Concurrently, adherent cells (monocytes) were subjected to a 7-day differentiation process into macrophages using 50 ng/mL of human macrophage colony-stimulating factor (M-CSF) (Thermo Fisher Scientific).

3.3. CO-CULTURES CONDITIONS

For co-cultures, 3×10^5 CAF154-hTERT were cultured for 2 hours with the proper medium in 6-well plates. After 2 hours, 1×10^5 tumorspheres from PC435 were cultured together with CAF154-hTERT in 50% of FBM and 50% SPH DMEM-F12 (tumorspheres medium) for 48 hours. Conditioned media (CM) from various conditions (PC435 tumorspheres or co-culture of PC435 tumorspheres + CAF154-hTERT) were collected. CM (treated or not with GAL3 monoclonal antibody (clone BC10)(100 ng·mL−1) (Thermo Fisher Scientific)) will be employed in the subsequent experiment to test the effect on the macrophage polarization and T_{REGS}.

3.4. NUCLEIC ACID ANALYSIS

Genomic DNA was extracted from cell cultures to assess the most common mutations in lung cancer patients. Furthermore, RNA was also extracted to perform gene expression analyses.

3.4.1. RNA AND DNA ISOLATION

The extraction of total RNA from cell pellets and frozen tissue samples was performed using standard TRIZol® LS Reagent (Ambion, life technologies) according to manufactures' instructions. EVs total RNA derived from cell cultures were isolated using the Total RNA Purification Kit (Norgen Biotek) following the manufactures' instructions. For tumor samples, a tissue sample of 10-15 mg was carefully dissected and 1 mL of TRIZol® LS Reagent (Ambion, life technologies) was added. The samples were then homogenized using a TissueLyser (Qiagen), and 200 µL of chloroform was incorporated to facilitate the separation of the aqueous phase, which contains the RNA. Subsequently,

isopropanol was employed to precipitate the nucleic acids, and ethanol was used for the purification steps. The total RNA was resuspended in nuclease-free water and preserved at -80°C until subsequent analysis. In the case of cell cultures, when tumor cells reached 80% of confluence, they were detached using 0.05% trypsin-EDTA and subsequently centrifuged. For monolayer cells, the centrifugation was performed at 290 g for 5 minutes, while for tumorspheres, it was conducted at 200 g for the same duration. The resulting cell pellets underwent two washes with PBS, following the same protocol as that employed for RNA extraction from fresh-frozen tissue specimens. In this case, the DNA interphase was carefully collected in absolute ethanol and washed, first with 10% ethanol/0.1 M sodium citrate buffer, and then with 75% ethanol. The resulting DNA was then dissolved in nuclease-free water and stored at -80°C until further analysis.

The quantity and quality of RNA and DNA were evaluated using a nano spectrophotometer, Nano Drop 2000C (Thermo Fisher Scientific).

3.4.2. DETERMINATION OF THE MUTATIONAL STATUS

The Oncomine™ Comprehensive Assay Plus (OCA-Plus) was used to analyze the mutational status of primary-derived cultures. OCA-Plus allows the detection of hundreds of variants, including target hotspots SNVs, indels, CNVs and gene fusion across more than 500 genes that are relevant in solid tumors. Briefly, libraries were prepared from 20 ng RNA on the Ion Chef™ Instrument. Four samples and one negative control were multiplexed on the Ion 550™ Chip and sequenced on the Ion Gene Studio™ S5 systems, using the workflow described in the user guide. The raw sequencing data were analyzed using the Ion Reporter Oncomine Comprehensive Plus - w3.0 workflow (all from Thermo Fisher Scientific).

3.4.3. QUANTIFICATION OF GENE EXPRESSION

3.4.3.1. REVERSE TRANSCRIPTION

Reverse transcription (RT) was carried out to convert RNA into complementary DNA (cDNA), which was necessary for subsequent analyses. This conversion was achieved using random hexanucleotides and a High-Capacity cDNA Reverse Transcription Kit (Applied Biosystems) according to the manufacturer's instructions. Each reaction

included the following components: 2 μL of RT buffer, 0.8 μL of dNTP mix, 2 μL of RT random primers, 1 μL of MultiScribe™ Reverse Transcriptase, 1 μL of RNase inhibitor, and a variable volume of RNA, depending on the sample concentration (1.0 μg of total RNA for frozen tissue, 0.5 μg of total RNA for cells samples and macrophages and 0.150 μg of total RNA for EVs samples). The total reaction volume was adjusted to 20 μL with nuclease-free water. The reactions were conducted in a Veriti™ 96-Well Thermal Cycler (Applied Biosystem) under the conditions described in Table 5, and the resultant cDNA was preserved at -80°C.

Table 5. Cycling program for reverse transcription reaction.

Phase	Time	Temperature
1	10 minutes	25°C
2	2 hours	37°C
3	5 seconds	85°C

3.4.3.2. QUANTITATIVE REAL TIME PCR

The resulting cDNA, used for target gene quantification, was employed in RT-qPCR reactions conducted with assays based on hydrolysis probes containing a reporter dye linked to the 5' end of the probe, known as TaqMan® probes (Applied Biosystems). A total of 28 genes were analyzed in this study, selected based on their relevance in the TME, along with an additional 8 genes chosen for their importance in macrophage polarization. The selection of these genes was made following a PubMed database search. Gene expression levels were evaluated using TaqMan® Gene Expression Assays and the specific assays employed are listed in Table 6. Various gene controls (Table 7) were examined in cell-cultures, EVs, macrophages, and fresh-frozen specimens to determine the most suitable internal control for each specific scenario, utilizing the GeNorm software. GeNorm software performs an automated calculation of the gene-stability measurement 'M' for all control genes and facilitates the removal of the least stable housekeeping genes (Vandesompele et al., 2002). Actin beta (*ACTB*), beta-glucuronidase (*GUSB*), and cyclin dependent kinase Inhibitor 1B (*CDKN1B*) were selected as endogenous controls for cells and frozen tissue, whereas *ACTB* and glyceraldehyde-3-phosphate dehydrogenase (*GAPDH)* were selected as endogenous controls for EVs

samples, and beta-2-microglobulin (*B2M)* was selected as endogenous control for macrophages.

Table 6. Genes analyzed in this study, their description, and TaqMan® assays used for RT-qPCR.

Gene	Description	Assay	Amplicon lenght
Immunoregulatory genes			
CD276	Cluster of Differentiation 276	Hs00987207_m1	65
CD200	Cluster of Differentiation 200	Hs01033303_m1	64
CD40LG	Cluster of Differentiation 40 Ligand	Hs00163934_m1	81
CD137L	TNF Superfamily Member 9	Hs00169409_m1	72
HLAG	Major Histocompatibility Complex Class I Antigen G	Hs03045108_m1	109
HLAE	Major Histocompatibility Complex Class I Antigen E	Hs03045171_m1	130
HLAF	Major Histocompatibility Complex Class I Antigen F	Hs01587840_m1	107
ICOSL	Inducible T Cell Costimulatory Ligand	Hs00323621_m1	59
IL4	Interleukin 4	Hs00174122_m1	70
IL10	Interleukin 10	Hs00961622_m1	74
IL6	Interleukin 6	Hs00985639_m1	66
IL8	Interleukin 8	Hs99999034_m1	81
IL12A	Interleukin 12A	Hs01073447_m1	52
IL12B	Interleukin 12B	Hs01057148_m1	64
IL17A	Interleukin 17A	Hs00174383_m1	80
IL13	Interleukin 13	Hs99999038_m1	68
IDO1	Indoleamine 2,3-Dioxygenase 1	Hs00984148_m1	66
INFγ	Interferon Gamma	Hs00989291_m1	73
LGALS3	Galectin 3	Hs00173587_m1	64
LGALS3BP	Galectin 3 Binding Protein	Hs00174774_m1	57
LGALS9	Galectin 9	Hs00371321_m1	82
MICA	Major Histocompatibility Complex Class I Polypeptide-Related Seq A	Hs00741286_m1	75
MICB	Major Histocompatibility Complex Class I Polypeptide-Related Seq B	Hs00792952_m1	138
OX40L	TNF Receptor Superfamily Member 4	Hs00182411_m1	72
PDL1	Programmed Cell Death 1 Ligand 1	Hs01125301_m1	89
PDL2	Programmed Cell Death 1 Ligand 2	Hs01057777_m1	61
STAT3	Signal Transducer and Activator of Transcription 3	Hs01047580_m1	87
TGFβ	Transforming Growth Factor Beta	Hs00998133_m1	57
Genes related to macrophages polarization			
IL6	Interleukin 6	Hs00985639_m1	66
CD206	Mannose receptor, C type 1	Hs00267207_m1	82
CD163	CD163 molecule	Hs00174705_m1	72
IL10	Interleukin 10	Hs00961622_m1	74
VEGFA	Vascular endothelial growth factor A	Hs00900055_m1	59
IL12A	Interleukin 12A	Hs01073447_m1	52
NOS2	Nitric oxide synthase 2	Hs00167248_m1	74
ARG2	Arginase 2	Hs00163660_m1	86

Table 7. Endogenous gene TaqMan® assays used for the normalization of the results.

Gene	Description	Assay	Amplicon length
ACTB	ATP-binding cassette, sub-family G	Hs 99999903_m1	171
GUSB	Glucuronidase, beta	Hs 01558067_m1	71
CDKN1A	Cyclin-dependent kinase inhibitor	Hs 00153277_m1	71
GAPDH	Glyceraldehyde-3-phosphate dehydrogenase	Hs 99999905_m1	122
B2M	beta-2-microglobulin	Hs 00187842_m1	64

Each reaction was performed in duplicates in 384-well plates with a final volume of 5 µl including: 1 µL of cDNA, 2,5 µL of TaqMan Gene Expression Master Mix (Applied Biosystems), and a 0.25 µL TaqMan Gene Expression Assay (Applied Biosystems). In every run, non-template controls (NTCs) were incorporated, along with a commercially available reference cDNA (Clontech) serving as the positive reference control. The reactions were carried out using a Light Cycler 480 thermocycler system (Applied Biosystems), adhering to the cycling conditions outlined in Table 8.

The efficiency of each TaqMan® assay was evaluated through a series of dilutions (50 ng/µl, 5 ng/µl, 0.5 ng/µl, 0.05 ng/µl, and 0.005 ng/µl) using the cDNA as a template. Efficiency was calculated by using the following equation: $E = 10^{-1/slope}$ and the results indicated that almost all the assays used were adequately efficient (Supplementary Table S1). However, it was not possible to evaluate the efficiency of the *IL4* assay.

Table 8. Cycling program for RT-qPCR.

	Step	Time	Temperature
Pre-PCR	UNG incubation	2 min	50°C
	Taq activation	10 min	95°C
PCR (40 cycles)	Denature	15 sec	95°C
	Anneal/Extend	1 min	60°C

Relative gene expression levels were calculated as the ratio of target gene expression to reference gene expression according to Pfaffl formula (Pfaffl, 2001). In this context, relative quantification measures changes in the steady-state mRNA levels of a target gene across numerous samples, and it presents these changes relative to the levels of control RNA. The expression is normalized against a reference gene, which is often a housekeeping gene. All samples were tested in triplicate.

3.5. PROTEIN ANALYSIS

Additionally, alongside the gene expression studies, protein analyses were conducted to determine their secretion, expression and location patterns using immunoassay, immunoblotting, flow cytometry (FC) and immunofluorescence (IF).

3.5.1. IMMUNOASSAY

The supernatants from cell cultures or plasma samples were analyzed using multiplex magnetic bead-based immunoassay technology, which relies on FC and based on Luminex® xMAP® technology (Luminex Corp) (Figure 12).
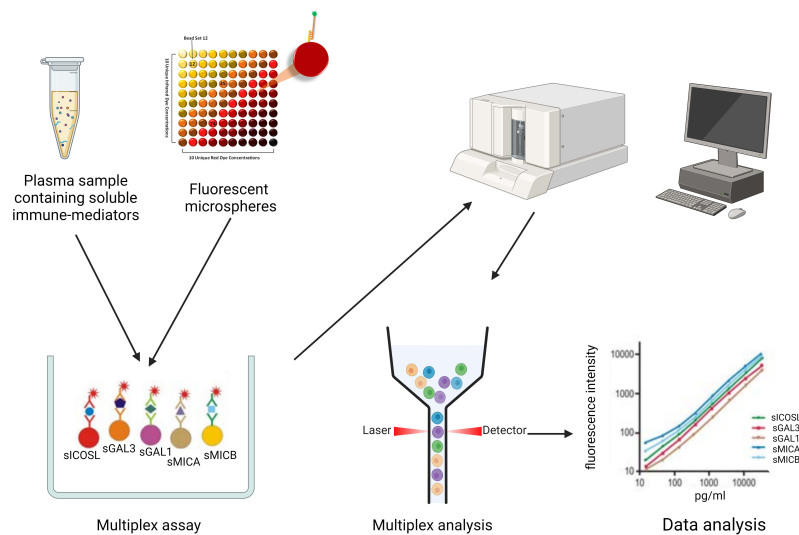
Figure 13. Luminex® xMAP® Technology and general principles. Own design created with BioRender.com.

For plasma samples, the soluble levels of sICOSL, sCD276, sFGL1, sGAL1, sGAL3, sMICA and sMICB, were measured using a multiparametric immunoassay commercial kit, MILLIPLEX® Human Immuno-Oncology Checkpoint Protein Panel 2 - Immuno-Oncology Multiplex Assay (Merck-Millipore).

For cell culture supernatants, 4 different commercial kits were used:

1) MILLIPLEX® Human Circulating Cancer Biomarker Magnetic Bead Panel 3 (Merck-Millipore) to quantify levels of sGAL3.

 2) MILLIPLEX® Human High Sensitivity T Cell Panel - Immunology Multiplex Assay (Merck-Millipore) to measure levels of sIFNγ, sIL13, sIL17A, sIL6 and sIL8.

 3) MILLIPLEX® Human Immuno-Oncology Checkpoint Protein Premixed 17-plex Panel 1 - Immuno-Oncology Multiplex Assay (Merck-Millipore) to quantify levels of sPDL1 and sPDL2.

4) MILLIPLEX® Human Immuno-Oncology Checkpoint Protein Panel 2 - Immuno-Oncology Multiplex Assay (Merck-Millipore) to determine levels of sICOSL, sMICA, sMICB and sCD276.

Quality controls (QC1 and QC2), as well as a calibration curve based on 1:4 dilutions of the highest standard, were used for quantification and as internal controls for intra- and inter-assay reproducibility. According to manufacturer's instructions, 25 µl of plasma were used for each sample and mixed with proper regents and monoclonal antibodies, which are attached to the surface of magnetic microspheres. These microspheres are labeled with precise amounts of red and infrared fluorophores, resulting in a distinct spectral signature for each one. The measurement of the different soluble proteins is determined fluorescently by labeled secondary antibodies, where the signal intensity is directly proportional to the concentration of the analyte detected. The fluorescent signals from all samples were then analyzed using a Luminex 100/200™ instrument (Luminex Corp). Utilizing measurements from seven diluted standard concentrations supplied by the manufacturer, a five-parameter standard curve was employed to convert optical density values into concentrations, expressed in picograms per milliliter (pg/mL). A minimum of 50 beads per cytokine were assessed for each standard and sample. The resulting concentrations (in pg/ml) were determined using Belysa™ software (Merck-Millipore). Notably, all inter-assay and intra-assay coefficients of variation (CV) were maintained below 15%. For HCKP2-11K, the lower limit of quantification (LLOQ) of sICOSL, sCD276, sFGL1, sGAL-1, sGAL3, sMICA, and sMICB was 12.2 pg/ml, 195 pg/ml, 48.8 pg/ml and 61 pg/ml, 48.8 pg/ml, 12.2 pg/ml, and 104 pg/ml, respectively. For HCCBP3MAG-58K, the LLOQ of sGAL3 was 4 pg/ml. For HSTCMAG-28SK, the LLOQ of sIFNγ, sIL13, sIL17A, sIL6 and sIL8 was 0.61 pg/ml, 0.24 pg/ml, 0.73 pg/ml, 0.18 pg/ml, and 0.31 pg/ml, respectively. For HCKP1-11K-PX17, the LLOQ of sPDL1 and sPDL2 was 5 pg/ml and 49 pg/ml, respectively.

3.5.2. IMMUNOBLOTTING

For protein isolation, the culture medium was aspirated from the tumorspheres, and they were washed with cold PBS. For adherent-cultured cells, they were scraped from the culture dishes prior to lysis. Protein pellets were lysed using a lysis buffer

containing 100mM Tris pH8, 2% NP40, 1% Na deoxycholate, 0.2% SDS and 300mM NaCl, 1mM sodium orthovanadate, 25mM NaF and protease inhibitor cocktail (Roche). All lysates were incubated for 30 minutes on ice and subsequently centrifuged at 10.000 g for 10 minutes at 4°C. Supernatants were collected and stored at -80°C. To determine the total protein concentration, spectrophotometry was employed using the bicinchoninic acid (BCA) Protein Assay (Thermo Fisher Scientific). Absorbance was measured at 570 nm using a Victor3^{TM}-1420 Multilabel Plate Counter (Perkin Elmer), and protein concentration was calculated by interpolating absorbance in a standard curve prepared with standard solutions of BSA. Next, proteins were separated by sodium dodecyl sulfate polyacrylamide gel electrophoresis (SDS-PAGE). A total of 30 μg of protein was mixed with Laemmli buffer containing 200mM Tris-HCl pH 6.8, 8% SDS, 40% glycerol and 2mg Bromophenol Blue, and then denatured for 5 minutes at 95°C. Protein separation was carried out on a 12% SDS-polyacrylamide gel, with electrophoresis conducted at 150 V for approximately 1 hour. Molecular weights were determined using a protein ladder, Rainbow Molecular Weight Markers (Amershan). Separated proteins were subsequently transferred to a 0.45 μm polyvinylidene difluoride (PVDF) membranes, Immobilion®-P (Sigma-Millipore) at 100 V and 4 °C for 60 minutes. Successful transfer was verified by staining the membranes with a solution containing 0.5% Ponceau S solution and 1% glacial acetic acid. Afterwards, this staining was cleared using a washing solution composed of 0.01% Tween 20 (Panreac) in PBS. Following this, the membranes were blocked with 5% skim milk for 1 hour to prevent nonspecific binding of antibodies. Subsequently, the membranes were incubated overnight at 4°C with the Anti-GAL3 antibody in blocking solution at [1:2000] working solution (Clone A3A12) (ab2785, Abcam). The membranes were then washed three times for 10 minutes each at room temperature (RT) with washing solution and incubated with an anti-IgG (whole molecule)-peroxidase secondary antibody at [1:5000] working solution (Thermo Fisher Scientific) for 1 hour at RT. After another three washes, peroxidase activity was detected by incubating the membranes with a chemiluminescent detection system using the high-sensitivity Amersham ECL Select™ detection reagent (GE Healthcare) and the Alliance Q9-series (Uviteq). Densitometric analysis was performed using ImageJ (NIH) and all results were normalized over β-actin (Sigma-Aldrich).

3.5.3. FLOW CYTOMETRY

To examine GAL3 membrane expression in tumor cells, the culture medium was removed and tumorspheres and adherent cells were trypsinized in single cells. Single-cell solutions were then washed with staining buffer (PBS 1× + 0.5% BSA + 2mM EDTA) and incubated for 30 minutes at 4°C with phycoerythrin (PE) anti-GAL3 (clone M3/38) (Biolegend). Afterwards, single cells were washed with PBS twice and incubated with 200 µl of 7-aminoactinomicina D (7AAD) Viability Staining (Thermo Fisher Scientific) for dead cells exclusion prior analysis.

For analysis of T_{REG} phenotype, T cells treated with CM (tumorspheres or co-culture) with and without GAL3 monoclonal antibody, were washed in staining buffer and incubated for 30 minutes at RT with Fixable Viability Stain 780 (BD Horizon) to exclude dead cell. Next, single cells were washed in staining buffer and incubated with surface antibodies in staining buffer for 30 minutes at 4°C: Brilliant Violet V510 (BV510) Mouse Anti-Human CD3 (Clone HIT3a), Brilliant Violet V421 (BV42) Anti-Human CD4 (Clone SK3), Allophycocyanin (APC) Anti-Human CD25 (clone M-A251). Then, single cells were washed with staining buffer and fixed and permeabilized with transcription factor buffer set (Thermo Fisher Scientific), following the instructions in the datasheet. Afterwards, single cells were washed with washing solution and finally incubated with PE anti-Human FoxP3 (Clone 259D/C7) for 30 minutes at 4°C. T_{REGS} were identified within live cell gate as CD3+CD4+Foxp3+CD25^{high}. For controls, we have used Fluorescence Minus One (FMOs) for FOXP3 and CD25, which are the markers with low expression levels.

Signal were acquired using a FC500 MPL Flow Cytometer and CytExpert v2.3 software (Beckman-Coulter). All antibodies used for FC analysis are listed in Table 9.

Table 9. List of antibodies used for flow cytometry. 7AAD, 7-aminoactinomicina D; PE, phycoerythrin; BV, brilliant violet; APC, allophycocyanin.

Antibody	Dilution	Catalog nº	Supplier
7AAD Viability Staining	1:10	00-6993-50	Thermofisher
PE anti-Gal3 (clone M3/38)	1:200	125408	Biolegend
Fixable Viability Stain 780	1:1000	565388	BD Horizon
BV421 Anti-Human CD4 (clone SK3)	1:50	565997	BD Horizon
BV510 Mouse Anti-Human CD3 (Clone HIT3a)	1:50	564713	BD Bioscience
APC Anti-Human CD25 (clone M-A251)	1:50	555434	BD Bioscience
PE anti-Human FoxP3 (Clone 259D/C7)	1:50	560046	BD Bioscience

3.5.4. IMMUNOFLUORESCENCE

For immunofluorescence analysis, adherent cells were cultured on coverslips until they reached 80% confluence. Tumorspheres were resuspended in PBS at a final concentration around 5×10^5 cell/mL. Then, 100 µL of the cell suspensions were centrifuged at 400 g for 5 minutes using a cytospin 3 (Thermo Shandon). Cells were fixed in 4% paraformaldehyde in PBS at RT for 15 minutes and washed with PBS three times for 5 minutes each washing step. Permeabilization of cell membranes was performed with 0.4% Triton X-100 in PBS for 10 min. Cells were washed three times again with PBS and blocked with PBS containing 1% BSA for 1 hour and subsequently incubated with GAL3 anti-mouse [1:200] (ab2785) antibody in blocking buffer overnight at 4 °C. Following this incubation, cells were washed with PBS three times. Thereafter, cells were incubated with Alexa Fluor 488-labelled IgG secondary antibodies [1:2000] (A11001, Thermo Fisher Scientific) in blocking buffer for 1 hour. Slides were incubated with 4',6-diamidino-2-phenylindole (DAPI) (Thermo Fisher Scientific) for 3 minutes at RT and washed with PBS for 5 minutes. Coverslips were mounted with Fluoromount Aqueous Mounting Medium (Sigma-Aldrich) and analyzed using a Leica confocal microscope (Leica Microsystems).

3.6. CIBERSORTX TOOL

Dataset for LUAD from the TCGA consortium was downloaded. Clinical information and RNA-sequencing data (Illumina HiSeq platform) were directly downloaded from the International Cancer Genome Consortium (ICGC) Data Portal (J. Zhang et al., 2011) (https://dcc.icgc.org/projects/LUAD-US). Only patients meeting specific eligibility criteria, which included a confirmed diagnosis of LUAD and a stage I-IIIA classification, were included in our subsequent analyses.

To assess immune cell subsets, we prepared and uploaded a composite dataset following the guidelines provided by the CIBERSORTx online analysis platform (https://cibersortx.stanford.edu/). To deconvolve the immune cell subsets, we employed the leukocyte 22 data matrix (LM22) signature matrix, a validated leukocyte gene signature matrix encompassing 547 genes that distinguish 22 human hematopoietic cell phenotypes. These include various T-cell types, naive and memory B cells, plasma cells, NK cells, and myeloid subsets (Newman et al., 2015). We selected "B-mode" for batch

correction and set the permutations to 500, while retaining other parameters at their default values.

Upon running CIBERSORTx, we obtained the absolute proportions of tumor-infiltrating immune cell (TIICs) in each sample, along with p-values indicating the confidence of the deconvolution results. All samples with p-values less than 0.05 were considered eligible for further analysis. Heatmap displaying various cellular subtypes is presented in Figure 14. Subsequently, our focus turned to exploring the proportions of specific immune cell types, including T_{REGS}, activated memory CD4$^+$ T cells, CD8$^+$ T cells, M1 macrophages, and M2 macrophages, in more detail. These exploratory analyses were conducted using R (version 4.3.0) and involved techniques such as k-means clustering and principal component analysis (PCA). Additionally, we analyzed RNA-seq data for 356 LUAD patients obtained from TCGA, dividing the data into two groups (high and low) according to the levels of expression of *LGALS3* taking the median value as a cut-off.
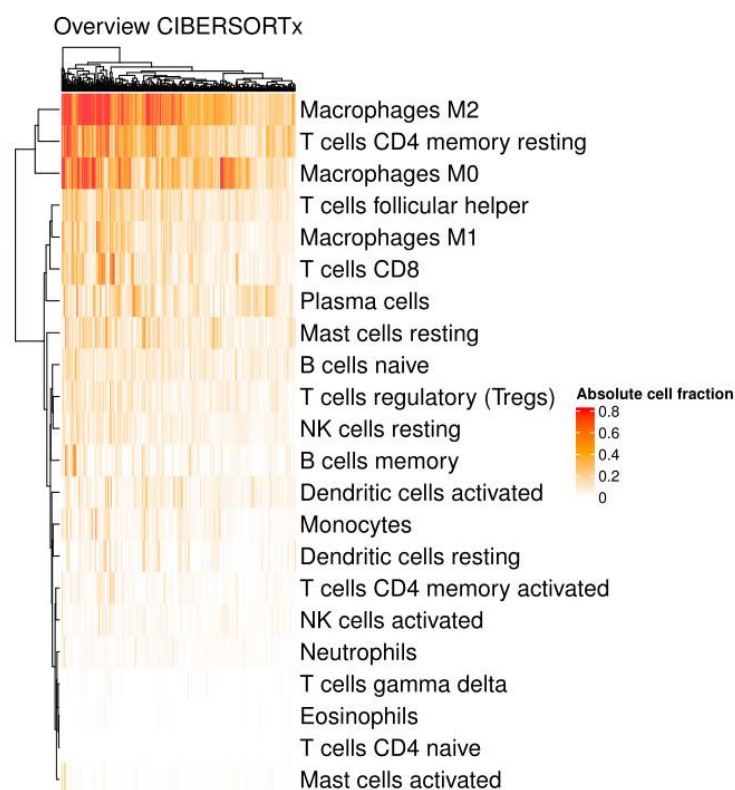
Figure 14. Heatmap of different cellular subtypes representing absolute cell fraction of different cellular subtypes.

3.7. STATISTICAL ANALYSIS

First, we assessed the normality of the variables using the Kolmogorov-Smirnov test. As the variables did not follow a normal distribution, statistical analyses were conducted using non-parametric tests. In cell culture experiments, we conducted triplicate trials for each sample and the results are presented as the median ± the interquartile range (IQR). We employed the non-parametric Wilcoxon's signed-rank test to analyze expression and secretion in both adherent-cultured cells and tumorspheres. Spearman rank test was used to test for correlations between continuous variables.

To study the correlation between soluble immunoregulatory genes and different clinicopathological variables, response, and survival, we used three different cohort. early-stage NSCLC test cohort from HGUV, TCGA validation cohort, and advance-stage NSCLC from HGUV. Clinical and RNA-seq information from TCGA consortium was directly downloaded from the ICGC (J. Zhang et al., 2011). To compare continuous variables, we performed a non-parametric Mann-Whitney U-test (for two groups) and Kruskal-Wallis (for more than two groups) to evaluate the median soluble levels of all tested immune-mediators. We assessed the association between discrete variables using the Chi-squared (X^2) tests.

Survival analysis was performed using a univariate Cox regression method using clinicopathological variables and dichotomized gene expression immune-mediators. We generated survival curves using the Kaplan-Meier method and assessed the statistical significance between survival curves using the log-rank test.

Receiving Operating Curve (ROC) method was used to determine a cut-off level for each biomarker with a significant difference for DCB and ORR. ROC curves were also used to evaluate the diagnostic power of biomarkers. Other predictive parameters were also evaluated, including sensitivity, specificity, cut-off value, positive predictive value (PPV), negative predictive value (NPV), and area under the ROC (AUC) with a 95% confidence interval (CI), to assess the discrimination power of individual biomarkers. The identification of the cut-point value requires a concurrent evaluation of sensitivity and specificity. One of the commonly employed methods is the Youden index method (Ruopp et al., 2008). This approach defines the optimal cutoff point as the point that maximizes

the Youden function, which represents the difference between the true positive rate and the false positive rate across all potential cut-off values. In general, an AUC of 0.5 suggests no discrimination, 0.7 to 0.8 is considered acceptable, 0.8 to 0.9 is considered excellent, and more than 0.9 is considered outstanding.

Finally, to assess the independent value of the tested biomarkers, a Cox proportional hazard model for multivariate analyses was used. All variables (both immune-meaditors and clinicopathological features) from the univariate analyses were entered into the multivariate analyses in a forward stepwise Cox regression analysis. We considered a probability of 95% (p < 0.05) as statistically significant for all analyses. Statistical analyses were performed using the Statistical Package for the Social Sciences (SPSS) version 23.0. PCA was performed with the SIMCA-P software (Umetrics) version 13.0 using unit variance scaling method. RNA-seq data analyses were performed using R 3.5., GraphPad Prism (GraphPad Software Inc.) version 8.0 was used to create the graphics presented here. Statistical significance was set at $p<0.05$ (*), $p<0.01$ (**), $p<0.001$(***).

IV. RESULTS & DISCUSSION

CHAPTER I. EXPLORATORY PHASE: *IN VITRO* STUDIES ON IMMUNE-MEDIATORS

1. *IN VITRO* MODELS: ADHERENT AND TUMORSPHERES CELL CULTURES

Short-term PDLCC cultures were successfully established in our laboratory in 40% of primary tumor tissue samples (Herreros-Pomares et al., 2019). During the present study, we established three long-term PDC, PC301, PC435 and PC471 which were able to grow tumor cells as monolayer and tumorspheres. A long-term primary culture was deemed successfully established when it exclusively consisted of cancer cells, without stromal fibroblasts, and could be preserved through cryopreservation, thawed, and re-grown. The clinicopathological characteristics of PC301, PC435, and PC471 are outlined in Table 3. Long-term PDLCC cultures were stablished and maintained for one month before undergoing their initial passage.

PDLCC cultures play a crucial role in cancer research, significantly contributing to our comprehension of tumor biology, molecular mechanisms, oncogene activation, and patient-specific gene expression patterns (Richter et al., 2021). Long-term establishment of PDLCC cultures presents several challenges, including excessive necrosis of tumor samples, inadequate preservation of tumor specimens, fibroblast overgrowth, limited cancer cells lifespan, and low sustained proliferation rated (Kodack et al., 2017). One of the primary obstacles to achieving long-term cultures is the limited lifespan of these cultures, resulting in the majority being short-term. To address this challenge, as our expertise in the culture process grew, we incorporate some improvements in the cell culture conditions. Initially, we employed standard culture media consisted of standard growth media, including DMEM/F12 with FBS, on collagen-I-coated dishes. However, we explored the use of a Rho-associated coiled-coil containing ROCKi, Y-27632, an innovative conditional reprogramming technique that have been suggested to overcome the limitations associated with conventional approaches (Chapman et al., 2010; Hong et al., 2019; X. Liu et al., 2012). ROCKi serves as a downstream effector of the small GTP-binding proteins RhoA and RhoC (Julian & Olson, 2014), playing a role in various cellular

processes, such as cell proliferation, differentiation, cytokinesis, motility, adhesion, and cytoskeletal organization (Etienne-Manneville & Hall, 2002). Studies have revealed that the ROCKi hampers myosin light chain phosphorylation and, as a result, suppresses cell death (Okumura et al., 2016).

Simultaneously, commercial cell lines were cultured under both conditions and subsequently included in additional analyses. The examination of long-term PDLCC cultures and commercial cell lines using bright field revealed significant heterogeneity in the adherent culture cells and tumorspheres among them (Figure 15) (see more details in Supplementary files).
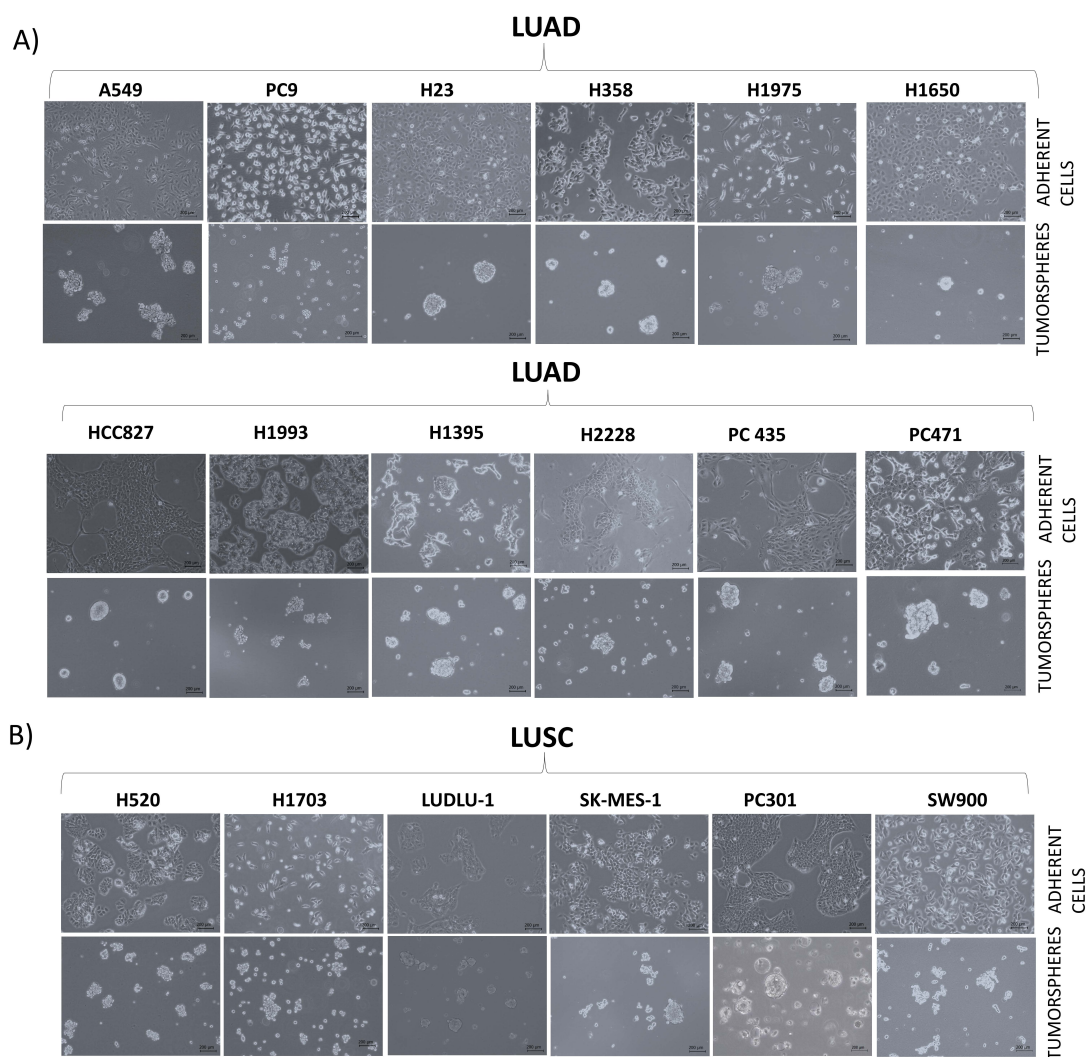
Figure 15. Representative images of the patient derived lung cancer cell cultures and cell lines grown under adherent conditions (adherent-cultured cells) and non-adherent conditions (tumorspheres). A) LUAD, lung adenocarcinoma cultures. B) LUSC, lung squamous cell carcinoma cultures. Scale bar, 200 μm.

2. GENE EXPRESSION ANALYSIS OF IMMUNOREGULATORY GENES

The relative expression of 28 immunoregulatory genes, described as inhibitory immune checkpoints (*ICOSL*, *CD276*, *PDL1*, *PDL2*), co-stimulatory immune checkpoints (*CD200*, *CD40L*, *CD137L*, *OX40L*), cytokines (*IL4*, *IL10*, *IL6*, *IL8*, *IL12A*, *IL12B*, *IL17A*, *IL13*, *IFNγ*, *TNFα*, *TGFβ*), galectins (*LGALS3*, *LGALS9*), ligands of NKG2D (*MICA*, *MICB*), non-classical MHC class I molecules (*HLAG*, *HLAE*, *HLAF*), signal transducer and activator (*STAT3*) and enzymes (*IDO1*), was analyzed in tumorspheres and compared with their adherent counterparts by using RT-qPCR. The relative expression levels of *IL17A*, *IFNγ*, *HLAG*, *IL4*, *IL10* and *IL13* were below the limit of detection of the technique in all samples and were excluded from the analysis. As previously mentioned, the efficiency of each TaqMan® assay was assessed with the Cp slope method. Supplementary Table 1 contains a compilation of the slopes and efficiency values for each assay. It is noteworthy that all the assays employed in this research demonstrated an amplification efficiency close to 100%, except for *IL4*.

To determine the optimal internal PCR control, we assessed the expression of four endogenous genes (*ACTB*, *GAPDH*, *GUSB* and *CDKN1B*) in all samples. GeNorm software (see details in the materials and methods section) was employed for this purpose, identifying the combination of *ACTB*, *GUSB*, and *CDKN1B* as the most stable option. Following the methodology proposed by Vandesompele et al. we calculated a normalization factor based on the expression of these three endogenous genes using the geometric mean (Vandesompele et al., 2002).

We conducted a Wilcoxon signed-rank test to assess relative gene expression, comparing samples from both culture conditions at two different times of seeded (12 hours and 24 hours), which included PDLCC cultures. The analysis was carried out independently in LUAD and LUSC cultures. In LUAD cultures, both at 12h and 24h, tumorspheres showed higher expression of 15 out of 21 genes compared to adherent-cultured cells, being a group of 11 genes (*CD276*, *STAT3*, *ICOSL*, *MICA*, *MICB*, *HLAE*, *LGALS3*, *HLAF*, *LGALS9*, *MICB*, *IL8* and *CD200*), significantly higher expressed according to

this test (Figure 16). In LUSC cultures, both at 12h and 24h, tumorspheres showed higher expression of 16 out of 21 genes compared to adherent-cultured cells, being a group of 3 genes (*MICA*, *LGALS9* and *CD200*) at 12h and 4 genes (*MICA*, *LGALS9*, *STAT3*, *ICOSL*) at 24h, significantly higher expressed compared to adherent-cultured cells according to this test (Figure 17).
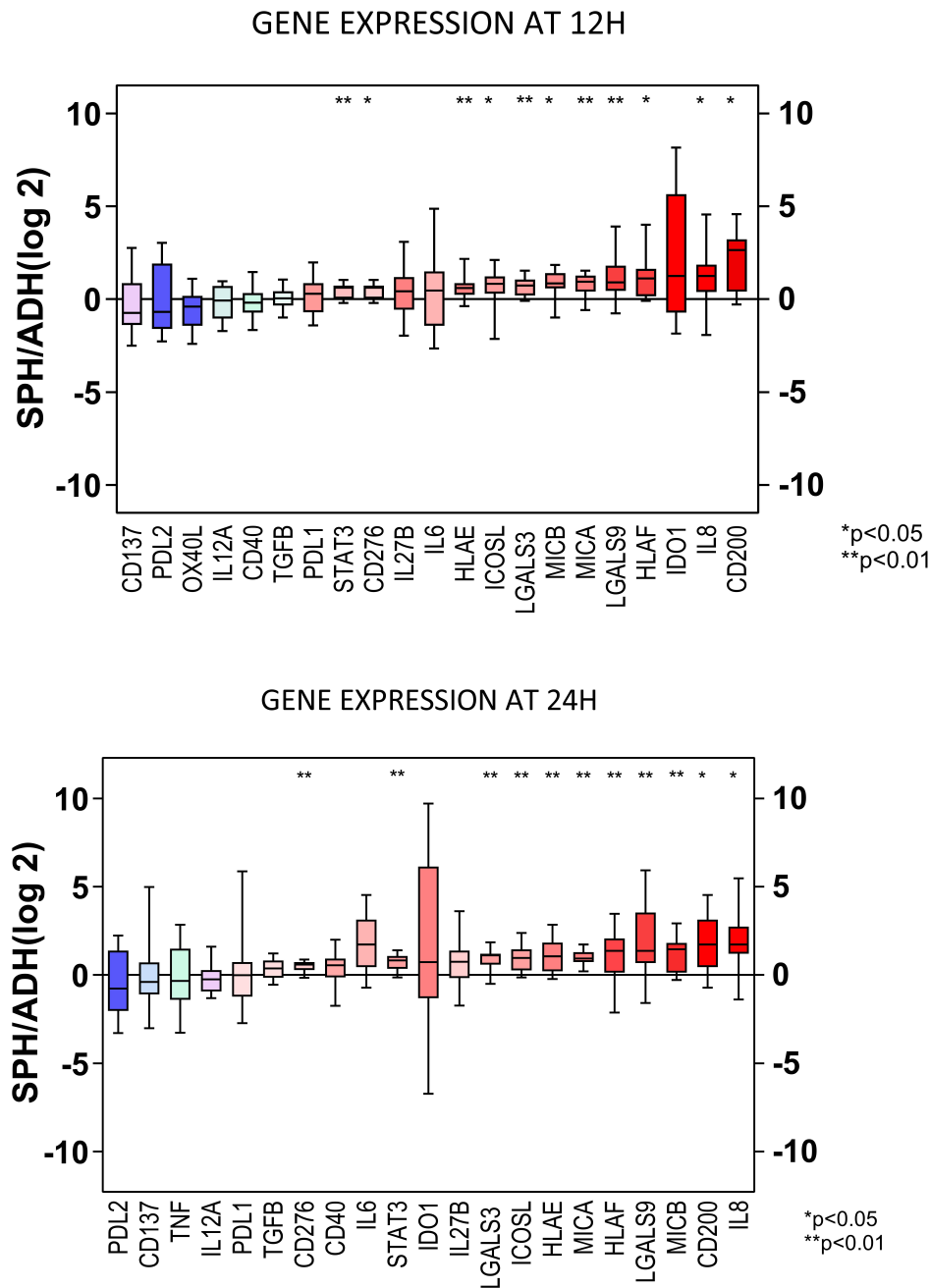
Figure 16. Transcription levels of the immunoregulatory genes in tumorspheres versus adherent-cultured cells in lung adenocarcinoma cultures (LUAD) at 12 (A) and 24 (B) hours after cell seeding. The results shown are the log2 of the ratio between the gene expression of tumorspheres and the gene expression of adherent-cultured cells. Error bars represent the maximum and minimum points. Statistical analysis was carried out with the Wilcoxon test. mRNA was measured by RT-qPCR. The experiment was repeated three times. ADH, adherent-cultured cells; SPH, tumorspheres; RT-qPCR, real time quantitative polymerase chain reaction. Significance values were *p<0.05, **p<0.01.

A)

B)
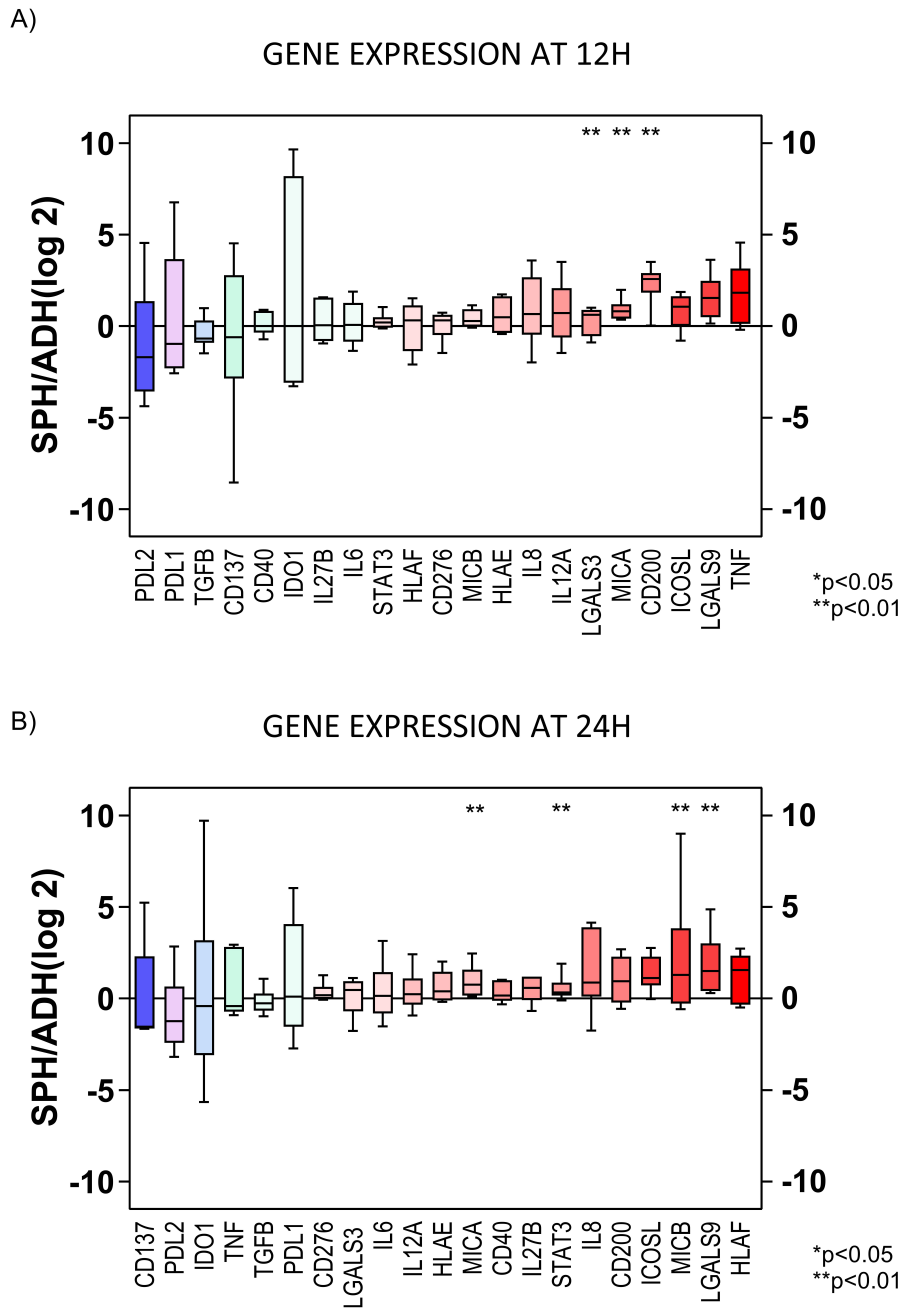
Figure 17. Transcription levels of the immunoregulatory genes in tumorspheres versus adherent-cultured cells in lung squamous cell carcinoma (LUSC) cultures at 12 (A) and 24 (B) hours after cell seeding. The results shown are the log2 of the ratio between the gene expression of tumorspheres and the gene expression of adherent-cultured cells. Error bars represent the maximum and minimum points. Statistical analysis was carried out with the Wilcoxon test. mRNA was measured by RT-qPCR. The experiment was repeated three times. ADH, adherent-culltured cells; SPH, tumorspheres; RT-qPCR, real time quantitative polymerase chain reaction. Significance values were *$p<0.05$, **$p<0.01$.

The evaluation of immune molecules' expression on tumor cells could provide the knowledge to comprehend better tumor immune evasion mechanisms. For this purpose, some studies have been focused on using tumorspheres such in our present study, a 3D

model system with outstanding applications for *in vitro* studies (Darvin et al., 2019; García-Rocha et al., 2022). Our results demonstrate that tumorspheres model expressed higher levels of most of immunoregulatory genes studied, elucidating that they may have better immunomodulatory abilities, making them a better model than conventional 2D models. Recently, Bertolini et al reports that spheroids from cell lines are enriched in metastasis initiating cells with immunosuppressive potential (Fortunato et al., 2020). In this work we proposed tumorspheres as a model to study the role of immunoregulatory proteins.

The gene encoding *CD200* was found to be the most expressed gene in both LUAD and LUSC cultures. CD200 is a cell surface glycoprotein implicated in various human cancer cells, where it has been suggested to play a pro-tumor role. *CD200* is known to be overexpressed in cancer cells in a variety of human tumors, including melanoma (Petermann et al., 2007), ovarian cancer (Moreaux et al., 2008) and some B cell malignancies. Studies on *CD200* in tumors have yielded controversial results. Interestingly, in animal research, the presence of *CD200* expression was identified in CSC of basal cell carcinoma and linked to tumor initiation capability (Colmont et al., 2013). Additionally, in squamous cell carcinoma, it was positively associated with metastatic potential (Stumpfova et al., 2010).

CD276, also known as B7-H3, is a member of the B7 family and overexpressed in tumor tissues, including NSCLC (C. Zhang & Hao, 2020). Although there are many controversial studies regarding the role of CD276 in lung cancer, it is generally observed to be highly expressed in cancer cells and is thought to be involved in evading the surveillance of cytotoxic T-cells and natural killer cells (Flem-Karlsen et al., 2018).

Regarding classical HLA molecules, we found the expression of *HLAG* and *HLAE* increased in tumorspheres. There is also strong evidence that cancer cells can express tolerogenic or immunosuppressive molecules, such as non-classical HLA E and G molecules, which are involved in tumor immune scape (Wischhusen et al., 2007).

Our analyses also showed that tumorspheres had greater expression of *MICA* and *MICB*. It has been studied that tumor cells utilize post-translational mechanisms, such as

the release of ligands (MICA and MICB) in soluble forms, to inhibit NK activating receptors, preventing the attachment of activating ligands on their surfaces. This strategy allows them to evade recognition by NK cells (Molfetta et al., 2019; Xing & Ferrari de Andrade, 2020).

STAT3 was also highly expressed in tumorspheres, suggesting a possible activation of this pathway in lung tumor cells. It has been studied that *STAT3* signaling pathway plays an important role in evading anti-tumor immunity in lung cancer (P. Dutta et al., 2014).

In terms of costimulatory immune checkpoints, in our study, *ICOSL* had greater expression in tumorspheres. There have been no prior reports of the expression of this gene in lung cancer. The binding between ICOS and ICOSL induces a range of activities within diverse T cell subpopulations, including T cell activation and effector functions, and, when sustained, can involve suppressive activities mediated by T$_{REGS}$ (Marinelli et al., 2018).

In terms of interleukins, *IL8* have been highly expressed by tumorspheres. IL8 is a potent angiogenic factor in many cancers including NSCLC (Smith et al., 1994) playing diverse roles in the progression of cancer, including immune evasion through its pro-inflammatory effects. In lung cancer, the most well-defined inflammatory roles of IL8 include the attraction of neutrophils and MDSCs (Schalper et al., 2020).

Focusing on galectins, which are part of a larger family of lectins, *LGALS3* and *LGALS9* were significantly highly expressed in tumorspheres. Both galectins have been associated with lung cancer. GAL3 is linked to the progression of lung cancer, whereas GAL9 relates to enhancing anti-cancer immune responses (Chang et al., 2017). Interestingly, data have shown that intracellular GAL3 promotes tumor growth, metastasis, and poor survival, while extracellular GAL3 may facilitate metastasis by promoting immune scape, although this aspect has been poorly investigated (Cardoso et al., 2016; Farhad et al., 2018; Fortuna-Costa et al., 2014). Ling-Yeng Chung et al. investigated *LGALS3* expression in NSCLC commercial cell lines (A549 and H1299) and discovered that spheroids, over successive passages, exhibited notably elevated levels of

this molecule in comparison to monolayer cells. GAL3 act as a cofactor by engaging with β-catenin, thereby enhancing the transcriptional activities of genes associated with stemness (Chung et al., 2015). Significantly, we have examined *LGALS3* expression and obtained consistent results not only in a substantial number of lung tumorspheres derived from cell lines but also in PDLCC cultures from *CHGUV*, which behave as a suitable and translational platform, as previously described by other authors (S. Y. Kim et al., 2019; Kodack et al., 2017b; Z. Zhang et al., 2018). Considering that in prior research conducted in our laboratory, we established that lung tumorspheres exhibit stem-like characteristics and additionally, in this study, we observe that lung tumorspheres express higher levels of *LGALS3* than adherent-cultured cells, it is reasonable to hypothesize that GAL3 could support the stemness properties according with Ling-Yeng Chung et al. results. In line with these findings, there are data in other tumor types indicating that GAL3 supports stemnes status in CSC (H. G. Kang et al., 2016; Nangia-Makker et al., 2018).

3. PROTEIN SECRETION ANALYSIS OF IMMUNE-MEDIATORS

Next, we analyzed the soluble forms (in culture media samples) of most of the genes evaluated previously. Levels of sPD-L1, sPD-L2, sICOSL, sMICA, sMICB, sCD276, sIFNγ and sIL17A were below the limit of detection of the technique in most of samples, preventing further analysis.

We analyzed the secretion of proteins from paired samples in 2D and 3D conditions, at two different time points and seeding densities, using a Wilcoxon signed-rank test. The analysis was performed separately for LUAD and LUSC cultures. In LUAD cultures, both at 12h and 24h and at low and high density, tumorspheres exhibited higher secretion of sGAL3 compared to adherent-culture cells (Figure 18A, left). Tumorspheres also express significant higher levels of sIL13 at 24h post-seeding (Figure 18B, left). In LUSC cultures, we only observed that sGAL3 was highly secreted by tumorspheres compared to adherent-cultured cells at 24h post-seeding compared with

their adherent counterpart (Figure 18B, right). No significant differences were found in the secretion of the other soluble immune-mediators analyzed.
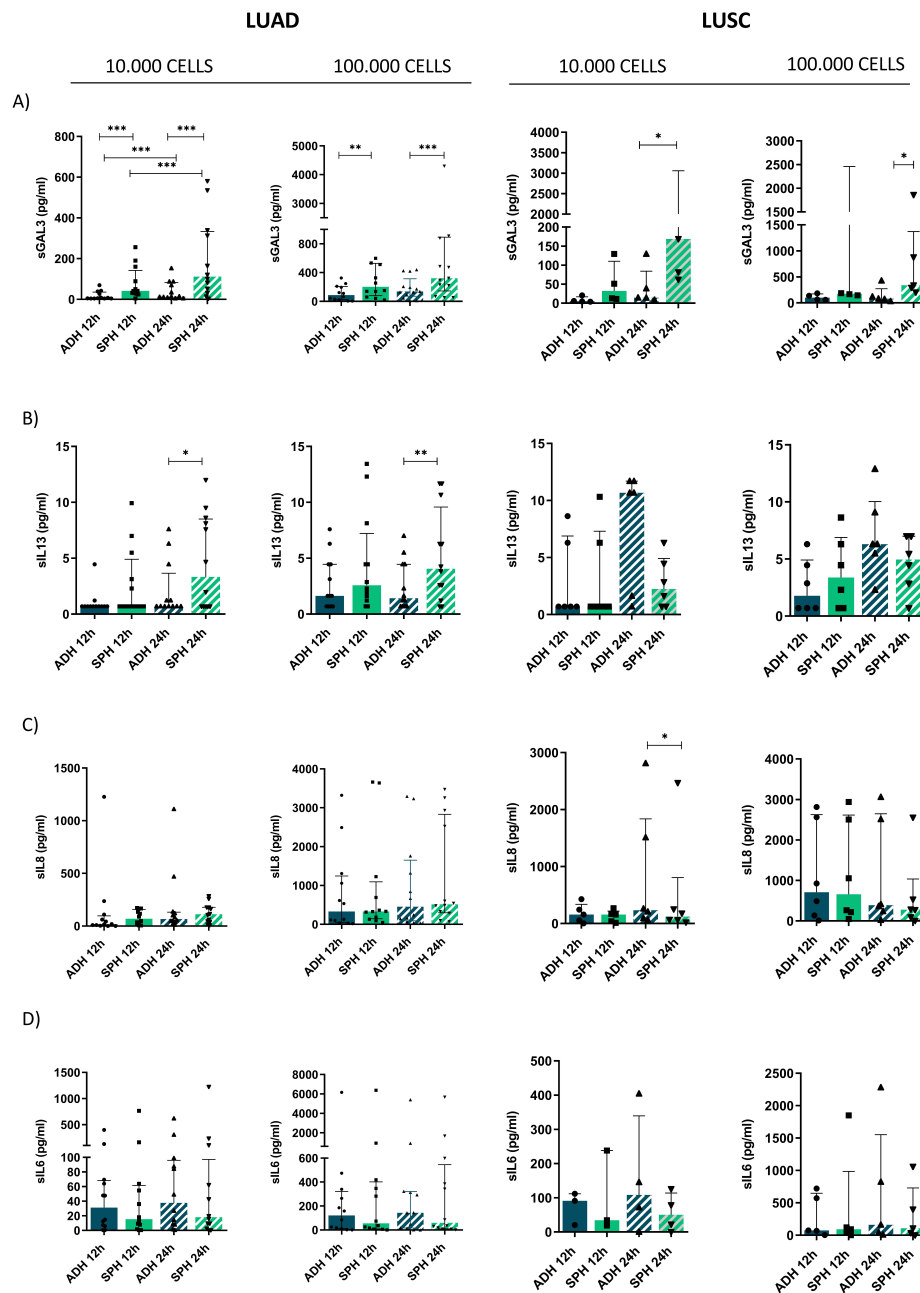
Figure 18. Immunoassay of soluble immune-mediators in lung adenocarcinoma (LUAD) and lung squamous cell carcinoma (LUSC) adherent-cultured cells and tumorspheres analyzed by Luminex® Technology at 12 and 24 hours after cell seeding at two different density (low-density 10.000 cells/ml and high density 100.000 cells/ml). A) Median levels of sGAL3 of all cell lines and patient derived lung cancer cell (PDLCC) cultures at 12 and 24 hours. B) Median levels of sIL13 of all cell lines and PDLCC cultures at 12 and 24 hours. C) Median levels of sIL8 of all cell lines and PDLCC cultures at 12 and 24 hours. D) Median levels of sIL6 of all cell lines and PDLCC cultures at 12 and 24 hours. LUAD, on the left; LUSC, on the right. Statistical analysis was carried out with the Wilcoxon test. Errors bars represent interquearlite range (IQR) of the median of all cell lines and primary cultures (n=12 for LUAD and n=6 for LUSC). ADH, adherent-cultured cells; SPH, tumorspheres; PDLCC, patient derived lung cancer cell; n, sample size; LUAD, lung adenocarcinoma; LUSC, lung squamous cell carcinoma; IQR, interquartile range; sGAL3 (Soluble galectin-3); sIL13 (soluble interleukine-13); sIL6 (soluble interleukine-6). Significance values were *$p<0.05$, **$p<0.01$, ***$p<0.001$.

While our results indicate that LUAD tumorspheres secrete higher levels of IL13 compared to adherent-cultured cells, it is important to note that there is considerable variability among samples, leading to a relatively wide IQR. Furthermore, it should be emphasized that many of the samples exhibited values below the detection limit, so these results should be interpreted with caution. IL13 is a proinflammatory cytokine correlated with various pathological conditions and the progression of metastasis in lung cancer (Joshi et al., 2006). Moreover, previous studies have revealed that IL13 is associated with PI3K/AKT signaling pathway (Grehan et al., 2005).

Furthermore, in line with our previous gene expression analysis, tumorspheres were found to secrete significantly higher levels of sGAL3 compared to adherent-cultured cells. It should be notice that GAL3 exerts different biological effects based on its cellular localization, which is achieved through specific interactions with intra- and extracellular proteins. These interactions influence a multitude of biological processes, including neoplastic transformation and metastasis (Ruvolo, 2016). Extracellular GAL3 exhibits numerous autocrine and paracrine effects (Dumic et al., 2006). It facilitates cell adhesion and activation and serves as a chemoattractant for specific cell types. GAL3 plays a role in regulating cellular homeostasis, immune responses, organ development, angiogenesis, as well as tumor invasion and metastasis (F. T. Liu & Rabinovich, 2005; Ochieng et al., 2002; Takenaka et al., 2002). However, it is important to note that many studies have utilized exogenously introduced GAL3 at elevated concentrations. Therefore, the biological functions of GAL3 in physiological conditions still require further clarification.

GAL3 lacks a signal sequence for translocation into the endoplasmic reticulum and Golgi compartments, and it does not follow the classical secretory pathways (Menon & Hughes, 1999). Studies have shown that GAL3 can undergo cleavage by matrix metalloproteinases (MMPs) and be detected freely in plasma (Nangia-Makker et al., 2007, 2010; Ochieng et al., 1998). Regarding its immunosupressive role in lung cancer, not many studies have been conducted. Generally, some studies have suggested that GAL3 can induce T-cell apoptosis and inhibit TCR-mediated signal transduction by forming multivalent interactions with glycans located on the TCR (H. Y. Chen et al., 2009; Demetriou et al., 2001). This subsequently impact hampers the lateral mobility of the

TCR complex, a critical factor in T-cell activation, ultimately resulting in the suppression of the T-cell response.

4. DEEPING IN THE STUDY OF GALECTIN-3

Among all the molecules analyzed, GAL3 has been the only one expressed and secreted at higher levels by tumorspheres compared to adherent-cultured cells (Figure 19). No significant differences were found between the expression and secretion of GAL3 in LUAD tumorspheres and LUSC tumorspheres. Additionally, given our results and the potential immunosuppressive role of GAL3 in tumor immune evasion within the TME, which has been poorly investigated, we propose further exploration of this molecule in the context of lung cancer.
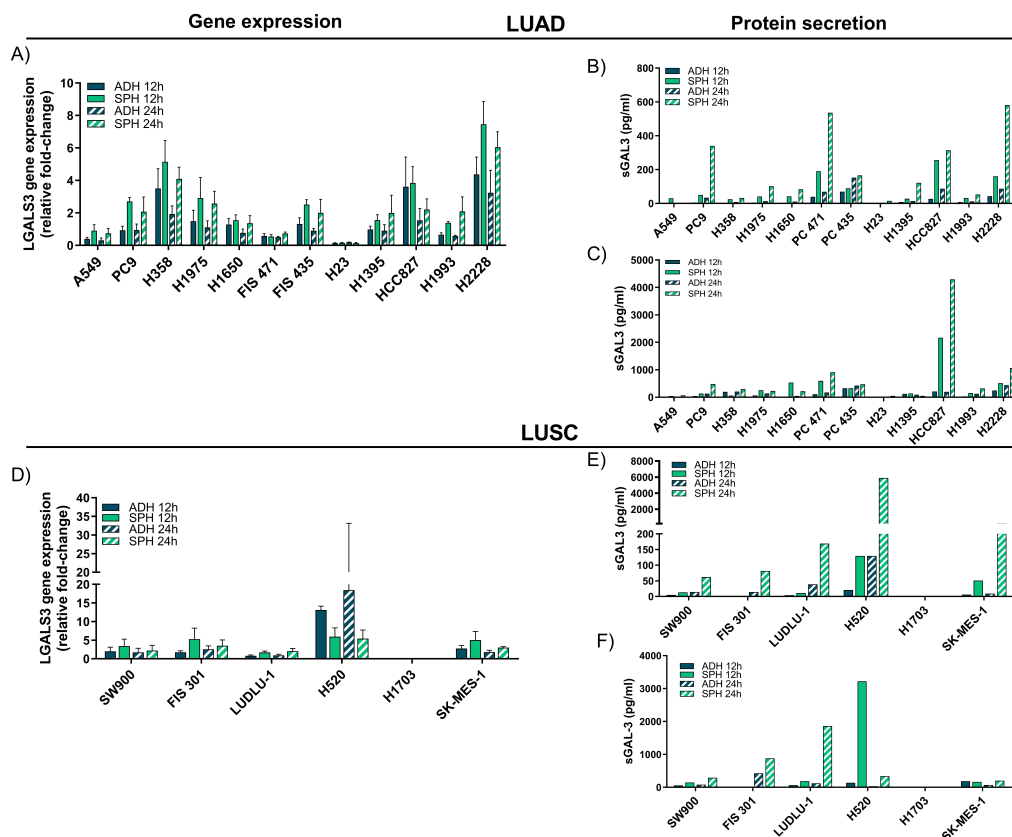
Figure 19. Transcription and secretion levels of GAL3 in adherent-cultured cells versus tumorspheres. A,D) Transcription levels of *LGALS3* in adherent-cultured cells vs. tumorspheres in lung adenocarcinoma (LUAD) patient derived lung cancer cell (PDLCC) cultures and cell lines A) and lung squamous cell carcinoma (LUSC) PDLCC cultures and cell lines D) analyzed by RT-qPCR at 12 and 24 hours after cell seeding. The results shown the relative fold-change gene expression of *LGALS3* to reference genes *ACTB*, *CDKN1B*, and *GUSB*. Errors bars represent standard deviation (SD) of three different experiments. B, C, E, F) Immunoassay of sGAL3 in adherent-cultured cells and tumorspheres analyzed by Luminex® Technology at 12 and 24 hours after cell seeding. B, E) Median levels of sGAL3 of all cell lines and PDLCC cultures at 12 and 24 hours after 10.000 cells/ml seeding (low density) in LUAD cultures B) and in LUSC cultures E). D, F) Median levels of sGAL3 of all cell lines PDLCC cultures at 12 and 24 hours after 100.000 cells/ml seeding (high density) in LUAD cultures D) and in LUSC cultures F). ADH, adherent-cultured cells; SPH, tumorspheres; LUAD, lung adenocarcinoma; LUSC, lung squamous cell carcinoma; RT-qPCR, real time quantitative polymerase chain reaction; PDLCC, patient derived lung cancer cell.

First, we performed immunoblotting analyses comparing again paired tumorspheres and adherent-cultured cells. In the LUAD cultures, GAL3 protein expression was significantly higher in almost all tumorspheres than in their adherent counterparts. Only one cell line, H1395, showed higher levels of GAL3 in the adherent-cultured cells than in tumorspheres (Figure 20 A,B,C). In the LUSC cohort, out of the 6 cultures, 3 of them indeed exhibited higher protein levels in tumorspheres than in adherent-cultured cells, one of them, H520, showed no differences, and finally, in line with previous results, the commercial H1703 cell line did not display GAL3 protein expression (Figure 20 D,E,F).

Comparing levels of GAL3 protein expression in LUAD and LUSC tumorspheres, the median protein levels (in Arbitrary Units) were 1.078 in LUAD cultures and 0.6168 in LUSC cultures, although these differences were not significative. Not many studies assert the differences of expression of GAL3 between LUAD and LUSC. R Buttery et al. found that GAL3 is highly expressed and found in both intracellular and extracellular compartments in NSCLC, whereas in SCLC, GAL3 is very poorly expressed by IHC (Buttery et al., 2004).

It should be highlighted that according with gene expression levels and secretion, both tumorspheres and adherent-cultured cells from LUAD cultures, H23 and A549, expressed the lowest levels of GAL3. This could be indicating that these cell lines may have an active inhibitory mechanism. These two lines are *KRAS* mutated, but no correlations were found between levels of GAL3 and *KRAS* mutational status since *KRAS* mutated cell lines such as H358, SW900, or the PC435 expressed high levels of *LGALS3*. Another possible mechanism could be via KEAP1/NRF2/GAL3. A549 and H23 have missense substitutions (p.G333C and p.Q193H, respectively) in the *KEAP1* gene. KEAP1 is a substrate receptor of a Cul3-RING ubiquitin ligase (CRL3) that, in physiological conditions, constitutively binds and targets NRF2, nuclear factor erythroid 2–related factor 2, for degradation. In response to oxidative stress or mutations, the KEAP1-NRF2 binding is inhibited and, consequently, NRF2 is stabilized and accumulated in the nucleus (Lignitto et al., 2019). Recently it has been revealed that the *LGALS3* expression was regulated by this classical antioxidant protein NFRS.

These authors revealed that using an NRF2-specific inhibitor increased GAL3 (Lan et al., 2023). Therefore, considering these publications, we can infer that *KEAP1* mutations in H23 and A549 could lead to the accumulation of the NRF2 factor, decreasing the amounts of GAL3.
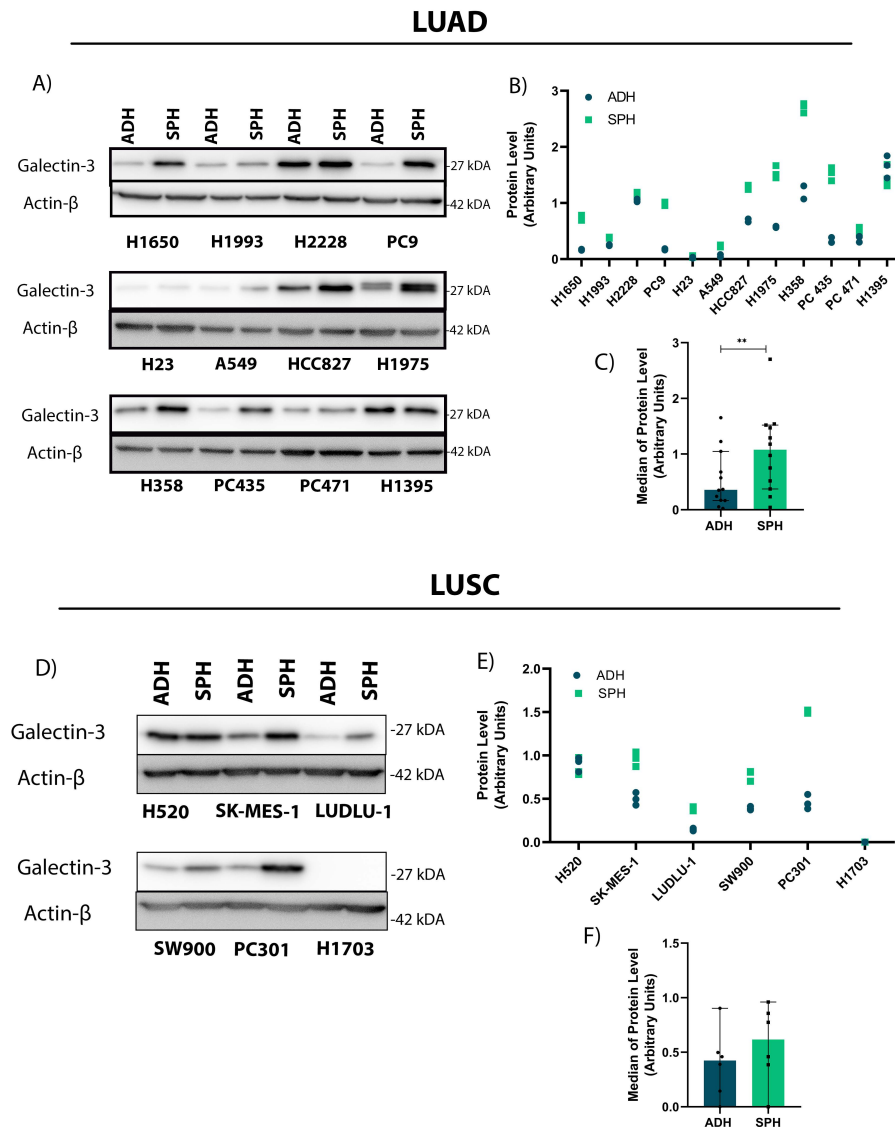
Figure 20. Expression of GAL3 at protein level. A) Immunoblots (IBs) showing the level of GAL3 in adherent-cultured cells and tumorspheres in lung adenocarcinoma (LUAD) cultures. Beta-actin (ACTB) was used as loading control. The experiment was repeated three times and representative western blot results from one experiment were shown. B) ImageJ analysis of IBs of panel A. Bar chart represents the relative expression of each protein according to immunoblots in LUAD cultures. Three grey values relative to the loading controls were measured in every case and averaged. C) Values relative to the loading controls were measured in every LUAD cultured and averaged. Statistical analysis was carried out with the Wilcoxon test. Errors bars represent interquartile range (IQR) of all cell lines and patient derived lung cancer cell (PDLCC) cultures median (n=12). D) IBs showing the level of GAL3 in adherent-cultured cells and tumorspheres in lung squamous cell carcinoma (LUSC) cultures. ACTB was used as loading control. The experiment was repeated three times and representative western blot results from one experiment were shown. E) ImageJ analysis of IBs of panel A. Bar chart represents the relative expression of each protein according to immunoblots in LUSC cultures. Three grey values relative to the loading controls were measured in every case and averaged. F) Values relative to the loading controls were measured in every LUSC cultures and averaged. Statistical analysis was carried out with the Wilcoxon test. Errors bars represent IQR of all cell lines and PDLCC cultures median (n=6). ADH, adherent-cultured cells; SPH, tumorspheres; LUAD, lung adenocarcinoma; LUSC, lung squamous cell carcinoma; n, sample size; PDLCC, patient derived lung cancer cell; IB, immunoblots. Significance values were **p<0.01.

4.1. FLOW CYTOMETRY ANALYSIS

In addition to western blotting, we performed FC to analyze GAL3 expression on the cell surface in both culture conditions. Interestingly, at membrane level, LUAD tumorspheres were highly enriched in GAL3+ cells (*p*=0.021) (Figure 21 A,B). H23 and A549 showed the lowest expression at membrane level of GAL3. These results are consistent with what had previously been observed in terms of gene expression, protein secretion, and protein expression. No significant differences were found in LUSC cells between tumorspheres and adherent-cultured cells (Figure 21 C,D).
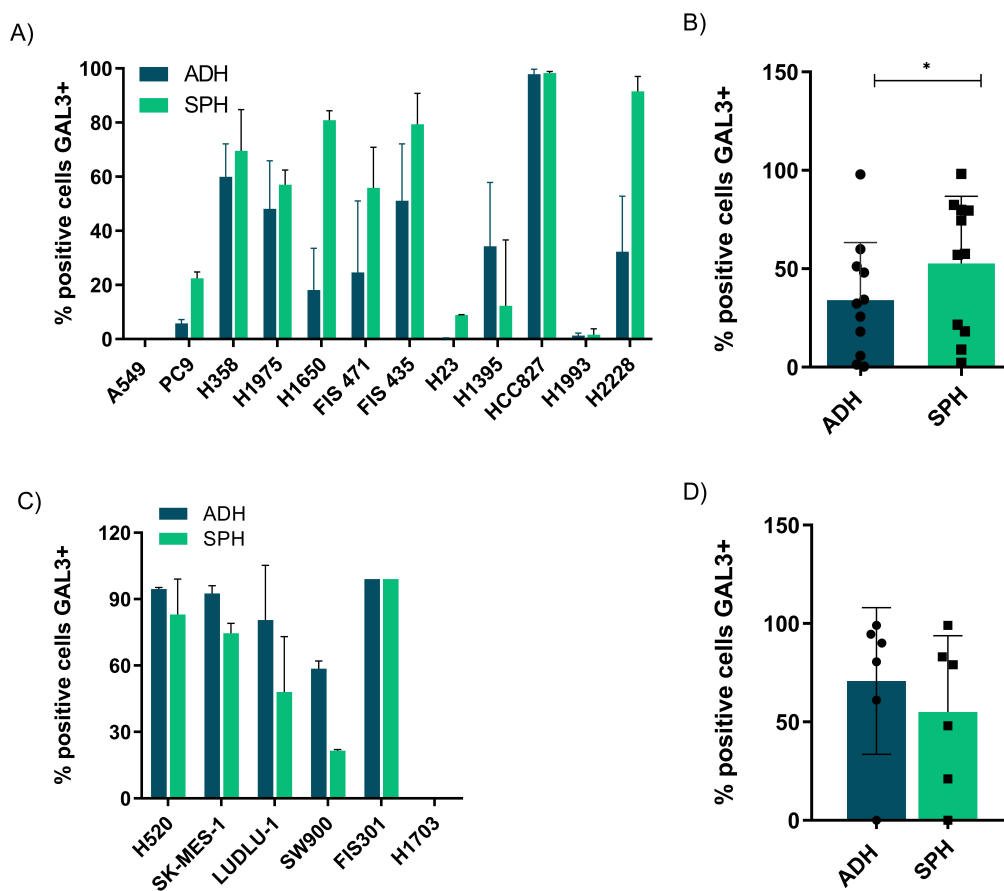
Figure 21. Flow cytometry (FC) analysis of GAL3. A,B) FC analysis of surface GAL3 in lung adenocarcinoma (LUAD) adherent-cultured cells and tumorspheres. A) The results shown are individual results for each cell line and patient derived lung cancer cell (PDLCC) cultures. Errors bars represent standard deviation (SD) of three different experiments. B) The results shown are the median of all cells lines and PDLCC cultures. Statistical analysis was carried out with the Wilcoxon test. Errors bars represent interquartile range (IQR) of the median. C,D) FC analysis of surface GAL3 in lung squamous cell carcinoma (LUSC) adherent-cultured cells and tumorspheres. C) The results shown are individual results for each cell line and PDLCC cultures. Errors bars represent SD of three different experiments. D) The results shown are the median of all cells lines and PDLCC cultures. Statistical analysis was carried out with the Wilcoxon test. Errors bars represent IQR of the median. ADH, adherent-cultured cells; SPH, tumorspheres; LUAD, lung adenocarcinoma; LUSC, lung squamous cell carcinoma; n, sample size; PDLCC, patient derived lung cancer cell; IQR, interquartile range. Significance values were *p<0.05.

Some ports confirm the extracellular location of GAL3 on the cell surface in different type of tissues. GAL3 exhibits a strong affinity for β1,6-GlcNAc-branched N-glycans and glycoproteins, leading to the formation of molecular complexes on the cell surface and ECM. This interaction consequently influences the distribution of glycoproteins and cell signal transduction (F. T. Liu & Rabinovich, 2005). Furthermore, GAL3 on the cell surface plays a role in the homotypic aggregation of tumor cells within the bloodstream during metastasis, achieved by binding to complementary serum glycoproteins. These glycoproteins serve as connecting links between neighboring cells (Inohara & Raz, 1995).

The presence of GAL3 in cell surface has also been linked to biological behaviors related to CSC. Specifically, Ilmer et al. exposed that GAL3 on the cell surface distinguishes a specific group of gastrointestinal tumor-initiating cancer cells resistant to chemotherapy, exhibiting elevated stem cell properties. To be specific, GAL3-positive CSCs were characterized by high ALDH, increased *in vitro* self-renewal capacity (sphere formation), and greater tumor-forming potential *in vivo*. They also demonstrate resistance to chemotherapeutic agents and apoptosis induced by death receptors in comparison to GAL3-negative CSCs (Ilmer et al., 2016). Considering that in previous studies in our laboratory, we demonstrated that lung tumorspheres possess stem-like properties, and furthermore, in this study, we observed that tumorspheres are enriched in GAL+ cells, we could speculate that cell surface GAL3 expression identifies a subset of CSCs in lung tumorspheres as well. Further analysis are being carried out to validate this hypothesis.

Other authors revealed that GAL3 on the cell surface confers resistance to tumor necrosis factor-related apoptosis-inducing ligand (TRAIL) by obstructing the movement of death receptors in metastatic colon adenocarcinoma cells (Mazurek et al., 2012).

4.2. IMMUNOFLUORESCENCE

In addition to the immunoblotting, we performed IF analysis of GAL3 localization patterns in both culture conditions from LUAD cultures. Remarkably, variations in the subcellular distribution of GAL3 (membranous, nuclear, and cytoplasmic) were noted, but without significant distinctions between lung tumorspheres and adherent-cultured cells, as observed through immunofluorescence (Figure 22). Notably, no signal was detected in A549 and H23, in concordance with the previously observed low levels of expression and secretion.

GAL3 can be either localized in the nucleus, cytoplasm, plasma membrane or secreted into extracellular space, however the primary location is in the cytoplasm according with our results (Farhad et al., 2018). Regarding cytoplasm, GAL3 could be implied in various intracellular events. Numerous cytosolic molecules were identified as GAL3 ligands (Dumic et al., 2006). The first cytosolic molecule identified as a GAL3 ligand *in vivo* was Bcl-2, a molecule involved in regulation of apoptosis (R. Y. Yang et al., 1996). Many other molecules involved in apoptotic signaling pathway have been recently identified as a novel GAL3 binding partners such as CD95 (APO-1/Fas) or Alix/AIP1 (Fukumori et al., 2004)(F. T. Liu & Rabinovich, 2005). Moreover, the role of cytosolic GAL3 in controlling cell proliferation, differentiation, survival, and apoptosis has been further validated through observations of its impact on K-Ras protein in other types of cancer cells (Shalom-Feuerstein et al., 2005) and Akt protein (Lee et al., 2003; Oka et al., 2005). Recently, it has been reported that GAL3 in cytoplasm activates TLR4 signaling thus affecting lung cancer cell proliferation and migration through TLR4/NF-κB/NEAT1 (Zhou et al., 2018).

In nucleus, the tumorigenic potential of GAL3 could be linked to its interactions with β-catenin, leading to the upregulation of cyclin D and c-MYC expression (Shimura et al., 2004) and facilitating cell cycle progression (Dumic et al., 2006). The nuclear presence of GAL3 has the capacity to modulate gene transcription by augmenting the association of transcription factors with Sp1 and CRE elements within gene promoter sequences (Dumic et al., 2006).
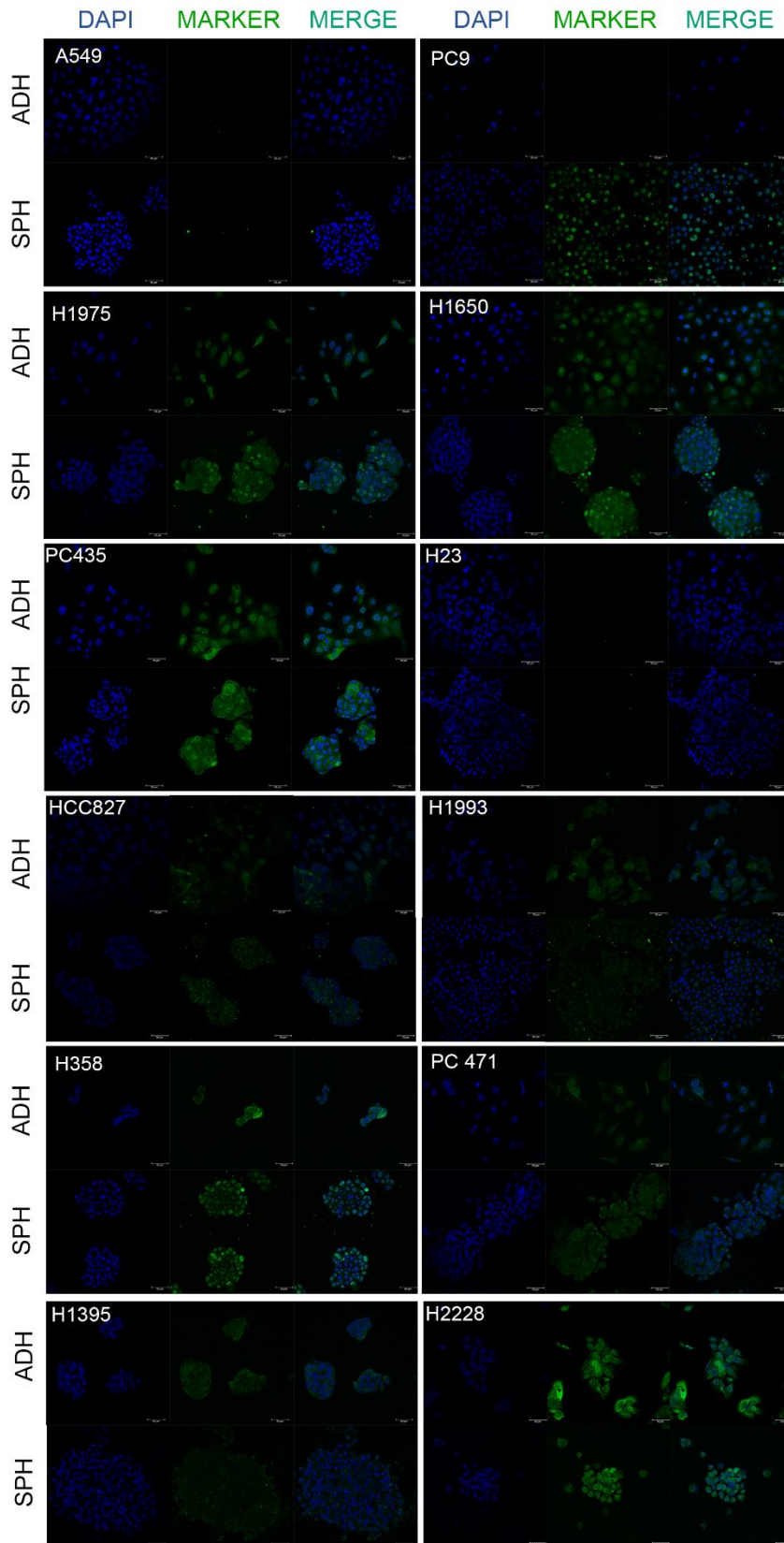
Figure 22. Representative immunofluorescence (IF) images of GAL3 in adherent-cultured cells and tumorspheres from LUAD cultures. Green channel in IF shows the indicated antibody staining GAL3, blue channel shows DAPI staining, and merge shows all channels merged. ADH, adherent-cultured cells; SPH, tumorspheres; IF, immunofluorescence; DAPI, 4',6-diamidino-2-fenilindol; LUAD, lung adenocarcinoma. Scale bar represents 50 µm.

4.3. CORRELATION OF LGALS3 AND LGALS3BP

Due to its relationship with GAL3, we decided to study the gene expression levels of galectin-3 binding protein (*LGALS3BP*) in LUAD cell cultures and its correlation with *LGALS3*. LUAD tumorspheres exhibited significantly higher *LGALS3BP* expression compared to adherent-culture cells at both 12-hour and 24-hour time points, as determined by Wilcoxon's signed-rank test across all cell lines and PDLCC cultures (Figure 23 A,B). Furthermore, the expression of *LGALS3BP* showed a positive correlation with *LGALS3* expression in LUAD cell cultures, encompassing both adherent-cultured cells and tumorspheres (R=0.62, *p*=0.0014 and R=0.64, *p*=0.00095, respectively) (Figure 23 C,D) .
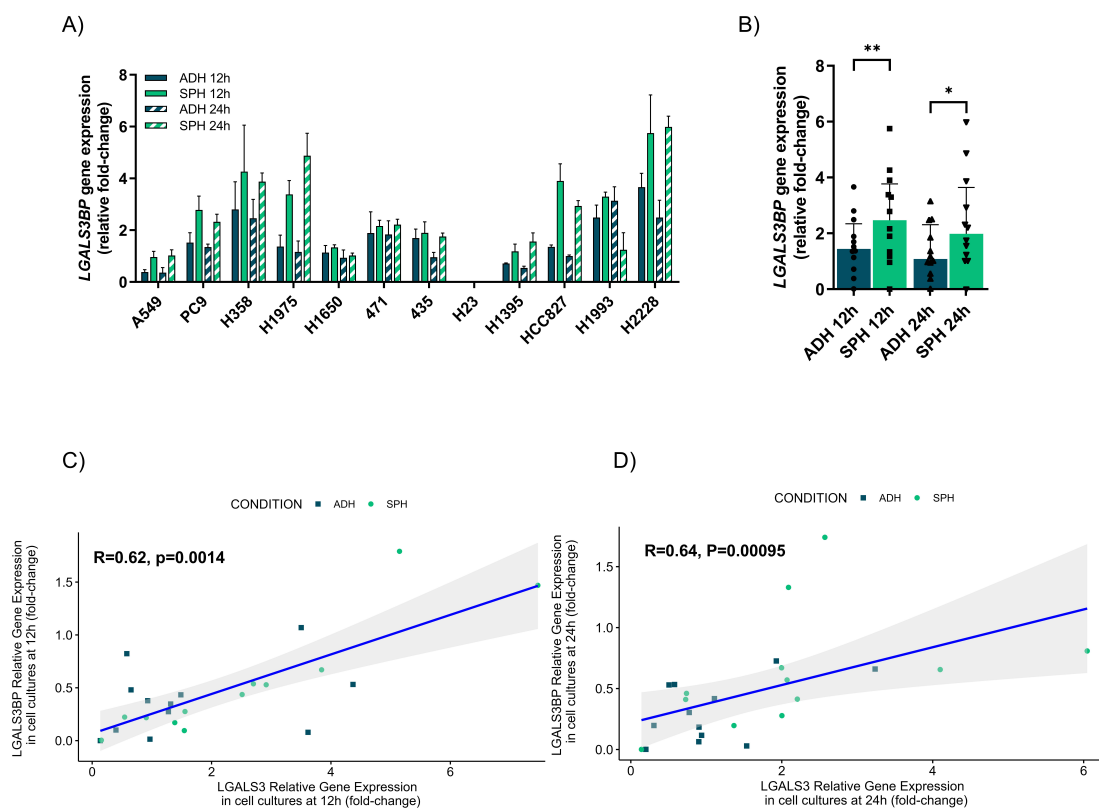
Figure 23. Transcription levels of *LGALS3BP* in adherent-cultured cells vs. tumorspheres in lung adenocarcinoma (LUAD) patient derived lung cancer cell (PDLCC) cultures and cell lines. mRNA was measured by RT-qPCR at 12 and 24 hours after cell seeding. A) The results shown the relative fold-change gene expression of *LGALS3BP* to reference genes *ACTB*, *CDKN1B*, and *GUSB* of each PDLCC cultures and cell line. Errors bars represent standard deviation (SD) of three different experiments. (B) The results shown are the median of relative fold-change gene expression of *LGALS3* to reference genes *ACTB*, *CDKN1B*, and *GUSB*. Errors bars represent interquartile range (IQR) of all samples (n=12). (C) Correlation between *LGALS3BP* expression levels and *LGALS3* expression levels in LUAD tumor cell cultures at 12 hours after cell seeding (n=12). (D) Correlation between *LGALS3BP* expression levels and *LGALS3* expression levels in LUAD tumor cell cultures after 24h after cell seeding (n=12). R represents the Spearman correlation coefficient. ADH, adherent; SPH, tumorspheres; n, sample size; LUAD, lung adenocarcinoma; PDLCC, patient derived lung cancer cell. Significance values were *p<0.05, ** p<0.01.

LGALS3BP is a heavily glycosylated protein that acts as a ligand for GAL3, promoting the survival of cancer cells throughout the metastatic process. (Capone et al., 2021). In a previous study, it was reported that in the microenvironment of human neuroblastoma, GAL3BP interacts with GAL3 in bone marrow mesenchymal stem cells, leading to the transcriptional upregulation of IL6 through the GAL3BP/GAL3/Ras/MEK/ERK signaling pathway (Fukaya et al., 2008; He et al., 2019). However, no prior studies have explored their correlation in lung cancer. Our findings suggest that these two genes may potentially cooperate in the pathological processes of cancer, but these data need further investigation.

4.4. ANALYSIS OF LGALS3 EXPRESSION IN EXTRACELLULAR VESICLES.

Next, we analyzed *LGALS3* expression in a large number of extracellular vesicle (EV) samples derived from NSCLC cell cultures under both adherent and tumorspheres conditions using RT-qPCR.

Consistent with our previous results, we confirmed that *LGALS3* exhibited significantly higher expression in LUAD secreted EVs originating from tumorspheres compared to those from adherent-cultured cells (*p*=0.001) (Figure 24 A,B). Conversely, there were no notable differences in *LGALS3* expression within the LUSC group (data not shown). The expression of *LGALS3* in LUAD cell-derived EVs displayed a positive correlation with *LGALS3* expression in LUAD cell cultures (R=0.54, *p*=0.011), and this correlation was even more pronounced when analyzing only the subgroup of tumorspheres (R=0.74, *p*=0.013) (Figure 24 C,D). Furthermore, a good correlation was observed between GAL3 secretion in LUAD cell cultures (sGAL3) and *LGALS3* expression in exosomes (R=0.74, *p*=0.00011) (Figure 24E). No significant correlations were detected in the LUSC group.
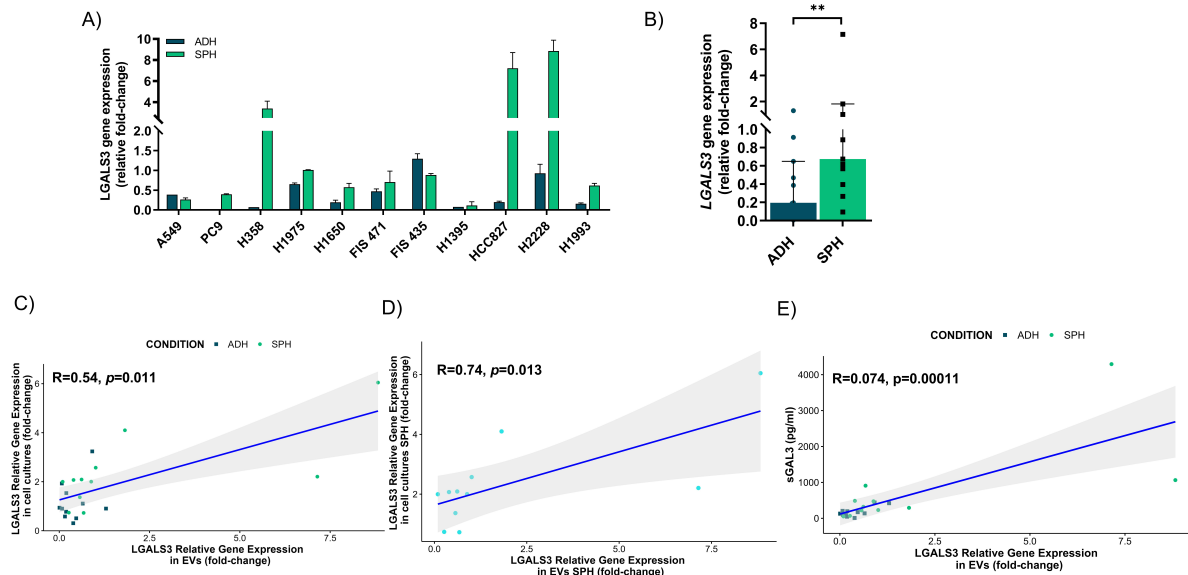
Figure 24. *LGALS3* **expression in lung adenocarcinoma (LUAD) tumor-derived extracellular vesicles (EVs) from adherent-cultured cells and tumorspheres and correlation with expression of *LGALS3* and secretion of sGAL3 in culture cells.** (A) The results shown the relative fold-change gene expression of *LGALS3* in LUAD tumor-derived EVs to reference genes *ACTB*, *CDKN1B*, and *GUSB*. Experiments were performed in duplicate. (B) The results shown are the median of relative fold-change gene expression of *LGALS3* in LUAD tumor derived-EVs to reference genes *ACTB*, *CDKN1B*, and *GUSB*. Statistical analysis was carried out with the Wilcoxon test. Errors bars represent interquartile range (IQR) of all samples (n=11). Significance values were ** *p*<0.01. (C) Correlation between *LGALS3* expression levels in LUAD tumor derived-EVs and *LGALS3* expression levels in LUAD tumor cell cultures (n=11). (D) Correlation between *LGALS3* expression levels in LUAD tumor derived-EVs from spheroids and *LGALS3* expression levels in LUAD tumorspheres cell cultures (n=22). E) Correlation between *LGALS3* expression levels in LUAD tumor derived-EVs and sGAL3 levels secreted by LUAD tumor cell cultures (n=11). Statistical analysis was carried out with the Spearman Correlation Coefficient. R represents the Spearman correlation coefficient. EVs, extracellular vesicles; LUAD, lung adenocarcinoma; ADH, adherent; SPH, tumorspheres; n, sample size; sGAL3 (soluble galectin-3). *P*-value was statistical significative *p*<0.05.

EVs represent a subgroup of small vesicles secreted by various cells, displaying a crucial role in intercellular communication. They have the potential to enhance cell proliferation and survival, influence the structure of the TME, and enhance invasive and metastatic behaviors. These EVs play a vital role in the TME by contributing as potent signaling molecules in the communication between cancer cells and neighboring cells (Dang et al., 2016). In our previous laboratory work, we conducted a comprehensive characterization on NSCLC EVs, revealing that the cargo within EVs can reflect molecular signatures and serve as a valuable tool for both diagnosis and prognosis (Duréndez-Sáez et al., 2022).

As we previously mentioned, GAL3 lacks a conventional signal sequence that would typically guide the protein to the ER/Golgi complex for subsequent secretion. Potential mechanisms involve the EVs (Hughes, 1999). GAL3 has been identified in EVs derived from DCs (Théry et al., 2001), bladder cancer (Welton et al., 2010), ovarian

cancer (B. Liang et al., 2013), melanoma (Lazar et al., 2015) and leukemia cells (Fei et al., 2015), but there have been no documented reports of its presence in EVs from lung cancer. Although the process by which GAL3 becomes cargo in exosomes remains unclear, a hypothesis suggests that it may bind with glycosphingolipids capable of forming exosomes independently of conventional cellular mechanisms (Phuyal et al., 2014; Takeda et al., 2008). An interesting study revealed not only that exosomes act as a vehicle for GAL3 secretion, but also that GAL3 recruitment into intraluminal vesicles (ILVs) interaction leads to its release at the plasma membrane as exosomes. Particularly, these authors identified a highly conserved tetrapeptide motif, P(S/T)AP, located in the amino terminal domain of GAL3. This motif engages in a direct interaction with the endosomal sorting complex required for transport (ESCRT) component Tsg101, ultimately leading to exosomal released (Bänfer et al., 2018). In summary, our findings demonstrate that GAL3 is expressed in LUAD tumor-derived EVs from tumorspheres and is correlated with expression and secretion of GAL3 by tumor cells, suggesting that exosomes serve as vehicles for GAL3 secretion.

4.5. GALECTIN-3 ANS ITS RELATIONSHIP WITH IMMUNE CELLS.

GAL3 plays a pivotal role in TME particularly in regulating T cell populations. Therefore, we aimed to investigate the role of GAL3 as a possible immunomodulator in lung cancer to advance our understanding of GAL3 and its potential role in NSCLC. With a specific focus on the immune TME, previous studies have shown that extracellular GAL3, secreted by tumor cells, hinders TCR movement, induces T cell apoptosis, and enhances TCR downregulation (H. Y. Chen et al., 2009; Guha et al., 2013; Kouo et al., 2015). However, the impact of GAL3 on macrophages and T_{REGS} remains relatively unexplored. This knowledge gap prompted us to undertake comprehensive research. Our approach encompasses a complex analysis, involving cell cultures and patient samples, with the ultimate goal of generating clinically relevant insights.

4.5.1. *IN VITRO* APPROACH

The initial approach, based on cell cultures, involved the use of CM collected from PC435 tumorspheres and co-culture of lung tumorspheres with a fibroblast cell line 154CAFh-TERT which has features of CAFs. These different CM were used for culturing macrophages and lymphocytes, with and without treatment using a blocking GAL3 monoclonal antibody. This approach aimed to examine their influence on macrophages and T_{REGS} and to evaluate the potential involvement of sGAL3 in these interactions.

First, we assessed the impact of CM derived from tumorspheres and co-cultures, with or without anti-GAL3 treatment, on the polarization of M0 macrophages toward TAM, which are characterized for their immunosuppressive properties. For this purpose, we measured gene expression of proinflammatory cytokines *IL12A, VEGFA* and *IL6*, typically expressed by M1 macrophages, as well as immunosuppressive cytokines *IL10*, *CD163*, *CD206*, *NOS2* and *ARG2*, commonly expressed by M2 macrophages. The expression of *B2M* gene was used as the internal control. The relative expression levels of *IL12A*, *NOS2*, *ARG1* were below the limit of detection of the technique in most samples and were excluded from the final analysis. No significant differences were observed in macrophage responses to CM, whether or not the anti-GAL3 treatment was added (Figure 25).

Previous studies have indicated that GAL3 plays a crucial role in regulating macrophage function, promoting an "M2" phenotype (MacKinnon et al., 2008; Vuong et al., 2019). However, our current approach did not reveal any significant effect of GAL3 secreted by lung tumorspheres on macrophage polarization. It might be worthwhile to explore potential differences using alternative techniques, such as FC, and expand our cohort to include more healthy volunteers.
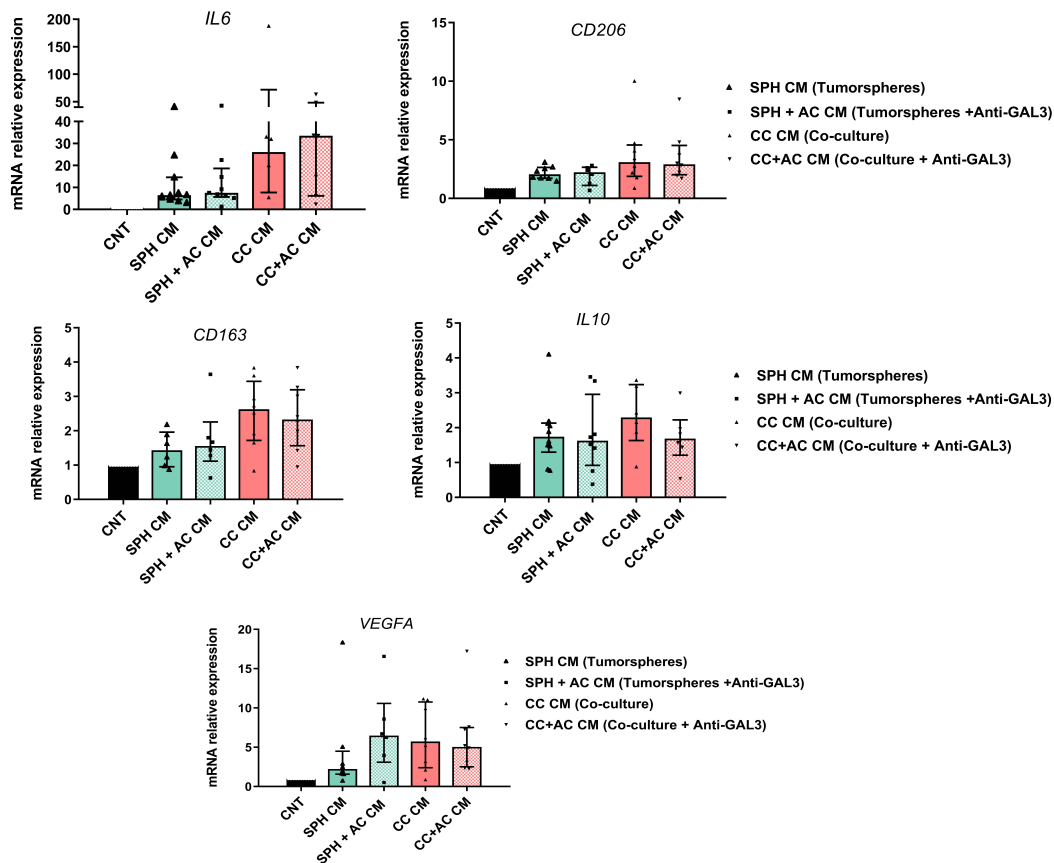
Figure 25. Effects of conditioned media (CM) from tumorspheres and co-culture with fibroblast on TAM polarization. RT-qPCR quantification of *IL6, CD206, CD163, IL10* and *VEGA* gene expression in macrophages derived from PBMCs from 9 healthy volunteers. Macrophages were incubated for 72 h with CM from tumorspheres or co-culture, untreated or treated with anti-GAL3 antibody. We used as a control (CNT) (50% of fibroblast medium (FBM) and 50% tumorspheres DMEM F12). Statistical analysis was carried out with the Wilcoxon test. Bars represent minimum and maximum points. CNT, control medium; CM, conditioned medium; SPH, tumorspheres; CC, co-culture; AC, anti-GAL3; TAM, tumor associated macrophages; RT-qPCR, real time quantitative polymerase chain reaction. P-value was statistical significative p<0.05.

Second, we evaluated the impact of CM derived from tumorspheres and co-cultures on the modulation of T_{REGS} (CD4+Foxp3+CD25+). CM from tumorspheres (SPH CM) and co-cultures (CC CM) significantly increased the proportion of T_{REGS} compared to the control group, showing a 1.9-fold and 1.7-fold-increased, respectively (*p*=0.008 and *p*=0.01, respectively). Remarkably, the blockade of sGAL3 in CC CM was sufficient to prevent the increase of T_{REGS} population significantly (*p*=0.028) (Figure 26).
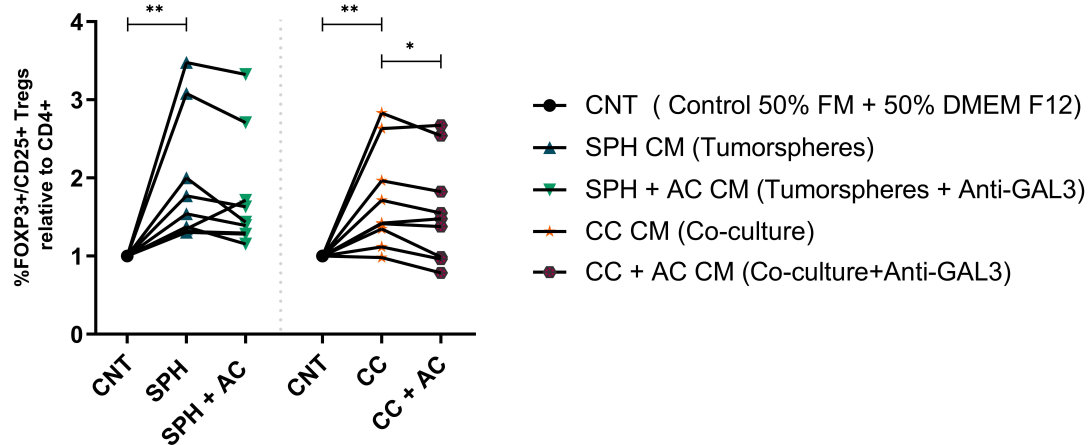
Figure 26. Conditioned media (CM) from tumorspheres induces T$_{REGS}$ that can be prevented by GAL3 blockade. Flow cytometry analysis for T$_{REG}$ population within T lymphocytes (T$_{REGS}$: CD4+Foxp3+CD25+), from n=9 healthy volunteers. T lymphocytes were incubated for 72 h with CM from tumorspheres or co-culture, untreated or treated with anti-GAL3 antibody. Data are the median value in % T$_{REG}$ population FOXP3+/CD25+ relative to CD4$^+$. We used a control (CNT) (50% of fibroblast medium (FBM) and 50% tumorspheres DMEM F12). Statistical analysis was carried out with the Wilcoxon test. Lines represent the decreased or increased. n, sample size; CNT, control medium; CM, conditioned medium; SPH, tumorspheres; CC, co-culture; AC, anti-GAL3; T$_{REGS,}$ regulatory T cells. Significance values were *p<0.05, **p<0.01.

In our approach, to partially recreate and analyze the role that sGAL3 might play in the modulation of T$_{REGS}$, we used CM from tumorspheres and tumorspheres co-cultured with fibroblast (another important component of TME), both treated and untreated with a GAL3 neutralizing antibody, to treat lymphocytes and study the implication of T$_{REGS}$. Our first approximation suggests that sGAL3 could have an impact on T$_{REGS}$ cells. No previous studied have elucidated the role of GAL3 on T$_{REGS}$.

Regarding the analysis of the modulatory role of factors in the tumor-stroma interactions, there are different approaches, such as CM, direct co-culture or indirect co-culture (via transwell). The CM strategy has been used extensively for studying tumor-stroma interactions over time. For instance, Nallasamy et al., used CM-derived from fibroblasts to investigate the interplay between CAFs and stemness properties in pancreatic tumors (Nallasamy et al., 2021). Other authors employed CM from fibroblast or macrophages to study the crosstalk between stromal components and tumor cells in triple negative breast cancer (K. Jin et al., 2017). Moreover, Michielsen et al., measured the degree of suppression by tumor-conditioned media (TCM) on lipopolysaccharide-induced DCs activation, both in the absence and presence of bevacizumab (anti VEGFR monoclonal antibody), to assess whether the immunosuppressive activity of tumors would influence the response to bevacizumab or patient survival (Michielsen et al.,

2012). Since we observed that our tumorspheres secrete high levels of GAL3, and CM was easy to obtain and reliable, we chose this approach over other possibilities.

While a validation using *in vivo* syngeneic models could be interesting, it is essential to acknowledge that current animal models for studying TME require further refinement due to their inherent complexity. Therefore, we have complemented our research with additional validation conducted using patient samples to explore the relationship between GAL3 with T$_{REGS}$.

4.5.2. A STRATEGY BASED ON FORMALIN-FIXED PARAFFIN-EMBEDDED SAMPLES FROM HGUV COHORT

Continuing this path, we aimed to delve deeper into the relationship between GAL3 and various T cell markers, including FOXP3, which is the most specific marker for T$_{REGS}$, within a more translational context to further support our prior findings. To achieve this, we established correlations between *LGALS3* expression in frozen tumor samples and the infiltration of FOXP3+, CD4+, and CD8+ lymphocytes, as well as the expression of these markers in FFPE samples from both the tumor and the tumor-adjacent stromal compartments.

In the stromal compartment, the count of positively stained cells per high-powered field (HPF) ranged from 0 to 21 for FOXP3+, 0 to 37 for CD4+, and 9 to 55 for CD8+. In contrast, within the tumor compartment, these counts ranged from 0 to 8 for FOXP3+, 0 to 12 for CD4+, and 1 to 24 for CD8+. Notably, we observed a positive correlation between patients who exhibited a high infiltration of FOXP3+ cells in the tumor and those with elevated expression of *LGALS3* in the tumor (R=0.6, *p*=0.019) (Figure 27). No other significative correlations were identified with the remaining T cell markers (Table 10).
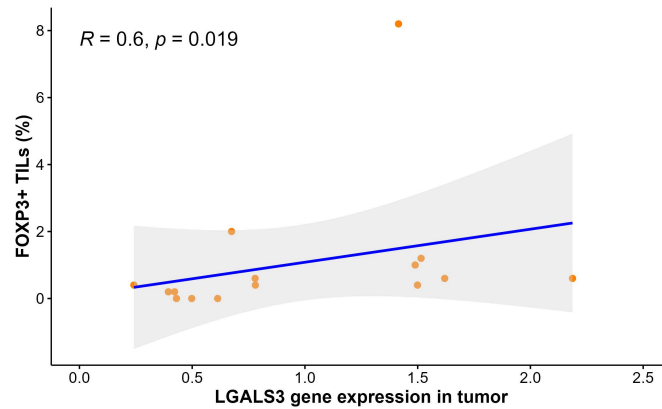
Figure 27. Correlations between infiltration of FOXP3⁺ lymphocytes from formalin-fixed paraffin-embedded (FPEE) samples and *LGALS3* expression levels in frozen tumor tissue (n=15). Statistical analysis was carried out with the Spearman Correlation Coefficient. R represents the Spearman correlation coefficient. P-value was statistical significative $p<0.05$.

Table 10. Correlations between infiltration of FOXP3⁺, CD4+ and CD8+ lymphocytes in tumor or stroma compartments from FPEE samples and LGALS3 expression levels in frozen tumor tissue though Spearman Correlation Coefficient.

		FOXP3+TILS in tumor	FOXP3+TILS in stroma	CD4+TILS in tumor	CD4+TILS in stroma	CD8+TILS in tumor	CD8+TILS in stroma
***LGALS3* in tumor**	R coefficient	0.6	0.121	-0.310	-0.516	0.075	0.021
	p-value	0.019*	0.666	0.260	0.05	0.789	0.940

Statistical analysis was carried out with the Spearman Correlation Coefficient. R represents the Spearman correlation coefficient. Significance values were *$p<0.05$.

Next, we assessed the correlation between *LGALS3* expression in the tumor and the gene expression levels of *FOXP3*, *CD4* and *CD8* in samples obtained through microdissection from FFPE tissues, including both the tumor and stromal areas. The results of individual correlations are shown in Table 11. In this case, we did not detect a correlation with FOXP3 levels. However, a significative negative correlation between *LGALS3* expression in the tumor with the expression levels of *CD8* in the stroma area was shown (R=-0.606, *p*=0.009) (Figure 28A). Subsequently, we attempted to identify additional correlations between *FOXP3* and *LGALS3* expression by combining these genes with other T cell markers. We opted to combined T cell markers such as CD4 (indicative of T helper cells) and CD8 (indicative of T cytotoxic cells) in conjunction with FOXP3. To achieve this, new variables based on the ratio of these markers were calculated, and the data correlations are presented in Table 12.

Table 11. Correlations between *LGALS3* expression levels in tumor and gene expression levels of *FOXP3*, *CD4* and *CD8* in samples obtained by microdissection from formalin-fixed paraffin-embedded (FFPE) tissues.

		FOXP3 in tumor	*FOXP3* in stroma	*CD4* in tumor	CD4 in stroma	*CD8* in tumor	*CD8* in stroma
***LGALS3* in tumor**	R coefficient	0.044	-2.13	-0.469	-0.475	-0.087	-0.606
	p-value	0.858	0.411	0.032*	0.040*	0.708	0.009**

R represents the Spearman correlation coefficient. Significance values were *p<0.05, **p<0.01.

Table 12. Correlations between *LGALS3* expression levels in tumor and ratios between gene expression levels of *FOXP3* in tumor and *CD4* and *CD8* in tumor and stroma in samples obtained by microdissection from formalin-fixed paraffin-embedded (FFPE) tissues.

		FOXP3 T/ CD4 T	*FOXP3* T/ CD4 S	*FOXP3* T/ CD8 T	*FOXP3* T/ CD8 S
***LGALS3* in**	R coefficient	0.589	0.589	0.089	0.549
tumor	*p-value*	0.008**	0.010*	0.716	0.022*

R represents the Spearman correlation coefficient. T,tumor; S, stroma. Significance values were *p<0.05, **p<0.01.

Among the various combinations we assessed for their correlation with *LGALS3* expression in the tumor, we identified a notable positive and significant correlation with *LGALS3* expression. This correlation was observed between the ratio of *FOXP3* expression within the tumor compartment and the expression of *CD8* in the stromal compartment (R=0.55, *p*=0.024) (Figure 28B). Additionally, we observed another positive and significant correlation with *LGALS3* expression, this time between the ratio of *FOXP3* expression within the tumor compartment and the *CD4* expression in either the tumor or stromal compartments (Figure 28 C,D).
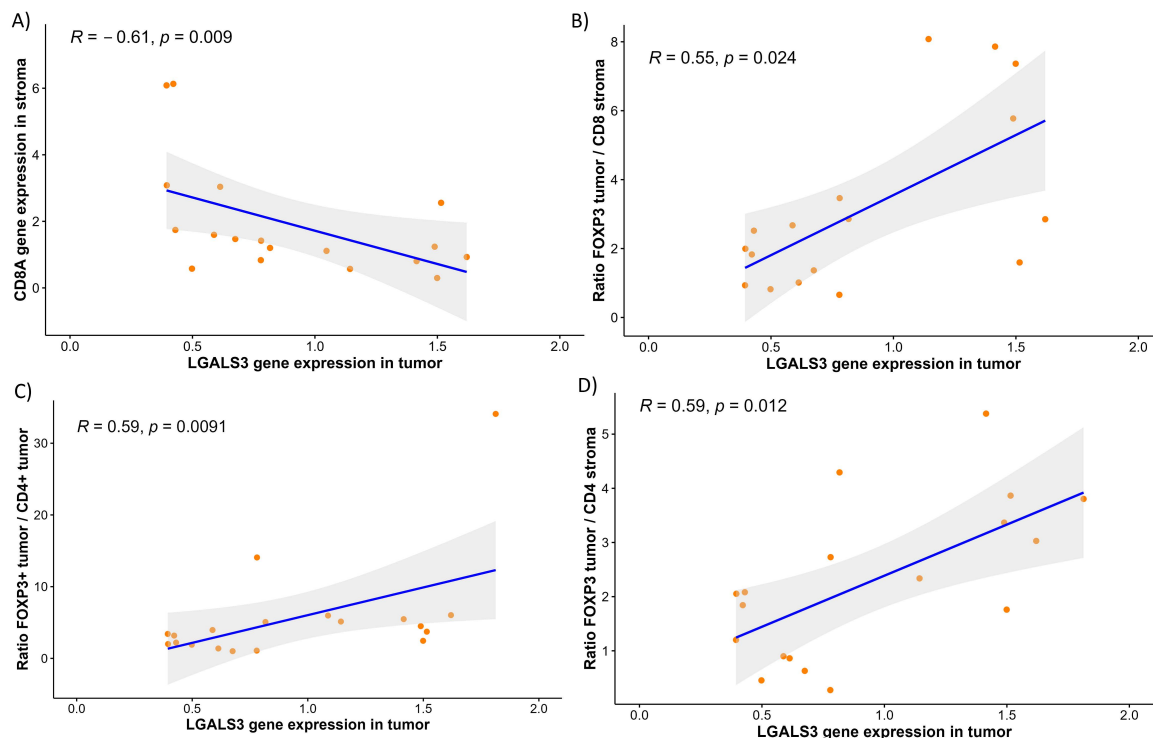
Figure 28. Correlation between *LGALS3* and *CD4* or *CD8* expression levels in tumor in samples obtained by microdissection from formalin-fixed paraffin-embedded (FFPE) tissues. A) Correlation between *LGALS3* expression levels in tumor and CD8 expression levels in tumor (n=18) B) Correlation between *LGALS3* expression levels in tumor and FOXP3 tumor/CD8 stroma ratio (n=17). C) Correlation between *LGALS3* expression levels in tumor and FOXP3 tumor/CD4 tumor ratio (n=19). D) Correlation between *LGALS3* expression levels in tumor and FOXP3 tumor/CD4 stroma ratio (n=18). Statistical analysis was carried out with the Spearman Correlation Coefficient. R represents the Spearman correlation coefficient. P-value was statistical significative *p*<0.05.

These results suggest that among the T cell populations we have studied, T_REGS (characterized by the expression of FOXP3) are the ones that exhibit a positive correlation with *LGALS3* levels. We have found that higher levels of *LGALS3* are associated with increased levels of FOXP3, both in terms of proportion and expression. T_REGS, an immunosuppressive subset of CD4+ T cells, play a role in compromising immune surveillance against cancer in healthy individuals and impairing the antitumor immune response in tumor-bearing hosts. T_REGS are crucial in the context of cancer immunotherapy, and elevated levels of tumor-infiltrating T_REGS are indicative of poor prognosis in patients with various types of cancers, including NSCLC (J. Liang et al., 2022; Usó et al., 2016). Mechanisms governing T_REGS accumulation, activation, and survival within the TME have been discovered for different tumor types. Based on the results obtained in this study, we can propose that one of the mechanisms by which lung tumor cells attract T_REGS to the tumor might involve GAL3.

Previously, only one study had reported a relationship between GAL3 and the frequency and function of T_REGS (Fermino et al., 2013). In their study, these authors revealed that endogenous GAL3 regulates the frequency and function of CD4+ CD25+ Foxp3+ T_REGS cells, thereby altering the course of Leishmania major infection. In contrast to our findings, their study indicated that GAL3 deficiency led to an increased frequency of peripheral T_REGS in both draining LNs and sites of infection. It's important to note that our study is fundamentally different because we focus on T_REGS within the TME, specifically in the context of lung cancer. Furthermore, Fermino et al. examined T_REGS in the settings of LNs and infection sites, related to a different disease entirely.

Conversely, our study has also unveiled a negative correlation between *LGALS3* expression in the tumor and the expression levels of *CD8* in stromal compartment. This finding is consistent with existing literature (Kouo et al., 2015; Vuong et al., 2019).

4.5.3. A STRATEGY BASED ON CIBERSOTX TOOL WITH TCGA DATABASE

Next, to validate the relationship between *LGALS3* expression and various cellular subtypes, including T_REGS, which is of particular interest to our research, we used the

CIBERSORTx platform to analyze a patient cohort from TCGA. This study was conducted including the proportions of T_{REGS}, activated CD4 memory T cells, CD8 T cells, M1 macrophages, and M2 macrophages within the tumors of 356 resectable LUAD patients. Our analysis resulted in the identification of four distinct subgroups through k-means clustering, categorized as follows: Hot tumors, Cold tumors, M2 high tumors, and T_{REGS} high tumors (Figure 29A). A scatterplot illustrating these four clusters through PCA is presented in Figure 29B. Furthermore, we investigated the correlation between patient clusters and *LGALS3* expression. As depicted in Figure 29A, a noticeable trend indicates that tumors with a higher proportion of T_{REGS} tend to have a greater percentage of patients exhibiting elevated *LGALS3* expression. More specifically, 65.45% of the patients within this cluster exhibited upregulated *LGALS3* (Figure 29C).
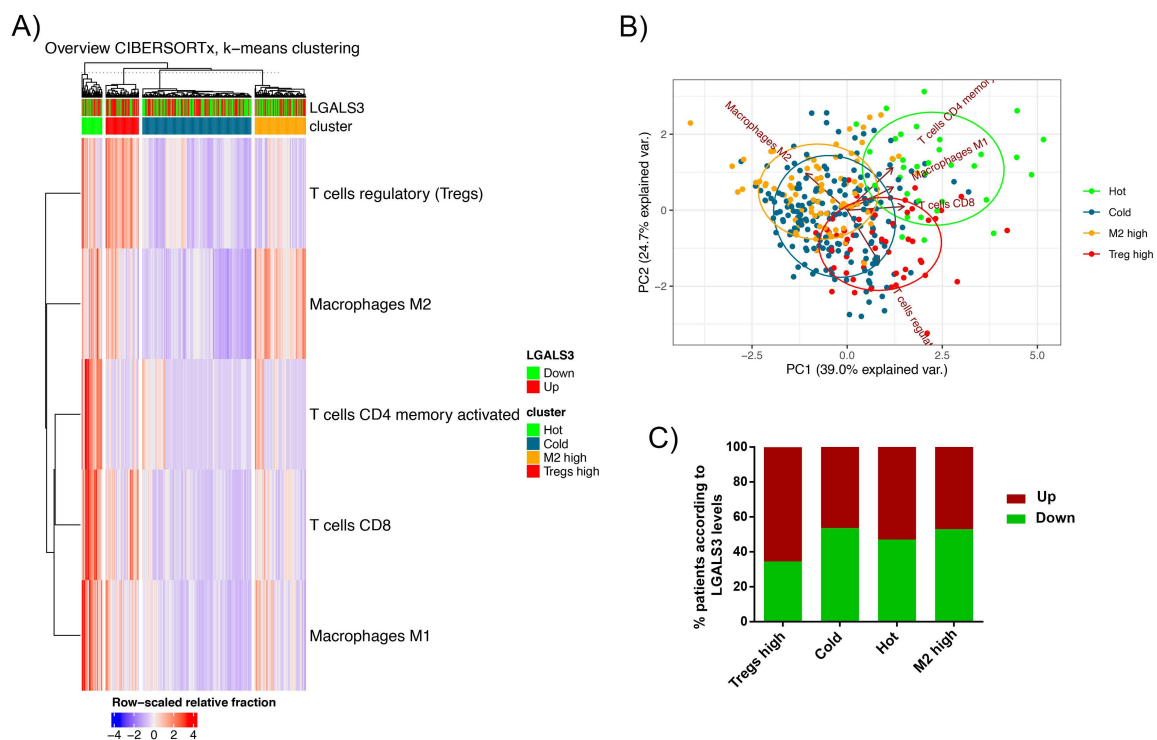
Figure 29. Results of immune cell infiltration clustering and expression of *LGALS3*. A) K-means heatmap. Four distinctive clusters of patients (n=356) were identified by using hierarchical clustering algorithm with Complex Heatmap package based on different immune cell infiltration. Clusters are distinguished by hot tumors (Hot), cold tumors (Cold), M2-enriched tumors (M2 high), and regulatory T cell-enriched tumors (T_{REGS} high). More red color designates higher expression for a given sample while blue designates lower expression. *LGALS3* expression is shown on top. Red color represents overexpression and green represents under expression. B) The scatterplot performed by principal component analysis (PCA) to show the four distinct clusters. C) Bar charts representing the percentage of patients with upregulated *LGALS3* and downregulated *LGALS3* in the 4 clusters.

Considering the outcomes of the three approaches we have presented, and the hypothesis that GAL3 modulates immune functions to facilitate tumor immunosuppression, we can affirm that our study suggests that, among the various T cell populations investigated, tumors may employ GAL3 as a mechanism to attract T_{REGS}, contributing to immune evasion. A graphical abstract of this part of the thesis (Chapter I) is shown in Figure 30.
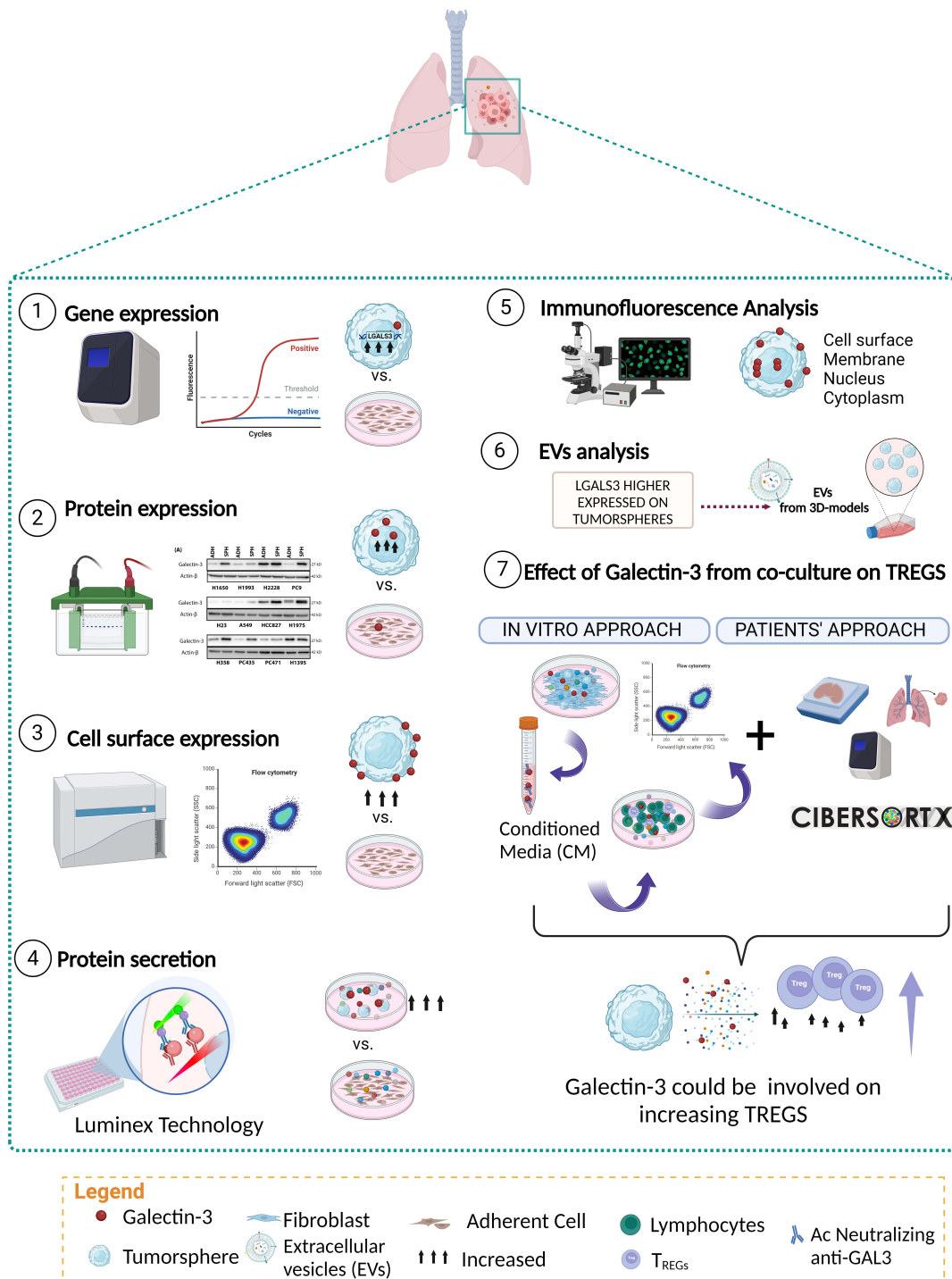
Figure 30. Chapter I graphical abstract. Own design created with BioRender.com.

CHAPTER II. TRANSLATIONAL PHASE: STUDY OF IMMUNE-MEDIATORS BIOMARKERS.

The implications of sGAL3 on NSCLC patients were studied in this second chapter through plasma samples. We employed an multiparametric immunoassay based on Luminex® xMAP®, a technology that allows the investigation of many analytes simultaneously with speed and sensitivity (*XMAP® Technology – The World's Most Used Multiplexing Technology*, 2023). This approach enabled us to examine not only sGAL3 but also other immune-mediators, including sFGL1, sCD276, sGAL1, sGAL3, sMICA and sMICB.

A) STUDY OF BIOMARKERS IN EARLY-STAGE NSCLC FROM CHGUV (TEST COHORT)

1. CLINICOPATHOLOGICAL VARIABLES

This study included 91 patients with NSCLC who underwent resection at CHGUV. This cohort included the two primary subtypes of NSCLC: LUAD and LUSC subtypes. Table 13 presents the most relevant demographic and clinicopathological characteristics of this cohort. The median patient age was 65 years [range: 42-84], with 73.6% being male, and 52.7% having LUADs. Additionally, 47.3% of the patients were diagnosed at stage I of the disease, and 65.6% presented a performance status (PS) = 0.

The prognostic value of the different clinicopathological variables was assessed using the univariate Cox regression method for RFS and OS and are shown in Table 14 along with the hazard ratios and *p*-value for each variable. Significant results obtained from the univariate Cox regression method were also analyzed using the Kaplan-Meier method (log-rank) to obtain the survival plots (Figure 31). The univariate analysis revealed that patients with large tumors, smokers, more advanced disease stages, and males had shorter RFS. In addition, individuals with large tumors, worse PS, advanced disease stages, and males had worse OS, consistent with previously published results (Garinet et al., 2022). Studies have revealed that women who underwent pulmonary resections for lung cancer had a significantly better prognosis than men (Cerfolio et al.,

2006; Sachs et al., 2021). Regarding PS there is some debate, but our results align with Powell et al. who demonstrated that a poor PS at diagnosis correlated with a higher risk of early death after resection (Powell et al., 2013). Additionally, some studies also revealed that active smokers at diagnosis have a worse prognosis compared to former or non-smokers (Andreas et al., 2013; Sheikh et al., 2021). Large tumors have also been correlated with poor prognosis in NSCLC (Cangir et al., 2004; K. Zhang et al., 2021). Finally, tumor staging is the most objective and reproducible prognostic factor studied, with advanced stages being associated with a worse prognosis (Goldstraw et al., 2016).

Table 13. Clinicopathological characteristics of early-stage NSCLC test cohort from CHGUV included in the study.

Characteristics	n	%
Age at surgery (median, range):	65 [IQR, 42–84]	
Gender		
Male	67	73.6
Female	24	26.4
Stage		
I	43	47.3
II	30	33
III	18	19.8
Histology		
LUSC	42	46.2
LUAD	48	52.7
Others	1	1.1
PS		
0	59	65.6
1	30	33.3
2	1	1.1
Smoking status		
Current	44	48.4
Former	34	37.4
Never	13	14.3
EGFR mutational status		
Mutated	9	9.9
Wildtype	66	72.5
NS	16	17.6
KRAS mutational status		
Mutated	11	12.1
Wildtype	55	60.4
NS	25	27.5

LUAD, lung adenocarcinoma; LUSC, lung squamous cell carcinoma; NS, non-specified; n, sample size: IQR; interquartile range; NSCLC, non-small cell lung cancer; CHGUV, *Consorcio Hospital General Universitario de Valencia*.

Table 14. Results from univariate survival analysis based on clinicopathological variables for the early-stage NSCLC test cohort.

Characteristics	RFS			OS		
Variable	**HR**	**95% CI**	***p*-value**	**HR**	**95% CI**	***p*-value**
Gender Male vs. Female	3.075	1.300-7.273	0.011*	3.090	1.207-7.928	0.019*
Age > 65 vs. ≤ 65	1.003	0.550-1.830	0.991	1.314	0.679-2.544	0.418
TNM Staging III vs. II vs. I	1.574	1.108-2.236	0.011*	1.568	1.071-2.296	0.021*
Histology LUAD vs. LUSC	0.905	0.534-1.532	0.710	0.894	0.501-1.956	0.704
Tumor Size T3/T4 vs. T2 vs. T1	1.818	1.132-2.919	0.013*	1.843	1.107-3.068	0.019*
LN involvement Yes vs. No	1.595	0.871-2.920	0.131	1.257	0.643-2.460	0.503
Smoking status Current/ Former vs. Never	3.412	1.054-11.047	0.041*	1.865	0.660-5.271	0.239
PS 0 vs. 1-2	1.658	0.910-3.022	0.099	1.950	1.027-3.704	0.041*

CI, confidence interval; HR, hazard ratio; LN, lymph node; RFS, relapse-free survival; OS, overall survival; PS, performance status; LUAD, lung adenocarcinoma; LUSC, lung squamous cell carcinoma; NSCLC, non-small cell lung cancer. The results were obtained using the univariate Cox regression method. Significance values were *p<0.05.

The prognostic value of the clinicopathological variables was also assessed according to the tumor histology. LUAD subcohort comprised 48 patients, of whom 22 (45.8%) experienced relapsed, and 21 (43.8%) died. Again, in the univariate analysis, gender and PS were found to be associated with RFS and OS (Table 15). Survival plots from Kaplan-Meier survival analysis are represented in Figure 32.

Table 15. Results from univariate survival analysis based on clinicopathological variables for the early-stage LUAD test subcohort.

Characteristics	RFS			OS		
Variable	**HR**	**95% CI**	***p*-value**	**HR**	**95% CI**	***p*-value**
Gender Male vs. Female	2.802	1.117-7.031	0.028*	2.870	1.049-7.848	0.040*
Age > 65 vs. ≤ 65	0.738	0.327-1.662	0.163	1.071	0.453-2.529	0.879
TNM Staging III vs. II vs. I	1.762	1.086-2.857	0.022*	1.653	0.977-2.797	0.061
Tumor Size T3/T4 vs. T2 vs. T1	1.792	0.976-3.293	0.060	1.506	0.805-2.815	0.200
LN involvement Yes vs. No	2.023	0.878-4.661	0.098	1.556	0.626-3.866	0.341
Smoking status Current/ Former vs. Never	3.311	0.981-11.17	0.054	1.803	0.599-5.427	0.294
PS 0 vs. 1-2	3.354	1.352-8.321	0.009**	2.803	1.072-7.331	0.036*

CI, confidence interval; HR, hazard ratio; LN, lymph node; RFS, relapse-free survival; OS, overall survival; LUAD, lung adenocarcinoma. The results were obtained using the univariate Cox regression method. Significance values were *p<0.05; **p<0.01.
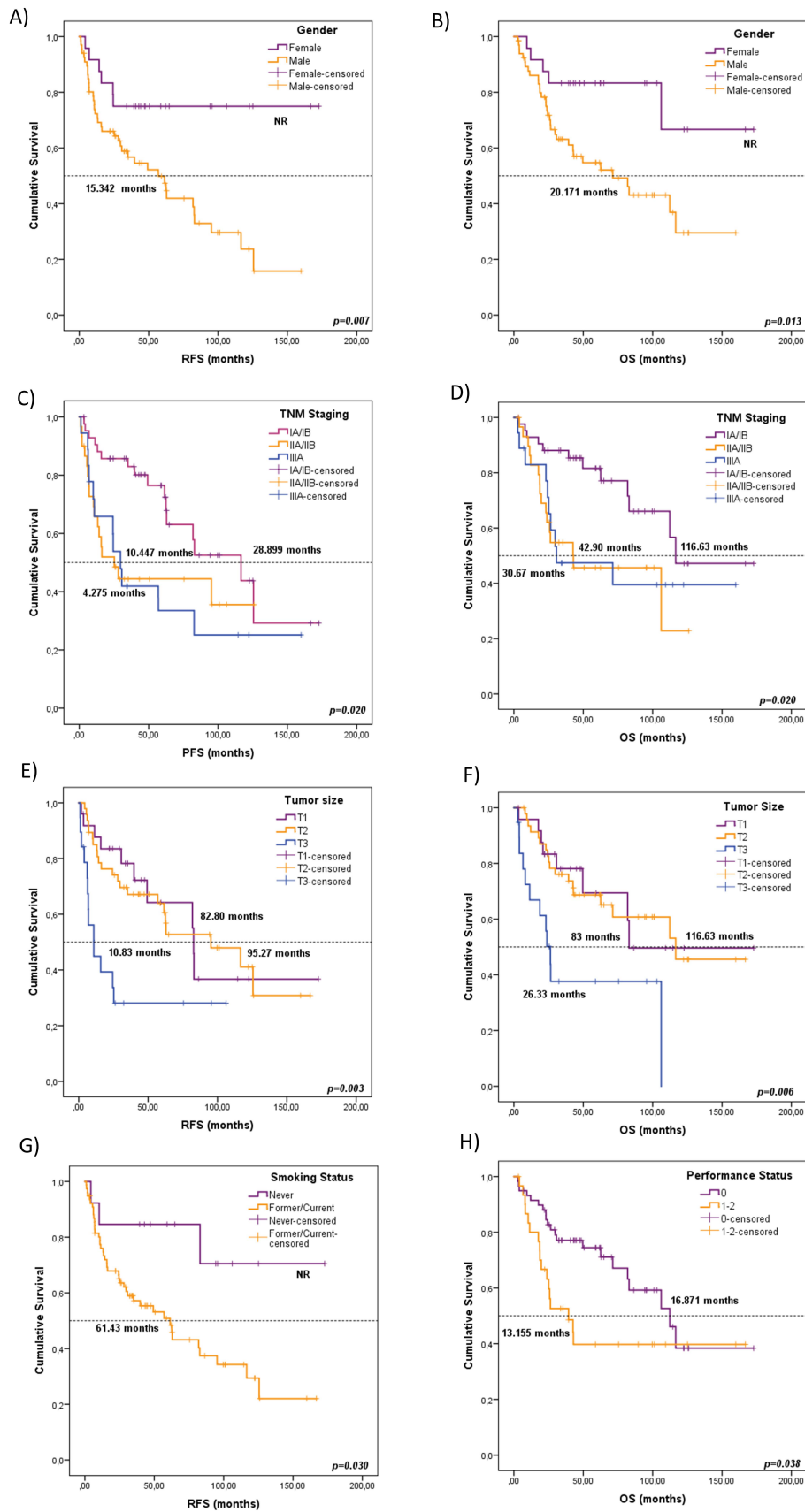
Figure 31. Kaplan-Meier plots for RFS and OS according to clinicopathological variables for the early-stage NSCLC test cohort. A-B. Gender; C-D. TNM staging; E-F. Tumor size; G. Smoking Status; H. Performance Status. RFS, relapse-free survival; OS, overall survival.**;** TNM, tumor-node-metastasis; NSCLC, non-small cell lung cancer; NR, not reached. *P*-values were calculated by log-rank test. *P*-value was statistical significative *p*<0.05.
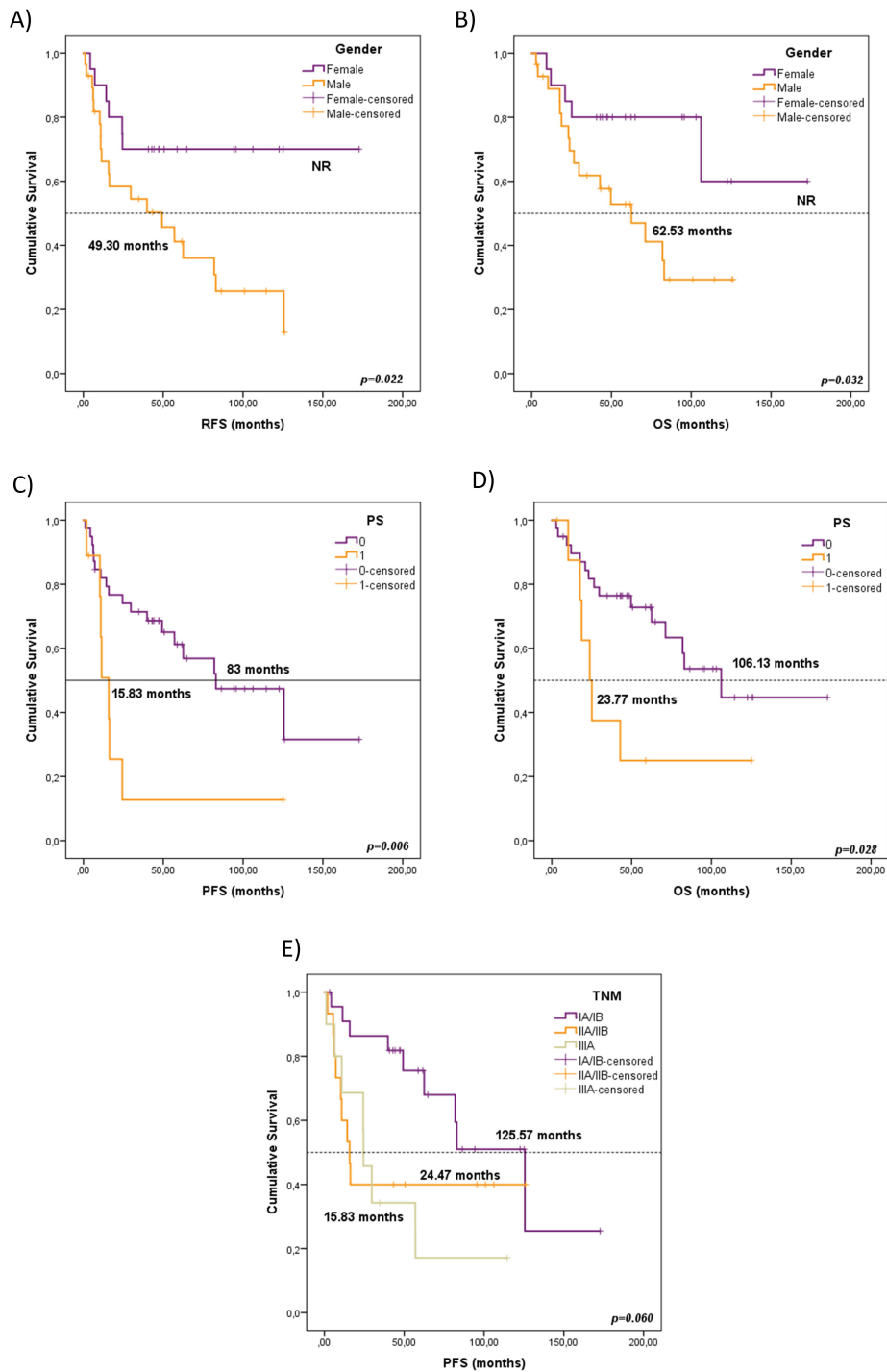
Figure 32. Kaplan-Meier plots for RFS and OS according to clinicopathological variables for the early-stage LUAD test subcohort. A-B. Gender; C-D. Performance Status; E. TNM Staging. P-values from the Kaplan-Meier test. PS, Performance Status; RFS, relapse-free survival; OS, overall survival; TNM, tumor-node-metastasis; LUAD, lung adenocarcinoma; NR, not reached. *P*-values were calculated by log-rank test. *P*-value was statistical significative *p*<0.05.

LUSC subcohort comprised 42 patients, with 19 (45.2%) experiencing relapsed and 17 (40.5%) dying. In contrast to the findings in LUAD patients, only tumor size was associated with RFS (*p*=0.017) and there was a trend for OS (*p*=0.051). No other significant associations were found between clinicopathological variables and RFS or OS in this group (Table 16). Survival plots from Kaplan-Meier survival analysis are represented in Figure 33.

Table 16. Results from univariate survival analysis based on clinicopathological variables for the early-stage LUSC test subcohort.

Characteristics	RFS			OS		
Variable	HR	95% CI	*p*-value	HR	95% CI	*p*-value
Gender Male vs. Female	24.503	0.025-24.503	0.362	24.840	0.028-22291.681	0.354
Age > 65 vs. ≤ 65	1.776	0.568-1.776	0.323	0.060	0.639-6.644	0.226
TNM Staging III vs. II vs. I	1.409	0.796-2.497	0.240	1.395	0.793-2.453	0.248
Tumor Size T3/T4 vs. T2 vs. T1	2.180	0.0997-4.769	0.051	1.639	1.094-2.454	0.017*
LN involvement Yes vs. No	0.954	0.351-2.591	0.926	0.929	0.342-2.522	0.885
Smoking status Current/ Former vs. Never	1.195	0.452-3.159	0.719	1.094	0.410-2.981	0.858
Performance status 0 vs. 1-2	1.811	0.669-4.409	0.243	1.834	0.676-4.972	0.233

CI, confidence interval; HR, hazard ratio; LN, lymph node; RFS, relapse-free survival; OS, overall survival; LUSC, lung squamous cell carcinoma. The results were obtained using the univariate Cox regression method. Significance values were **p*<0.05.
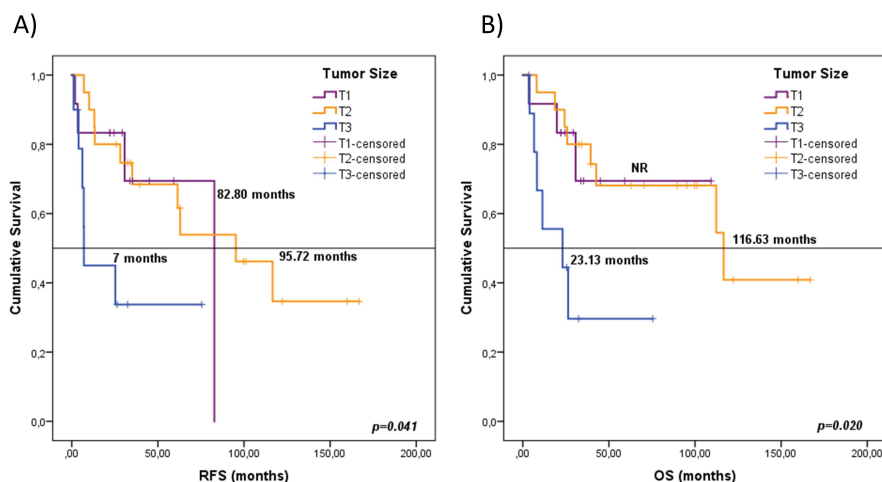
Figure 33. Kaplan-Meier plots for RFS and OS according to tumor size for the early-stage LUSC test subcohort. RFS, relapse-free survival; OS, overall survival; LUSC, lung squamous cell carcinoma; NR, not reached. *P*-values were calculated by Kaplan-Meier test. *P*-value was statistical significative *p*<0.05.

2. INDIVIDUAL SOLUBLE BIOMARKERS

2.1. BIOMARKERS WITH DIAGNOSTIC VALUE

First, we aimed to elucidate whether certain immunoregulatory soluble mediators, including sGAL3, could hold diagnostic value. Among the seven analytes analyzed, the median plasma levels of sFGL1, sGAL1, sGAL3 and sMICB in early-stages NSCLC patients were significantly higher than the controls (Figure 34).

Among these 4 factors, ROC analysis was performed to test their ability to diagnose early-stage NSCLC. The summary of measurements for various individual immune-mediators and their predictive values in diagnosing early-stage NSCLC can be found in Table 17. sGAL3 emerged as the biomarker with the best overall diagnostic accuracy, displaying the highest AUC (AUC=0.849, 95% CI: 0.772-0.926). We employed a logistic regression to investigate whether the combination of two or three plasma biomarkers could enhance the diagnostic precision. The combination of sFGL1 and sGAL3 yielded a better optimal diagnostic efficacy for cancer patients (AUC=0.913, 95% CI: 0.9815-0.946) than the individual biomarkers. This combination demonstrated a sensitivity of 91.3%, a specificity of 76.5%, PPV of 91.3% and a NPV of 76.5% for predicting early-stage NSCLC (Figure 35).
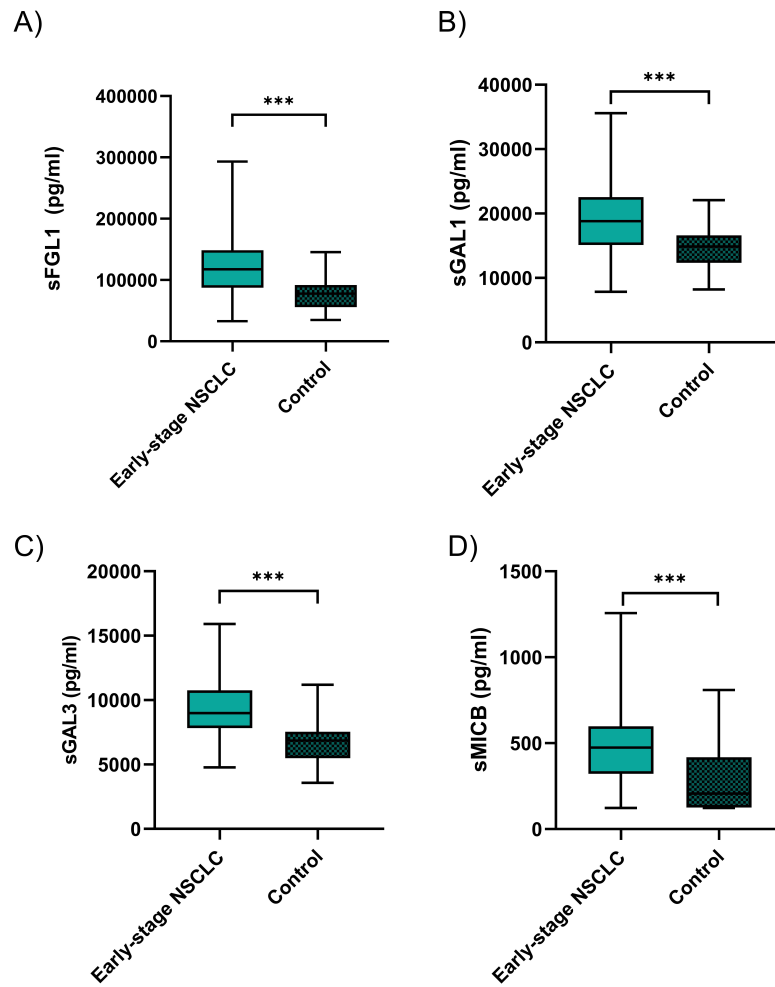
Figure 34. Levels of plasma immune-mediator biomarkers between early-stage NSCLC samples and controls. The bold horizontal lines in the box plots are medians and bars represent minimum and maximum values. NSCLC, Non-small cell lung cancer. *P*-values were calculated by the Mann-Whitney test. Significance values were ***$p<0.001$.

Table 17. Diagnostic accuracies of plasma immune-mediator biomarkers of early-stage NSCLC.

	AUC (95% CI)	Sensitivity	Specificity	PPV	NPV
Early-stage NSCLC vs. Control					
sFGL1	0.791 (0.709-0.873)	0.696	0.824	0.914	0.500
sGAL3	**0.849 (0.772-0.926)**	**0.815**	**0.794**	**0.915**	**0.614**
sGAL-1	0.777 (0.693-0.861)	0.609	0.853	0.918	0.446
sMICB	0.675 (0.554-0.796)	0.641	0.706	0.855	0.421
Model (sGAL3, sFGL1)	**0.880 (0.815-0.946)**	**0.913**	**0.765**	**0.913**	**0.765**

CI, confidence interval; NSCLC, Non-Small Cell Lung Cancer; AUC, Area Under Curve; PPV, positive predictive value; NPV, negative predictive value. The results were obtained using the ROC analysis.
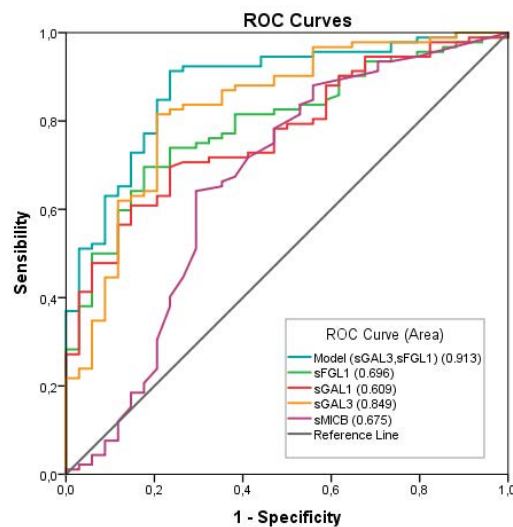
Figure 35. Receiver operating characteristic (ROC) curves of individual or combination of Model, sFGL1, sGAL3, sGAL-1 and sMICB plasma tumor biomarkers early-stage NSCLC comparing to the controls.

These preliminary results suggest that sGAL3 could have diagnostic value. No studies were found about the value of GAL3 as a diagnostic biomarker in lung cancer, whether in tissue or non-invasive samples. In addition to its tissue expression, which has shown potential diagnostic value in certain types of cancer, preoperative serum/plasma sGAL3 levels also displayed diagnostic value in certain types of cancer. In line with our findings, certain studies have reported elevated serum sGAL3 levels in individuals with pancreatic carcinoma compared to those with benign pancreatic conditions and healthy individuals, suggesting its potential as a diagnostic biomarker in pancreatic tumors (Xie et al., 2012). Additionally, patients with metastatic prostate cancer have exhibited higher serum sGAL3 levels when compared to control subjects without cancer (Balan et al., 2013). Serum sGAL3 levels were also significantly elevated in thyroid cancer patients (Yilmaz et al., 2015). Finally, breast cancer patients have also displayed significantly increased serum sGAL3 levels compared to healthy control subjects (C. Chen et al., 2014).

FGL1 is also upregulated in tumor tissues (including lung, prostate, melanoma, colorectal, breast and brain tumors) based on meta-analysis of the oncomine databases (J. Wang et al., 2019). Furthermore, our research demonstrates that combining sFGL1 and sGAL3 results in improved diagnostic effectiveness for early-stages NSCLC patients. Notably, both analytes are ligands of LAG-3, which is one of the most promising immune checkpoints alongside PD1 and CTLA4. It can be hypothesized that tumors secrete

elevated levels of sFGLF1 and sGAL3 as a mechanism to evade the immune system by activating LAG-3, an immune checkpoint inhibitor that prevents T-cell activation.

2.2. BIOMARKERS WITH PROGNOSTIC VALUE

The prognostic value of the immunoregulatory soluble mediators, including sGAL3, was assessed using the univariate Cox regression method for RFS and OS. Levels of soluble proteins were dichotomized according to their median, and the results obtained are shown in Table 18. No significant correlations were found in the Univariant Cox regression analysis.

Table 18. Results from univariate survival analysis based on levels of soluble factors for the early-stage NSCLC test cohort.

	RFS			OS		
Gene	HR	95% CI	*p*-value	HR	95% CI	*p*-value
sFGLF1						
High vs. Low	1.653	0.914-2.989	0.097	1.816	0.947-3.483	0.073
sICOSL						
High vs. Low	0.722	0.397-1.311	0.284	0.817	0.428-1.558	0.539
sCD276						
High vs. Low	1.211	0.672-2.182	0.524	1.282	0.676-2.432	0.446
sGAL3						
High vs. Low	1.374	0.764-2.470	0.289	1.637	0.858-3.123	0.135
sGAL1						
High vs. Low	1.723	0.948-3.130	0.074	1.731	0.903-3.319	0.099
sMICA						
High vs. Low	0.995	0.551-1.797	0.987	1.028	0.539-1.960	0.933
sMICB						
High vs. Low	1.071	0.594-1.928	0.820	1.058	0.558-2.006	0.863

CI, confidence interval; HR, hazard ratio; RFS, relapse-free survival; OS, overall survival; NSCLC, non-samll cell lung cancer. The results were obtained using the univariate Cox regression method. *P*-value was statistical significative *p*<0.05.

It is known that NSCLC exhibits remarkable genomic diversity, with various molecularly-defined patient subgroups. Distinct driver mutations have been discerned within the LUSC and LUAD histological classifications. Our previous results, as shown in Chapter I, have revealed substantial disparities between them concerning *LGALS3* expression. This has led us to consider them as potentially distinct molecular diseases. Consequently, we conducted survival analysis based on patients' histology. Regarding LUSC patients, no significant correlations were found in univariate Cox regression analysis (Table 19).

Table 19. Results from univariate survival analysis based on levels of soluble factors for the early-stage LUSC test subcohort.

	RFS			OS		
Gene	**HR**	**95% CI**	**p-value**	**HR**	**95% CI**	**p-value**
sFGLF1	1.533	0.619-3.796	0.356	1.948	0.718-5.285	5.285
sICOSL	0.551	0.220-1.383	0.204	0.747	0.284-1.970	0.556
sCD276	0.784	0.320-1.921	0.595	0.621	0.233-1.655	0.341
sGAL3	0.992	0.406-2.424	0.986	1.195	0.456-3.130	0.717
sGAL1	1.594	0.645-3.941	0.313	1.889	0.687-5.189	0.218
sMICA	1.146	0.473-2.776	0.762	1.664	0.620-4.462	0.312
sMICB	1.376	0.567-3.339	0.481	1.373	0.517-3.648	0.415

CI, confidence interval; HR, hazard ratio; RFS, relapse-free survival; OS, overall survival; LUSC, lung squamous cell carcinoma. The results were obtained using the univariate Cox regression method. *P*-value was statistical significative *p*<0.05.

On the other hand, outcomes of univariate Cox regression analysis for LUAD patients are detailed in Table 20.

Table 20. Results from univariate survival analysis based on levels of soluble factors for the early-stage LUAD test subcohort.

	RFS			OS		
Gene	**HR**	**95% CI**	***p*-value**	**HR**	**95% CI**	***p*-value**
sFGLF1 *High vs. Low*	1.541	0.695-3.419	0.288	1.425	0.601-3.380	0.421
sICOSL *High vs. Low*	1.076	0.490-2.364	0.855	1.072	0.454-2.530	0.873
sCD276 *High vs. Low*	1.331	0.602-1.942	0.480	1.733	0.725-4.145	0.216
sGAL3 *High vs. Low*	2.269	0.985-5.230	0.054	2.844	1.127-7.176	0.027*
sGAL1 *High vs. Low*	1.458	0.660-3.219	0.351	1.316	0.558-3.103	0.530
sMICA *High vs. Low*	1.048	0.477-2.303	0.908	0.849	0.356-2.021	0.711
sMICB *High vs. Low*	0.887	0.401-1.963	0.768	0.904	0.381-2.146	0.818

CI, confidence interval; HR, hazard ratio; RFS, relapse-free survival; OS, overall survival; LUAD, lung adenocarcinoma. The results were obtained using the univariate Cox regression method. Significance values were *p*<0.05.

In this case the univariate Cox regression model performed with LUAD patients revealed that high levels of sGAL3 were associated with shorter RFS [HR, 2.269; 95% CI 0.985-5.230; *p*=0.054] and worse OS [HR, 2.844; 95% CI 1.127-7.176; *p*=0.027]. Kaplan-Meier analyses were carried out in order to obtain the survival plots (Figure 36).
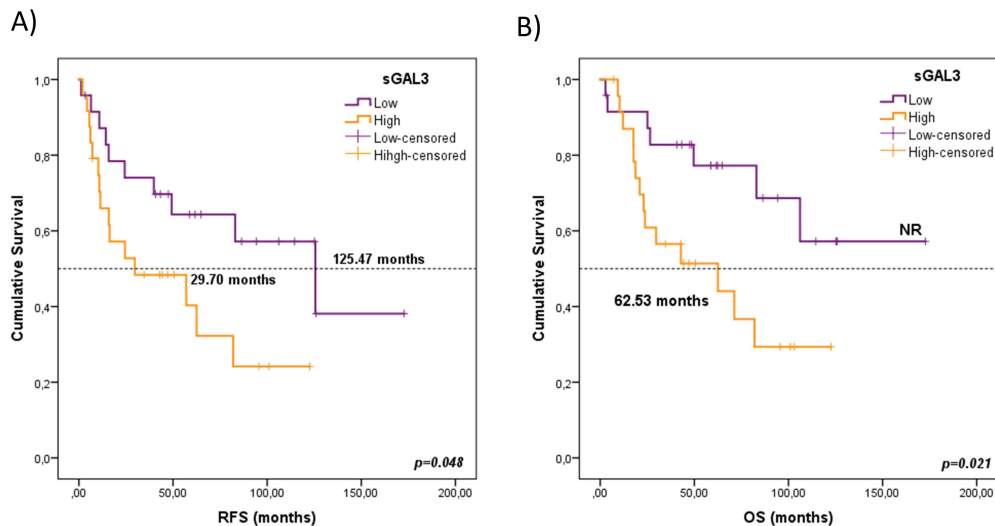
Figure 36. Kaplan-Meier plots for RFS and OS according to soluble levels of sGAL3 for early-stage LUAD test subcohort. (A) Relapse-free survival (RFS) and B) Overall survival (OS). The groups were divided as low and high according to its median. Purple lines represent patients with low levels of sGAL3 on plasma, whilst yellow lines represent patients with high levels of sGAL3 on plasma. LUAD, lung adenocarcinoma; RFS, relapse-free survival; OS, overall survival; NR, not reached. *P*-values were calculated by log-rank test. *P*-value was statistical significative *p*<0.05.

As expected, sGAL3, which was found significantly higher expressed in lung tumorspheres compared to adherent-cultured cells and correlated with T$_{REGS}$, is also associated with worse prognosis in early-stage LUAD patients. Using non-invasive methodologies, Kataoka et al. were also assessed sGAL3 in 42 early NSCLC sera using conventional enzyme-linked immunosorbent assays (ELISA), but no prognostic role was found (Kataoka et al., 2019). There are some differences between this study and ours: 1) liquid biopsy sources used, 2) technique employed, and 3) number of patients included. First, they used serum as a source, which may be affected by interference from coagulation or hemolysis, potentially causing errors in biomarker measurements (J. Paul & Veenstra, 2022). Moreover, plasma offers a richer source of proteins, and the Human Proteome Project recommends that plasma prepared using EDTA should be used for all proteomic studies. Second, in our case, the use of Luminex® MAP technology, as opposed to the conventional ELISA, offers several advantages, including increased throughput, reduced sample volume requirements, and enhanced sensitivity. Furthermore, this technology simplifies the simultaneous assessment of multiple mediators (DuPont et al., 2005). Finally, the study of Kataoka et al. comprises a cohort of 42 patients with NSCLC, of which 27 had LUAD. In our study, we employed a large cohort of 91 patients, in which we did not observe prognostic value of sGAL3 as these authors. However, when we analyzed only the LUAD subcohort consisting of 48 patients, we

100

found a correlation between sGAL3 and prognosis. No more previous studies have been performed on soluble GAL3 in NSCLC. In contrast, some studies have been published in other type of cancers. Higher soluble levels of sGAL3 has been shown to be an independent prognostic factor in pancreatic and colorectal cancer (Shimura et al., 2017; Tao et al., 2017).

The precise way GAL3 influences prognosis remains unclear, although multiple hypotheses have been proposed to explain these mechanisms. Some investigations have revealed when tumors release extracellular GAL3, it binds to glycoproteins located on the surface of tumor cells, including integrins and receptor tyrosine kinases. This binding hinders the receptors' endocytosis, thereby enhancing signal transduction and facilitating tumor progression. Additionally, GAL3 induces leukocyte migration, favoring the entry of leukocytes into the TME (Cardoso et al., 2016). Based on our previous results, it is plausible that sGAL3 could attract T_{REGS} to the lung TME, inducing immunosuppression.

3. MULTIVARIATE ANALYSIS

To determine the independent prognostic value of sGAL3 in LUAD subcohort, a multivariate Cox regression analysis was performed. To construct RFS and OS multivariate models, all clinicopathological variables (gender, age, TNM staging, KRAS mutation status, EGFR mutation status and smoking status) were included. Results obtained from this multivariate analysis confirmed that sGAL3 was a prognosis independent biomarker for RFS and OS with a HR at 3.580 (95% CI 1.185-10.81; *p*=0.024) and 2.862 (95% CI 1.057-7.753; *p*=0.039) in LUAD subcohort, respectively (Table 21). Moreover, performance status for RFS and gender for OS were also confirmed as prognosis independent factors.

Table 21. Significant results from multivariate Cox regression model including all clinicopathological variables from this part of the study.

Variables	RFS			OS		
	HR	95% CI	*p*-value	HR	95% CI	*p*-value
sGAL3 (High vs Low)	2.862	1.057-7.753	0.039*	3.580	1.185-10.81	0.024*
Gender Male vs Female	-	-	-	3.238	1.043-10.05	0.042*
PS 0 vs 1-2	3.139	1.116-8.829	0.030*	-	-	-

CI, confidence interval; HR, hazard ratio; PS, performance status; RFS, relapse-free survival; OS, overall survival. The results were obtained using the multivariate Cox regression method. Significance values were *p<0.05.

According with our results, a study conducted by the International Staging Committee from IASLC revealed that gender was an independent prognostic factor for survival in stage I-IIA NSCLC cases (Yoshizawa et al., 2011). Additionally, Sachs et al. also demonstrated that the survival advantage observed in woman who underwent pulmonary resections for lung cancer was independent of age, physical performance, tumor characteristics and stage of disease (Sachs et al., 2021). Another Norwegian study analyzing sex-specific long-term survival after lung cancer surgery also found that female sex was associated independently with better outcome (Båtevik et al., 2005). Yoshida et al. similarly revealed that female gender was a favorable prognostic factor in NSCLC patients who underwent surgery (Yoshida et al., 2016). Furthermore, PS has also been studied as independent prognostic factor by other authors. PS evaluates the patient's capacity to carry out daily activities, and Buccheri et al. documented the independent predictive validity of PS in discriminating patients with different prognosis, but in NSCLC including all stages (Buccheri et al., 1996).

Regarding the independent prognostic impact of sGAL3 in early-stage NSCLC, only one prior study has attempted to elucidate its prognosis impact by using non-invasive methodologies, with negative results as we presented before (Kataoka et al., 2019). However, some studies employing invasive methods have elucidated the independent prognostic value of GAL3 in NSCLC patients who underwent curative resection. Szöke et al. suggested that GAL3 expression could be an independent prognostic biomarker for OS in stage II NSCLC, and Puglisi et al. found that nuclear GAL3 was also independently associated with shorter OS (Puglisi et al., 2004; Szöke et al., 2007). Contrary to our study, these two reports did not provide detailed information about RFS, which adds value to our study. In this regard, whether GAL3 expression in tumor cells could serve as a predictive biomarker for recurrence has not been clarified. Kusuhara et al. and Katoka et al. were the only one to report that GAL3 expression (measured by IHC) was an independent predictive factor of RFS rather than OS (Kataoka et al., 2019; Kusuhara et al., 2021). It should be highlighted that in these studies, 64.2% and 73% of patients, respectively, had LUAD histological type, which was the predominant histology. However, no analysis of subcohorts based on histology were conducted by these groups. In contrast to these studies, the strength of our study lies in the fact that we used a non-

invasive methodology with plasma samples, which facilitates translation to clinical practice. Furthermore, our study suggests that not only GAL3 expression in early-stages LUAD patients can not only serve as an independent factor for OS prognosis but also for predicting recurrences.

To validate our finding, we evaluated the prognostic value of *LGALS3* expression in an independent cohort of NSCLC patients from TCGA Consortium.

B) VALIDATION STUDY: TCGA EARLY-STAGE NSCLC COHORT (VALIDATION COHORT)

1. CLINICOPATHOLOGICAL VARIABLES

661 patients were included in this part of the study. This cohort included the two primary subtypes of NSCLC: LUAD and LUSC. Table 22 shows the most relevant demographic and clinicopathological characteristics of this cohort. The median patient age was 68 years [range: 38-88], with 73.6% being male, and 51.9% having LUADs. Moreover, 57.3% of the patients were diagnosed at stage I of the disease, only 17.1 never smoked, 208 (31.5%) experienced relapse, and 261 (39.5%) died during the follow-up.

The prognostic value of the different clinicopathological variables was assessed using the univariate Cox regression method for RFS and OS and is shown in Table 23. Significant results obtained from the univariate Cox regression method were also analyzed using the Kaplan-Meier method (log-rank) to obtain the survival plots (Figure 37). This univariate analysis showed that patients over 65 years, those with LNs involvement, bigger tumors, or more advanced stage had shorter RFS and worse OS, which is consistent with our previous results in the test cohort.

Table 22. Clinicopathological characteristics of the TCGA patients included in the study.

Characteristics	n	%
Age at surgery (median, range):	68[IQR 38–88]	
Gender		
Male	395	59.8
Female	266	40.2
Stage		
I	375	56.7
II	179	27.1
III	107	16.2
Histology		
LUAD	345	52.2
LUSC	316	47.8
Smoking status		
Current	165	25.0
Former	382	57.8
Never	114	17.2
Exitus		
No	400	60.5
Yes	261	39.5
Relapse		
No	394	59.6
Yes	208	31.5
NS	59	17.2

IQR, interquartile range; LUAD, lung adenocarcinoma; LUSC, lung squamous cell carcinoma; n, sample size. The results were obtained using the multivariate Cox regression method. Significance values were *$p<0.05$.

Table 23. Results from univariate survival analysis based on clinicopathological variables for the validation cohort from TCGA.

Characteristics	RFS			OS		
Variable	HR	95% CI	*p*-value	HR	95% CI	*p*-value
Gender						
Male vs. Female	0.877	0.701-1.096	0.248	0.798	0.619-1.029	0.081
Age						
> 65 vs. ≤ 65	1.278	1.013-1.612	0.039*	1.327	1.019-1.727	0.036*
TNM Staging						
III vs. II vs. I	1.261	1.099-1.447	0.001**	1.312	1.125-1.529	0.001**
Tumor Size						
T3/T4 vs. T2 vs. T1	1.107	1.038-1.179	0.002**	1.362	1.116-1.663	0.002**
LN involvement						
Yes vs. No	1.395	1.116-1.744	0.003**	1.565	1.219-2.008	0.000***
Smoking status						
Current/ Former vs. Never	0.851	0.640-1.131	0.266	0.923	0.663-1.286	0.638
Histology						
LUAD vs. LUSC	0.931	0.749-1.157	0.519	1.204	0.941-1.541	0.141

LUAD, lung adenocarcinoma; LUSC, lung squamous cell carcinoma; CI, confidence interval; HR, hazard ratio; LN, lymph node; TNM, tumor node metastasis; RFS, relapse-free survival. OS, overall survival. The results were obtained using the univariate Cox regression method. Significance values were *$p<0.05$; **$p<0.01$; ***$p<0.001$.
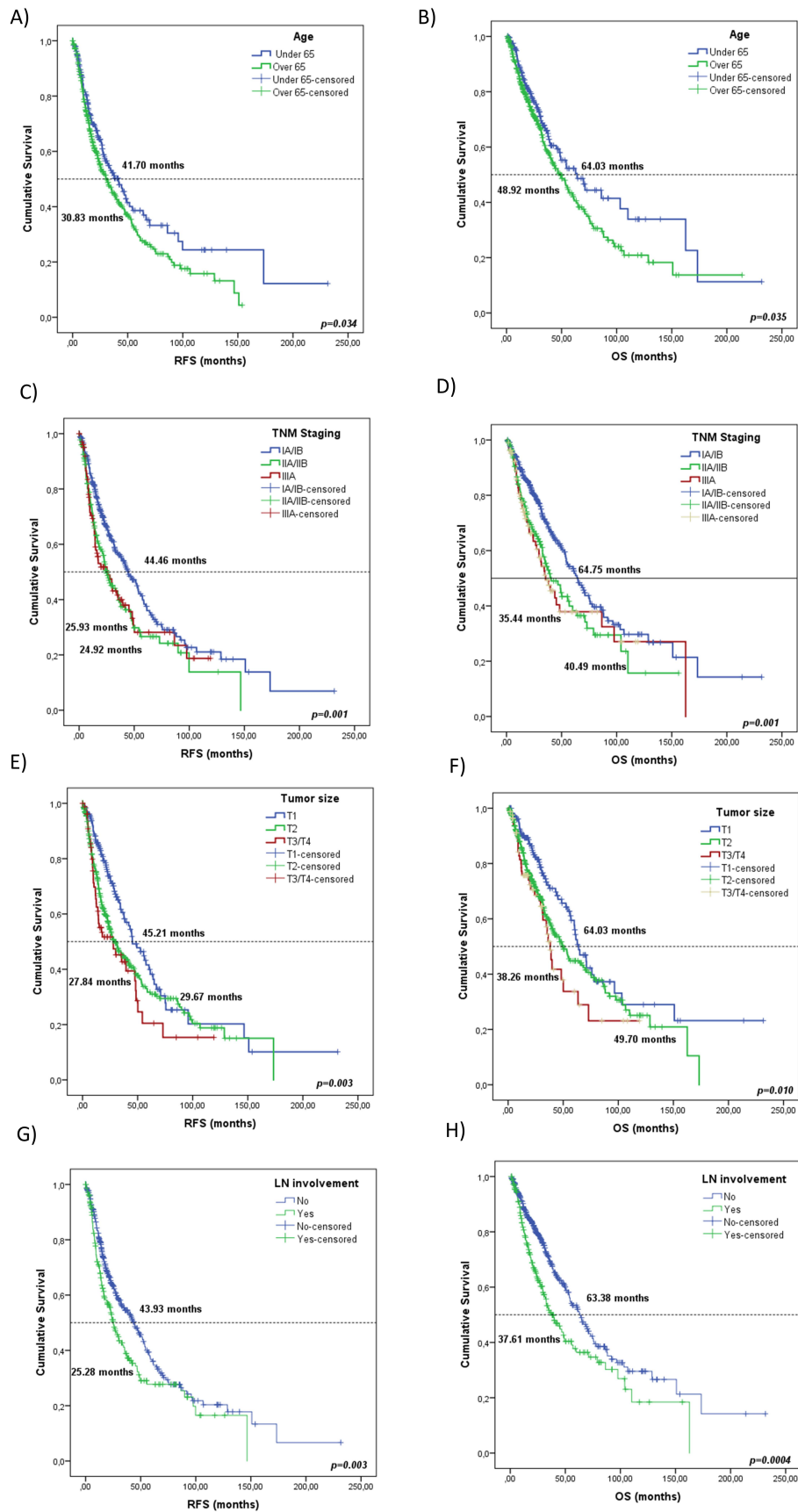
Figure 37. Kaplan-Meier plots for RFS and OS according to clinicopathological variables for the validation cohort from TCGA. A-B). Age; C-D). TNM staging; E-F). Tumor size; G-H). LN involvement. P-values from the Kaplan-Meier test. LN; lymph node; RFS, relapse-free survival; OS, overall survival; TNM, tummor-node-metastasis. *P*-values were calculated by log-rank test. *P*-value was statistical significative *p*<0.05.

The prognostic value of the clinicopathological variables was also assessed according to the tumor histology. The LUAD subcohort comprised 345 patients, 123 (35.7%) of whom experienced relapse, and 114 (33.0%) died. Once again, in the univariate Cox analysis, TNM staging, tumor size and LN involvement were associate with RFS and OS (Table 24), consistent with our previous results in the LUAD subcohort. Survival plots from Kaplan-Meier survival analysis are represented in Figure 38.

Table 24. Results from univariate survival analysis based on clinicopathological variables for the LUAD validation subcohort from TCGA.

Characteristics	RFS			OS		
Variable	HR	95% CI	*p*-value	HR	95% CI	*p*-value
Gender Male vs. Female	0.878	0.647-1.191	0.401	0.899	0.622-1.299	0.570
Age > 65 vs. ≤ 65	1.328	0.364-1.831	0.083	1.1339	0.908-1.975	0.140
TNM Staging III vs. II vs. I	1.1446	1.195-1.748	0.0001***	1.547	1.232-1.943	p<0.0001***
Tumor Size T3/T4 vs. T2 vs. T1	1.573	1.223-2.024	0.0004***	1.481	1.086-2.020	0.013*
LN involvement Yes vs. No	1.731	1.269-2.361	0.001**	2.118	1.461-3.070	p<0.0001***
Smoking status Current/ Former vs. Never	0.819	0.583-1.151	0.251	0.744	0.497-1.113	0.150

CI, confidence interval; HR, hazard ratio; LN, lymph node; TNM, tumor node metastasis; OS, overall survival; RFS, relapse-free survival; LUAD, lung adenocarcinoma. The results were obtained using the univariate Cox regression method. Significance values were *p<0.05; **p<0.01; ***p<0.001.

The LUSC subcohort comprised 316 patients, 85 (26.9%) of whom experienced relapse, and 147 (15.5%) died during follow up. In contrast to the findings in LUAD patients, no significant associations were found between clinicopathological variables and relapse or survival in this group (Table 25).

Table 25. Results from univariate survival analysis based on clinicopathological variables for the LUSC validation subcohort from TCGA.

Characteristics	RFS			OS		
Variable	HR	95% CI	*p*-value	HR	95% CI	*p*-value
Gender Male vs. Female	0.712	0.48-1.055	0.090	0.766	0.521-1.127	0.176
Age > 65 vs. ≤ 65	1.184	0.815-1.721	0.376	1.292	0.898-1.86	0.168
TNM Staging III vs. II vs. I	1.083	0.863-1.36	0.489	1.142	0.926-1.408	0.215
Tumor Size T3/T4 vs. T2 vs. T1	1.263	0.966-1.651	0.088	1.269	0.976-1.65	0.076
LN involvement Yes vs. No	1.021	0.712-1.464	0.909	1.203	0.855-1.694	0.289
Smoking status Current/ Former vs. Never	1.295	0.658-2.548	0.454	1.311	0.642-2.644	0.457

CI, confidence interval; HR, hazard ratio; LN, lymph node; RFS, relapse-free survival; OS, overall survival; LUSC, lung squamous cell carcinoma. The results were obtained using the univariate Cox regression method. *P*-value was statistical significative p<0.05.
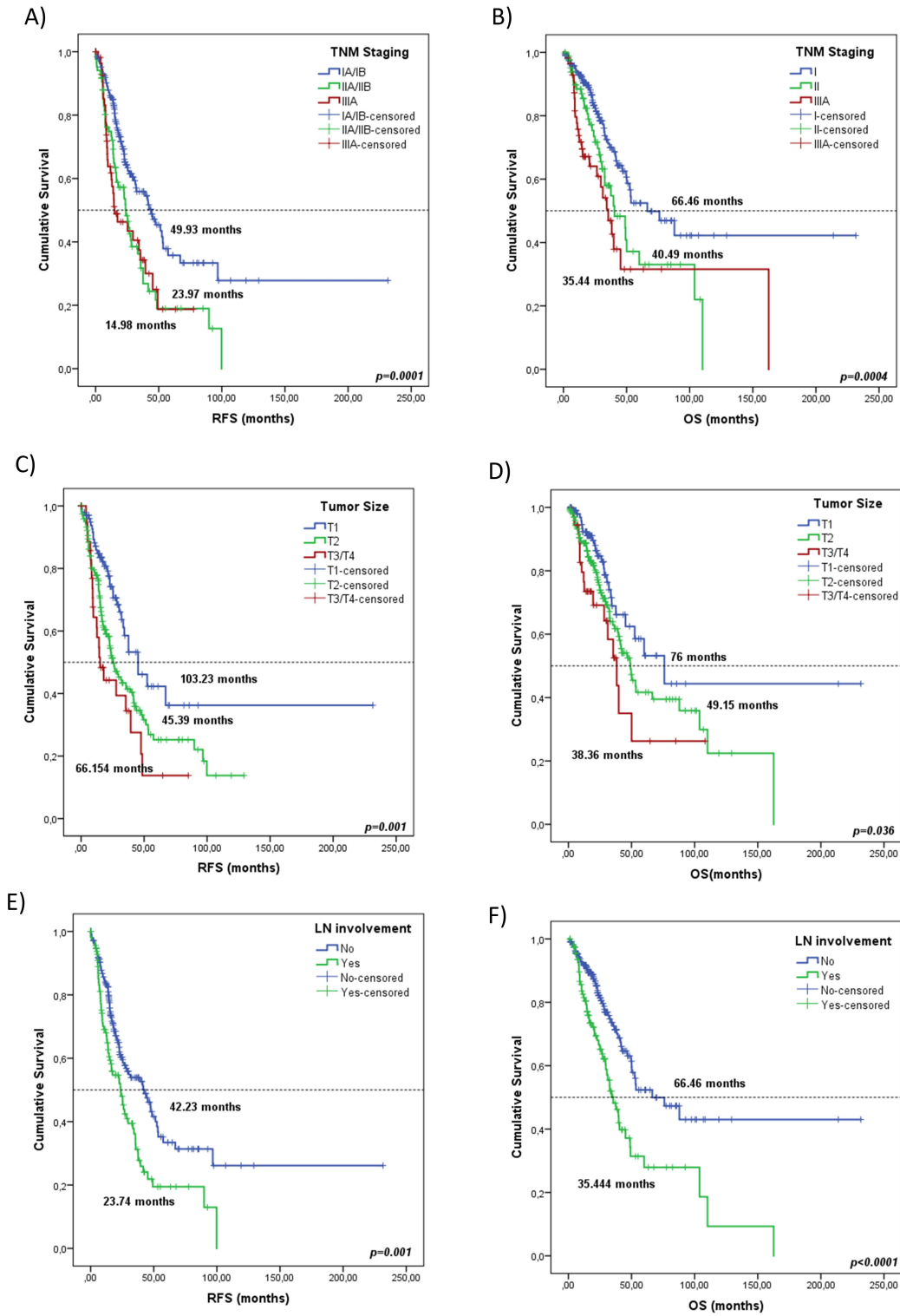
Figure 38. Kaplan-Meier plots for RFS and OS according to clinicopathological variables for the LUAD subcohort from TCGA. A-B. TNM staging; C-D. Tumor size; E-F. LN involvement. RFS, relapse-free survival; OS, overall survival; LN, lymph node; TNM, tumor-node-metastasis. *P*-values were calculated by log-rank test. *P*-value was statistical significative *p*<0.05.

2. INDIVIDUALS BIOMARKERS

Our next step was the study of the *LGALS3* expression as prognostic biomarker for RFS and OS, assessed by Cox regression statistics. Gene expression levels were dichotomized according to their median. Consistent with our previous study in the HGUV cohort on plasma, no significant results were found for *LGALS3* in the entire validation cohort for RFS [HR, 0.933; CI 95% 0.731-1.160, *p*=0.535] and OS [HR, 0.846; CI 95% 0.661-1.082, *p*=0.183]. In addition, we perform the univariate survival analysis in the two histologic subgroups: LUAD and LUSC. No significant differences were found for LUSC validation subcohort for RFS [HR, 0.784; CI 95% 0.576-1.068, *p*=0.123] and OS [HR, 0.751; CI 95% 0.540-1.043 *p*=0.088], whereas significant differences were observed in LUAD validation subcohort. Univariate Cox regression analysis revealed that expression levels above the median of *LGALS3* were associated with worse PFS [HR, 1.551; 95% CI 1.136-2.117; *p*=0.003] and OS [HR, 1.968; 95% CI 1.341-2.888; *p*=0.0001]. Survival plots from Kaplan-Meier analyses are shown in Figure 39.
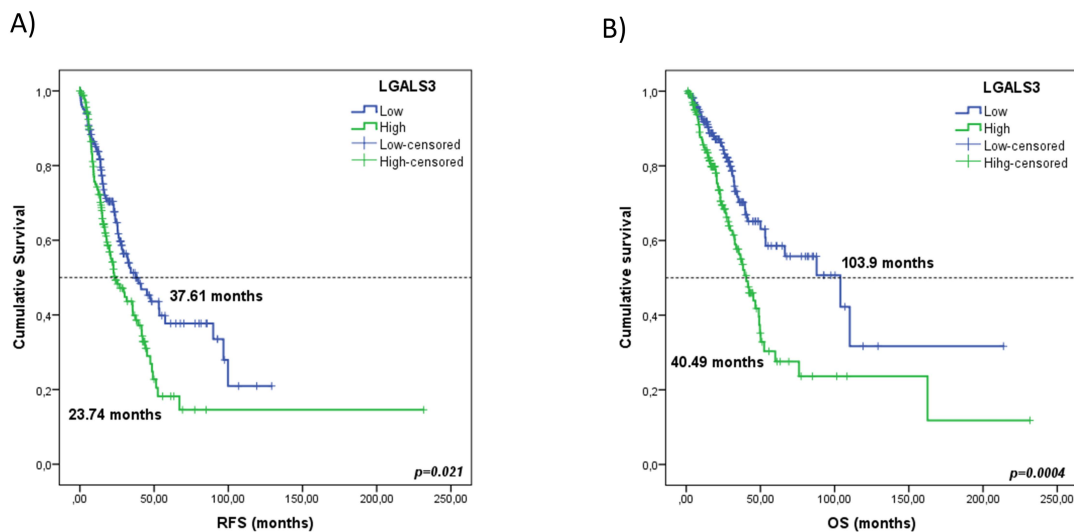
Figure 39. Kaplan-Meier survival curves for RFS and OS according to *LGALS3* from LUAD subcohort from TCGA. A) Relapse-free survival (RFS) and B) Overall survival (OS). Gene expression levels were dichotomised according to the median. Green lines represent patients with high levels of expression, whereas blue lines represent patients with low levels of expression. OS, overall survival; RFS, relapse-free survival; LUAD, lung adenocarcinoma. *P*-values were calculated by log-rank test. *P*-value was statistical significative *p*<0.05.

3. MULTIVARIATE ANALYSIS

In order to determine the independent prognostic value of *LGALS3* in the LUAD validation subcohort, a multivariate Cox regression analysis was performed. To construct PFS and OS multivariate models, we introduce all clinicopathological variables (gender, age, TNM staging and smoking status). Results obtained from this multivariate analysis confirmed that *LGALS3* and TNM staging were independent biomarkers for RFS and OS in LUAD validation subcohort from TCGA (Table 26).

Table 26. Significant results from multivariate Cox regression model including all clinicopathological variables from LUAD validation subcohort.

Variables	RFS			OS		
	HR	95% CI	*p*-value	HR	95% CI	*p*-value
LGALS3 (High vs Low)	1.908	1.294-2.814	0.001**	1.513	1.092-2.096	0.013*
TNM III vs. II vs. I	1.568	1.249-1.968	<0.0001***	1.451	1.193-1.763	<0.0001***

TNM; tumor node metastasis; CI, confidence interval; HR, hazard ratio; RFS, relapse-free survival; OS, overall survival. The results were obtained using the multivariate Cox regression method. Significance values were *p<0.05; **p<0.01; ***p<0.001.

The association between high *LGALS3* expression and worse prognosis was confirmed in this independent TCGA validation cohort for the LUAD cases, supporting the prognostic power of GAL3 in this lung cancer subtype.

For the validation of our results in plasma, we used data from TCGA (data from RNA-sequencing). The TCGA validation cohort is a public database, providing massive information that allow us to perform in silico analysis, as previously done in our laboratory (Duréndez-Sáez et al., 2022; Herreros-Pomares et al., 2019). However, we need to consider some limitations, such as partial outcome information, which might lead to some uncertainties. Currently, we are actively collecting more plasma samples from resected patients to complete a plasma validation cohort for further analysis.

Based on our findings, it was expected that sGAL3 (in plasma), as well as *LGALS3* expression in tissue, would be a prognostic marker for LUAD overall survival and predictive marker for LUAD recurrence.

C) STUDY OF BIOMARKERS IN ADVANCED-STAGE NSCLC COHORT FROM HGUV

Despite the progress made in ICIs therapies for advanced NSCLC, there is an urgent need to explore new biomarkers for patient selection and treatment optimization. Plasmatic biomarkers offer several advantages, including repeatability, easy accessibility, the ability to conduct sequential analysis during follow-up, and the potential to better recapitulate tumor heterogeneity. For these reasons, this chapter holds great relevance, as we investigated the value of seven plasmatic biomarkers: sFGL1, sCD276, sICOSL, sGAL1 and sGAL3, sMICB, sMICA, both at PRE and at FR in advanced-stage NSCLC patients treated with anti-PD1.

1. CLINICOPATHOLOGICAL VARIABLES

Fifty-two advanced-stage NSCLC patients, who received first-line treatment with pembrolizumab, were enrolled in this study. The most relevant demographic and clinicopathological characteristics of the cohort are shown in Table 27. The median patient age was 67 years [range: 51-89], 75% were male, and 65.4% had LUADs. Moreover, 51.9% of the patients were diagnosed at stage IVB of the disease and 84.6% presented a PS=0-1 at initiation of pembrolizumab. None of the patients had targetable driver mutations approved by the European Medicines Agency (EMA). According to the guidelines, all patients treated with pembrolizumab in monotherapy exhibited PDL1 expression ≥ 50% in their tumor samples (Reck et al., 2016).

The median follow-up duration was 18.41 months (ranging from 1.37 to 21.191 months) in the entire group. The ORR was at 40.4% (21 out of 52), consistent with the literature (Aguilar et al., 2019; Reck et al., 2021). Moreover, 29 patients showed DCB, including 4 CR, 15 PR, and 10 SD. Two patients achieved PR at the initial assessment but progressed before reaching the 6-month mark. At data cut-off, 38 patients (73.1%) had experienced disease progression, with a median PFS of 7 months (range 0.1-13.36 months). More detailed demographic and clinicopathological variables of the patients can be found in Supplementary Table S2.

Table 27. Clinicopathological characteristics in advanced-stage NSCLC cohort.

Characteristics	n	%
Age at surgery (median, range):	67 [IQR 51–89]	
Gender		
Male	39	75
Female	13	25
Stage		
IIIB	12	23.1
IVA	13	25
IVB	27	51.9
Histology		
LUSC	13	25
LUAD	34	65.4
Others	5	9.6
Performance Status		
0-1	44	84.6
2	7	13.5
Smoking status		
Current	37	71.2
Former	11	21.2
Never	4	7.7
Progression		
Yes	38	73.1
No	14	26.9
Exitus		
Yes	36	69.2
No	16	30.8

LUAD, lung adenocarcinoma; LUSC, lung squamous cell carcinoma; IQR, interquartile range; n, sample size: IQR; interquartile range; NSCLC, non-small cell lung cancer.

Median soluble levels of the immune-mediators determined at PRE and FR (4 months of treatment) are presented in Table 28.

Table 28. Median levels of soluble analytes measured by Luminex technology in advanced-stage NSCLC cohort.

Analyte	Median at PRE (pg/ml)	IQR at PRE (pg/ml)	Median at FR (pg/ml)	IQR at FR (pg/ml)
sICOSL	6413.32	259.88-8220.46	6411.42	5336.64-9826.69
sCD276	611.78	238.45-1247.62	885.78	231.51-1749.88
sFGL1	151042.76	121193.97-189434.59	156594.82	125794.24-211091.35
sGAL1	20506.60	16678.27-25437.53	21408.75	18321.44-26125.93
sGAL3	9991.40	8066.19-12776.39	10252.91	8728.84-13004.53
sMICA	28.22	19.00-54.07	13.33	16.53-41.62
sMICB	611.08	343.44-929.92	512.27	393.76-825.87
sICOSL	6413.32	259.88-8220.46	6411.42	5336.64-9826.69

IQR, Interquartile range; PRE, baseline; FR, first response assessment; NSCLC, non-small cell lung cancer.

The correlations between plasma levels of immune-mediators at PRE and the clinical features of the patients was assessed using the Mann-Whitney test and summarized in Table 29. At PRE, patients aged more than 70 years had high levels of sICOSL. Interestingly, former or never smokers exhibited higher levels of co-inhibitory immune checkpoints, including sICOSL, sCD276 and sMICA, compared with current smokers (Figure 40).

No correlations were found between immune-mediators and variables such as with sex, histology, and stage (data not shown).

Table 29. Associations between plasma levels and clinicopathological variables in advanced-stage NSCLC cohort.

Characteristics	Nº of patient	Analyte	Plasma levels median (IQR) pg/ml	*p*
Age				
<70	33	sICOSL	5946.01 (4613.23-7958.96)	0.047*
>70	19		7190.05 (5966.16-10302.75)	
Smoking Status				
Current	37	sICOSL	6064.42 (5187.47-7958.96)	0.049*
Former or Never	15		8192.04 (5966.16-10301.75)	
Smoking Status				
Current	37	sCD276	433.32 (212.94-926.29)	0.006**
Former or Never	15		1250.45 (503.86-2394.42)	
Smoking Status				
Current	37	sMICA	23.64 (17.03-47.69)	0.029*
Former or Never	15		44.07 (24.88-89.76)	

IQR, Interquartile range; PRE, baseline; FR, first response assessment; NSCLC, non-small cell lung cancer; IQR, interquartile range. *P*-values were calculated by the Mann-Whitney test. Significance values were *p*<0.05; **p*<0.01.
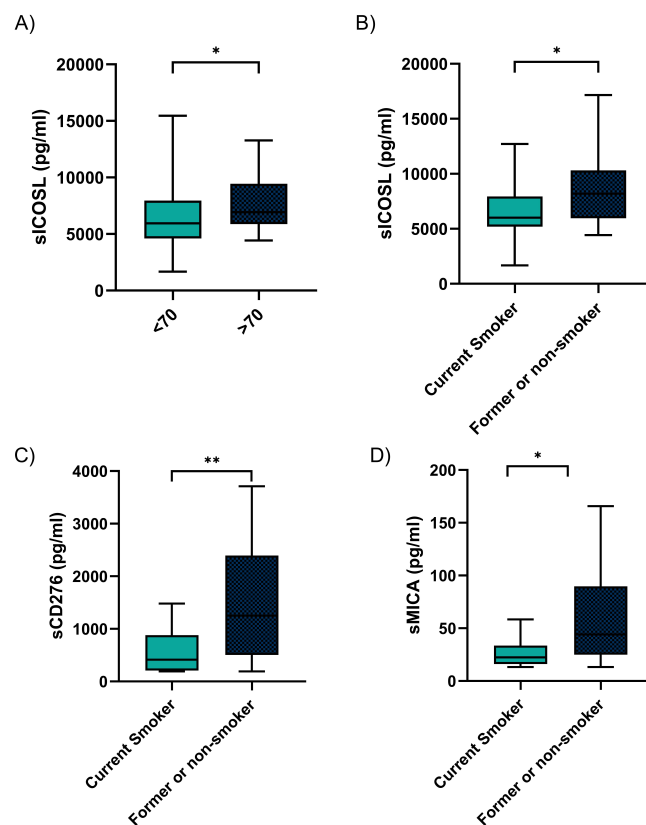
Figure 40. Correlations between soluble biomarkers and clinicopathological variables in advanced-stage NSCLC cohort. A) sICOSL levels at baseline in patients with <70 years (n=33) and patients with >70 years (n=19). B, C, D) sICOSL, sCD276, sMICA at baseline in patient current smokers (n=37) and patients former or never smokers (n=15). The bold horizontal lines in the box plots are medians and bars represent minimum and maximum values. n; sample size; NSCLC, non-small cell lung cancer. *P*-values were calculated by the Mann-Whitney test. Significance values were *p*<0.05, **p*<0.01.

Our results revealed significant differences between smorkers who exhibited low levels of sICOSL, sCD276, and sMICA, compared to never or non-smokers. These three molecules play a crucial role as immunosuppressive factors within the TME (Terry et al., 2017). Smokers' lung cancers are characterized by an activated immune micronvironment with increased immunogenicity and upregulation of immune modulators such as chemokines (CXCL5, CXCL10), cytolytic activity-related genes (PRF1, GZMA), and immune checkpoint biomarkers (CD274, IDOI). In contrast, the immune microenvironment of tumor from the non-smoking group is enriched for immunosuppressive related cells, including T_{REGS} and M2 macrophages (de Alencar et al., 2022; Y. Sun et al., 2021). No previous associations between ICOSL, MICA, CD276 and tobacco history have been reported.

Next, the prognostic value of the different clinicopathological variables was assessed using the univariate Cox regression method for PFS and OS (Table 30).

Table 30. Results from univariate survival analysis based on clinicopathological variables for the in advanced-stage NSCLC cohort.

Characteristics	PFS			OS		
Variable	HR	95% CI	*p*-value	HR	95% CI	*p*-value
Gender Male vs. Female	1.333	0.660-2.693	0.423	0.852	0.397-1.830	0.682
Age > 65 vs. ≤ 65	1.032	0.527-2.024	0.926	1.418	0.711-2.830	0.322
TNM Staging III/IVA vs. IVB	3.107	0.939-10.280	0.063	0.592	0.303-1.159	0.126
Smoking status Current vs Former/Never	1.143	0.55-2.357	0.717	1.624	0.773-3.413	0.201
Performance status 0 vs. 1-2	1.820	0.748-4.425	0.187	2.248	0.822-6.146	0.114

CI, confidence interval; HR, hazard ratio; PFS, progression-free survival; OS, overall survival; NSCLC, non-small cell lung cancer. The results were obtained using the univariate Cox regression method. *P*-value was statistical significative *p*<0.05.

The prognostic value of the clinicopathological variables was also assessed according to the tumor histology. In the advanced-stage LUAD subcohort (n=34) the univariate Cox analysis (Table 31) show a significant correlation in OS with the smoking status, which agreed with previously published results. Survival Kaplan Meier plots according to smoking status are depicted in Figure 41. Multiple studies demonstrate significantly better therapeutics outcomes in smokers as compared with never smokers when single-agent immunotherapy is applied. This effect is thought to be due to tobacco

product-induced upregulation of PD-L1/PD-1 expression and TMB score (Popat et al., 2022; Zaleskis et al., 2021; W. Zhao et al., 2021).

Table 31. Results from univariate survival analysis based on clinicopathological variables for the advanced-stage LUAD subcohort.

Characteristics	PFS			OS		
Variable	HR	95% CI	*p*-value	HR	95% CI	*p*-value
Gender Male vs. Female	2.278	0.925-5.609	0.073	1.055	0.387-2.872	0.917
Age > 65 vs. ≤ 65	1.184	0.482-2.911	0.712	2.474	0.973-6293	0.057
TNM Staging III/IVA vs. IVB	1.044	0.465-2.347	0.916	0.779	0.335-1.811	0.561
Smoking status Current vs Former/Never	1.725	0.673-4.423	0.256	3.426	1.201-9.775	0.021*
PS 0 vs. 1-2	1.565	0.457-5.354	0.476	1.381	0.302-6.312	0.677

CI, confidence interval; HR, hazard ratio; PS, performance status; TNM, tumor-node-metastasis; PFS, progression-free survival; OS, overall survival. The results were obtained using the univariate Cox regression method. Significance values were *p<0.05.
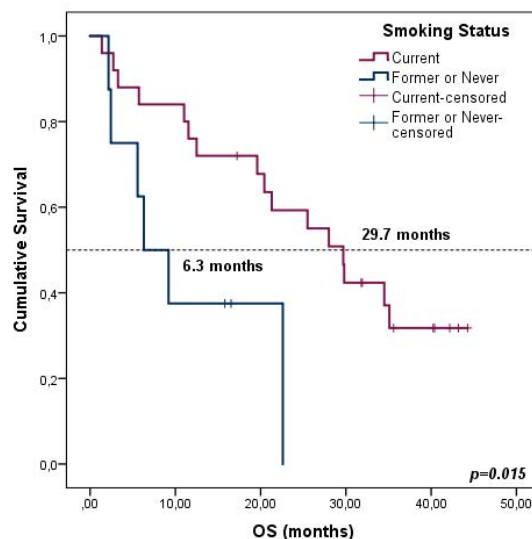
Figure 41. Kaplan-Meier plots for OS according to smoking status in the advanced-stage LUAD subcohort. OS; overall survival; LUAD, lung adenocarcinoma. *P*-values were calculated by log-rank test. *P*-value was statistical significative *p<0.05.*

In the LUSC subgroup, the number of included patients was a total of 13, which represents a too small number of samples to perform statistical analyses. We did not find any statistical association in this subcohort (data not shown).

2. INDIVIDUALS SOLUBLE BIOMARKERS

2.1. BIOMARKERS WITH DIAGNOSTIC VALUE

With the aim of analyzing the potential diagnostic value of previously examined soluble immune-mediators, the next step was to compare the plasma levels of patients in advanced stages of lung cancer with those of a control group (selected based on similar age and gender characteristics). We found that the median plasma biomarkers levels of advanced-stage NSCLC patients were significantly higher than those of the controls (Figure 42).
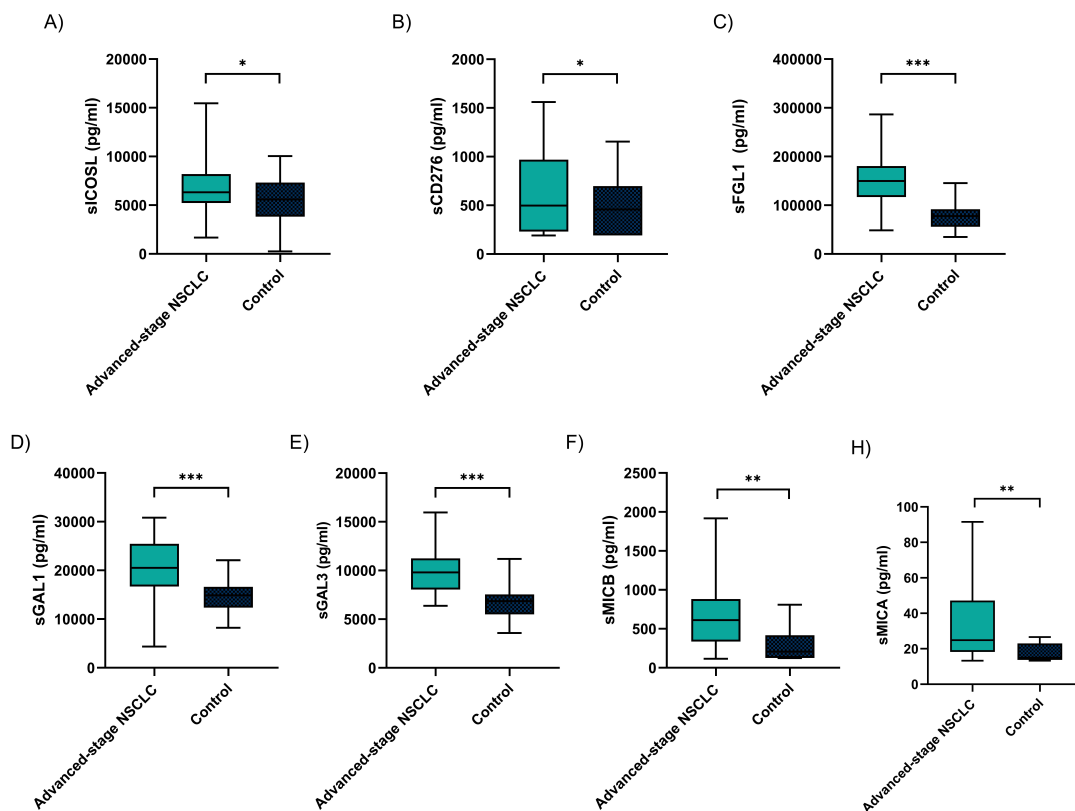
Figure 42. Levels of plasma biomarkers between advanced-stage NSCLC cohort and controls. A) sICOSL B) sCD276 C) sFGL1 D) sGAL1 E) sGAL3 F) sMICB G) sMICA. The bold horizontal lines in the box plots are medians and bars represent minimum and maximum values. NSCLC, Non-small cell lung cancer. The results were obtained the Mann-Whitney test. Significance values were *p<0.05, **p<0.01, ***p<0.001.

ROC analysis was also performed to test the potential diagnostic value of the selected biomarkers in NSCLC. The evaluation of the different individual markers and their predictive values in the diagnosis of advanced-stage NSCLCs is summarized in Table 32. Among these, sFGL1 and sGAL3 emerged as biomarkers with good diagnostic

accuracy (Figure 43). sFGL1 exhibited the highest AUC at 0.919 (95% CI: 0.860-0.978), followed by sGAL3 with an AUC of 0.889 (95% CI: 0.827-0.960). To assess whether combining these two plasma immune-mediators could enhance diagnostic accuracy, logistic regression was employed. This combination demonstrated superior diagnostic effectiveness in advanced-stage cancer patients, achieving an optimal AUC of 0.963 (95% CI: 0.929-0.996) with a sensitivity of 82.7%, specificity of 97.1%, a PPV of 99.7%, and a NPV of 78.5% for the prediction of advanced-stage NSCLC.

Table 32. Diagnostic accuracies of plasma biomarkers of advanced-stage NSCLC cohort.

	AUC (95% CI)	Sensitivity	Specificity	PPV	NPV
Advanced-stage NSCLC vs. Control					
sFGL1	0.919 (0.860-0.978)	0.885	0.853	0.902	0.828
sGAL3	0.889 (0.817-0.960)	0.904	0.794	0.904	0.794
sGAL1	0.801 (0.709-0.894)	0.596	0.941	0.939	0.604
sMICB	0.711 (0.592-0.830)	0.712	0.706	0.712	0.706
sMICA	0.691 (0.575-0.807)	0.538	0.818	0.824	0.529
sICOSL	0.651 (0.535-0.769)	0.808	0.471	0.700	0.615
sCD276	0.624 (0.504-0.743)	0.269	0.971	0.933	0.465
Model (sGAL3, sFGL1)	0.963 (0.929-0.996)	0.827	0.971	0.997	0.785

CI, confidence interval; NSCLC, non-small cell lung cancer; AUC, Area Under Curve; PPV, positive predictive value; NPV, negative predictive value. The results were obtained using the ROC analysis.
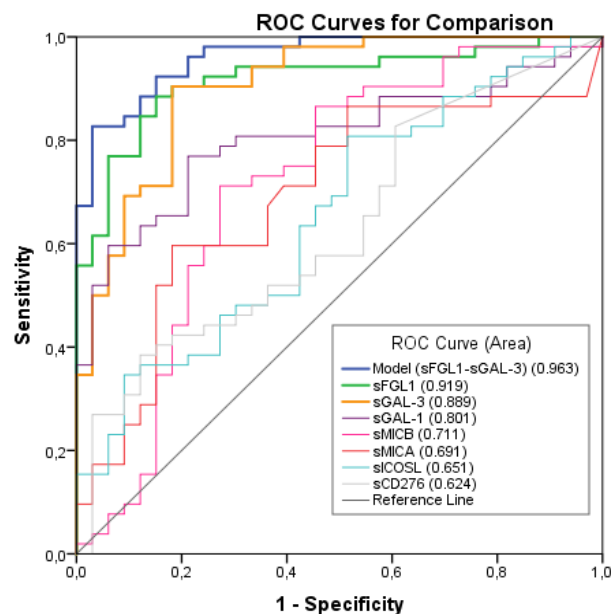
Figure 43. Receiver operating characteristic (ROC) curves of individual or combine model. Experimental variables included in the analysis comprises: sFGL1, sGAL3, sGAL1, sMICB, sMICA, sICOSL, sCD276 plasma tumor in advanced-stage NSCLC cohort comparing to the controls. NSCLC, non-small cell lung cancer.

In concordance with our previous findings in early-stage NSCLC patients, sGAL3 shows good capability as a diagnostic biomarker also in advanced-stage patients.

Moreover, the combination of sGAL3 and sFGL1 outperforms the diagnostic capacity of each biomarker analyzed individually.

Regarding sFGL1 (also ligand of LAG3), which we have also observed to have good diagnostic sensitivity, this immune mediator has been found upregulated in different type of tumors (including lung, prostate, melanoma, colorectal, breast and brain tumors) based on the data published by Wang and coworkers (J. Wang et al., 2019). Consistent with our findings, Li et al. reported that FGL1 exhibited normal expression in patients with other pulmonary pathologies (n=10) but showed upregulation in the advanced LUAD group (n=7) (W. Li et al., 2018). However, their study suffered from a limited sample size, leading to reduced statistical power. Additionally, they employed isobaric tags for relative and absolute quantification (iTRAQ) labeling in conjunction with multidimensional liquid chromatography-tandem mass spectrometry (iTRAQ-coupled 2D LC-MS/MS), a labor-intensive, time-consuming, and costly technology (Beretov et al., 2014)4). In contrast, our approach utilized Luminex® MAP technology, which offers faster processing, higher throughput, reduced sample volume requirements, and enhanced sensitivity (DuPont et al., 2005).

2.2. BIOMARKERS THAT PREDICT RESPONSE TO IMMUNOTHERAPY

After conduction the analysis of the diagnostic value, to assess the value of these immunoregulatory soluble factors to predict response to pembrolizumab in first-line, we analyzed their correlation with the ORR and the DCB at PRE and FR.

The correlations between ORR with soluble levels of immunoregulatory mediators was assessed using the Mann-Whitney analysis and are shown in Table 33. This analysis showed that median sCD276 levels were significantly higher in patients without tumor response, with a median value of 874.05 pg/ml (IQR, 399.52-1306.96), compared to 326.38 pg/ml (IQR, 206.40-696.52) in patients with tumor response (*p*=0.035) at PRE (Figure 44). The ORR was 26.9% (n=7) in the case of those with high levels of sCD276 (n=26) (≥median of 611.7850 pg/ml) versus 53.8% (n=14) in the case of those with low

levels of sCD276 (n=26) (< median of 611.7850 pg/ml) (*p*=0.048). No statistical differences were found in the rest of factors analyzed.

Table 33. Associations between plasma levels and objective response in advanced-stage NSCLC cohort.

Objective Response	Nº of patient	Analyte	Plasma levels median (IQR) pg/ml	p
Responders (PR/CR)	21	sCD276 PRE	326.38 (206.40-696.52)	0.035*
Non-Responders (SD/PD)	31		874.05 (399.52-1306.96)	
Responders (PR/CR)	16	sCD276 FR	414.05 (190.35-1720.33)	0.141
Non-Responders (SD/PD)	24		1126.44 (550.53-1749.88)	
Responders (PR/CR)	21	sMICB PRE	610.03 (390.76-805.08)	0.391
Non-Responders (SD/PD)	31		721.90 (334.50-988.36)	
Responders (PR/CR)	16	sMICB FR	500.36 (415.61-597.23)	0.594
Non-Responders (SD/PD)	24		625.97 (334.50-846.53)	
Responders (PR/CR)	21	sGAL3 PRE	9858.75 (8026.30-11820.17)	0.496
Non-Responders (SD/PD)	31		10233.28 (8105.84-12951.68)	
Responders (PR/CR)	16	sGAL3 FR	10032.54 (8358.81-12863.93)	0.404
Non-Responders (SD/PD)	24		10557.82 (9095.70-13396.13)	
Responders (PR/CR)	21	sGAL1 PRE	19427.16 (12989.25-22525.05)	0.095
Non-Responders (SD/PD)	31		20933.01 (17246.30-26497.31)	
Responders (PR/CR)	16	sGAL1 FR	20166.88 (16676.29-24794.85)	0.113
Non-Responders (SD/PD)	24		21890.26 (19278.92-27561.02)	
Responders (PR/CR)	21	sICOSL PRE	6901.21 (5549.56-9101.50)	0.275
Non-Responders (SD/PD)	31		5966.16 (4791.58-8192.04)	
Responders (PR/CR)	16	sICOSL FR	11597.87 (3117.96-NR)	0.902
Non-Responders (SD/PD)	24		4584.47 (3723.56-7682.73)	
Responders (PR/CR)	21	sMICA PRE	36.04 (21.16-84.81)	0.221
Non-Responders (SD/PD)	31		24.88 (17.46-52.21)	
Responders (PR/CR)	16	sMICA FR	24.73 (15.60-80.64)	0.557
Non-Responders (SD/PD)	24		24.88 (16.53-34.80)	
Responders (PR/CR)	21	sFGL1 PRE	139042.05 (99865.75-164719.51)	0.086
Non-Responders (SD/PD)	31		151910.48 (122234.84-211183.97)	
Responders (PR/CR)	16	sFGL1 FR	144309 (122536.64-180918.75)	0.318
Non-Responders (SD/PD)	24		159358.85 (126852.32-275000.31)	

PRE, baseline; FR, first response assessment; IQR, interquartile range; PR, partial response; CR, complete response; SD, stable disease; PD, progression disease; NSCLC, non-small cell lung cancer. *P*-values were calculated by the Mann-Whitney test. Significance values were **p*<0.05.
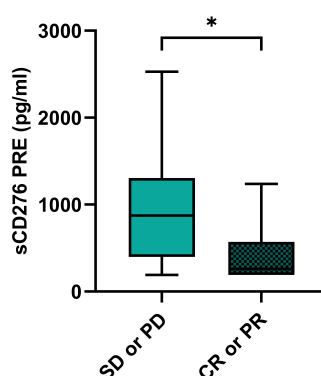
Figure 44. sCD276 and tumor response in advanced-stage NSCLC cohort. sCD276 levels at PRE in patients with tumor response (n=21) and patients without tumor response (n=31) in the entire cohort. The bold horizontal lines in the box plots are medians and bars represent minimum and maximum values. SD, stable disease; PD, progression; PR, partial response; CR, complete response; PRE, baseline; NSCLC, non-small cell lung cancer. *P*-values were calculated by the Mann-Whitney test. Significance values were **p*<0.05.

Regarding, CD276, it was initially believed to have a co-stimulatory function in the immune response, which would not be in line with our results. Nevertheless, recent research has revealed its co-inhibitory role in T-cells, contributing to the immune evasion of tumor cells (Hofmeyer et al., 2008). Our results would be in consonance with this statement, as non-responding patients to immunotherapy could have an immunosuppressive TME in which sCD276 may be involved.

Next, the correlations between DCB with soluble levels of immunoregulatory factors was assessed using the Mann-Whitney analysis and are shown in Table 34.

Table 34. Associations between plasma levels and durable clinical benefit in advanced-sage NSCLC cohort.

Clinical Benefit	Nº of patient	Analyte	Plasma levels median (IQR) pg/ml	p
DCB	29	sCD276 PRE	399.50 (228.17-958.58)	0.209
Non-DCB	23		844.65 (336.42-1457.30)	
DCB	24	sCD276 FR	633.93 (190.35-1714.75)	0.318
Non-DCB	16		994.44 (680.54-1763.11)	
DCB	29	sMICB PRE	501.27 (334.50-774.94)	0.049*
Non-DCB	23		832.81 (448.04-1000.22)	
DCB	24	sMICB FR	446.73 (348.31-555.70)	0.027*
Non-DCB	16		777.35 (786.55-983.07)	
DCB	29	sGAL3 PRE	9801.43 (7941.03-11820.17)	0.214
Non-DCB	23		10297.75 (8105.84-14298.70)	
DCB	24	sGAL3 FR	9970.82 (8251.78-12617.99)	0.048*
Non-DCB	16		11460.30 (9774.59-20760.98)	
DCB	29	sGAL1 PRE	19427.16 (16435.84-27534.96)	0.324
Non-DCB	23		20933.01 (17246.30-26497.31)	
DCB	24	sGAL1 FR	20795.18(17495.34-24794.85)	0.090
Non-DCB	16		22876.46 (19286.19-28165.29)	
DCB	29	sICOSL PRE	6646.33 (5507.54-8212.98)	0.324
Non-DCB	23		5907.39 (4424.38-8864.95)	
DCB	24	sICOSL FR	6981.89 (5527.96-9001.39)	0.331
Non-DCB	16		5867.20 (3218.53-10581.34)	
DCB	29	sMICA PRE	33.55 (20.43-173.40)	0.412
Non-DCB	23		24.88 (17.46-54.70)	
DCB	24	sMICA FR	26.12 (17.46-56.75)	0.420
Non-DCB	16		23.49 (15.29-34.23)	
DCB	29	sFGL1 PRE	139042.05 (116153.19-172003.06)	0.151
Non-DCB	23		162802.37 (121432.96-242133.79)	
DCB	24	sFGL1 FR	152508.45 (118659.75-192999.08)	0.404
Non-DCB	16		159358.85 (131996.26-228745.92)	

DCB, durable clinical benefit; Non-DCB, non-durable clinical benefit; PRE, baseline; FR, first response assessment; IQR, interquartile range; NSCLC, non-small cell lung cancer. *P*-values were calculated by the Mann-Whitney test. Significance values were *p<0.05.

At FR median sGAL3 levels were significantly higher in patients with non-DCB with a median value of 10297.75 pg/ml (IQR, 8105.84-14298.70) compared to 9970.82 pg/ml (8251.78-12617.99) in patients with DCB (p=0.03) (Figure 45A). Moreover, median sMICB

levels at PRE were significantly higher in patients non-DCB with a median value of 832.81 pg/ml (IQR, 448.04-1000.22) compared to 460.30 pg/ml (IQR, 9774.59-20760.98) in patients with DCB (*p*=0.049) (Figure 45B). Similarly, at FR, sMICB levels were significantly higher in patients with non-DCB with a median value of 777.35 pg/ml (IQR, 786.55-983.07) compared to 446.73 pg/ml (IQR, 348.31-555.70) in patients with DCB (*p*=0.027) (Figure 45C). There were no statistical differences in the rest of the immunoregulatory factors in patients with DCB compared to non-DCB.
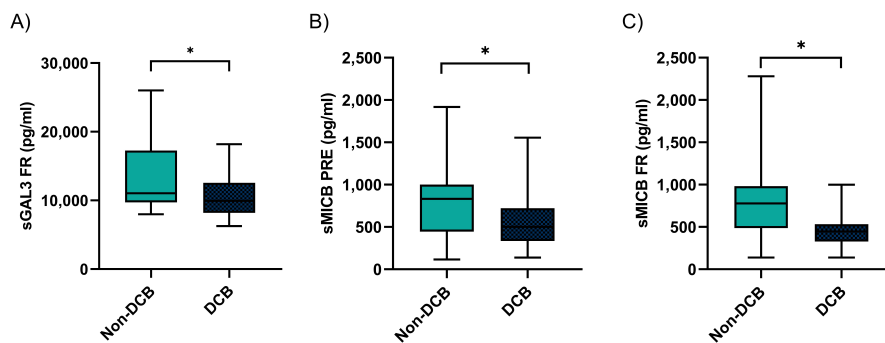
Figure 45. Associations between plasma levels of immune-mediators and durable clinical benefit (DCB) in advanced-stage NSCLC entire cohort. A) sGAL3 levels at first response assessment (FR) in patients without durable clinical benefit (non-DCB) (n=16) and patients with DCB (n=24). B) sMICB levels at baseline (PRE) in patients with non-DCB (n=23) and patients with DCB (n=29). B) sMICB levels at FR in patients with non-DCB (n=16) and patients with DCB (n=24). The bold horizontal lines in the box plots are medians and bars represent minimum and maximum values. Horizontal lines in the box plots are medians and bars represent minimum and maximum values. non-DCB, non-durable clinical benefit; DCB, durable clinical benefit; PRE, baseline; FR, first response assessment; NSCLC, non-small cell lung cancer. *P*-values were calculated by the Mann-Whitney test. Significance values were **p<0.05*.

Using ROC Curves, we test the ability of sGAL3 and sMICB to predict the clinical benefit. The summary of measurements for various individual immune-mediators and their predictive values in clinical benefit can be found in Table 35. Among these, sMICB at FR emerged as the biomarker with the highest overall predictive accuracy. sMICB cut-off levels of 583.39 pg/ml were associated with a sensitivity of 75%, a specificity of 79.2%, a PPV of 70.6% and an NPV of 82.6% to predict DCB at FR. Using this cut-off, patients with low sMICB (n=23) had a CBR of 82.6% while patients who had high sMICB (n=17) had a CBR of 29.4% (*p*=0.001) (Figure 46).

Table 35. Predictive accuracies of plasma biomarkers of advanced-stage NSCLC.

	AUC (95% CI)	Sensitivity	Specificity	PPV	NPV
DCB vs. non-DCB					
sGAL3 at FR	0.688 (0.519-0.856)	0.688	0.625	0.550	0.750
sMICB at PRE	0.660 (0.507-0.813)	0.565	0.793	0.684	0.697
sMICB at FR	0.707 (0.527-0.887)	0.750	0.790	0.706	0.826

non-DCB, non-durable clinical benefit; DCB, durable clinical benefit; PRE, baseline; FR, first response assessment; PPV, predictive positive value; NPV, negative predictive valur; NSCLC, non-small cell lung cancer.
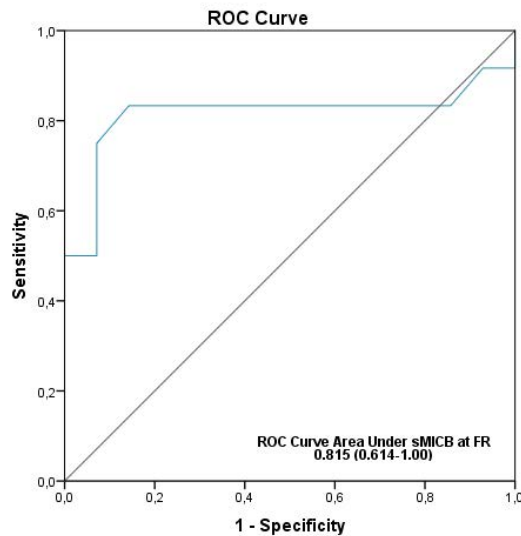
Figure 46. Receiver operating characteristic (ROC) curve of sMICB plasma levels at first response assessment (FR) in advanced-stage NSCLC with durable clinical benefit comparing to the patients without durable clinical benefit.

Despite extensive efforts to identify novel predictive biomarkers for immunotherapy in advanced NSCLC, the available data remain limited and characterized by significant heterogeneity. Even though there are currently three biomarkers (PDL1 expression, MSI, or TMB) approved by the FDA for patient selection in immunotherapy, each of them has inherent limitations at present. The expression level of PDL1 on immune cells within the tumor has emerged as the first reliable predictive biomarker for assessing the responsiveness to ICIs in advanced-stage NSCLC patients undergoing immunotherapy (Patel & Kurzrock, 2015). Nonetheless, the utility of tissue-based PDL1 expression as a predictive biomarker comes with certain limitations, including the use of various antibodies across clinical trials, varying positive threshold criteria, tumor heterogeneity in PDL1 staining, inadequate tumor tissue availability, and even patients with a negative baseline PDL1 stain might still respond to ICIs, while tumors with high PDL1 expression may be resistant to treatment (Davis & Patel, 2019). This challenge has prompted the exploration of non-invasive methods for assessing biomarkers in advanced NSCLC, including the examination of circulating tumor-derived material known as the 'tumor circulome,' which offers an innovative approach in precision oncology to address the current constraints associated with tissue biopsies (Abate et al., 2020; Malapelle et al., 2021). Within the tumor circulome, plasmatic soluble proteins offer numerous advantages due to their repeatability and easy of accessibility. Therefore, our study focuses on the research of soluble immune-mediators in plasma that hold predictive

value for immunotherapy. As far as we know, this study reports for the first time novel potential predictive plasmatic biomarkers, sMICB, sCD276 and sGAL3, in advanced-stage NSCLC patients treated with immunotherapy.

Some studies have been performed on tissue samples regarding GAL3. Our results agree with previous data that proposed a GAL3 signature by IHC for the selection of candidates for immunotherapy in 34 NSCLC patients. This study showed that patients exhibiting high GAL3 tumor expression prior to treatment, experienced an early and pronounced progression after three treatment cycles. In contrast, patients with negative or low/intermediate GAL3 expression demonstrated early and durable objective responses (Capalbo et al., 2019). In contrast to Capalbo's study, we conducted an analysis that encompassed PRE and FR samples, obtaining significant results in FR samples. Our findings support the use of a fast and high-sensitivity methodology that could be employed to assess the secretion of sGAL3 in plasma samples. Our results reflect the impact of pembrolizumab on the immune-mediators' production, providing valuable insights for identifying non-responders in the initial radiological evaluation. No other studies have been carried out about the predictive role to immunotherapy of sCD276 and sMICB.

Other studies about new plasmatic biomarkers as putative predictive biomarkers associated with ICIs efficacy in NSCLC has also been carried out. Okuma et al. revealed that clinical benefit by nivolumab therapy was significantly associated with baseline plasma sPDL1 levels in NSCLC patients (Okuma et al., 2017, 2018). Other plasmatic biomarkers such as sGranB were associated with the response to nivolumab (Costantini et al., 2018).

As we seen previously, significant differences were found between LUSC and LUAD analysis, which led to the assumption that they are molecularly different diseases. In our previous analysis in early-stage NSCLC, only in LUAD patients did sGAL3 have an impact on the prognosis. For this reason, a Mann-Whitney analysis was also performed according to patients' histology. Regarding LUSC patients, the low number of patients (n=13) renders the analyses statistically underpowered, and results were no significant, so they are not displayed in the current thesis. The correlations between ORR and soluble

levels of immune-mediators in advanced-stage LUAD patients was assessed using the Mann-Whitney analysis. According with the results in the entire cohort, this analysis also showed that median sCD276 levels at PRE were significantly higher in patients without tumor response with a median value of 844.65 pg/ml (IQR, 395.99-1250.45) compared to 326.23 pg/ml (IQR, 190.35-647.27) in patients with tumor response (*p*=0.043) (Figure 47). No statistical differences were found in the rest of factors analyzed.
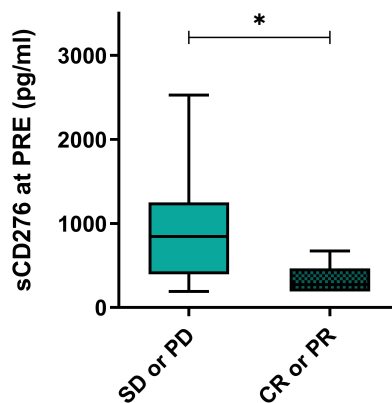
Figure 47. sCD276 and tumor response in advanced-stage LUAD subcohort. sCD276 levels at baseline in patients with tumor response (n=21) and patients without objective response (n=31) in LUAD subcohort. The bold horizontal lines in the box plots are medians and bars represent minimum and maximum values. SD, stable disease; PD, progression; PR, partial response; CR, complete response; PRE, baseline; LUAD, lung adenocarcinoma. P-values were calculated by the Mann-Whitney test. Significance values were **p* <0.05.

Next, the correlations between DCB with soluble levels of immune-mediators in advanced-stage LUAD patients was assessed using the Mann-Whitney analysis and are shown in Table 36. Consistent with the results in the entire cohort, at PRE, median sMICB levels were significantly higher in patients with non-DCB compared to patients with DCB (*p*=0.049) (Figure 48A). At FR, median sMICB and sGAL3 levels were significantly higher in patients with non-DCB compared to patients with DCB (*p*=0.005 and *p*=0.017, respectively) (Figure 48 B,C). Moreover, in the LUAD subcohort median sGAL1 levels were significantly higher in patients with non-DCB compared to patients with DCB (Figure 48D). There were no statistical differences in the rest of the immune-mediatoris in patients with DCB compared to those with non-DCB.

Table 36. Associations between plasma levels and durable clinical benefit in advanced-stage LUAD subcohort.

Durable Clinical Benefit	Nº of patient	Analyte	Plasma levels median (IQR) pg/ml	*p*
DCB	19	sCD276 PRE	395.99 (222.46-671.97)	0.167
Non-DCB	15		844.65 (235.68-1285.98)	
DCB	14	sCD276 FR	440.06 (190.35-1368.7975)	0.212
Non-DCB	12		994.44 (551.49-1763.11)	
DCB	19	sMICB PRE	485.11 (306.89-721.90)	0.004*
Non-DCB	15		832.81 (583.49-1110.41-9	
DCB	14	sMICB FR	446.73 (431.21-555.70)	0.005*
Non-DCB	12		805.08 (611.60-1045.58)	
DCB	19	sGAL3 PRE	9218.35 (7587.89-11242.48)	0.089
Non-DCB	15		11208.02 (8014.89-14623.86)	
DCB	14	sGAL3 FR	8880.89 (7582.85-10768.98)	0.017*
Non-DCB	12		11972.50 (9844.79-23224.59)	
DCB	19	sGAL1 PRE	17434.43 (13813.95-20458.16)	0.096
Non-DCB	15		21433.74 (17246.30-24572.79)	
DCB	14	sGAL1 FR	18141.46 (16457.60-21422.51)	0.015*
Non-DCB	12		22876.46 (19371.66-27030.29)	
DCB	19	sICOSL PRE	6646.33 (5502.57-7959.70)	0.391
Non-DCB	15		5717.13 (4424.38-8864.95)	
DCB	14	sICOSL FR	6166.43 (5567.95-7952.21)	.0.595
Non-DCB	12		5867.20 (2638.22-9623.41)	
DCB	19	sMICA PRE	29.08 (19.93-44.74)	0.336
Non-DCB	15		37.25 (19.93-58.45)	
DCB	14	sMICA FR	23.02 (16.84-44.11)	0.860
Non-DCB	12		24.73 (17.64-37.95)	
DCB	19	sFGL1 PRE	139042.05 (94695.67-211183.97)	0.391
Non-DCB	15		151910.48 (121432.96-190373.31)	
DCB	14	sFGL1 FR	156594.82 (111035.84-205654.16)	0.667
Non-DCB	12		154094.95 (131996.26-183530.29)	

DCB, durable clinical benefit; Non DCB, non-durable clinical benefit; PRE, baseline; FR, First response assessment; IQR, interquartile range. P-values were calculated by the Mann-Whitney test. Significance values were *p*<0.05.
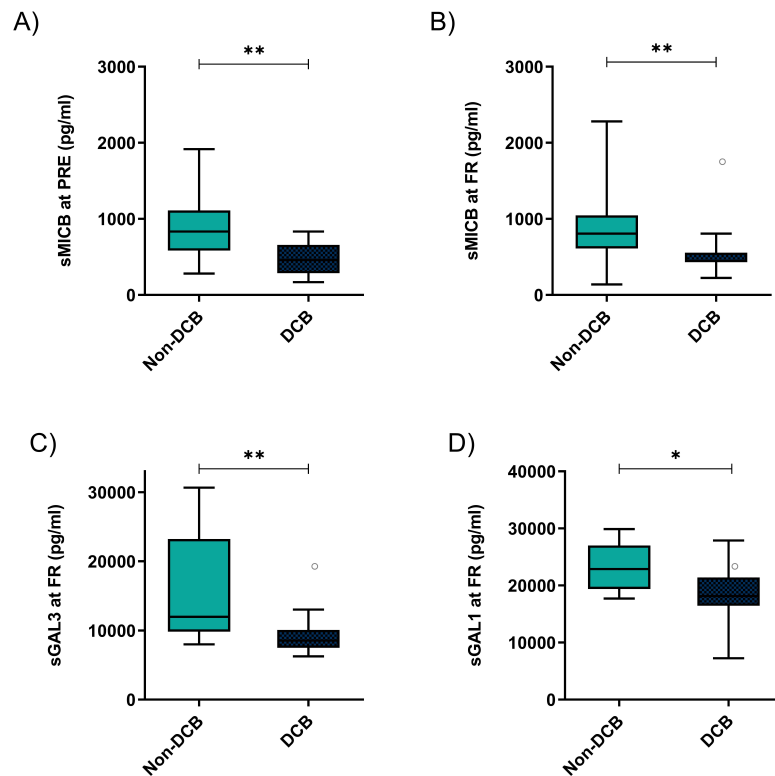
Figure 48. Associations between plasma levels of immune-mediators and durable clinical benefit (DCB) in advanced-stage LUAD subcohort. A) sMICB levels at baseline (PRE) in patients with non-DCB (n=15) and patients with DCB (n=19). B) sMICB levels at first response assessment (FR) in patients with non-DCB (n=12) and patients with DCB (n=14). C) sGAL3 levels at FR in patients with non-DCB (n=12) and patients with DCB (n=14). C) sGAL1 levels at FR in patients with non-DCB (n=12) and patients with DCB (n=14). The bold horizontal lines in the box plots are medians and bars represent minimum and maximum values. horizontal lines in the box plots are medians and bars represent minimum and maximum values. non-DCB, non-durable clinical benefit; DCB, durable clinical benefit; PRE, baseline; FR, first response assessment; LUAD, lung adenocarcinoma. *P*-values were calculated by the Mann-Whitney test. Significance values were *$p<0.05$, **$p<0.01$.

Using ROC Curves, we test the ability of sGAL3, sMICB and sGAL1 to predict the clinical benefit. The summary of measurements for various individual immune-mediators at PRE and at FR and their predictive values in DCB can be found in Table 37. Among these, sMICB at FR emerged as the biomarker with the highest overall predictive accuracy also in the advanced-stage LUAD subcohort. sMICB cut-off levels of 612.12 pg/ml were associated with a sensitivity of 75%, a specificity of 95.9%, a PPV of 90% and an NPV of 81.3% to predict DCB at FR. Using this cut-off, patients with low sMICB (n=23) had a CBR of 81.3% while patients who had high sMICB (n=17) had a CBR of 10% (*$p<0.001$*) (Figure 49).

Table 37. Predictive accuracies of plasma biomarkers of advanced-stage LUAD subcohort.

	AUC (95% CI)	Sensitivity	Specificity	PPV	NPV
DCB vs. non-DCB					
sMICB at PRE	0.782 (0.620-0.945)	0.667	0.895	0.833	0.773
sMICB at FR	0.815 (0.614-1.000)	0.750	0.929	0.900	0.813
sGAL3 at FR	0.801 (0.625-0.977)	0.750	0.846	0.818	0.786
sGAL1 at FR	0.780 (0.602-0.958)	0.917	0.571	0.647	0.889

CI, confidence interval; non-DCB, non-durable clinical benefit; DCB, durable clinical benefit; PPV, positive predictive value; NPV, negative predictive value; PRE, baseline; FR, first response assessment; LUAD, lung adenocarcinoma.
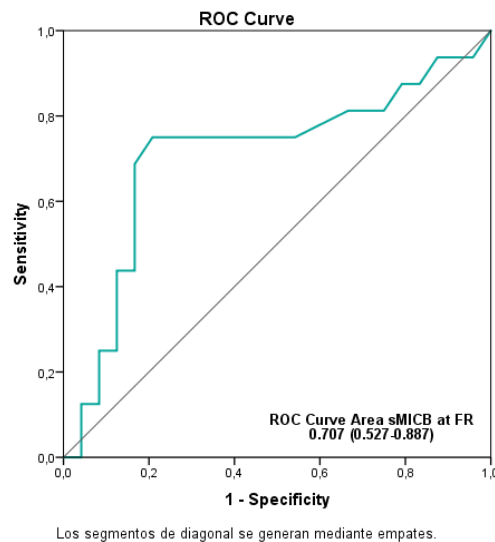
Figure 49. Receiver operating characteristic (ROC) curve of sMICB plasma levels at first response assessment in advanced-stage LUAD subcohort with durable clinical benefit comparing to the patients without durable clinical benefit.

In advance LUAD subcohort, we have observed the same results as in the entire NSCLC cohort but with greater significance. Since the majority of our cohort consists of LUAD cases, this histology may have the greatest impact on the overall cohort results.

2.3. BIOMARKERS WITH PROGNOSTIC VALUE

The prognostic value of the soluble immune-mediators, including sGAL3, was performed using the univariate Cox regression method for PFS and OS. Levels of soluble proteins were dichotomized according to their median, and the results obtained are shown in Table 38. Kaplan-Meier analyses were carried out to obtain the survival plots (Figure 50). In this case the Univariate Cox regression model performed revealed that high sGAL3 levels (>median) at PRE were associated with worse PFS [HR, 2.024; 95% CI 1.053-3.890; p=0.034] and OS [HR, 1.949; CI 95% 0.992-3.830, p=0.049] (Figure 50 A,B). Moreover, we observed a tendency that patients with low sCD276 levels at PRE tended to have better PFS and OS than those with high sCD276 levels (Figure 50 C,D). Finally,

126

high sMICB levels (>median) at FR were associated with worse PFS [HR, 2.348; 95% CI 1.129-4.883; *p*=0.022] (Figure 50E). Similarly, patients with low sMICB levels at FR tended to have better OS [HR, 1.827; 95% CI 0.838-3.983; *p*=0.129] (Figure 50F).

Table 38. Results from univariate survival analysis based on levels of soluble immune-mediators in the advanced-stage NSCLC cohort.

	PFS			OS		
Gene	**HR**	**95% CI**	**p-value**	**HR**	**95% CI**	**p-value**
sFGLF1 PRE						
High vs. Low	0.908	0.477-1.729	0.770	1.163	0.598-2.260	0.657
sFGLF1 FR						
High vs. Low	0.939	0.458-1.923	0.862	1.035	0.479-2.2236	0.930
sICOSL PRE						
High vs. Low	0.847	0.448-1.603	0.610	1.010	0.520-1.963	0.976
sICOSL FR						
High vs. Low	0.688	0.333-1.420	0.312	0.723	0.372-1.596	0.422
sCD276 PRE						
High vs. Low	1.861	0.976-3.547	0.059	1.688	0.866-3.292	0.124
sCD276 FR						
High vs. Low	1.674	0.811-3.455	0.163	1.140	0.528-2.462	0.738
sGAL3 PRE						
High vs. Low	2.024	1.053-3.890	0.034*	1.949	0.992-3.830	0.049*
sGAL3 FR						
High vs. Low	1.507	0.733-3.097	0.265	1.964	0.899-4.290	0.090
sGAL1 PRE						
High vs. Low	1.431	0.755-2.712	0.273	1.175	0.604-2.284	0.653
sGAL1 FR						
High vs. Low	1.155	0.564-2.368	0.693	1.089	0.503-2.357	0.828
sMICA PRE						
High vs. Low	0.634	0.333-1.209	0.634	0.979	0.504-1.903	0.951
sMICA FR						
High vs. Low	0.808	0.388-1.682	0.568	0.917	0.418-2.013	0.830
sMICB PRE						
High vs. Low	1.700	0.898 -3.220	0.103	1.440	0.740-2.804	0.283
sMICB FR						
High vs. Low	2.348	1.129-4.0883	0.022*	1.827	0.838-3.983	0.129

CI, confidence interval; HR, hazard ratio; PFS, progression-free survival; OS, overall survival; PRE, baseline; FR, first response assessment; NSCLC, non-small cell lung cancer. *P*-values were calculated by univariate Cox regression method. Significance values were **p*<0.05.
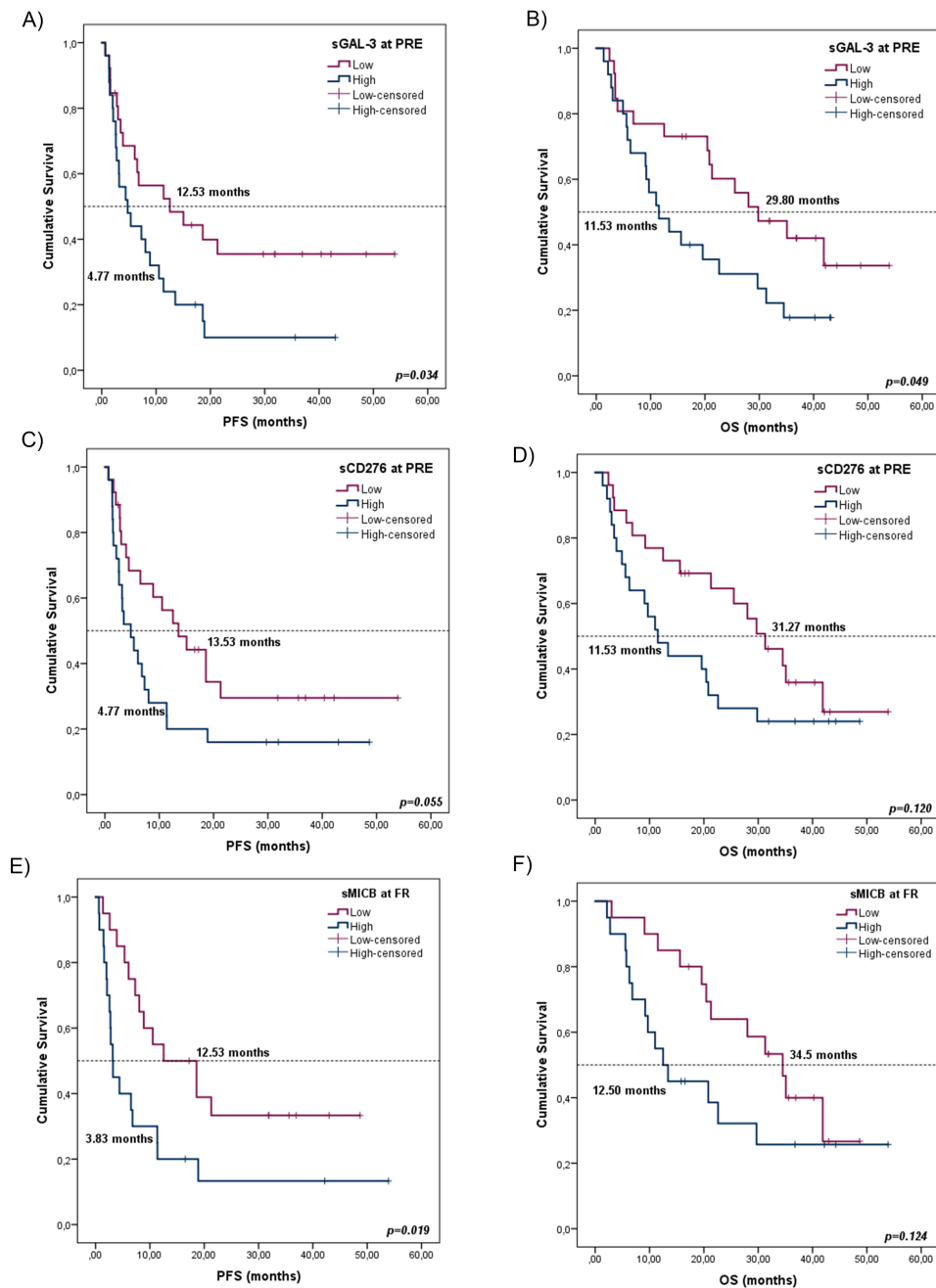
Figure 50. Kaplan-Meier plots for PFS and OS according to the plasma levels of immune-mediators in the advanced-stage NSCLC cohort. A,B) Progression-free survival (PFS) and overall survival (OS) based on sGAL3 levels at baseline (PRE), respectively. Cut-off values correspond to the median soluble levels. Red lines represent patients with high levels of sGAL3 (n=25), whereas blue lines represent patients with low levels of sGAL3 (n=26). C,D) PFS and OS based on sCD276 levels at PRE, respectively. Cut-off values correspond to the median soluble levels. Red lines represent patients with high levels of sCD276 (n=25), whereas blue lines represent patients with low levels of sGAL3 (n=26). E,F) PFS and OS in line with sMICB levels at first response assessment (FR), respectively. Cut-off values correspond to the median soluble levels. Red lines represent patients with high levels of sMICB (n=20), whereas blue lines represent patients with low levels of sMICB (n=20). PFS, progression-free survival; OS, overall surviva; PRE, baseline; FR, First response assessment; NSCLC, non-small cell lung cancer; n, sample size. *P*-values were calculated by log-rank test. *P*-value was statistical significative *p*<0.05.

Next, we performed the same analysis through an univariant Cox regression analysis using the percentile 75th instead of the median. Interestingly, low sMICB levels at PRE and FR (considering the 75th percentile of sMICB <825.87 pg/ml) were also associated with improved PFS and OS. At PRE, patients with sMICB levels below the 75th percentile had worse PFS [HR, 2.454; 95% CI 1.180-5.102; *p*=0.016] and OS [HR, 2.378; 95% CI1.104-5.125; *p*=0.027]. Furthermore, at FR, high sMICB levels were associated with worse PFS [HR, 3.643; 95% CI 1.611-8.241; *p*=0.002] and OS [HR, 2.938; 95% CI 1.232-7.005; *p*=0.015]. Kaplan-Meier analyses were carried out to obtain the survival plots (Figure 51).
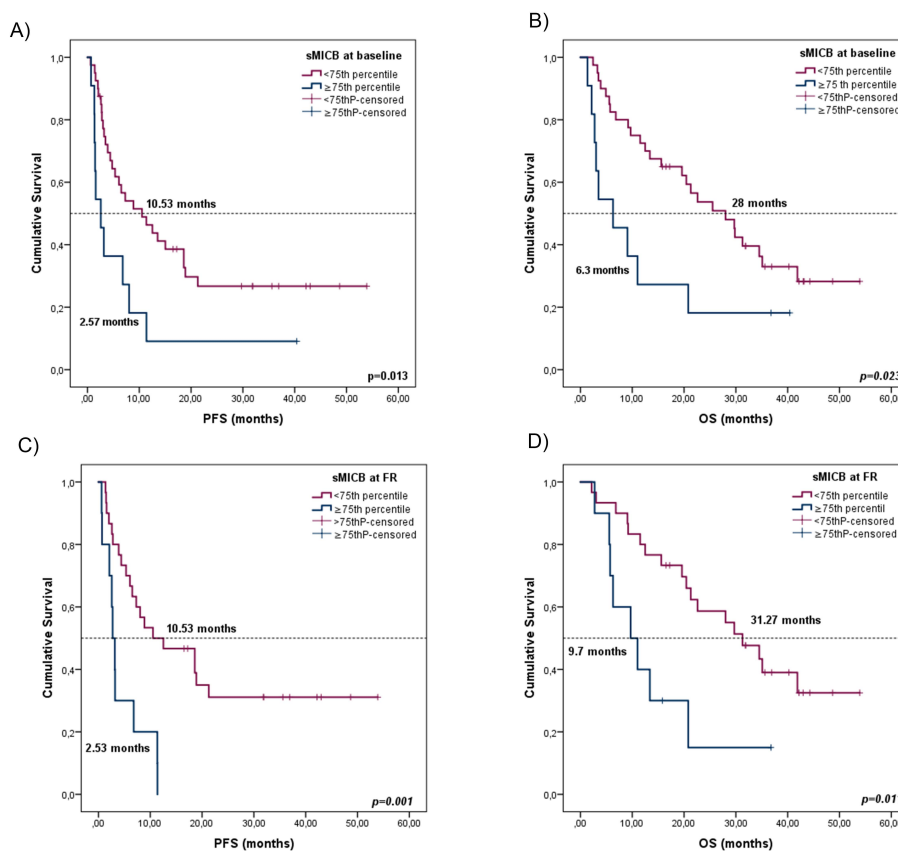
Figure 51. sMICB and PFS and OS using 75ᵗʰ percentile in advanced-stage NSCLC cohort. A, B) Progression-free survival (PFS) and overall survival (OS) in compliance with sMICB levels (above (n=11) or below (n=40) the 75th percentile) at baseline (PRE). C, D) PFS and OS according to sMICB levels (above (n=10) or below (n=30) the 75th percentile at first response assessment (FR). PFS, progression-free survival; OS, overall survival; FR, first response assessment; PRE, baseline; n, sample size; NSCLC, non-small cell lung cancer. *P*-values were calculated by log-rank. test. *P*-value was statistical significative *p*<0.05.

Recently, a study by Jun Sun Kim et al. examined the involvement of sGAL3 in NSCLC patients treated with ICIs measured through a conventional immunoassay. The results were in line with our findings, indicating that patients with elevated sGAL3 levels in their serum or plasma (depending on the availability before treatment) had a poorer

OS (n=56) (J. Sun et al., 2022). No significant results were found for PFS. However, this study lacked a measurement of levels at FR and did not conduct a dynamic analysis as in our study. Additionally, the heterogeneity in sample types (plasma or serum), prior lines of treatment, type of ICIs used may introduce variability in their results.

Regarding sMICB, the soluble isoform of MICB in bloodstream is derived from alternative splicing, Phosphatidylinositol-Specific Phospholipase C-mediated cleavage, a proteolytic shedding, or via exosome secretion (Chitadze et al., 2013). Contrary to the membrane-bound form, the soluble form of MICB has been reported to induce a reduction in *NKG2D* expression on both systemic and tumor-infiltrated NK and T cells, leading to their functional impairment (Doubrovina et al., 2003; Groh et al., 2002; Raffaghello et al., 2004; J. D. Wu et al., 2004). To our knowledge, this is the first study to determine the significance of sMICB in advanced-stage NSCLC patients. The relation of high levels of sMICB with poor prognosis could be explained because the shedding of sMICB in the bloodstream cause the ineffectiveness of NKG2D–mediated immunity, which has been investigated in epithelial cancer including lung, ovarian, colon, breast, neuroblastoma, melanoma and prostate cancer (Groh et al., 2002).

Finally, we attempted to assess if variations in levels between PRE and FR could have an implication on prognosis. Levels of soluble immune-meadiators calculated as the ratio of FR/PRE were dichotomized according to >2 (two-fold increase) and <2(decreased or stable levels), and the results obtained are shown in Table 39. Interestingly, patients with increased sGAL3 levels at FR had shorter OS in comparison with patients harboring stable or decreased levels of sGAL3 at FR (3.9 vs. 22.6 months, *p*=0.033) (Figure 52). Changes in the rest of the biomarkers levels between PRE and FR did not predict patients' outcomes.

We showed that a decreased in sGAL3 after 4 cycles of pembrolizumab was associated with an improvement of OS. Assessing sGAL3 kinetics between PRE and FR reflects the impact of pembrolizumab on the biomarker's production or destruction and may be helpful to identify non-responders before the first radiological evaluation, which usually occurs after 4 to 6 cycles.

Table 39. Results from univariate survival analysis based on the differences between levels of soluble factors in PRE and FR for the advanced-stage NSCLC cohort.

	PFS			OS		
Gene	**HR**	**95% CI**	**p-value**	**HR**	**95% CI**	**p-value**
sFGLF1 FR/PRE						
Increased vs. Decreased or Stable	0.962	0.455-2.033	0.918	1.227	0.572-2.633	0.599
sICOSL FR/PRE						
Increased vs. Decreased or Stable	1.204	0.551-2.631	0.216	1.993	0.929-4.275	0.077
sCD276 FR/PRE						
Increased vs. Decreased or Stable	1.290	0.666-2.501	0.450	1.690	0.857-3.335	0.130
sGAL3 FR/PRE						
Increased vs. Decreased or Stable	1.501	0.726-3.104	0.273	2.147	1.046-4.409	0.037*
sGAL1 FR/PRE						
Increased vs. Decreased or Stable	1.204	0.551-2.631	0.641	1.993	0.929-4.275	0.077
sMICA FR/PRE						
Increased vs. Decreased or Stable	0.951	0.435-2.076	0.899	1.602	0.747-3.434	0.226
sMICB FR/PRE						
Increased vs. Decreased or Stable	0.971	0.471-2.000	0.936	1.661	0.810-3.304	0.166

CI, confidence interval; HR, hazard ratio; OS, overall survival; PFS, progression-free survival; PRE, baseline; FR, first response assessment. *P*-values were calculated by univariate Cox regression method. Significance values were *p<0.05, **p<0.01.
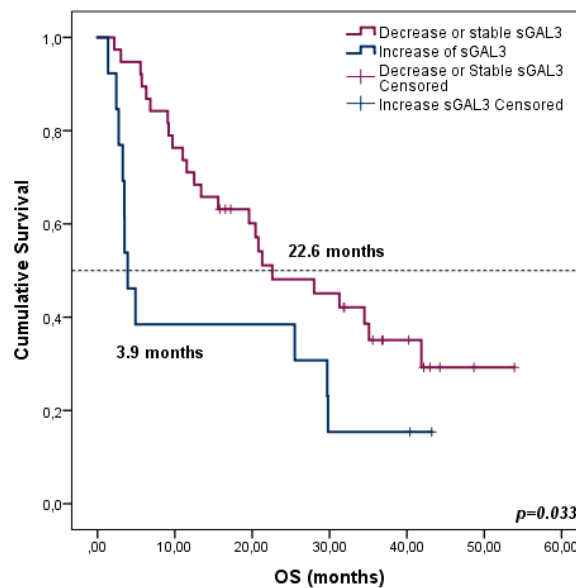
Figure 52. Kaplan-Meier survival curves based on the evolution of sGAL3 levels between PRE and FR. Overall survival (OS) stratified in decreased or stable sGAL3 levels (n=38) vs. increase sGAL3 levels (n=13). Red lines represent patients with decreased or stable levels of sGAL3 whereas blue lines represent patients with decrease levels of sGAL3. PRE, baseline; FR, first response assessment; OS, overall survival; n, sample size. *P*-values were calculated by log-rank test. P-value was statistical significative *p<0.05.

As we have seen previously, significant differences were found between LUSC and LUAD analysis, which led to the assumption that they are molecularly different diseases. In our previous analysis in early-stage NSCLC, only in LUAD patients sGAL3 did have an impact in the prognosis. For this reason, the univariate Cox regression method for PFS and OS was performed in advanced-stage LUAD subcohort. Levels of soluble immune-

mediators were dichotomized according to their median, and the results obtained are shown in Table 40. Kaplan-Meier analyses were carried out to obtain the survival plots for significant analytes (Figure 53).

Table 40. Results from univariate survival analysis based on levels of soluble immune-mediators for the advanced-stage LUAD subcohort.

	PFS			OS		
Gene	**HR**	**95% CI**	**p-value**	**HR**	**95% CI**	**p-value**
sFGLF1 PRE						
High vs. Low	0.964	0.430-2.159	0.029	1.201	0.528-2.730	0.662
sFGLF1 FR						
High vs. Low	0.802	0.332-1.937	0.624	1.151	0.442-2.996	0.773
sICOSL PRE						
High vs. Low	0.512	0.225-1.163	0.110	0.651	0.284-1.493	0.311
sICOSL FR						
High vs. Low	0.656	0.271-1.1587	0.349	0.659	0.251-1.733	0.398
sCD276 PRE						
High vs. Low	2.363	1.043-5.355	0.039*	1.700	0.742-3.895	0.210
sCD276 FR						
High vs. Low	2.055	0.813-5.084	0.119	1.252	0.482-3.253	0.645
sGAL3 PRE						
High vs. Low	2.275	0.995-5.202	0.079	1.171	0.750-3.931	0.201
sGAL3 FR						
High vs. Low	2.913	1.119-7.581	0.028*	3.458	1.248-9.577	0.017*
sGAL1 PRE						
High vs. Low	1.368	0.612-3.057	0.446	0.878	0.431-2.220	0.978
sGAL1 FR						
High vs. Low	1.506	0.620-3661	0.366	2.075	0.785-5.484	0.141
sMICA PRE						
High vs. Low	1.042	0.463-2.348	0.920	2.722	1.145-6.473	0.023*
sMICA FR						
High vs. Low	1.334	0.540-3.293	0.532	1.907	0.709-5.126	0.201
sMICB PRE						
High vs. Low	1.634	0.731-3.651	0.232	1.279	0.552-2.962	0.566
sMICB FR						
High vs. Low	4.279	1.688-10.846	0.002**	2.352	0.896-6175	0.082

CI, confidence interval; HR, hazard ratio; OS, overall survival; PFS, progression-free survival; PRE, baseline; FR, First response assessment; LUAD, lung adenocarcinoma. *P*-values were calculated by univariate Cox regression method. Significance values were *$p<0.05$, **$p<0.01$.

In this case the Univariate Cox regression model performed revealed that LUAD patients with low sCD276 levels (<median) at PRE were associated with worse PFS [HR, 2.363; 95% CI 1.043-5.355; *p*=0.039]. This association was significant, unlike in the case of the entire cohort (Figure 53A). Consistent with the entire cohort, in LUAD patients, high sMICB levels (>median) at FR were associated with worse PFS [HR, 4.279; 95% CI 1.688-10.846; *p*=0.002] (Figure 53B). Similarly, patients with low sMICB levels at FR tended to have better OS [HR, 2.352; 95% CI 0.896-6175; *p*=0.082] (Figure 53C). Finally, in LUAD subcohort, high sGAL3 levels (>median) at FR were associated with worse PFS [HR, 2.913;

95% CI 1.119-7.581; *p*=0.028] and OS [HR, 3.458; 95% CI 1.248-9.577, *p*=0.017] (Figure 53 D,E).
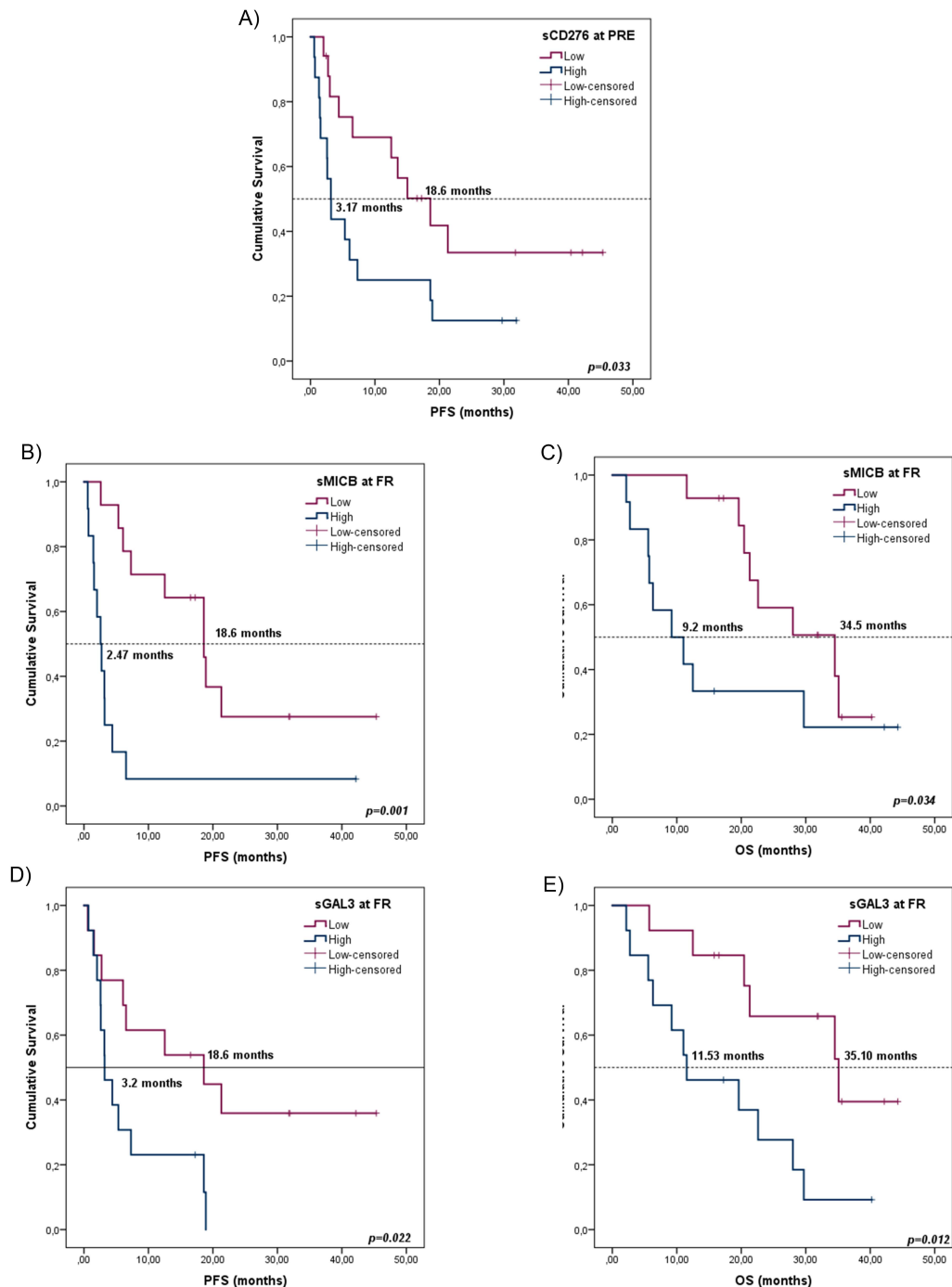
Figure 53. Kaplan-Meier plots for PFS and OS according to the plasma levels of immune-mediators in the advanced-stage LUAD subcohort. A) Progression-free survival (PFS) based on sCD276 levels at baseline (PRE), respectively. Cut-off values correspond to the median soluble levels. Purple lines represent patients with high levels of sGAL3 (n=17), whereas blue lines represent patients with low levels of sGAL3 (n=16). B,C) PFS and overall survival (OS) based on sMICB levels at first response assessment (FR), respectively. Cut-off values correspond to the median soluble levels. Purple lines represent patients with high levels of sMICB (n=14), whereas blue lines represent patients with low levels of sMICB (n=12). D,E) PFS and OS in line with sGAL3 levels at FR, respectively. Cutoff values correspond to the median soluble levels. Purple lines represent patients with high levels of SGAL3 (n=13), whereas blue lines represent patients with low levels of sGAL3 (n=13). OS, overall survival; PFS, progression-free survival; PRE, baseline; FR, first response assessment; LUAD, lung adenocarcinoma; n, sample size. *P*-values were calculated by Kaplan-Meier test. *P*-value was statistical significative *p*<0.05.

Contrary to the entire cohort, when we analyzed only LUAD subcohort we observed that sGAL3 has prognosis value at FR. This discrepancy could be attributable to the size of the sample utilized.

Regarding sCD276, we found that patients with low levels of sCD276 have better prognosis for PFS. The value of prognosis of sCD276 has already been explored in a few cancer studies. In accordance with our findings, previous studies have reported that elevated levels of sCD276 are linked to unfavorable prognoses in ovarian cancer and gastric adenocarcinoma patients (Huang et al., 2022; Kovaleva et al., 2021). However, a recent study in NSCLC reported opposites results, showing that higher sCD276 levels were associated with improved outcomes, in contrast to our study (Genova et al., 2023). It's worth noting that our results are aligned with most studies conducted on tissue specimens, where CD276 expression has consistently been correlated with a poor prognosis, underscoring the significance of our findings (Malapelle et al., 2022).

3. MULTIVARIATE ANALYSIS

In order to determine the independent prognostic value of sGAL3 and sMICB, a multivariate Cox regression analysis was performed. To build multivariate PFS and OS models, we introduce all clinicopathological variables (gender, age, TNM staging, histology and smoking status), as well as all soluble immune-mediators analyzed. Results obtained from this multivariate analysis confirmed that sGAL3 at PRE was an independent biomarker for PFS and OS. Moreover, sMICB at FR for PFS was also confirmed as prognostic independent factor (Table 41).

Table 41. Significant results from multivariate Cox regression model including all clinicopathological variables from advanced-stage NSCLC.

	PFS			OS		
Variables	**HR**	**95% CI**	**p-value**	**HR**	**95% CI**	**p-value**
sGAL3 PRE (High vs Low)	2.450	1.143-5.252	0.021*	4.915	1.897-12.731	0.001**
sMICB FR (High vs Low)	2.576	1.228-5.402	0.012*	-	-	-

CI, confidence interval; HR, hazard ratio; OS, overall survival; PFS, progression-free survival. PRE, baseline; FR, first response assessment; NSCLC, non-small cell lung cancer. *P*-value were obtained using the multivariate Cox regression method. Significance values were *$p<0.05$, **$p<0.01$.

The multivariate Cox regression method for PFS and OS was also performed in advanced-stage LUAD subcohort. Results obtained from this multivariate analysis confirmed that sGAL3 at FR was an independent biomarker for OS. Moreover, sMICB at FR for PFS and OS was also confirmed as prognostic independent factor (Table 42).

Table 42. Significant results from multivariate Cox regression model including all clinicopathological variables from advanced-stage LUAD subcohort.

Variables	PFS			OS		
	HR	95% CI	p-value	HR	95% CI	p-value
sGAL3 FR (High vs Low)	-	-	-	4.824	1.101-21.144	0.037*
sMICB FR (High vs Low)	43.278	7.652-244.784	*p*<0.001***	29.410	4.535-190.739	*p*<0.001***

CI, confidence interval; HR, hazard ratio; OS, overall survival; PFS, progression-free survival. PRE, baseline; FR, first response assessment; LUAD, lung adenocarcinoma. *P*-value were obtained using the multivariate Cox regression method. Significance values were *p<0.05, **p<0.01, ***p<0.001.

Despite the exciting findings we have uncovered, our research does come with certain limitations. In spite of the small group of patients in our cohort, it's important to note that we still observed significant results in terms of ORR, DCB, and survival rates. To further validate the predictive and prognostic value of sMICB and sGAL3, it would be necessary to use a validation cohort of advanced-stage NSCLC patients. Nevertheless, our study in advanced-stage NSCLC has also several strengths. First, we employed a prospective cohort of patients with previously well-characterized plasma samples, subject to rigorous pre-analytical conditioning. Second, our research involved the analysis of two distinct samples: one at the PRE and another at the FR for each patient, allowing the dynamic analyses. Third, we used an ultrasensitive multiplex methodology, which not only enhanced sensitivity but also reduced costs, time, and sample usage.

Additionally, the robust immunoassay we employed minimized the potential for assay-dependent variability. A graphical abstract of this part of the thesis (Chapter II) is shown in Figure 54.
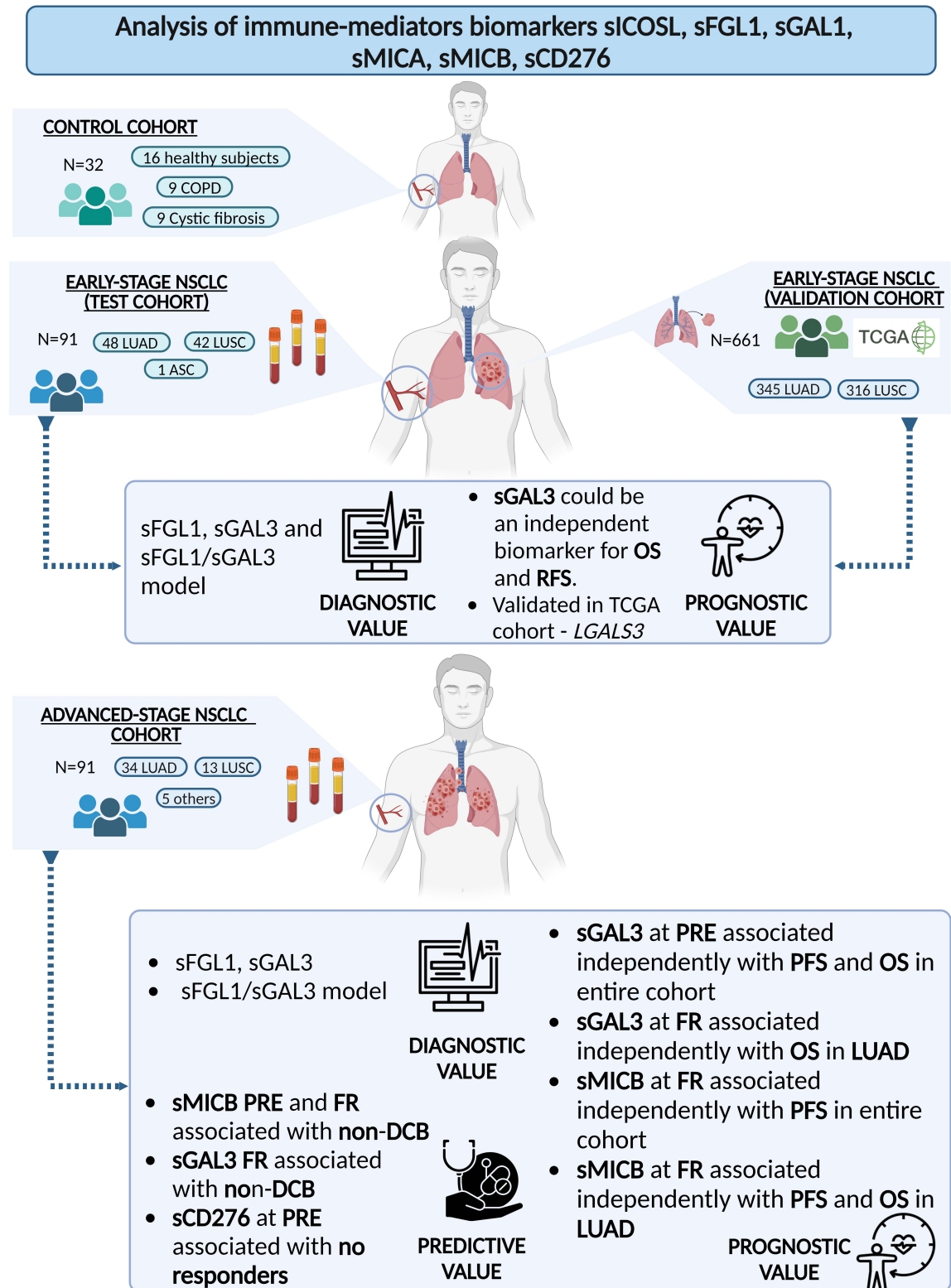
Figure 54. Chapter II graphical abstract. LUAD, lung adenocarcinoma; LUSC, lung squamous cell carcinoma, COPD, chronic obstructive pulmonary disease; ASC, adenosquamous carcinoma; TCGA, The Cancer Genome Atlas; PRE, baseline, FR, first response assessment, non-DCB, non-durable clinical benefit; OS, overall survival; RFS, relapse-free survival; PFS, progression-free survival. Own design created with BioRender.com.

INTEGRATION OF RESULTS CHAPTER I AND CHAPTER II

One of the hallmarks of cancer highlights the key role of immune systems in tumorigenesis. Since interactions between tumor cells and immune cells are involved in the down-regulation of the immune response, allowing tumors to escape from immunosurveillance, a better understanding on how tumor cells interact with their immune TME in NSCLC will result in an improved characterization of patient`s immune contexture, and new immunotherapeutic protocols that may overcome the limitations of conventional therapeutic strategies. Consequently, it is essential to delve into the study of the interplay between lung tumor cells and their immune microenvironment, translating the findings into the search of biomarkers that can help better characterize tumor behaviour.

In the first part of this study, we employed 3 long-term PDLCC cultures and 15 commercial cell lines in two cell culture conditions: sphere-forming assays for tumorspheres (3D models) and standard adherent-cultured conditions (2D models) for their corresponding control counterparts. We analyzed the immune gene expression profile of 3D versus 2D culture cells in an attempt to identify molecules that could modulate the anti-tumor activities of immune cells. The relative gene expression of immunoregulatory genes described as inhibitory or co-stimulatory immune checkpoints, cytokines, galectins, ligands of NKG2D, non-classical MHC class I molecules and signal transducer/activator were determined by RT-qPCR, which is considered the gold standard in gene expression quantification with major advantages compared to other methods like low time consuming, high sensitivity, and the low amount of RNA required. Using Wilcoxon signed-rank test, *CD276*, *STAT3*, *ICOSL*, *MICA*, *MICB*, *HLAE*, *LGALS3*, *HLAF*, *LGALS9*, *MICB*, *IL8* and *CD200* for LUAD cultures and *MICA*, *LGALS9*, *STAT3*, *ICOSL* for LUSC cultures were found significantly higher expressed in tumorspheres compared with their 2D counterparts. This point led us to consider that tumorspheres possessed superior immunomodulatory properties compared to adherent-cultured cells. At that point, we analyzed the soluble factors secreted to the culture media of most of these molecules and GAL3 was selected as one of the major contributors in the TME modulation. Therefore, the expression of the protein encoded by this gene was selected for further analysis. Immunoblotting and FC confirmed previous

finding, showing that tumorspheres from LUAD cultures produced higher levels of GAL3 compared with adherent-cultured cells. IF analysis showed differential localization pattern between both culture conditions. Moreover, the study of *LGALS3* on EVs, which are an important part of TME acting as effective signaling mediators, elucidated that not only GAL3 from tumor cells but also a vesicular form of GAL3 could facilitate communication between cells in the TME.

Given these evidences suggesting that GAL3 plays an important role in TME, we decided to delve deeper into this study. At this point, the literature revealed that extracellular sGAL3 secreted by tumor cells restricts T-cell receptor (TCR) gene rearrangement, induces T cell apoptosis, and potentiate TCR downregulation, but the relationship with T$_{REGS}$ has been poorly studied. To analyze the role of GAL3 in the lung TME and elucidated its role on T$_{REGS,}$ two different strategies were employed: i) *in vitro* cell cultures and ii) analysis of GAL3 in NSCLC samples.

In the first strategy, CM from co-cultures between tumorspheres from PC435 and a fibroblast cell line were used to culture lymphocytes from healthy donors. CM effectively increased the proportion of T$_{REGS}$ compared to the control group. Blockade of GAL3 in CM was sufficient to prevent the increase of T$_{REGS}$ population significantly.

In the second strategy, we observed a positive correlation between patients exhibiting high FOXP3+ cells infiltration and those with elevated expression of *LGALS3* in the tumor. Moreover, in terms of gene expression, we discovered a positive and significant correlation of *LGALS3* expression with the ratio between *FOXP3* expression within the tumor compartment and the expression of *CD4* within both the stroma and the tumor region. To validate these results, CIBERSORTx tool with the TCGA database was used. We identified 4 clusters, where the one characterized by high levels of T$_{REGS}$ also had the highest percentage of patients with high levels of *LGALS3* expression. From these results, we can propose that some components of TME in lung cancer, such as tumor cells with stem-like properties and fibroblast, could be favors an immunosuppressive microenvironment, possibly recruiting T$_{REGS}$ through sGAL3 (results published in Molecular Oncology (Torres-Martínez et al., 2023)).

In the second part of this study, the prognostic value of GAL3 was analyzed in patients using both an early-stage and an advanced-stage NSCLC cohorts. Due to the significant differences reported according to lung cancer histologies and based on our previous results, survival analyses were also performed according to the histologic subtypes. For this purpose, we used plasma from the peripheral blood of patients. A liquid biopsy sample can be obtained from patients in a non-invasive way, at any time during disease providing a clear picture of tumor heterogeneity and evolution over time. Moreover, we used a multiplexed immunoassay which allowed us to analyze other immunoregulatory factors besides GAL-3 at the same time. The analysis of immune mediators in early and advanced NSCLC could provide useful prognostic information and could also predict response to treatment in certain clinical settings.

First, ROC analysis elucidated that sFGL1, sGAL3, and its combinations allowed an optimal diagnostic efficacy for early-stage NSCLC patients. Moreover, survival analysis revealed that high levels of sGAL3 are associated with worse PFS and OS in a test subcohort of 48 early-stage LUAD patients, being independent prognostic factor. Furthermore, we validated the prognostic value of GAL3 in an independent validation cohort of 661 early-stage NSCLC patients (validation cohort) from TCGA, finding that high levels of *LGALS3* was associated independently with worse PFS and OS in LUAD patients, but not for LUSC patients. The use of this *in silico* cohort, while not the most suitable for validation due to being based on RNA-seq data from tissue sample, is public and provide massive information. Even though, we obtained concordant results in plasma and in tissue. As far as we know, this is the first study elucidating the diagnostic and prognostic value of sGAL3 on early-stage LUAD patients undergoing surgery.

Second, we evaluated the diagnostic, prognosis, and predictive value of sGAL3 at PRE and at FR in a cohort of 52 advanced-stage NSCLC patients from *CHGUV* treated in first-line with pembrolizumab. As previously investigated in early-stage NSCLC patients, the diagnostic value of sFGL1 and sGAL3 individually and combined was also found in advanced stage NSCLC patients. Moreover, sGAL3 at FR and sMICB at PRE and FR were associated with durable clinical benefit in the entire cohort and in the LUAD subcohort. sCD276 was also associated with objective response in the entire cohort and in the LUAD subcohort. No significant results were obtained for the subcohort of LUSC patients

(n=13), probably because the low number of patients. In terms of prognosis, we found sMICB at FR to be an independent prognostic biomarker for PFS in the entire cohort and for PFS and OS for LUAD subcohort. Interestingly, we also revealed that sGAL3 at PRE could serve as an independent biomarker for OS and PFS in the entire cohort and sGAL3 at FR was found to be independent biomarker for OS. Finally, we also attempted to find prognostic value in the differences that may arise upon treatment. A decreased in FR levels of sGAL3 was associated with reduction in OS in the entire cohort.

Our study suggests that plasma sMICB and sGAL3 levels could add important information for the selection of patients for pembrolizumab treatment in advanced-stage NSCLC, potentially by excluding those with high plasma levels of sGAL3 and sMICB. Some limitations should be considered: i) includes a small number of patients, ii) the results need confirmation in a large cohort of patients with a longer follow-up. If these results are confirmed, a better selection of candidates for immunotherapy using these soluble biomarkers could be feasible, preventing ineffective treatments.

Finally, as we move towards the era of precision medicine, liquid biopsy and circulating biomarkers are central to identifying the best treatment for individual patients. As demonstrated in our study, the use of liquid biopsy highlights the importance of continuing the quest for novel immune biomarkers that can enhance our ability to identify patients who will derive maximum benefit from surgery in early-stage LUAD patients and from immunotherapy in advance-stage NSCLC patients (results published at IJMS (Torres-Martínez et al., 2023)). The novelty of these recently published results opens up potential new avenues of research on these molecules as biomarkers in lung cancer.

A graphical abstract of the integration of results is shown in Figure 55.
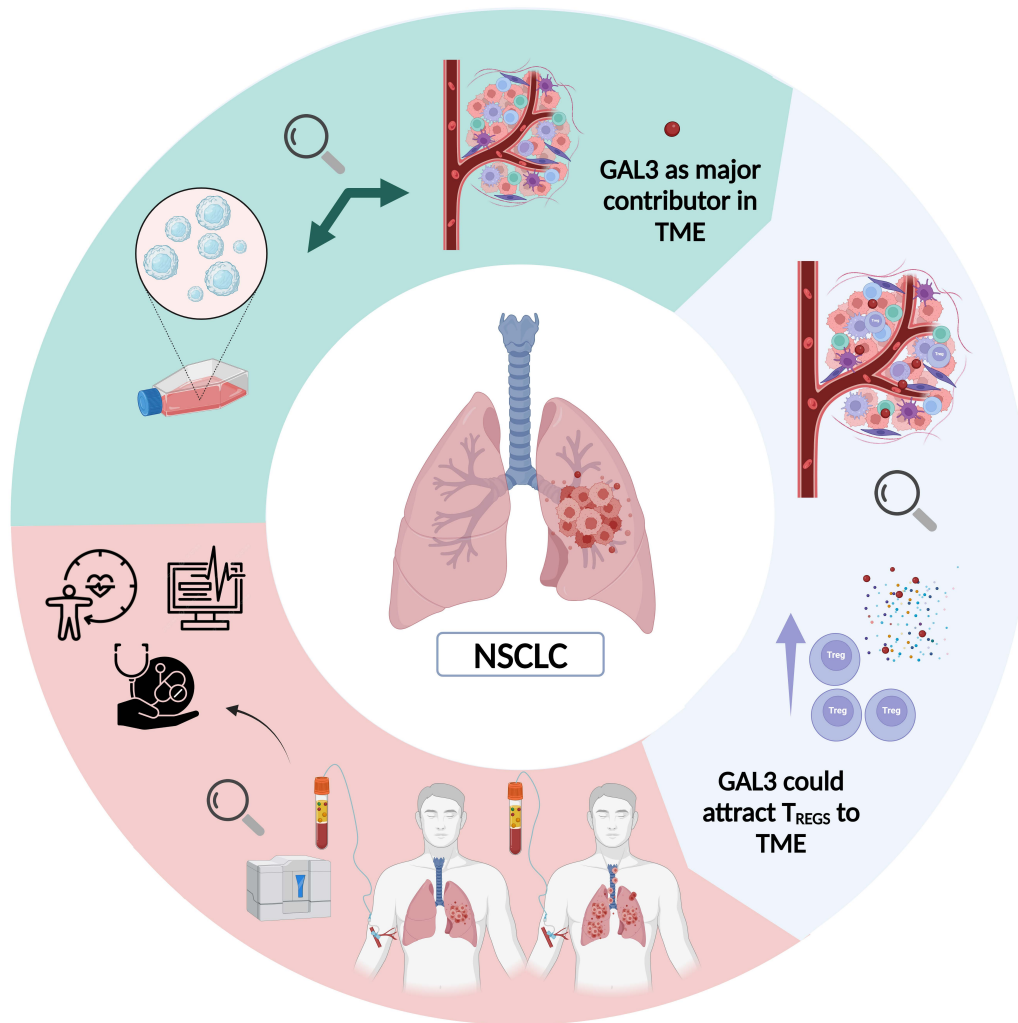
Figure 55. Integration of results emcompassed in this tesis. Own design created with BioRender.com. GAL3; Galectin-3; NSCLC, non-small cell lung cancer; TME, tumor micronvironment.

V.CONCLUSIONS

Exploratory phase:

1. Tumorspheres (3D models) from lung cancer cells expressed higher levels of immunoregulatory genes than their adherent counterparts 2D models), indicating enhanced immunomodulatory abilities.

2. LUAD tumorspheres secrete significantly higher levels of sGAL3 into the culture medium than adherent-cultured cells, indicating a possible role as a key modulator of TME in this scenario.

3. GAL3 expression (at the mRNA and protein levels) was found to be increased in tumorspheres from LUAD cultures. Moreover, a differential localization pattern of GAL3 protein was discovered among 3D and 2D LUAD cultures, with the membrane form being higher in tumorspheres.

4. We revealed that certain components of TME in lung cancer, such as tumor cells with stem-like properties and CAFs, may promote an immunosuppressive microenvironment, possibly recruiting T_{REGS} through GAL3. Translational analysis corroborated the correlation between GAL3 and proportion of T_{REGS}.

Translational phase:

5. The analysis in of blood-based immune-mediator biomarkers in NSCLC patients revealed that:

    5.A. In early-stage NSCLC: sGAL3, sFGL1 and its combination were found to have a diagnostic value with adequate sensitivity and specificity. Moreover, sGAL3 was also identified as an independent prognostic factor in LUAD patients (test cohort), findings that were confirmed also in tissue samples from a validation TCGA cohort, demonstrating that patients with high LGALS3 have significantly shorter RFS and OS.

    5.B. In advanced-stage NSCLC: sGAL3, sFGL1 and its combination were also found to have a diagnostic value in this clinical setting. sGAL3, sMICB,

and/or CD276 showed a relationship with response, PFS, or OS, in some cases at PRE or in others at FR sample, emphasizing that once again and consistently with our results, sGAL3 demonstrated value as an independent prognostic biomarker for OS in LUAD.

6. The integration of our results indicated that GAL3 could be an important immune-mediator in the modulation of TME in LUAD, having diagnostic and prognostic value in early-stage LUAD and diagnostic, predictive, and prognostic value in advanced-stage LUAD patients.

VI. REFERENCES

Abate, R. E., Frezzetti, D., Maiello, M. R., Gallo, M., Camerlingo, R., De Luca, A., De Cecio, R., Morabito, A., & Normanno, N. (2020). Next generation sequencing-based profiling of cell free DNA in patients with advanced non-small cell lung cancer: Advantages and pitfalls. *Cancers*, *12*(12), 1–17. https://doi.org/10.3390/cancers12123804

Abbosh, C., Birkbak, N. J., Wilson, G. A., Jamal-Hanjani, M., Constantin, T., Salari, R., Le Quesne, J., Moore, D. A., Veeriah, S., Rosenthal, R., Marafioti, T., Kirkizlar, E., Watkins, T. B. K., McGranahan, N., Ward, S., Martinson, L., Riley, J., Fraioli, F., Al Bakir, M., … Dessimoz, C. (2017). Phylogenetic ctDNA analysis depicts early-stage lung cancer evolution. *Nature*, *545*(7655), 446–451. https://doi.org/10.1038/nature22364

Aguilar, E. J., Ricciuti, B., Gainor, J. F., Kehl, K. L., Kravets, S., Dahlberg, S., Nishino, M., Sholl, L. M., Adeni, A., Subegdjo, S., Khosrowjerdi, S., Peterson, R. M., Digumarthy, S., Liu, C., Sauter, J., Rizvi, H., Arbour, K. C., Carter, B. W., Heymach, J. V., … Awad, M. M. (2019). Outcomes to first-line pembrolizumab in patients with non-small-cell lung cancer and very high PD-L1 expression. *Annals of Oncology*, *30*(10), 1653–1659. https://doi.org/10.1093/annonc/mdz288

Airoldi, I., Lualdi, S., Bruno, S., Raffaghello, L., Occhino, M., Gambini, C., Pistoia, V., & Corrias, M. V. (2003). Expression of costimulatory molecules in human neuroblastoma. Evidence that CD40 + neuroblastoma cells undergo apoptosis following interaction with CD40L. *British Journal of Cancer*, *88*(10), 1527–1536. https://doi.org/10.1038/sj.bjc.6600951

Alexandrov, L. B., Nik-zainal, S., Wedge, D. C., & Aparicio, S. A. J. R. (2014). Signatures of mutational processes in human cancer. *Nature*, *500*(7463), 415–421. https://doi.org/10.1038/nature12477

Altorki, N. K., Markowitz, G. J., Gao, D., Port, J. L., Saxena, A., Stiles, B., McGraw, T., & Mittal, V. (2019). The lung microenvironment: an important regulator of tumour growth and metastasis. *Nature Reviews Cancer*, *19*(1), 9–31. https://doi.org/10.1038/s41568-018-0081-9

Andreas, S., Rittmeyer, A., Hinterthaner, M., & Huber, R. M. (2013). Smoking cessation in lung cancer - Achievable and effective. *Deutsches Arzteblatt International*, *110*(43), 719–724. https://doi.org/10.3238/arztebl.2013.0719

Andriani, F., Majorini, M. T., Mano, M., Landoni, E., Miceli, R., Facchinetti, F., Mensah, M., Fontanella, E., Dugo, M., Giacca, M., Pastorino, U., Sozzi, G., Delia, D., Roz, L., & Lecis, D. (2018). MiR-16 regulates the pro-tumorigenic potential of lung fibroblasts through the inhibition of HGF production in an FGFR-1- and MEK1-dependent manner. *Journal of Hematology and Oncology*, *11*(1), 1–17. https://doi.org/10.1186/s13045-018-0594-4

Balan, V., Wang, Y., Nangia-Makker, P., Kho, D., Bajaj, M., Smith, D., Heilbrun, L., Raz, A., & Heath, E. (2013). Galectin-3: A possible complementary marker to the PSA blood test. *Oncotarget*, *4*(4), 542–549. https://doi.org/10.18632/oncotarget.923

Bänfer, S., Schneider, D., Dewes, J., Strauss, M. T., Freibert, S. A., Heimerl, T., Maier, U. G., Elsässer, H. P., Jungmann, R., & Jacob, R. (2018). Molecular mechanism to recruit galectin-3 into multivesicular bodies for polarized exosomal secretion. *Proceedings of the National Academy of Sciences of the United States of America*, *115*(19), 4396–4405. https://doi.org/10.1073/pnas.1718921115

Båtevik, R., Grong, K., Segadal, L., & Stangeland, L. (2005). The female gender has a positive effect on survival independent of background life expectancy following surgical resection of primary non-small cell lung cancer: a study of absolute and relative survival over 15 years. *Lung Cancer*, *47*(2), 173–181. https://doi.org/10.1016/j.lungcan.2004.08.014.

Beretov, J., Wasinger, V. C., Graham, P. H., Millar, E. K., Kearsley, J. H., & Li, Y. (2014). Proteomics for breast cancer urine biomarkers. *Advances in Clinical Chemistry*, *63*, 123–167. https://doi.org/10.1016/B978-0-12-800094-6.00004-2

Bong, S., Xianhua, Y., Lee, H. J., Jheon, S., & Choe, C. L. G. (2011). Loss of PTEN Expression is an Independent Poor Prognostic Factor in Non-small Cell Lung

Cancer. *Journal of Pathology and Translational Medicine*, *45*(4), 329–335. https://doi.org/10.4132/KoreanJPathol.2011.45.4.329

Bosch-Barrera, J., Baldo, X., Rubio, M., Buxó, M., Vilardell, L., Porta, R., Marmol, E., Basté, N., Izquierdo, A., & Sebastian, F. (2012). Impact of Adenocarcinoma Versus Squamous-Cell-Carcinoma Histology on Survival of Resected Stage I-II Non-Small Cell Lung Cancer (NSCLC) in a Cohort of 509 Patients. *Annals of Oncology*, *23*, ix388. https://doi.org/10.1016/s0923-7534(20)33742-x

Buccheri, G., Ferrigno, D., & Tamburini, M. (1996). Karnofsky and ECOG performance status scoring in lung cancer: a prospective, longitudinal study of 536 patients from a single institution. *European Journal of Cancer*, *32A*(7), 1135–1141. https://doi.org/10.1016/0959-8049(95)00664-8

Buttery, R., Monaghan, H., Salter, D. M., & Sethi, T. (2004). Galectin-3: Differential expression between small-cell and non-small-cell lung cancer. *Histopathology*, *44*(4), 339–344. https://doi.org/10.1111/j.1365-2559.2004.01815.x

Cabel, L., Riva, F., Servois, V., Livartowski, A., Daniel, C., Rampanou, A., Lantz, O., Romano, E., Milder, M., Buecher, B., Piperno-Neumann, S., Bernard, V., Baulande, S., Bieche, I., Y. Pierga, J., Proudhon, C., & Bidard, F. C. (2017). Circulating tumor DNA changes for early monitoring of anti-PD1 immunotherapy: a proof-of-concept study. *Annals of Oncology*, *28*(8), 1996–2001. https://doi.org/10.1093/annonc/mdx212

Cangir, A. K., Kutlay, H., Akal, M., Güngör, A., Özdemir, N., & Akay, H. (2004). Prognostic value of tumor size in non-small cell lung cancer larger than five centimeters in diameter. *Lung Cancer*, *46*(3), 325–331. https://doi.org/10.1016/j.lungcan.2004.05.004

Cao, X., Cai, S. F., Fehniger, T. A., Song, J., Collins, L. I., Piwnica-Worms, D. R., & Ley, T. J. (2007). Granzyme B and Perforin Are Important for Regulatory T Cell-Mediated Suppression of Tumor Clearance. *Immunity*, *27*(4), 635–646. https://doi.org/10.1016/j.immuni.2007.08.014

Capalbo, C., Scafetta, G., Filetti, M., Marchetti, P., & Bartolazzi, A. (2019). Predictive Biomarkers for Checkpoint Inhibitor-Based Immunotherapy: The Galectin-3 Signature in NSCLCs. *International Journal of Molecular Sciences*, *20*(7). https://doi.org/10.3390/IJMS20071607

Capone, E., Iacobelli, S., & Sala, G. (2021). Role of galectin 3 binding protein in cancer progression: a potential novel therapeutic target. *Journal of Translational Medicine*, *19*(1), 405. https://doi.org/10.1186/s12967-021-03085-w

Cardoso, A. C. F., Andrade, L. N. de S., Bustos, S. O., & Chammas, R. (2016). Galectin-3 determines tumor cell adaptive strategies in stressed tumor microenvironments. *Frontiers in Oncology*, *23*(6), 127. https://doi.org/10.3389/fonc.2016.00127

Carrega, P., Morandi, B., Costa, R., Frumento, G., Forte, G., Altavilla, G., Ratto, G. B., Mingari, M. C., Moretta, L., & Ferlazzo, G. (2008). Natural killer cells infiltrating human nonsmall-cell lung cancer are enriched in CD56brightCD16- cells and display an impaired capability to kill tumor cells. *Cancer*, *112*(4), 863–875. https://doi.org/10.1002/cncr.23239

Carter, E. P., Roozitalab, R., Gibson, S. V., & Grose, R. P. (2021). Tumour microenvironment 3D-modelling: simplicity to complexity and back again. *Trends in Cancer*, *7*(11), 1033–1046. https://doi.org/10.1016/j.trecan.2021.06.009

Cerfolio, R. J., Bryant, A. S., Scott, E., Sharma, M., Robert, F., Spencer, S. A., & Garver, R. I. (2006). Women with pathologic stage I, II, and III non-small cell lung cancer have better survival than men. *Chest*, *130*(6), 1796–1802. https://doi.org/10.1378/chest.130.6.1796

Chaintreuil, P., Kerreneur, E., Bourgoin, M., Savy, C., Favreau, C., Robert, G., Jacquel, A., & Auberger, P. (2023). The generation, activation, and polarization of

monocyte-derived macrophages in human malignancies. *Frontiers in Immunology*, *14*, 1178337. https://doi.org/10.3389/fimmu.2023.1178337

Chan, B. A., & Hughes, B. G. M. (2015). Targeted therapy for non-small cell lung cancer: Current standards and the promise of the future. *Translational Lung Cancer Research*, *4*(1), 36–54. https://doi.org/10.3978/j.issn.2218-6751.2014.05.01

Chang, W. A., Tsai, M. J., Kuo, P. L., & Hung, J. Y. (2017). Role of galectins in lung cancer. *Oncology Letters*, *14*(5), 5077–5084. https://doi.org/10.3892/ol.2017.6882

Chapman, S., Liu, X., Meyers, C., Schlegel, R., & McBride, A. A. (2010). Human keratinocytes are efficiently immortalized by a Rho kinase inhibitor. *Journal of Clinical Investigation*, *120*(7), 2619–2626. https://doi.org/10.1172/JCI42297

Chemi, F., Rothwell, D. G., McGranahan, N., Gulati, S., Abbosh, C., Pearce, S. P., Zhou, C., Wilson, G. A., Jamal-Hanjani, M., Birkbak, N., Pierce, J., Kim, C. S., Ferdous, S., Burt, D. J., Slane-Tan, D., Gomes, F., Moore, D., Shah, R., Al Bakir, M., … Dive, C. (2019). Pulmonary venous circulating tumor cell dissemination before tumor resection and disease relapse. *Nature Medicine*, *25*(10), 1534–1539. https://doi.org/10.1038/s41591-019-0593-1

Chen, C., Duckworth, C. A., Fu, B., Pritchard, D. M., Rhodes, J. M., & Yu, L. G. (2014). Circulating galectins-2,-4 and-8 in cancer patients make important contributions to the increased circulation of several cytokines and chemokines that promote angiogenesis and metastasis. *British Journal of Cancer*, *110*(3), 741–752. https://doi.org/10.1038/bjc.2013.793

Chen, H. Y., Fermin, A., Vardhana, S., Weng, I. C., Lo, K. F. R., Chang, E. Y., Maverakis, E., Yang, R. Y., Hsu, D. K., Dustin, M. L., & Liu, F. T. (2009). Galectin-3 negatively regulates TCR-mediated CD4+ T-cell activation at the immunological synapse. *Proceedings of the National Academy of Sciences of the United States of America*, *106*(34), 14496–14501. https://doi.org/10.1073/pnas.0903497106

Chen, J., Song, Y., Miao, F., Chen, G., Zhu, Y., Wu, N., Pang, L., Chen, Z., & Chen, X. (2021). PDL1-positive exosomes suppress antitumor immunity by inducing tumor-specific CD8+ T cell exhaustion during metastasis. *Cancer Science*, *112*(9), 3437–3454. https://doi.org/10.1111/cas.15033

Chitadze, G., Bhat, J., Lettau, M., Janssen, O., & Kabelitz, D. (2013). Generation of Soluble NKG2D Ligands: Proteolytic Cleavage, Exosome Secretion and Functional Implications. *Scandinavian Journal of Immunology*, *78*(2), 120–129. https://doi.org/10.1111/sji.12072

Cho, J. W., Hong, M. H., Ha, S. J., Kim, Y. J., Cho, B. C., Lee, I., & Kim, H. R. (2020). Genome-wide identification of differentially methylated promoters and enhancers associated with response to anti-PD-1 therapy in non-small cell lung cancer. *Experimental and Molecular Medicine*, *52*(9), 1550–1563. https://doi.org/10.1038/s12276-020-00493-8

Chung, L. Y., Tang, S. J., Sun, G. H., Chou, T. Y., Yeh, T. S., Yu, S. L., & Sun, K. H. (2012). Galectin-1 promotes lung cancer progression and chemoresistance by upregulating p38 MAPK, ERK, and cyclooxygenase-2. *Clinical Cancer Research*, *18*(15), 4037–4047. https://doi.org/10.1158/1078-0432.CCR-11-3348

Chung, L. Y., Tang, S. J., Wu, Y. C., Sun, G. H., Liu, H. Y., & Sun, K. H. (2015). Galectin-3 augments tumor initiating property and tumorigenicity of lung cancer through interaction with β-catenin. *Oncotarget*, *6*(7), 4936. https://doi.org/10.18632/oncotarget.3210

Collisson, E. A., Campbell, J. D., Brooks, A. N., Berger, A. H., Lee, W., Chmielecki, J., Beer, D. G., Cope, L., Creighton, C. J., Danilova, L., Ding, L., Getz, G., Hammerman, P. S., Hayes, D. N., Hernandez, B., Herman, J. G., Heymach, J. V., Jurisica, I., Kucherlapati, R., … Cheney, R. (2014). Comprehensive molecular profiling of lung adenocarcinoma: The cancer genome atlas research network. *Nature*, *511*(7511), 543–550. https://doi.org/10.1038/nature13385

Colmont, C. S., BenKetah, A., Reed, S. H., Hawk, N. V., Telford, W. G., Ohyama, M., Udey, M. C., Yee, C. L., Vogel, J. C., & Patel, G. K. (2013). CD200-expressing human basal cell carcinoma cells initiate tumor growth. *Proceedings of the National Academy of Sciences of the United States of America*, *110*(4), 1434–1439. https://doi.org/10.1073/pnas.1211655110

Contini, P., Ghio, M., Poggi, A., Filaci, G., Indiveri, F., Ferrone, S., & Puppo, F. (2003). Soluble HLA-A,-B,-C and -G molecules induce apoptosis in T and NK CD8+ cells and inhibit cytotoxic T cell activity through CD8 ligation. *European Journal of Immunology*, *33*(1), 125–134. https://doi.org/10.1002/immu.200390015

Cook, J. H., Melloni, G. E. M., Gulhan, D. C., Park, P. J., & Haigis, K. M. (2021). The origins and genetic interactions of KRAS mutations are allele- and tissue-specific. *Nature Communications*, *12*(1), 1808. https://doi.org/10.1038/s41467-021-22125-z

Cooper, A. J., Sequist, L. V., & Lin, J. J. (2022). Third-generation EGFR and ALK inhibitors: mechanisms of resistance and management. *Nature Reviews Clinical Oncology*, *19*(8), 499–514. https://doi.org/10.1038/s41571-022-00639-9

Corrales, L., Rosell, R., Cardona, A. F., Martín, C., Zatarain-Barrón, Z. L., & Arrieta, O. (2020). Lung cancer in never smokers: The role of different risk factors other than tobacco smoking. *Critical Reviews in Oncology/Hematology*, *148*, 102895. https://doi.org/10.1016/j.critrevonc.2020.102895

Costantini, A., Julie, C., Dumenil, C., Hélias-Rodzewicz, Z., Tisserand, J., Dumoulin, J., Giraud, V., Labrune, S., Chinet, T., Emile, J. F., & Giroux Leprieur, E. (2018). Predictive role of plasmatic biomarkers in advanced non-small cell lung cancer treated by nivolumab. *OncoImmunology*, *7*(8), 1–11. https://doi.org/10.1080/2162402X.2018.1452581

Cox, A. D., Fesik, S. W., Kimmelman, A. C., Luo, J., & Der, C. J. (2014). Drugging the undruggable RAS: Mission Possible? *Nature Reviews Drug Discovery*, *13*(11), 828–851. https://doi.org/10.1038/nrd4389

Dang, C. Van, Zhao, H., Yang, L., Baddour, J., Achreja, A., Bernard, V., Moss, T., Marini, J. C., Tudawe, T., Seviour, E. G., Anthony, F., Lucas, S., Alvarez, H., Gupta, S., Maiti, S. N., Cooper, L., Peehl, D., Ram, P. T., Maitra, A., & Nagrath, D. (2016). Tumor microenvironment derived exosomes pleiotropically modulate cancer cell metabolism. *ELife*, *5*, e10250. https://doi.org/10.7554/eLife.10250.001

Darvin, P., Sasidharan Nair, V., & Elkord, E. (2019). PD-L1 Expression in Human Breast Cancer Stem Cells Is Epigenetically Regulated through Posttranslational Histone Modifications. *Journal of Oncology*, *2019*, 3958908. https://doi.org/10.1155/2019/3958908

Davis, A. A., & Patel, V. G. (2019). The role of PD-L1 expression as a predictive biomarker: an analysis of all US Food and Drug Administration (FDA) approvals of immune checkpoint inhibitors. *Journal for ImmunoTherapy of Cancer*, *7*(1), 278. https://doi.org/10.1186/S40425-019-0768-9

de Alencar, V. T. L., Figueiredo, A. B., Corassa, M., Gollob, K. J., & Cordeiro de Lima, V. C. (2022). Lung cancer in never smokers: Tumor immunology and challenges for immunotherapy. *Frontiers in Immunology*, *13*, 984349. https://doi.org/10.3389/fimmu.2022.984349

de Koning, H. J., van der Aalst, C. M., de Jong, P. A., Scholten, E. T., Nackaerts, K., Heuvelmans, M. A., Lammers, J.-W. J., Weenink, C., Yousaf-Khan, U., Horeweg, N., van 't Westeinde, S., Prokop, M., Mali, W. P., Mohamed Hoesein, F. A. A., van Ooijen, P. M. A., Aerts, J. G. J. V., den Bakker, M. A., Thunnissen, E., Verschakelen, J., … Oudkerk, M. (2020). Reduced Lung-Cancer Mortality with Volume CT Screening in a Randomized Trial. *New England Journal of Medicine*, *382*(6), 503–513. https://doi.org/10.1056/nejmoa1911793

de Miguel-Perez, D., Russo, A., Arrieta, O., Ak, M., Barron, F., Gunasekaran, M., Mamindla, P., Lara-Mejia, L., Peterson, C. B., Er, M. E., Peddagangireddy, V., Buemi, F., Cooper, B., Manca, P., Lapidus, R. G., Hsia, R. C., Cardona, A. F., Naing, A., Kaushal, S., … Rolfo, C. (2022). Extracellular vesicle PD-L1 dynamics

predict durable response to immune-checkpoint inhibitors and survival in patients with non-small cell lung cancer. *Journal of Experimental and Clinical Cancer Research*, *41*(1). https://doi.org/10.1186/s13046-022-02379-1

Dearden, S., Stevens, J., Wu, Y. L., & Blowers, D. (2013). Mutation incidence and coincidence in non small-cell lung cancer: Meta-analyses by ethnicity and histology (mutMap). *Annals of Oncology*, *24*(9), 2371–2376. https://doi.org/10.1093/annonc/mdt205

Demetriou, M., Granovsky, M., Quaggin, S., & Dennis, J. W. (2001). Negative regulation of T-cell activation and autoimmunity by Mgat5 N-glycosylation. *Nature*, *409*(6821), 733–739. https://doi.org/10.1038/35055582

Demotte, N., Wieërs, G., Van Der Smissen, P., Moser, M., Schmidt, C., Thielemans, K., Squifflet, J. L., Weynand, B., Carrasco, J., Lurquin, C., Courtoy, P. J., & Van Der Bruggen, P. (2010). A galectin-3 ligand corrects the impaired function of human CD4 and CD8 tumor-infiltrating lymphocytes and favors tumor rejection in mice. *Cancer Research*, *70*(19), 7476–7488. https://doi.org/10.1158/0008-5472.CAN-10-0761

Dick, J. E. (2008). Stem cell concepts renew cancer research. *The American Society of Hematology*, *112*(13), 4793–4807. https://doi.org/10.1182/blood-2008-08-077941.

Diwakar R Pattabiraman and Robert A. Weinberg. (2014). Tackling the cancer stem cells – what challenges do they pose? *Nature Reviews Drug Discovery*, *13*(7), 497–512. https://doi.org/10.1038/nrd4253.Tackling

Dong, N., Moreno-Manuel, A., Calabuig-Fariñas, S., Gallach, S., Zhang, F., Blasco, A., Aparisi, F., Meri-Abad, M., Guijarro, R., Sirera, R., Camps, C., & Jantus-Lewintre, E. (2021). Characterization of circulating t cell receptor repertoire provides information about clinical outcome after pd-1 blockade in advanced non-small cell lung cancer patients. *Cancers*, *13*(12). https://doi.org/10.3390/cancers13122950

Doubrovina, E. S., Doubrovin, M. M., Vider, E., Sisson, R. B., O'Reilly, R. J., Dupont, B., & Vyas, Y. M. (2003). Evasion from NK Cell Immunity by MHC Class I Chain-Related Molecules Expressing Colon Adenocarcinoma. *The Journal of Immunology*, *171*(12), 6891–6899. https://doi.org/10.4049/jimmunol.171.12.6891

Dumic, J., Dabelic, S., & Flögel, M. (2006). Galectin-3: An open-ended story. *Biochimica et Biophysica Acta*, *1760*(4), 616–635. https://doi.org/10.1016/J.BBAGEN.2005.12.020

DuPont, N. C., Wang, K., Wadhwa, P. D., Culhane, J. F., & Nelson, E. L. (2005). Validation and comparison of luminex multiplex cytokine analysis kits with ELISA: Determinations of a panel of nine cytokines in clinical sample culture supernatants. *Journal of Reproductive Immunology*, *66*(2), 175. https://doi.org/10.1016/J.JRI.2005.03.005

Duréndez-Sáez, E., Calabuig-Fariñas, S., Torres-Martínez, S., Moreno-Manuel, A., Herreros-Pomares, A., Escorihuela, E., Mosqueda, M., Gallach, S., Guijarro, R., Serna, E., Suárez-Cabrera, C., Paramio, J. M., Blasco, A., Camps, C., & Jantus-Lewintre, E. (2022). Analysis of Exosomal Cargo Provides Accurate Clinical, Histologic and Mutational Information in Non-Small Cell Lung Cancer. *Cancers*, *14*(13), 1–23. https://doi.org/10.3390/cancers14133216

Duruisseaux, M., Martínez-Cardús, A., Calleja-Cervantes, M. E., Moran, S., Castro de Moura, M., Davalos, V., Piñeyro, D., Sanchez-Cespedes, M., Girard, N., Brevet, M., Giroux-Leprieur, E., Dumenil, C., Pradotto, M., Bironzo, P., Capelletto, E., Novello, S., Cortot, A., Copin, M. C., Karachaliou, N., … Esteller, M. (2018). Epigenetic prediction of response to anti-PD-1 treatment in non-small-cell lung cancer: a multicentre, retrospective analysis. *The Lancet Respiratory Medicine*, *6*(10), 771–781. https://doi.org/10.1016/S2213-2600(18)30284-4

Dutta, P., Sabri, N., Li, J., & Li, W. X. (2014). Role of STAT3 in lung cancer. *JAK-STAT*, *3*(4), e999503. https://doi.org/10.1080/21623996.2014.999503

Dutta, S., Ganguly, A., Chatterjee, K., Spada, S., & Mukherjee, S. (2023). Targets of Immune Escape Mechanisms in Cancer: Basis for Development and Evolution of Cancer Immune Checkpoint Inhibitors. *Biology*, *12*(2), 218. https://doi.org/10.3390/biology12020218

Elizabeth A. Vasievich and Leaf Huang. (2011). The Suppressive Tumor Microenvironment: A Challenge in Cancer Immunotherapy. *Molecular Pharmaceutics*, *8*(3), 635–641. https://doi.org/10.1021/mp1004228

Etienne-Manneville, S., & Hall, A. (2002). Rho GTPases in cell biology. *Nature*, *420*(6916), 629–635. https://doi.org/10.1038/nature01148

Farhad, M., Rolig, A. S., & Redmond, W. L. (2018). The role of Galectin-3 in modulating tumor growth and immunosuppression within the tumor microenvironment. *Oncoimmunology*, *7*(6), e1434467. https://doi.org/10.1080/2162402X.2018.1434467

Fei, F., Joo, E. J., Tarighat, S. S., Schiffer, I., Paz, H., Fabbri, M., Abdel-Azim, H., Groffen, J., & Heisterkamp, N. (2015). B-cell precursor acute lymphoblastic leukemia and stromal cells communicate through Galectin-3. *Oncotarget*, *6*(13), 11378–11394. https://doi.org/10.18632/oncotarget.3409

Feng, B., Wu, J., Shen, B., Jiang, F., & Feng, J. (2022). Cancer-associated fibroblasts and resistance to anticancer therapies: status, mechanisms, and countermeasures. *Cancer Cell International*, *22*(1), 166. https://doi.org/10.1186/s12935-022-02599-7

Fermino, M. L., Dias, F. C., Lopes, C. D., Souza, M. A., Cruz, Â. K., Liu, F. T., Chammas, R., Roque-Barreira, M. C., Rabinovich, G. A., & Bernardes, E. S. (2013). Galectin-3 negatively regulates the frequency and function of CD4+CD25+Foxp3+ regulatory T cells and influences the course of Leishmania major infection. *European Journal of Immunology*, *43*(7), 1806–1817. https://doi.org/10.1002/eji.201343381

Flem-Karlsen, K., Fodstad, Ø., Tan, M., & Nunes-Xavier, C. E. (2018). B7-H3 in Cancer – Beyond Immune Regulation. *Trends in Cancer*, *4*(6), 401–404. https://doi.org/10.1016/J.TRECAN.2018.03.010

Fontana, F., Marzagalli, M., Sommariva, M., Gagliano, N., & Limonta, P. (2021). In vitro 3D cultures to model the tumor microenvironment. *Cancers*, *13*(12), 2970. https://doi.org/10.3390/cancers13122970

Fortuna-Costa, A., Gomes, A. M., Kozlowski, E. O., Stelling, M. P., & Pavão, M. S. G. (2014). Extracellular galectin-3 in tumor progression and metastasis. *Frontiers in Oncology*, *4*, 138. https://doi.org/10.3389/fonc.2014.00138

Fortunato, O., Belisario, D. C., Compagno, M., Giovinazzo, F., Bracci, C., Pastorino, U., Horenstein, A., Malavasi, F., Ferracini, R., Scala, S., Sozzi, G., Roz, L., Roato, I., & Bertolini, G. (2020). CXCR4 Inhibition Counteracts Immunosuppressive Properties of Metastatic NSCLC Stem Cells. *Frontiers in Immunology*, *11*(October), 1–13. https://doi.org/10.3389/fimmu.2020.02168

Freeman, G. J., Long, A. J., Iwai, Y., Bourque, K., Chernova, T., Nishimura, H., Fitz, L. J., Malenkovich, N., Okazaki, T., Byrne, M. C., Horton, H. F., Fouser, L., Carter, L., Ling, V., Bowman, M. R., Carreno, B. M., Collins, M., Wood, C. R., & Honjo, T. (2000). Engagement of the PD-1 Immunoinhibitory Receptor by a Novel B7 Family Member Leads to Negative Regulation of Lymphocyte Activation. *Journal of Experimental Medicine*, *192*(7). https://doi.org/10.1084/jem.192.7.1027

Fukaya, Y., Shimada, H., Wang, L. C., Zandi, E., & DeClerck, Y. A. (2008). Identification of galectin-3-binding protein as a factor secreted by tumor cells that stimulates interleukin-6 expression in the bone marrow stroma. *Journal of Biological Chemistry*, *283*(27), 18573–18581. https://doi.org/10.1074/jbc.M803115200

Fukumori, T., Takenaka, Y., Oka, N., Yoshii, T., Hogan, V., Inohara, H., Kanayama, H. O., Kim, H. R. C., & Raz, A. (2004). Endogenous galectin-3 determines the

routing of CD95 apoptotic signaling pathways. *Cancer Research*, *64*(10), 3376–3379. https://doi.org/10.1158/0008-5472.CAN-04-0336

Galli, G., & Rossi, G. (2020). Lung cancer histology-driven strategic therapeutic approaches. *Shanghai Chest*, *4*, 29. https://doi.org/10.21037/shc.2020.01.03

Ganesan, A.-P., Johansson, M., Ruffell, B., Yagui-Beltrán, A., Lau, J., Jablons, D. M., & Coussens, L. M. (2013). Tumor-infiltrating regulatory T cells inhibit endogenous cytotoxic T cell responses to lung adenocarcinoma. *The Journal of Immunology*, *191*(10), 5319–5319. https://doi.org/10.4049/jimmunol.1390059

García-Rocha, R., Monroy-García, A., Carrera-Martínez, M., Hernández-Montes, J., Don-López, C. A., Weiss-Steider, B., Monroy-Mora, K. A., Ponce-Chavero, M. de los Á., Montesinos-Montesinos, J. J., Escobar-Sánchez, M. L., Castillo, G. M., Chacón-Salinas, R., Vallejo-Castillo, L., Pérez-Tapia, S. M., & Mora-García, M. de L. (2022). Evidence that cervical cancer cells cultured as tumorspheres maintain high CD73 expression and increase their protumor characteristics through TGF-β production. *Cell Biochemistry and Function*, *40*(7), 760–772. https://doi.org/10.1002/cbf.3742

Garinet, S., Wang, P., Mansuet-Lupo, A., Fournel, L., Wislez, M., & Blons, H. (2022). Updated Prognostic Factors in Localized NSCLC. *Cancers*, *14*(6), 1400. https://doi.org/10.3390/cancers14061400

Genova, C., Tasso, R., Rosa, A., Rossi, G., Reverberi, D., Fontana, V., Marconi, S., Croce, M., Giovanna, M., Bello, D., Dellepiane, C., Tagliamento, M., Ciferri, M. C., Zullo, L., Fedeli, A., Alama, A., Cortese, K., Gentili, C., Cella, E., … Coco, S. (2023). Prognostic Role of Soluble and Extracellular Vesicle-Associated PD-L1, B7-H3 and B7-H4 in Non-Small Cell Lung Cancer Patients Treated with Immune Checkpoint Inhibitors. *Cells*, *12*(6), 832. https://doi.org/10.3390/cells12060832.

Gkolfinopoulos, S., & Mountzios, G. (2018). Beyond EGFR and ALK: targeting rare mutations in advanced non-small cell lung cancer. *Annals of Translational Medicine*, *6*(8), 142–142. https://doi.org/10.21037/atm.2018.04.28

Goh, K. Y., Cheng, T. Y. De, Tham, S. C., & Lim, D. W. T. (2023). Circulating Biomarkers for Prediction of Immunotherapy Response in NSCLC. *Biomedicines*, *11*(2), 508. https://doi.org/10.3390/biomedicines11020508

Goldberg, S. B., Narayan, A., Kole, A. J., Decker, R. H., Teysir, J., Carriero, N. J., Lee, A., Nemati, R., Nath, S. K., Mane, S. M., Deng, Y., Sukumar, N., Zelterman, D., Boffa, D. J., Politi, K., Gettinger, S. N., Wilson, L. D., Herbst, R. S., & Patel, A. A. (2018). Early Assessment of Lung Cancer Immunotherapy Response via Circulating Tumor DNA. *Clinical Cancer Research*, *24*(8), 1872–1880. https://doi.org/10.1158/1078-0432.CCR-17-1341

Goldstraw, P., Chansky, K., Crowley, J., Rami-Porta, R., Asamura, H., Eberhardt, W. E. E., Nicholson, A. G., Groome, P., Mitchell, A., Bolejack, V., Ball, D., Beer, D. G., Beyruti, R., Detterbeck, F., Edwards, J., Galateau-Sallé, F., Giroux, D., Gleeson, F., Huang, J., … Yokoi, K. (2016). The IASLC lung cancer staging project: Proposals for revision of the TNM stage groupings in the forthcoming (eighth) edition of the TNM Classification for lung cancer. *Journal of Thoracic Oncology*, *11*(1), 39–51. https://doi.org/10.1016/j.jtho.2015.09.009

Grehan, J. F., Levay-Young, B. K., Fogelson, J. L., François-Bongarçon, V., Benson, B. A., & Dalmasso, A. P. (2005). IL-4 and IL-13 Induce Protection of Porcine Endothelial Cells from Killing by Human Complement and from Apoptosis through Activation of a Phosphatidylinositide 3-Kinase/Akt Pathway 1. *The Journal of Immunology*, *175*(3), 1903–1910. https://doi.org/10.4049/jimmunol.175.3.1903

Groh, V., Wu, J., Yee, C., & Spies, T. (2002). Tumour-derived soluble MIC ligands impair expression of NKG2D and T-cell activation. *Nature*, *419*(6908), 734–738. https://doi.org/10.1038/nature01112

Guha, P., Kaptan, E., Bandyopadhyaya, G., Kaczanowska, S., Davila, E., Thompson, K., Martin, S. S., Kalvakolanu, D. V., Vasta, G. R., & Ahmed, H. (2013). Cod glycopeptide with picomolar affinity to galectin-3 suppresses T-cell apoptosis and prostate cancer metastasis. *Proceedings of the National Academy of*

Sciences of the United States of America, *110*(13), 5052–5057. https://doi.org/10.1073/pnas.1202653110

Guibert, N., Delaunay, M., Lusque, A., Boubekeur, N., Rouquette, I., Clermont, E., Mourlanette, J., Gouin, S., Dormoy, I., Favre, G., Mazieres, J., & Pradines, A. (2018). PD-L1 expression in circulating tumor cells of advanced non-small cell lung cancer patients treated with nivolumab. *Lung Cancer*, *120*, 108–112. https://doi.org/10.1016/j.lungcan.2018.04.001

Gurda, G. T., Zhang, L., Wang, Y., Chen, L., Geddes, S., Cho, W. C., Askin, F., Gabrielson, E., & Li, Q. K. (2015). Utility of five commonly used immunohistochemical markers TTF-1, Napsin A, CK7, CK5/6 and P63 in primary and metastatic adenocarcinoma and squamous cell carcinoma of the lung: a retrospective study of 246 fine needle aspiration cases. *Clinical and Translational Medicine*, *4*(1), 16. https://doi.org/10.1186/s40169-015-0057-2

Hammerman, P. S., Sos, M. L., Ramos, A. H., Xu, C., Dutt, A., Zhou, W., Brace, L. E., Woods, B. A., Lin, W., Zhang, J., Deng, X., Lim, S. M., Heynck, S., Peifer, M., Simard, J. R., Lawrence, M. S., Onofrio, R. C., Salvesen, H. B., Seidel, D., … Koker, M. (2012). Mutations in the DDR2 kinase gene identify a novel therapeutic target in squamous cell lung cancer. *Cancer Discovery*, *1*(1), 78–89. https://doi.org/10.1158/2159-8274.CD-11-0005

Hanahan, D. (2022). Hallmarks of Cancer: New Dimensions. *Cancer Discovery*, *12*(1), 31–46. https://doi.org/10.1158/2159-8290.CD-21-1059

Hanahan, D., & Weinberg, R. A. (2000). The Hallmarks of Cancer Review Douglas. *Cell*, *100*(7), 57–70. https://doi.org/10.1016/j.cell.2011.02.013.

Hanahan, D., & Weinberg, R. A. (2011). Hallmarks of cancer: The next generation. *Cell*, *144*(5), 646–674. https://doi.org/10.1016/j.cell.2011.02.013

Hao, B., Li, F., Wan, X., Pan, S., Li, D., Song, C., Li, N., & Geng, Q. (2022). Squamous cell carcinoma predicts worse prognosis than adenocarcinoma in stage IA lung

cancer patients: A population-based propensity score matching analysis. *Frontiers in Surgery*, *9*, 944032. https://doi.org/10.3389/fsurg.2022.944032

He, X., Zhang, S., Chen, J., & Li, D. (2019). Increased LGALS3 expression independently predicts shorter overall survival in patients with the proneural subtype of glioblastoma. *Cancer Medicine*, *8*(5), 2031–2040. https://doi.org/10.1002/cam4.2075

Hecht, S. S. (2011). Tobacco smoke carcinogens and lung cancer. *Current Cancer Research*, *6*(14), 53–74. https://doi.org/10.1007/978-1-61737-995-6_3

Helena A. Yu, Maria E. Arcilla, Natasha Rekhtman, Camelia S. Sima, Maureen F. Zakowski, William Pao, Mark G. Kris, Vincent A. Miller, Marc Ladanyi, & Gregory J. Riely. (2014). Analysis of Tumor Specimens at the Time of Acquired Resistance to EGFR TKI therapy in 155 patients with EGFR mutant Lung Cancers. *Clinical Cancer Research*, *19*(8), 2240–2247. https://doi.org/10.1158/1078-0432.CCR-12-2246

Hendriks, L. E., Kerr, K. M., Menis, J., Mok, T. S., Nestle, U., Passaro, A., Peters, S., Planchard, D., Smit, E. F., Solomon, B. J., Veronesi, G., & Reck, M. (2023). Non-oncogene-addicted metastatic non-small-cell lung cancer: ESMO Clinical Practice Guideline for diagnosis, treatment and follow-up. *Annals of Oncology*, *34*(4), 358–376. https://doi.org/10.1016/j.annonc.2022.12.013

Hernández-Prieto, S., Romera, A., Ferrer, M., Subiza, J. L., López-Asenjo, J. A., Jarabo, J. R., Gómez, A. M., Molina, E. M., Puente, J., González-Larriba, J. L., Hernando, F., Pérez-Villamil, B., Díaz-Rubio, E., & Sanz-Ortega, J. (2015). A 50-gene signature is a novel scoring system for tumor-infiltrating immune cells with strong correlation with clinical outcome of stage I/II non-small cell lung cancer. *Clinical and Translational Oncology*, *17*(4), 330–338. https://doi.org/10.1007/s12094-014-1235-1

Herreros-Pomares, A., de-Maya-Girones, J. D., Calabuig-Fariñas, S., Lucas, R., Martínez, A., Pardo-Sánchez, J. M., Alonso, S., Blasco, A., Guijarro, R., Martorell,

M., Escorihuela, E., Chiara, M. D., Duréndez, E., Gandía, C., Forteza, J., Sirera, R., Jantus-Lewintre, E., Farràs, R., & Camps, C. (2019). Lung tumorspheres reveal cancer stem cell-like properties and a score with prognostic impact in resected non-small-cell lung cancer. *Cell Death and Disease*, *10*(9). https://doi.org/10.1038/S41419-019-1898-1

Hirsch, F. R., Scagliotti, G. V., Mulshine, J. L., Kwon, R., Curran, W. J., Wu, Y. L., & Paz-Ares, L. (2017). Lung cancer: current therapies and new targeted treatments. *The Lancet*, *389*(10066), 299–311. https://doi.org/10.1016/S0140-6736(16)30958-8

Hofmeyer, K. A., Ray, A., & Zang, X. (2008). The contrasting role of B7-H3. *Proceedings of the National Academy of Sciences of the United States of America*, *105*(30), 10277–10278. https://doi.org/10.1073/pnas.0805458105

Holmgaard, R. B., Zamarin, D., Li, Y., Gasmi, B., Munn, D. H., Allison, J. P., Merghoub, T., & Wolchok, J. D. (2015). Tumor-Expressed IDO Recruits and Activates MDSCs in a Treg-Dependent Manner. *Cell Reports*, *13*(2), 412–424. https://doi.org/10.1016/j.celrep.2015.08.077

Hong, H. K., Pyo, D. H., Kim, T. W., Yun, N. H., Lee, Y. S., Song, S. J., Lee, W. Y., & Cho, Y. B. (2019). Efficient primary culture model of patient-derived tumor cells from colorectal cancer using a Rho-associated protein kinase inhibitor and feeder cells. *Oncology Reports*, *42*(5), 2029–2038. https://doi.org/10.3892/or.2019.7285

Huang, L., Zhou, Y., Sun, Q., Cao, L., & Zhang, X. (2022). Evaluation of the role of soluble B7-H3 in association with membrane B7-H3 expression in gastric adenocarcinoma. *Cancer Biomarkers*, *33*(1), 123–129. https://doi.org/10.3233/CBM-210178

Hughes, R. C. (1999). Secretion of the galectin family of mammalian carbohydrate-binding proteins. *Biochimica et Biophysica Acta*, *6*(1473), 172–175. https://doi.org/10.1016/s0304-4165(99)00177-4.

Ilmer, M., Mazurek, N., Byrd, J. C., Ramirez, K., Hafley, M., Alt, E., Vykoukal, J., & Bresalier, R. S. (2016). Cell surface galectin-3 defines a subset of chemoresistant gastrointestinal tumor-initiating cancer cells with heightened stem cell characteristics. *Cell Death and Disease*, *7*(8). https://doi.org/10.1038/cddis.2016.239

Inohara, H., & Raz, A. (1995). Functional Evidence that Cell Surface Galectin-3 Mediates Homotypic Cell Adhesion. *Cancer Research*, *55*(15), 3267–3271.

Inoue, A., Kobayashi, K., Maemondo, M., Sugawara, S., Oizumi, S., Isobe, H., Gemma, A., Harada, M., Yoshizawa, H., Kinoshita, I., Fujita, Y., Okinaga, S., Hirano, H., Yoshimori, K., Harada, T., Saijo, Y., Hagiwara, K., Morita, S., & Nukiwa, T. (2013). Updated overall survival results from a randomized phase III trial comparing gefitinib with carboplatin-paclitaxel for chemo-naïve non-small cell lung cancer with sensitive EGFR gene mutations (NEJ002). *Annals of Oncology*, *24*(1), 54–59. https://doi.org/10.1093/annonc/mds214

Islami, F., Torre, L. A., & Jemal, A. (2015). Global trends of lung cancer mortality and smoking prevalence. *Translational Lung Cancer Research*, *4*(4), 327–338. https://doi.org/10.3978/j.issn.2218-6751.2015.08.04

Jänne, P. A., Riely, G. J., Gadgeel, S. M., Heist, R. S., Ou, S.-H. I., Pacheco, J. M., Johnson, M. L., Sabari, J. K., Leventakos, K., Yau, E., Bazhenova, L., Negrao, M. V., Pennell, N. A., Zhang, J., Anderes, K., Der-Torossian, H., Kheoh, T., Velastegui, K., Yan, X., … Spira, A. I. (2022). Adagrasib in Non–Small-Cell Lung Cancer Harboring a KRAS G12C Mutation. *New England Journal of Medicine*, *387*(2), 120–131. https://doi.org/10.1056/nejmoa2204619

Jantus-Lewintre, E., Usó, M., Sanmartín, E., & Camps, C. (2012). Update on biomarkers for the detection of lung cancer. *Lung Cancer: Targets and Therapy*, *3*, 21–29. https://doi.org/10.2147/LCTT.S23424

Jarnicki, A. G., Lysaght, J., Todryk, S., & Mills, K. H. G. (2006). Suppression of Antitumor Immunity by IL-10 and TGF-β-Producing T Cells Infiltrating the

Growing Tumor: Influence of Tumor Environment on the Induction of CD4 + and CD8 + Regulatory T Cells. *The Journal of Immunology*, *177*(2), 896–904. https://doi.org/10.4049/jimmunol.177.2.896

Jin, K., Pandey, N. B., & Popel, A. S. (2017). *Crosstalk between stromal components and tumor cells of TNBC via secreted factors enhances tumor growth and metastasis*. *8*(36), 60210–60222. https://doi.org/10.18632/oncotarget.19417

Jin, R., Peng, L., Shou, J., Wang, J., Jin, Y., Liang, F., Zhao, J., Wu, M., Li, Q., Zhang, B., Wu, X., Lan, F., Xia, L., Yan, J., Shao, Y., Stebbing, J., Shen, H., Li, W., & Xia, Y. (2021). EGFR-Mutated Squamous Cell Lung Cancer and Its Association With Outcomes. *Frontiers in Oncology*, *11*, 680804. https://doi.org/10.3389/fonc.2021.680804

Joshi, B. H., Hogaboam, C., Dover, P., Husain, S. R., & Puri, R. K. (2006). Role of Interleukin-13 in Cancer, Pulmonary Fibrosis, and Other TH2-Type Diseases. *Vitamins and Hormones*, *74*, 479–504. https://doi.org/10.1016/S0083-6729(06)74019-5

Julian, L., & Olson, M. F. (2014). Rho-associated coiled-coil containing kinases (ROCK), structure, regulation, and functions. *Small GTPases*, *5*(2), e29846. https://doi.org/10.4161/sgtp.29846

Kadota, K., Nitadori, J. I., Woo, K. M., Sima, C. S., Finley, D. J., Rusch, V. W., Adusumilli, P. S., & Travis, W. D. (2014). Comprehensive pathological analyses in lung squamous cell carcinoma: Single cell invasion, nuclear diameter, and tumor budding are independent prognostic factors for worse outcomes. *Journal of Thoracic Oncology*, *9*(8), 1126–1139. https://doi.org/10.1097/JTO.0000000000000253

Kadowaki, T., Arikawa, T., Shinonaga, R., Oomizu, S., Inagawa, H., Soma, G., Niki, T., & Hirashima, M. (2012). Galectin-9 signaling prolongs survival in murine lung-cancer by inducing macrophages to differentiate into plasmacytoid dendritic

cell-like macrophages. *Clinical Immunology*, *142*(3), 296–307. https://doi.org/10.1016/j.clim.2011.11.006

Kang, D. H., Park, C. K., Chung, C., Oh, I. J., Kim, Y. C., Park, D., Kim, J., Kwon, G. C., Kwon, I., Sun, P., Shin, E. C., & Lee, J. E. (2020). Baseline Serum Interleukin-6 Levels Predict the Response of Patients with Advanced Non-small Cell Lung Cancer to PD-1/PD-L1 Inhibitors. *Immune Network*, *20*(3), 1–11. https://doi.org/10.4110/IN.2020.20.E27

Kang, H. G., Kim, D.-H., Kim, S.-J., Cho, Y., Jung, J., Jang, W., & Chun, K.-H. (2016). Galectin-3 supports stemness in ovarian cancer stem cells by activation of the Notch1 intracellular domain. *Oncotarget*, *7*(42), 68229–68241. https://doi.org/10.18632/oncotarget.11920

Kanwal, M., Ding, X. J., & Cao, Y. (2017). Familial risk for lung cancer. *Oncology Letters*, *13*(2), 535–542. https://doi.org/10.3892/ol.2016.5518

Kashyap, A., Rapsomaniki, M. A., Barros, V., Fomitcheva-Khartchenko, A., Martinelli, A. L., Rodriguez, A. F., Gabrani, M., Rosen-Zvi, M., & Kaigala, G. (2022). Quantification of tumor heterogeneity: from data acquisition to metric generation. *Trends in Biotechnology*, *40*(6), 647–676. https://doi.org/10.1016/j.tibtech.2021.11.006

Kataoka, Y., Igarashi, T., Ohshio, Y., Fujita, T., & Hanaoka, J. (2019). Predictive importance of galectin-3 for recurrence of non-small cell lung cancer. *General Thoracic and Cardiovascular Surgery*, *67*(8), 704–711. https://doi.org/10.1007/s11748-019-01074-x

Kazakov, J., Hegde, P., Tahiri, M., Thiffault, V., Ferraro, P., & Liberman, M. (2017). Endobronchial and Endoscopic Ultrasound-Guided Transvascular Biopsy of Mediastinal, Hilar, and Lung Lesions. *Annals of Thoracic Surgery*, *103*(3), 951–955. https://doi.org/10.1016/j.athoracsur.2016

Keegan, A., Ricciuti, B., Garden, P., Cohen, L., Nishihara, R., Adeni, A., Paweletz, C., Supplee, J., Jänne, P. A., Severgnini, M., Awad, M. M., & Walt, D. R. (2020).

Plasma IL-6 changes correlate to PD-1 inhibitor responses in NSCLC. *Journal for ImmunoTherapy of Cancer*, *8*(2), e00678. https://doi.org/10.1136/JITC-2020-000678

Kim, C. H., Lee, Y. C. A., Hung, R. J., McNallan, S. R., Cote, M. L., Lim, W. Y., Chang, S. C., Kim, J. H., Ugolini, D., Chen, Y., Liloglou, T., Andrew, A. S., Onega, T., Duell, E. J., Field, J. K., Lazarus, P., Le Marchand, L., Neri, M., Vineis, P., … Zhang, Z. F. (2014). Exposure to secondhand tobacco smoke and lung cancer by histological type: A pooled analysis of the International Lung Cancer Consortium (ILCCO). *International Journal of Cancer*, *135*(8), 1918–1930. https://doi.org/10.1002/ijc.28835

Kim, S. Y., Lee, J. Y., Kim, D. H., Joo, H. S., Yun, M. R., Jung, D., Yun, J., Heo, S. G., Ahn, B. C., Park, C. W., Pyo, K. H., Chun, Y. J., Hong, M. H., Kim, H. R., & Cho, B. C. (2019). Patient-Derived Cells to Guide Targeted Therapy for Advanced Lung Adenocarcinoma. *Scientific Reports*, *9*(1), 1–12. https://doi.org/10.1038/s41598-019-56356-4

Kocher, F., Hilbe, W., Seeber, A., Pircher, A., Schmid, T., Greil, R., Auberger, J., Nevinny-Stickel, M., Sterlacci, W., Tzankov, A., Jamnig, H., Kohler, K., Zabernigg, A., Frötscher, J., Oberaigner, W., & Fiegl, M. (2015). Longitudinal analysis of 2293 NSCLC patients: A comprehensive study from the TYROL registry. *Lung Cancer*, *87*(2), 193–200. https://doi.org/10.1016/j.lungcan.2014.12.006

Kodack, D. P., Farago, A. F., Dastur, A., Held, M. A., Dardaei, L., Friboulet, L., von Flotow, F., Damon, L. J., Lee, D., Parks, M., Dicecca, R., Greenberg, M., Kattermann, K. E., Riley, A. K., Fintelmann, F. J., Rizzo, C., Piotrowska, Z., Shaw, A. T., Gainor, J. F., … Benes, C. H. (2017). Primary Patient-Derived Cancer Cells and Their Potential for Personalized Cancer Patient Care. *Cell Reports*, *21*(11), 3298–3309. https://doi.org/10.1016/j.celrep.2017.11.051

Koneru, M., Schaer, D., Monu, N., Ayala, A., & Frey, A. B. (2005). Defective Proximal TCR Signaling Inhibits CD8 + Tumor-Infiltrating Lymphocyte Lytic Function. *The*

Journal of Immunology, *174*(4), 1830–1840. https://doi.org/10.4049/jimmunol.174.4.1830

Kouo, T., Huang, L., Pucsek, A. B., Cao, M., Solt, S., Armstrong, T., & Jaffee, E. (2015). Galectin-3 shapes antitumor immune responses by suppressing CD8+ T cells via LAG-3 and inhibiting expansion of plasmacytoid dendritic cells. *Cancer Immunology Research*, *3*(4), 412. https://doi.org/10.1158/2326-6066.CIR-14-0150

Kovaleva, O. V., Belova, T. P., Korotkova, E. A., Kushlinskii, D. N., Gratchev, A. N., Petrikova, N. A., Kudlay, D. A., & Kushlinskii, N. E. (2021). Soluble B7-H3 in Ovarian Cancer and Its Predictive Value. *Bulletin of Experimental Biology and Medicine*, *171*(4), 472–474. https://doi.org/10.1007/s10517-021-05253-w

Kreso, A., & Dick, J. E. (2014). Evolution of the Cancer Stem Cell Model. *Cell Stem Cell*, *14*(3), 275–291. https://doi.org/10.1016/j.stem.2014.02.006

Kuhn, E., Morbini, P., Cancellieri, A., Damiani, S., Cavazza, A., & Comin, C. E. (2018). Adenocarcinoma classification: Patterns and prognosis. *Pathologica*, *110*(1), 5–11.

Kuo, P.-L., Hung, J.-Y., Huang, S.-K., Chou, S.-H., Cheng, D.-E., Jong, Y.-J., Hung, C.-H., Yang, C.-J., Tsai, Y.-M., Hsu, Y.-L., & Huang, M.-S. (2011). Lung Cancer-Derived Galectin-1 Mediates Dendritic Cell Anergy through Inhibitor of DNA Binding 3/IL-10 Signaling Pathway. *The Journal of Immunology*, *186*(3), 1521–1530. https://doi.org/10.4049/JIMMUNOL.1002940

Kusuhara, S., Igawa, S., Ichinoe, M., Nagashio, R., Kuchitsu, Y., Hiyoshi, Y., Shiomi, K., Murakumo, Y., Saegusa, M., Satoh, Y., Sato, Y., & Naoki, K. (2021). Prognostic significance of galectin-3 expression in patients with resected NSCLC treated with platinum-based adjuvant chemotherapy. *Thoracic Cancer*, *12*(10), 1570–1578. https://doi.org/10.1111/1759-7714.13945

Lakins, M. A., Ghorani, E., Munir, H., Martins, C. P., & Shields, J. D. (2018). Cancer-associated fibroblasts induce antigen-specific deletion of CD8 + T Cells to

protect tumour cells. *Nature Communications*, *9*(1), 1–9. https://doi.org/10.1038/s41467-018-03347-0

Lan, Y. jiao, Cheng, M. han, Ji, H. min, Bi, Y. qian, Han, Y. yue, Yang, C. yang, Gu, X., Gao, J., & Dong, H. liang. (2023). Melatonin ameliorates bleomycin-induced pulmonary fibrosis via activating NRF2 and inhibiting galectin-3 expression. *Acta Pharmacologica Sinica*, *44*(5), 1029–1037. https://doi.org/10.1038/s41401-022-01018-x

Lawson, D. A., Kessenbrock, K., Davis, R. T., Pervolarakis, N., & Werb, Z. (2018). Tumour heterogeneity and metastasis at single-cell resolution. *Nature Cell Biology*, *20*(12), 1349–1360. https://doi.org/10.1038/s41556-018-0236-7

Lazar, I., Clement, E., Ducoux-Petit, M., Denat, L., Soldan, V., Dauvillier, S., Balor, S., Burlet-Schiltz, O., Larue, L., Muller, C., & Nieto, L. (2015). Proteome characterization of melanoma exosomes reveals a specific signature for metastatic cell lines. *Pigment Cell and Melanoma Research*, *28*(4), 464–475. https://doi.org/10.1111/pcmr.12380

Le, D. T., Durham, J. N., Smith, K. N., Wang, H., Bartlett, B. R., Aulakh, L. K., Lu, S., Kemberling, H., Wilt, C., Luber, B. S., Wong, F., Azad, N. S., Rucki, A. A., Laheru, D., Donehower, R., Zaheer, A., Fisher, G. A., Crocenzi, T. S., Lee, J. J., … Diaz, L. A. (2017). Mismatch repair deficiency predicts response of solid tumors to PD-1 blockade. *Science*, *357*(6349), 409–413. https://doi.org/10.1126/science.aan6733

Leach, D. R., Krummel, M. F., & Allison, J. P. (1996). Enhancement of Antitumor Immunity by CTLA-4 Blockade. *Science*, *271*(5256), 1734–1736. https://doi.org/10.1126/science.271.5256.1734

Lee, Y. J., Song, Y. K., Song, J. J., Siervo-Sassi, R. R., Kim, H. R. C., Li, L., Spitz, D. R., Lokshin, A., & Kim, J. H. (2003). Reconstitution of galectin-3 alters glutathione content and potentiates TRAIL-induced cytotoxicity by dephosphorylation of

Akt. *Experimental Cell Research*, *288*(1), 21–34. https://doi.org/10.1016/S0014-4827(03)00211-8

Lenschow, D. J., & Bluestone, J. A. (1993). T cell co-stimulation and in vivo tolerance. *Current Opinion in Immunology*, *5*(2), 747–752. https://doi.org/10.1016/0952-7915(93)90132-c

Lenschow, D. J., Walunas, T. L., & Bluestone, J. A. (1996). CD28/B7 System of T Cell Coestimulation. *Annual Review of Immunology*, *14*(1), 233–258. https://doi.org/10.1146/annurev.immunol.14.1.233

Leonetti, A., Sharma, S., Minari, R., Perego, P., Giovannetti, E., & Tiseo, M. (2019). Resistance mechanisms to osimertinib in EGFR-mutated non-small cell lung cancer. *British Journal of Cancer*, *121*(9), 725–737. https://doi.org/10.1038/s41416-019-0573-8

Li, C., Jiang, P., Wei, S., Xu, X., & Wang, J. (2020). Regulatory T cells in tumor microenvironment: New mechanisms, potential therapeutic strategies and future prospects. *Molecular Cancer*, *19*(1), 1–23. https://doi.org/10.1186/s12943-020-01234-1

Li, P., Qin, P., Fu, X., Zhang, G., Yan, X., Zhang, M., Zhang, X., Yang, J., Wang, H., & Ma, Z. (2021). Associations between peripheral blood lymphocyte subsets and clinical outcomes in patients with lung cancer treated with immune checkpoint inhibitor. *Annals of Palliative Medicine*, *10*(3), 3039–3049. https://doi.org/10.21037/APM-21-163

Li, W., Liu, J. Bin, Hou, L. K., Yu, F., Zhang, J., Wu, W., Tang, X. M., Sun, F., Lu, H. M., Deng, J., Bai, J., Li, J., Wu, C. Y., Lin, Q. L., Lv, Z. W., Wang, G. R., Jiang, G. X., Ma, Y. S., & Fu, D. (2022). Liquid biopsy in lung cancer: significance in diagnostics, prediction, and treatment monitoring. *Molecular Cancer*, *21*(1), 25. https://doi.org/10.1186/s12943-022-01505-z

Li, W., Zheng, H., Qin, H., Liu, G., Ke, L., Li, Y., Li, N., & Zhong, X. (2018). Exploration of differentially expressed plasma proteins in patients with lung

adenocarcinoma using iTRAQ-coupled 2D LC-MS/MS. *The Clinical Respiratory Journal*, *12*(6), 2036–2045. https://doi.org/10.1111/CRJ.12771

Liang, B., Peng, P., Chen, S., Li, L., Zhang, M., Cao, D., Yang, J., Li, H., Gui, T., Li, X., & Shen, K. (2013). Characterization and proteomic analysis of ovarian cancer-derived exosomes. *Journal of Proteomics*, *80*, 171–182. https://doi.org/10.1016/j.jprot.2012.12.029

Liang, J., Bi, G., Shan, G., Jin, X., Bian, Y., & Wang, Q. (2022). Tumor-Associated Regulatory T Cells in Non-Small-Cell Lung Cancer: Current Advances and Future Perspectives. *Journal of Immunology Research*, *2022*, 4355386. https://doi.org/10.1155/2022/4355386

Lignitto, L., LeBoeuf, S. E., Homer, H., Jiang, S., Askenazi, M., Karakousi, T. R., Pass, H. I., Bhutkar, A. J., Tsirigos, A., Ueberheide, B., Sayin, V. I., Papagiannakopoulos, T., & Pagano, M. (2019). Nrf2 Activation Promotes Lung Cancer Metastasis by Inhibiting the Degradation of Bach1. *Cell*, *178*(2), 316-329.e18. https://doi.org/10.1016/j.cell.2019.06.003

Lim, W., Ridge, C. A., Nicholson, A. G., & Mirsadraee, S. (2018). The 8th lung cancer TNM classification and clinical staging system: Review of the changes and clinical implications. *Quantitative Imaging in Medicine and Surgery*, *8*(7), 709–718. https://doi.org/10.21037/qims.2018.08.02

Liu, D., Wang, S., & Bindeman, W. (2017). Clinical applications of PD-L1 bioassays for cancer immunotherapy. *Journal of Hematology and Oncology*, *10*(1), 1–6. https://doi.org/10.1186/s13045-017-0479-y

Liu, F. T., & Rabinovich, G. A. (2005). Galectins as modulators of tumour progression. *Nature Reviews Cancer*, *5*(1), 29–41. https://doi.org/10.1038/NRC1527

Liu, X., Ory, V., Chapman, S., Yuan, H., Albanese, C., Kallakury, B., Timofeeva, O. A., Nealon, C., Dakic, A., Simic, V., Haddad, B. R., Rhim, J. S., Dritschilo, A., Riegel, A., McBride, A., & Schlegel, R. (2012). ROCK inhibitor and feeder cells induce

the conditional reprogramming of epithelial cells. *American Journal of Pathology*, *180*(2), 599–607. https://doi.org/10.1016/j.ajpath.2011.10.036

MacKinnon, A. C., Farnworth, S. L., Hodkinson, P. S., Henderson, N. C., Atkinson, K. M., Leffler, H., Nilsson, U. J., Haslett, C., Forbes, S. J., & Sethi, T. (2008). Regulation of Alternative Macrophage Activation by Galectin-3. *The Journal of Immunology*, *180*(4), 2650–2658. https://doi.org/10.4049/jimmunol.180.4.2650

Malapelle, U., Parente, P., Pepe, F., Di Micco, M. C., Russo, A., Clemente, C., Graziano, P., & Rossi, A. (2022). B7-H3/CD276 Inhibitors: Is There Room for the Treatment of Metastatic Non-Small Cell Lung Cancer? *International Journal of Molecular Sciences*, *23*(24), 16077. https://doi.org/10.3390/ijms232416077

Malapelle, U., Tiseo, M., Vivancos, A., Kapp, J., Serrano, M. J., & Tiemann, M. (2021). Liquid Biopsy for Biomarker Testing in Non-Small Cell Lung Cancer: A European Perspective. *Journal of Molecular Pathology*, *2*(3), 255–273. https://doi.org/10.3390/jmp2030022

Mao, X., Ou, M. T., Karuppagounder, S. S., Kam, T. I., Yin, X., Xiong, Y., Ge, P., Umanah, G. E., Brahmachari, S., Shin, J. H., Kang, H. C., Zhang, J., Xu, J., Chen, R., Park, H., Andrabi, S. A., Kang, S. U., Gonçalves, R. A., Liang, Y., … Dawson, T. M. (2016). Pathological α-synuclein transmission initiated by binding lymphocyte-activation gene 3. *Science*, *353*(6307), aah3374. https://doi.org/10.1126/science.aah3374

Marcus, L., Fashoyin-Aje, L. A., Donoghue, M., Yuan, M., Rodriguez, L., Gallagher, P. S., Philip, R., Ghosh, S., Theoret, M. R., Beaver, J. A., Pazdur, R., & Lemery, S. J. (2021). FDA Approval Summary: Pembrolizumab for the treatment of tumor mutational burden-high solid tumors. *Clinical Cancer Research*, *27*(17), 4685. https://doi.org/10.1158/1078-0432.CCR-21-0327

Marincola, F. M., Jaffee, E. M., Hickljn, D. J., & Ferrone, S. (2000). Escape of human solid tumors from t-cell recognition: molecular mechanisms and functional

significance. *Advances in Immunology*, *74*(74), 181–273. https://doi.org/10.1016/s0065-2776(08)60911-6

Marinelli, O., Nabissi, M., Morelli, M. B., Torquati, L., Amantini, C., & Santoni, G. (2018). ICOS-L as a Potential Therapeutic Target for Cancer Immunotherapy. *Current Protein and Peptide Science*, *19*(11), 1107–1113. https://doi.org/10.2174/1389203719666180608093913

Marjanovic, N. D., Weinberg, R. A., & Chaffer, C. L. (2013). Cell plasticity and heterogeneity in cancer. *Clinical Chemistry*, *59*(1), 168–179. https://doi.org/10.1373/clinchem.2012.184655

Markowitz, G. J., Havel, L. S., Crowley, M. J., Ban, Y., Lee, S. B., Thalappillil, J. S., Narula, N., Bhinder, B., Elemento, O., Wong, S. T., Gao, D., Altorki, N. K., & Mittal, V. (2018). Immune reprogramming via PD-1 inhibition enhances early-stage lung cancer survival. *JCI Insight*, *3*(13), e96836. https://doi.org/10.1172/jci.insight.96836

Marusyk, A., Almendro, V., & Polyak, K. (2012). Intra-tumour heterogeneity: a looking glass for cancer? *Nature Reviews Cancer*, *12*(5), 323–334. https://doi.org/10.1038/nrc3261

Mathew, M., Safyan, R. A., & Shu, C. A. (2017). PD-L1 as a biomarker in NSCLC: Challenges and future directions. *Annals of Translational Medicine*, *5*(18), 375. https://doi.org/10.21037/atm.2017.08.04

Mazurek, N., Byrd, J. C., Sun, Y., Hafley, M., Ramirez, K., Burks, J., & Bresalier, R. S. (2012). Cell-surface galectin-3 confers resistance to TRAIL by impeding trafficking of death receptors in metastatic colon adenocarcinoma cells. *Cell Death and Differentiation*, *19*(3), 523–533. https://doi.org/10.1038/cdd.2011.123

Mcelnay, P., & Lim, E. (2014). Adjuvant or neoadjuvant chemotherapy for NSCLC. *Journal of Thoracic Disease*, *6*(S2), 224–227. https://doi.org/10.3978/j.issn.2072-1439.2014.04.26

McGrail, D. J., Pilié, P. G., Rashid, N. U., Voorwerk, L., Slagter, M., Kok, M., Jonasch, E., Khasraw, M., Heimberger, A. B., Lim, B., Ueno, N. T., Litton, J. K., Ferrarotto, R., Chang, J. T., Moulder, S. L., & Lin, S. Y. (2021). High tumor mutation burden fails to predict immune checkpoint blockade response across all cancer types. *Annals of Oncology*, *32*(5), 661–672. https://doi.org/10.1016/j.annonc.2021.02.006

Meacham, C. E., & Morrison, S. J. (2013). Tumour heterogeneity and cancer cell plasticity. *Nature*, *501*(7467), 328–337. https://doi.org/10.1038/nature12624

Menon, R. P., & Hughes, R. C. (1999). Determinants in the N-terminal domains of galectin-3 for secretion by a novel pathway circumventing the endoplasmic reticulum-Golgi complex. *European Journal of Biochemistry*, *264*(2), 569–576. https://doi.org/10.1046/j.1432-1327.1999.00671.x

Meza, R., Meernik, C., Jeon, J., & Cote, M. L. (2015). Lung cancer incidence trends by gender, race and histology in the United States, 1973-2010. *PLoS ONE*, *10*(3), 1–14. https://doi.org/10.1371/journal.pone.0121323

Miao, J. L., Liu, R. J., Zhou, J. H., & Meng, S. H. (2016). *Fibroblast Growth Factor Receptor 1 Gene Amplification in Non-Small Cell Lung Cancer*. *129*(23), 2868–2872. https://doi.org/10.4103/0366-6999.194649

Michielsen, A. J., Ryan, E. J., & O'Sullivan, J. N. (2012). Dendritic cell inhibition correlates with survival of colorectal cancer patients on bevacizumab treatment. *OncoImmunology*, *1*(8), 1445–1447. https://doi.org/10.4161/onci.21318

Mirlekar, B. (2022). Tumor promoting roles of IL-10, TGF-β, IL-4, and IL-35: Its implications in cancer immunotherapy. *SAGE Open Medicine*, *10*, 20503121211069012. https://doi.org/10.1177/20503121211069012

Mok, T. S. K., Wu, Y., Kudaba, I., Kowalski, D. M., Cho, B. C., Turna, H. Z., Jr, G. C., & Srimuninnimit, V. (2019). Pembrolizumab versus chemotherapy for previously untreated, PD-L1-expressing, locally advanced or metastatic non-small-cell lung

cancer (KEYNOTE-042): a randomised, open-label , controlled, phase 3 trial. *The Lancet*, *6736*(18), 1–12. https://doi.org/10.1016/S0140-6736(18)32409-7

Molfetta, R., Zingoni, A., Santoni, A., & Paolini, R. (2019). Post-translational mechanisms regulating nk cell activating receptors and their ligands in cancer: Potential targets for therapeutic intervention. *Frontiers in Immunology*, *10*, 2557. https://doi.org/10.3389/fimmu.2019.02557

Moreaux, J., Veyrune, J. L., Reme, T., De Vos, J., & Klein, B. (2008). CD200: A putative therapeutic target in cancer. *Biochemical and Biophysical Research Communications*, *366*(1), 117–122. https://doi.org/10.1016/j.bbrc.2007.11.103

Myrna L. Ortiz, Lily Lu, Indu Ramachandran, and D. I. G. (2014). Myeloid-derived suppressor cells in the development of lung cancer. *Cancer Immunology Research*, *2*(1), 50–58. https://doi.org/10.1158/2326-6066.CIR-13-0129

Nagahara, K., Arikawa, T., Oomizu, S., Kontani, K., Nobumoto, A., Tateno, H., Watanabe, K., Niki, T., Katoh, S., Miyake, M., Nagahata, S.-I., Hirabayashi, J., Kuchroo, V. K., Yamauchi, A., & Hirashima, M. (2008). Galectin-9 Increases Tim-3+ Dendritic Cells and CD8+ T Cells and Enhances Antitumor Immunity via Galectin-9-Tim-3 Interactions. *The Journal of Immunology*, *181*(11), 7660–7669. https://doi.org/10.4049/jimmunol.181.11.7660

Nallasamy, P., Nimmakayala, R. K., Karmakar, S., Leon, F., Seshacharyulu, P., Lakshmanan, I., Rachagani, S., Mallya, K., Zhang, C., Ly, Q. P., Myers, M. S., Josh, L., Grabow, C. E., Gautam, S. K., Kumar, S., Lele, S. M., Jain, M., Batra, S. K., & Ponnusamy, M. P. (2021). Pancreatic Tumor Microenvironment Factor Promotes Cancer Stemness via SPP1–CD44 Axis. *Gastroenterology*, *161*(6), 1998-2013.e7. https://doi.org/10.1053/j.gastro.2021.08.023

Nangia-Makker, P., Hogan, V., & Raz, A. (2018). Galectin-3 and cancer stemness. *Glycobiology*, *28*(4), 172–181. https://doi.org/10.1093/glycob/cwy001

Nangia-Makker, P., Raz, T., Tait, L., Hogan, V., Fridman, R., & Raz, A. (2007). Galectin-3 cleavage: A novel surrogate marker for matrix metalloproteinase activity in

growing breast cancers. *Cancer Research*, *67*(24), 11760–11768. https://doi.org/10.1158/0008-5472.CAN-07-3233

Nangia-Makker, P., Wang, Y., Raz, T., Tait, L., Balan, V., Hogan, V., & Raz, A. (2010). Cleavage of galectin-3 by matrix metalloproteases induces angiogenesis in breast cancer. *International Journal of Cancer*, *127*(11), 2530–2541. https://doi.org/10.1002/ijc.25254

Nasim, F., Sabath, B. F., & Eapen, G. A. (2019). Lung Cancer. *Medical Clinics of North America*, *103*(3), 463–473. https://doi.org/10.1016/j.mcna.2018.12.006

Nazareth, M. R., Broderick, L., Simpson-Abelson, M. R., Kelleher, R. J., Yokota, S. J., & Bankert, R. B. (2007). Characterization of Human Lung Tumor-Associated Fibroblasts and Their Ability to Modulate the Activation of Tumor-Associated T Cells. *The Journal of Immunology*, *178*(9), 5552–5562. https://doi.org/10.4049/jimmunol.178.9.5552

Newman, A. M., Liu, C. L., Green, M. R., Gentles, A. J., Feng, W., Xu, Y., Hoang, C. D., Diehn, M., & Alizadeh, A. A. (2015). Robust enumeration of cell subsets from tissue expression profiles. *Nature Methods*, *12*(5), 453–457. https://doi.org/10.1038/nmeth.3337

Nicolazzo, C., Raimondi, C., Mancini, M., Caponnetto, S., Gradilone, A., Gandini, O., Mastromartino, M., Del Bene, G., Prete, A., Longo, F., Cortesi, E., & Gazzaniga, P. (2016). Monitoring PD-L1 positive circulating tumor cells in non-small cell lung cancer patients treated with the PD-1 inhibitor Nivolumab. *Scientific Reports*, *6*, 31726. https://doi.org/10.1038/SREP31726

Nowell, P. C. (1976). The Clonal Evolution of Tumor Cell Populations. *Science*, *194*(4260), 23–28. https://doi.org/10.1126/science.959840

Ochieng, J., Furtak, V., & Lukyanov, P. (2002). Extracellular functions of galectin-3. *Glycoconjugate Journal*, *19*(7–9), 527–535. https://doi.org/10.1023/B:GLYC.0000014082.99675.2F/METRICS

Ochieng, J., Green, B., Evans, S., James, O., & Warfield, P. (1998). Modulation of the biological functions of galectin-3 by matrix metalloproteinases. *Biochimica et Biophysica Acta*, *1379*(1), 97–106.

Ohue, Y., & Nishikawa, H. (2019). Regulatory T (Treg) cells in cancer: Can Treg cells be a new therapeutic target? *Cancer Science*, *110*(7), 2080–2089. https://doi.org/10.1111/cas.14069

Oka, N., Nakahara, S., Takenaka, Y., Fukumori, T., Hogan, V., Kanayama, H. O., Yanagawa, T., & Raz, A. (2005). Galectin-3 inhibits tumor necrosis factor-related apoptosis-inducing ligand-induced apoptosis by activating Akt in human bladder carcinoma cells. *Cancer Research*, *65*(17), 7546–7553. https://doi.org/10.1158/0008-5472.CAN-05-1197

Okada, K., Araki, M., Sakashita, T., Ma, B., Kanada, R., Yanagitani, N., Horiike, A., Koike, S., Oh-hara, T., Watanabe, K., Tamai, K., Maemondo, M., Nishio, M., Ishikawa, T., Okuno, Y., Fujita, N., & Katayama, R. (2019). Prediction of ALK mutations mediating ALK-TKIs resistance and drug re-purposing to overcome the resistance. *EBioMedicine*, *41*, 105–119. https://doi.org/10.1016/j.ebiom.2019.01.019

Okuma, Y., Hosomi, Y., Nakahara, Y., Watanabe, K., Sagawa, Y., & Homma, S. (2017). High plasma levels of soluble programmed cell death ligand 1 are prognostic for reduced survival in advanced lung cancer. *Lung Cancer*, *104*, 1–6. https://doi.org/10.1016/j.lungcan.2016.11.023

Okuma, Y., Wakui, H., Utsumi, H., Sagawa, Y., Hosomi, Y., Kuwano, K., & Homma, S. (2018). Soluble Programmed Cell Death Ligand 1 as a Novel Biomarker for Nivolumab Therapy for Non–Small-cell Lung Cancer. *Clinical Lung Cancer*, *19*(5), 410-417.e1. https://doi.org/10.1016/j.cllc.2018.04.014

Okumura, N., Fujii, K., Kagami, T., Makiko, N., Kitahara, M., Kinoshita, S., & Koizumi, N. (2016). Activation of the rho/rho kinase signaling pathway is involved in cell

death of corneal endothelium. *Investigative Ophthalmology and Visual Science*, *57*(15), 6843–6851. https://doi.org/10.1167/iovs.16-20123

Ottonello, S., Genova, C., Cossu, I., Fontana, V., Rijavec, E., Rossi, G., Biello, F., Dal Bello, M. G., Tagliamento, M., Alama, A., Coco, S., Boccardo, S., Vanni, I., Ferlazzo, G., Moretta, L., Grossi, F., Mingari, M. C., Carrega, P., & Pietra, G. (2020). Association Between Response to Nivolumab Treatment and Peripheral Blood Lymphocyte Subsets in Patients With Non-small Cell Lung Cancer. *Frontiers in Immunology*, *11*, 125. https://doi.org/10.3389/FIMMU.2020.00125

Overman, M. J., McDermott, R., Leach, J. L., Lonardi, S., Lenz, H. J., Morse, M. A., Desai, J., Hill, A., Axelson, M., Moss, R. A., Goldberg, M. V., Cao, Z. A., Ledeine, J. M., Maglinte, G. A., Kopetz, S., & André, T. (2017). Nivolumab in patients with metastatic DNA mismatch repair-deficient or microsatellite instability-high colorectal cancer (CheckMate 142): an open-label, multicentre, phase 2 study. *The Lancet Oncology*, *18*(9), 1182–1191. https://doi.org/10.1016/S1470-2045(17)30422-9

Pao, W., Miller, V., Zakowski, M., Doherty, J., Politi, K., Sarkaria, I., Singh, B., Heelan, R., Rusch, V., Fulton, L., Mardis, E., Kupfer, D., Wilson, R., Kris, M., & Varmus, H. (2004). EGF receptor gene mutations are common in lung cancers from "never smokers" and are associated with sensitivity of tumors to gefitinib and erlotinib. *Proceedings of the National Academy of Sciences of the United States of America*, *101*(36), 13306–13311. https://doi.org/10.1073/pnas.0405220101

Papadaki, M. A., Sotiriou, A. I., Vasilopoulou, C., Filika, M., Aggouraki, D., Tsoulfas, P. G., Apostolopoulou, C. A., Rounis, K., Mavroudis, D., & Agelaki, S. (2020). Optimization of the Enrichment of Circulating Tumor Cells for Downstream Phenotypic Analysis in Patients with Non-Small Cell Lung Cancer Treated with Anti-PD-1 Immunotherapy. *Cancers*, *12*(6), 1–26. https://doi.org/10.3390/cancers12061556

Pardoll, D. M. (2012). The blockade of immune checkpoints in cancer immunotherapy. *Nature Reviews Cancer*, *12*(4), 252–264. https://doi.org/10.1038/nrc3239

Patel, S. P., & Kurzrock, R. (2015). PD-L1 expression as a predictive biomarker in cancer immunotherapy. *Molecular Cancer Therapeutics*, *14*(4), 847–856. https://doi.org/10.1158/1535-7163.MCT-14-0983/86482/AM/PD-L1-EXPRESSION-AS-A-PREDICTIVE-BIOMARKER-IN

Paul, J., & Veenstra, T. D. (2022). Separation of Serum and Plasma Proteins for In-Depth Proteomic Analysis. *Separations*, *9*(4), 89. https://doi.org/10.3390/separations9040089

Pavan, A., Bragadin, A. B., Calvetti, L., Ferro, A., Zulato, E., Attili, I., Nardo, G., Maso, A. D., Frega, S., Menin, A. G., Fassan, M., Calabrese, F., Pasello, G., Guarneri, V., Aprile, G., Conte, P. F., Rosell, R., Indraccolo, S., & Bonanno, L. (2021). Role of next generation sequencing-based liquid biopsy in advanced non-small cell lung cancer patients treated with immune checkpoint inhibitors: Impact of STK11, KRAS and TP53 mutations and co-mutations on outcome. *Translational Lung Cancer Research*, *10*(1), 202–220. https://doi.org/10.21037/tlcr-20-674

Petermann, K. B., Rozenberg, G. I., Zedek, D., Groben, P., McKinnon, K., Buehler, C., Kim, W. Y., Shields, J. M., Penland, S., Bear, J. E., Thomas, N. E., Serody, J. S., & Sharpless, N. E. (2007). CD200 is induced by ERK and is a potential therapeutic target in melanoma. *Journal of Clinical Investigation*, *117*(12), 3922–3929. https://doi.org/10.1172/JCI32163

Petrova, M. P., Eneva, M. I., Arabadjiev, J. I., Conev, N. V., Dimitrova, E. G., Koynov, K. D., Karanikolova, T. S., Valev, S. S., Gencheva, R. B., Zhbantov, G. A., Ivanova, A. I., Sarbianova, I. I., Timcheva, C. V., & Donev, I. S. (2020). Neutrophil to lymphocyte ratio as a potential predictive marker for treatment with pembrolizumab as a second line treatment in patients with non-small cell lung cancer. *Bioscience Trends*, *14*(1), 48–55. https://doi.org/10.5582/BST.2019.01279

Pfaffl, M. W. (2001). A new mathematical model for relative quantification in real-time RT–PCR. *Nucleic Acids Research*, *29*(9), e45–e45. https://doi.org/10.1093/NAR/29.9.E45

Phuyal, S., Hessvik, N. P., Skotland, T., Sandvig, K., & Llorente, A. (2014). Regulation of exosome release by glycosphingolipids and flotillins. *FEBS Journal*, *281*(9), 2214–2227. https://doi.org/10.1111/febs.12775

Pikor, L. A., Ramnarine, V. R., Lam, S., & Lam, W. L. (2013). Genetic alterations defining NSCLC subtypes and their therapeutic implications. *Lung Cancer*, *82*(2), 179–189. https://doi.org/10.1016/j.lungcan.2013.07.025

Platonova, S., Cherfils-Vicini, J., Damotte, D., Crozet, L., Vieillard, V., Validire, P., André, P., Dieu-Nosjean, M. C., Alifano, M., Régnard, J. F., Fridman, W. H., Sautès-Fridman, C., & Cremer, I. (2011). Profound coordinated alterations of intratumoral NK cell phenotype and function in lung carcinoma. *Cancer Research*, *71*(16), 5412–5422. https://doi.org/10.1158/0008-5472.CAN-10-4179

Popat, S., Liu, S. V., Scheuer, N., Gupta, A., Hsu, G. G., Ramagopalan, S. V., Griesinger, F., & Subbiah, V. (2022). Association between Smoking History and Overall Survival in Patients Receiving Pembrolizumab for First-Line Treatment of Advanced Non-Small Cell Lung Cancer. *JAMA Network Open*, *5*(5), E2214046. https://doi.org/10.1001/jamanetworkopen.2022.14046

Postmus, P. E., Kerr, K. M., Oudkerk, M., Senan, S., Waller, D. A., Vansteenkiste, J., Escriu, C., & Peters, S. (2017). Early and locally advanced non-small-cell lung cancer (NSCLC): ESMO Clinical Practice Guidelines for diagnosis, treatment and follow-up. *Annals of Oncology*, *28*(suppl_4), iv1–iv21. https://doi.org/10.1093/annonc/mdx222

Powell, H. A., Tata, L. J., Baldwin, D. R., Stanley, R. A., Khakwani, A., & Hubbard, R. B. (2013). Early mortality after surgical resection for lung cancer: An analysis of

the English National Lung cancer audit. *Thorax*, *68*(9), 826–834. https://doi.org/10.1136/thoraxjnl-2012-203123

Puglisi, F., Minisini, A. M., Barbone, F., Intersimone, D., Aprile, G., Puppin, C., Damante, G., Paron, I., Tell, G., Piga, A., & Loreto, C. Di. (2004). Galectin-3 expression in non-small cell lung carcinoma. *Cancer Letters*, *212*(2), 233–239. https://doi.org/10.1016/j.canlet.2004.03.006

Qiu, Z., Chen, Z., Zhang, C., & Zhong, W. (2019). Achievements and futures of immune checkpoint inhibitors in non-small cell lung cancer. *Experimental Hematology & Oncology*, *8*, 1–19. https://doi.org/10.1186/s40164-019-0143-z

Rabinovich, G. A., Gabrilovich, D., & Sotomayor, E. M. (2007). Immunosuppressive Strategies that are Mediated by Tumor Cells. *Annual Review of Immunology*, *25*(1), 267–296. https://doi.org/10.1146/annurev.immunol.25.022106.141609

Raffaghello, L., Prigione, I., Airoldi, I., Camoriano, M., Levreri, I., Gambini, C., Pende, D., Steinte, A., Ferrone, S., & Pistoia, V. (2004). Downregulation and/or release of NKG2D ligands as immune evasion strategy of human neuroblastoma. *Neoplasia*, *6*(5), 558–568. https://doi.org/10.1593/neo.04316

Raju, S., Joseph, R., & Sehgal, S. (2018). Review of checkpoint immunotherapy for the management of non-small cell lung cancer. *Immuno Targets and Therapy*, *7*, 63–75. https://doi.org/10.2147/itt.s125070

Ramachandran, S., Verma, A. K., Dev, K., Goyal, Y., Bhatt, D., Alsahli, M. A., Rahmani, A. H., Almatroudi, A., Almatroodi, S. A., Alrumaihi, F., & Khan, N. A. (2021). Role of Cytokines and Chemokines in NSCLC Immune Navigation and Proliferation. *Oxidative Medicine and Cellular Longevity*, *2021*, 5563746. https://doi.org/10.1155/2021/5563746

Ramalingam, S. S., Vansteenkiste, J., Planchard, D., Cho, B. C., Gray, J. E., Ohe, Y., Zhou, C., Reungwetwattana, T., Cheng, Y., Chewaskulyong, B., Shah, R., Cobo, M., Lee, K. H., Cheema, P., Tiseo, M., John, T., Lin, M.-C., Imamura, F., Kurata, T., … Soria, J.-C. (2020). Overall Survival with Osimertinib in Untreated, EGFR -

Mutated Advanced NSCLC. *New England Journal of Medicine*, *382*(1), 41–50. https://doi.org/10.1056/nejmoa1913662

Reck, M., & Rabe, K. F. (2017). Precision Diagnosis and Treatment for Advanced Non–Small-Cell Lung Cancer. *New England Journal of Medicine*, *377*(9), 849–861. https://doi.org/10.1056/nejmra1703413

Reck, M., Rodríguez-Abreu, D., Robinson, A. G., Hui, R., Csöszi, T., Fülöp, A., Gottfried, M., Peled, N., Tafreshi, A., Cuffe, S., O'Brien, M., Rao, S., Hotta, K., Leal, T. A., Riess, J. W., Jensen, E., Zhao, B., Pietanza, M. C., & Brahmer, J. R. (2021). Five-Year Outcomes with Pembrolizumab Versus Chemotherapy for Metastatic Non–Small-Cell Lung Cancer with PD-L1 Tumor Proportion Score ‡ 50%. *Journal of Clinical Oncology*, *39*(21), 2339–2349. https://doi.org/10.1200/JCO.21.00174

Reck, M., Rodríguez-Abreu, D., Robinson, A. G., Hui, R., Csőszi, T., Fülöp, A., Gottfried, M., Peled, N., Tafreshi, A., Cuffe, S., O'Brien, M., Rao, S., Hotta, K., Leiby, M. A., Lubiniecki, G. M., Shentu, Y., Rangwala, R., & Brahmer, J. R. (2016). Pembrolizumab versus Chemotherapy for PD-L1–Positive Non–Small-Cell Lung Cancer. *New England Journal of Medicine*, *375*(19), 1823–1833. https://doi.org/10.1056/NEJMOA1606774/SUPPL_FILE/NEJMOA1606774_DISCLOSURES.PDF

Reynolds, B. A., & Weiss, S. (1992). Generation of neurons and astrocytes from isolated cells of the adult mammalian central nervous system. *Science*, *255*(5052), 1707–1710. https://doi.org/10.1126/SCIENCE.1553558

Rich, J. N. (2016). Cancer stem cells: understanding tumor hierarchy and heterogeneity. *Medicine*, *95*(S1), e4764. https://doi.org/10.1097/MD.0000000000004764

Richter, M., Piwocka, O., Musielak, M., Piotrowski, I., Suchorska, W. M., & Trzeciak, T. (2021). From Donor to the Lab: A Fascinating Journey of Primary Cell Lines.

Frontiers in Cell and Developmental Biology, *9*, 711381. https://doi.org/10.3389/fcell.2021.711381

Ricordel, C., Friboulet, L., Facchinetti, F., & Soria, J. (2018). Molecular mechanisms of acquired resistance to third-generation EGFR-TKIs in EGFR T790M-mutant lung cancer. *Annals of Oncology*, *29*(Supplement 1), i28–i37. https://doi.org/10.1093/annonc/mdx705

Robinson, C. G., & Bradley, J. D. (2010). The Treatment of Early-Stage Disease. *Seminars in Radiation Oncology*, *20*(3), 178–185. https://doi.org/10.1016/j.semradonc.2010.01.004

Rosell, R., Codony-Servat, J., Nieto, J. G., Santarpia, M., Jain, A., Chandan, S., Wang, Y., Giménez-Capitán, A., Molina-Vila, M. A., Nilsson, J., & González-Cao, M. (2023). KRAS G12C-mutant driven non-small cell lung cancer (NSCLC). *Critical Reviews in Oncology/Hematology*, 104228. https://doi.org/10.1016/j.critrevonc.2023.104228

Rui, L., Xiaofei, Z., Hongjuan, Y., & Liang, L. (2020). Four generations of EGFR TKIs associated with different pathogenic mutations in non-small cell lung carcinoma. *Journal of Drug Targeting*, *28*(9), 861–872. https://doi.org/10.1080/1061186X.2020.1737934

Ruopp, M. D., Perkins, N. J., Whitcomb, B. W., & Schisterman, E. F. (2008). Youden Index and Optimal Cut-Point Estimated from Observations Affected by a Lower Limit of Detection. *Biom J.*, *50*(3), 419430. https://doi.org/10.1002/bimj.200710415

Ruvolo, P. P. (2016). Galectin 3 as a guardian of the tumor microenvironment. *Biochimica et Biophysica Acta*, *1863*(3), 427–437. https://doi.org/10.1016/J.BBAMCR.2015.08.008

Sachs, E., Sartipy, U., & Jackson, V. (2021). Sex and Survival After Surgery for Lung Cancer: A Swedish Nationwide Cohort. *Chest*, *159*(5), 2029–2039. https://doi.org/10.1016/j.chest.2020.11.010

Sánchez-Paulete, A. R., Teijeira, A., Cueto, F. J., Garasa, S., Pérez-Gracia, J. L., Sánchez-Arráez, A., Sancho, D., & Melero, I. (2017). Antigen cross-presentation and T-cell cross-priming in cancer immunology and immunotherapy. *Annals of Oncology*, *28*(suppl_12), xii44–xii55. https://doi.org/10.1093/annonc/mdx237

Sanmamed, M. F., Perez-Gracia, J. L., Schalper, K. A., Fusco, J. P., Gonzalez, A., Rodriguez-Ruiz, M. E., Oñate, C., Perez, G., Alfaro, C., Martín-Algarra, S., Andueza, M. P., Gurpide, A., Morgado, M., Wang, J., Bacchiocchi, A., Halaban, R., Kluger, H., Chen, L., Sznol, M., & Melero, I. (2017). Changes in serum interleukin-8 (IL-8) levels reflect and predict response to anti-PD-1 treatment in melanoma and non-small-cell lung cancer patients. *Annals of Oncology*, *28*(8), 1988–1995. https://doi.org/10.1093/ANNONC/MDX190

Santarpia, M., Liguori, A., D'Aveni, A., Karachaliou, N., Gonzalez-Cao, M., Daffinà, M. G., Lazzari, C., Altavilla, G., & Rosell, R. (2018). Liquid biopsy for lung cancer early detection. *Journal of Thoracic Disease*, *10*(suppl_7), S882–S897. https://doi.org/10.21037/jtd.2018.03.81

Schalper, K. A., Carleton, M., Zhou, M., Chen, T., Feng, Y., Huang, S. P., Walsh, A. M., Baxi, V., Pandya, D., Baradet, T., Locke, D., Wu, Q., Reilly, T. P., Phillips, P., Nagineni, V., Gianino, N., Gu, J., Zhao, H., Perez-Gracia, J. L., … Melero, I. (2020). Elevated serum interleukin-8 is associated with enhanced intratumor neutrophils and reduced clinical benefit of immune-checkpoint inhibitors. *Nature Medicine*, *26*(5), 688–692. https://doi.org/10.1038/s41591-020-0856-x

Schneider, T., Hoffmann, H., Dienemann, H., Schnabel, P. A., Enk, A. H., Ring, S., & Mahnke, K. (2011). Non-small cell lung cancer induces an immunosuppressive phenotype of dendritic cells in tumor microenvironment by upregulating B7-H3. *Journal of Thoracic Oncology*, *6*(7), 1162–1168. https://doi.org/10.1097/JTO.0b013e31821c421d

Sequist, L. V., Soria, J.-C., Goldman, J. W., Wakelee, H. A., Gadgeel, S. M., Varga, A., Papadimitrakopoulou, V., Solomon, B. J., Oxnard, G. R., Dziadziuszko, R., Aisner, D. L., Doebele, R. C., Galasso, C., Garon, E. B., Heist, R. S., Logan, J., Neal, J. W.,

Mendenhall, M. A., Nichols, S., … Camidge, D. R. (2015). Rociletinib in EGFR - Mutated Non–Small-Cell Lung Cancer. *New England Journal of Medicine*, *372*(18), 1700–1709. https://doi.org/10.1056/nejmoa1413654

Shalom-Feuerstein, R., Cooks, T., Raz, A., & Kloog, Y. (2005). Galectin-3 regulates a molecular switch from N-Ras to K-Ras usage in human breast carcinoma cells. *Cancer Research*, *65*(16), 7292–7300. https://doi.org/10.1158/0008-5472.CAN-05-0775

Shao, A., & Owens, D. M. (2023). The immunoregulatory protein CD200 as a potentially lucrative yet elusive target for cancer therapy. *Oncotarget*, *14*, 96–103. https://doi.org/10.18632/oncotarget.28354.

Shaw, A. T., Bauer, T. M., de Marinis, F., Felip, E., Goto, Y., Liu, G., Mazieres, J., Kim, D.-W., Mok, T., Polli, A., Thurm, H., Calella, A. M., Peltz, G., & Solomon, B. J. (2020). First-Line Lorlatinib or Crizotinib in Advanced ALK -Positive Lung Cancer. *New England Journal of Medicine*, *383*(21), 2018–2029. https://doi.org/10.1056/nejmoa2027187

Shaw, A. T., Kim, D. W., Nakagawa, K., Seto, T., Crinó, L., Ahn, M. J., De Pas, T., Besse, B., Solomon, B. J., Blackhall, F., Wu, Y. L., Thomas, M., O'Byrne, K. J., Moro-Sibilot, D., Camidge, D. R., Mok, T., Hirsh, V., Riely, G. J., Iyer, S., … Jänne, P. A. (2013). Crizotinib versus chemotherapy in advanced ALK-positive lung cancer. *New England Journal of Medicine*, *368*(25), 2385–2394. https://doi.org/10.1056/NEJMoa1214886

Sheikh, M., Mukeriya, A., Shangina, O., Brennan, P., & Zaridze, D. (2021). Postdiagnosis Smoking Cessation and Reduced Risk for Lung Cancer Progression and Mortality. *Annals of Internal Medicine*, *174*(9), 1232–1239. https://doi.org/10.7326/M21-0252

Shimada, Y., Matsubayashi, J., Kudo, Y., Maehara, S., Takeuchi, S., Hagiwara, M., Kakihana, M., Ohira, T., Nagao, T., & Ikeda, N. (2021). Serum-derived exosomal PD-L1 expression to predict anti-PD-1 response and in patients with non-small

cell lung cancer. *Scientific Reports*, *11*(1). https://doi.org/10.1038/s41598-021-87575-3

Shimura, T., Shibata, M., Gonda, K., Kofunato, Y., Okada, R., Ishigame, T., Kimura, T., Kenjo, A., Kono, K., & Marubashi, S. (2017). Significance of circulating galectin-3 in patients with pancreatobiliary cancer. *Anticancer Research*, *37*(9), 4979–4986. https://doi.org/10.21873/anticanres.11909

Shimura, T., Takenaka, Y., Tsutsumi, S., Hogan, V., Kikuchi, A., & Raz, A. (2004). Galectin-3, a novel binding partner of β-catenin. *Cancer Research*, *64*(18), 6363–6367. https://doi.org/10.1158/0008-5472.CAN-04-1816

Siegelin, M. D., & Borczuk, A. C. (2014). Epidermal growth factor receptor mutations in lung adenocarcinoma. *Laboratory Investigation*, *94*(2), 129–137. https://doi.org/10.1038/labinvest.2013.147

Singhal, S., Bhojnagarwala, P. S., O'Brien, S., Moon, E. K., Garfall, A. L., Rao, A. S., Quatromoni, J. G., Stephen, T. L., Litzky, L., Deshpande, C., Feldman, M. D., Hancock, W. W., Conejo-Garcia, J. R., Albelda, S. M., & Eruslanov, E. B. (2016). Origin and Role of a Subset of Tumor-Associated Neutrophils with Antigen-Presenting Cell Features in Early-Stage Human Lung Cancer. *Cancer Cell*, *30*(1), 120–135. https://doi.org/10.1016/j.ccell.2016.06.001

Skoulidis, F., Li, B. T., Dy, G. K., Price, T. J., Falchook, G. S., Wolf, J., Italiano, A., Schuler, M., Borghaei, H., Barlesi, F., Kato, T., Curioni-Fontecedro, A., Sacher, A., Spira, A., Ramalingam, S. S., Takahashi, T., Besse, B., Anderson, A., Ang, A., … Govindan, R. (2021). Sotorasib for Lung Cancers with KRAS p.G12C Mutation. *New England Journal of Medicine*, *384*(25), 2371–2381. https://doi.org/10.1056/nejmoa2103695

Smith, D. R., Polverini, P. J., Kunkel, S. L., Orringer, M. B., Whyte, R. I., Burdick, M. D., Wilke, C. A., & Strieter, R. M. (1994). Inhibition of Interleukin 8 Attenuates Angiogenesis in Bronchogenic Carcinoma. *Journal of Experimental Medicine*, *179*(5), 1409–1415. https://doi.org/10.1084/jem.179.5.1409

Sociedad Española de Oncologia Médica. (2023). *Las cifras del cáncer en España 2023*. https://seom.org/images/Las_cifras_del_Cancer_en_Espana_2023.pdf

Socinski, M. A., Obasaju, C., Gandara, D., Hirsch, F. R., Bonomi, P., Bunn, P., Kim, E. S., Langer, C. J., Natale, R. B., Novello, S., Paz-Ares, L., Pérol, M., Reck, M., Ramalingam, S. S., Reynolds, C. H., Spigel, D. R., Stinchcombe, T. E., Wakelee, H., Mayo, C., & Thatcher, N. (2016). Clinicopathologic features of advanced squamous NSCLC. *Journal of Thoracic Oncology*, *11*(9), 1411–1422. https://doi.org/10.1016/j.jtho.2016.05.024

Soda, M., Choi, Y. L., Enomoto, M., Takada, S., Yamashita, Y., Ishikawa, S., Fujiwara, S. I., Watanabe, H., Kurashina, K., Hatanaka, H., Bando, M., Ohno, S., Ishikawa, Y., Aburatani, H., Niki, T., Sohara, Y., Sugiyama, Y., & Mano, H. (2007). Identification of the transforming EML4-ALK fusion gene in non-small-cell lung cancer. *Nature*, *448*(7153), 561–566. https://doi.org/10.1038/nature05945

Soda, M., Takada, S., Takeuchi, K., Young, L. C., Enomoto, M., Ueno, T., Haruta, H., Hamada, T., Yamashita, Y., Ishikawa, Y., Sugiyama, Y., & Mano, H. (2008). A mouse model for EML4-ALK-positive lung cancer. *Proceedings of the National Academy of Sciences of the United States of America*, *105*(50), 19893–19897. https://doi.org/10.1073/pnas.0805381105

Sojka, D. K., Huang, Y. H., & Fowell, D. J. (2008). Mechanisms of regulatory T-cell suppression - A diverse arsenal for a moving target. *Immunology*, *124*(1), 13–22. https://doi.org/10.1111/j.1365-2567.2008.02813.x

Solomon, B. J., Besse, B., Bauer, T. M., Felip, E., Soo, R. A., Camidge, D. R., Chiari, R., Bearz, A., Lin, C. C., Gadgeel, S. M., Riely, G. J., Tan, E. H., Seto, T., James, L. P., Clancy, J. S., Abbattista, A., Martini, J. F., Chen, J., Peltz, G., … Shaw, A. T. (2018). Lorlatinib in patients with ALK-positive non-small-cell lung cancer: results from a global phase 2 study. *The Lancet Oncology*, *19*(12), 1654–1667. https://doi.org/10.1016/S1470-2045(18)30649-1

Spyratos, D., Zarogoulidis, P., Porpodis, K., Tsakiridis, K., Machairiotis, N., Katsikogiannis, N., Kougioumtzi, I., Dryllis, G., Kallianos, A., Rapti, A., Li, C., & Zarogoulidis, K. (2013). Occupational exposure and lung cancer. *Journal of Thoracic Disease*, *5*(suppl_4), S440–S445. https://doi.org/10.3978/j.issn.2072-1439.2013.07.09

Srivastava, M. K., Zhu, L., Harris-white, M., Kar, U., Huang, M., Johnson, M. F., Lee, J. M., Elashoff, D., Strieter, R., Dubinett, S., & Sharma, S. (2012). Myeloid Suppressor Cell Depletion Augments Antitumor Activity in Lung Cancer. *PLoS ONE*, *7*(7), e40677. https://doi.org/10.1371/journal.pone.0040677

St. Paul, M., & Ohashi, P. S. (2020). The Roles of CD8+ T Cell Subsets in Antitumor Immunity. *Trends in Cell Biology*, *30*(9), 695–704. https://doi.org/10.1016/j.tcb.2020.06.003

Stillman, B. N., Hsu, D. K., Pang, M., Brewer, C. F., Johnson, P., Liu, F.-T., & Baum, L. G. (2006). Galectin-3 and galectin-1 bind distinct cell surface glycoprotein receptors to induce T cell death. *Journal of Immunology*, *176*(2), 778–789. https://doi.org/10.4049/JIMMUNOL.176.2.778

Stumpfova, M., Ratner, D., Desciak, E. B., Eliezri, Y. D., & Owens, D. M. (2010). The immunosuppressive surface ligand CD200 augments the metastatic capacity of squamous cell carcinoma. *Cancer Research*, *70*(7), 2962–2972. https://doi.org/10.1158/0008-5472.CAN-09-4380

Sumitomo, R., Hirai, T., Fujita, M., Murakami, H., Otake, Y., & Huang, C. (2019). M2 tumor-associated macrophages promote tumor progression in non-small-cell lung cancer. *Experimental and Therapeutic Medicine*, *18*, 4490–4498. https://doi.org/10.3892/etm.2019.8068

Sun, J., Soyeon, K., Koh, J., Kim, M., Keam, B., Kim, T. M., Lindmark, B., & Kim, D. W. (2022). Predictive role of galectin - 3 for immune checkpoint blockades (ICBs) in advanced or metastatic non - small cell lung cancer : a potential new marker

for ICB resistance. *Journal of Cancer Research and Clinical Oncology*, *149*, 2355–2365. https://doi.org/10.1007/s00432-022-04275-9

Sun, Y., Yang, Q., Shen, J., Wei, T., Shen, W., Zhang, N., Luo, P., & Zhang, J. (2021). The Effect of Smoking on the Immune Microenvironment and Immunogenicity and Its Relationship With the Prognosis of Immune Checkpoint Inhibitors in Non-small Cell Lung Cancer. *Frontiers in Cell and Developmental Biology*, *9*, 745859. https://doi.org/10.3389/fcell.2021.745859

Sung, H., Ferlay, J., Siegel, R. L., Laversanne, M., Soerjomataram, I., Jemal, A., & Bray, F. (2021). Global Cancer Statistics 2020: GLOBOCAN Estimates of Incidence and Mortality Worldwide for 36 Cancers in 185 Countries. *CA: A Cancer Journal for Clinicians*, *71*(3), 209–249. https://doi.org/10.3322/caac.21660

Szöke, T., Kayser, K., Trojan, I., Kayser, G., Furak, J., Tiszlavicz, L., Baumhäkel, J. D., & Gabius, H. J. (2007). The role of microvascularization and growth/adhesion-regulatory lectins in the prognosis of non-small cell lung cancer in stage II. *European Journal of Cardio-Thoracic Surgery*, *31*(5), 783–787. https://doi.org/10.1016/J.EJCTS.2007.01.072

Takeda, S., Gapper, C., Kaya, H., Bell, E., Kuchitsu, K., & Dolan, L. (2008). Local positive feedback regulation determines cell shape in root hair cells. *Science*, *319*(5867), 1241–1244. https://doi.org/10.1126/science.1152505

Takenaka, Y., Fukumori, T., & Raz, A. (2002). Galectin-3 and metastasis. *Glycoconjugate Journal*, *19*(7–9), 543–549. https://doi.org/10.1023/B:GLYC.0000014084.01324.15/METRICS

Tao, L., Jin, L., Dechun, L., Hongqiang, Y., Changhua, K., & Guijun, L. (2017). Galectin-3 expression in colorectal cancer and its correlation with clinical pathological characteristics and prognosis. *Open Medicine*, *12*(1), 226–230. https://doi.org/10.1515/med-2017-0032

Terry, S., Savagner, P., Ortiz-Cuaran, S., Mahjoubi, L., Saintigny, P., Thiery, J. P., & Chouaib, S. (2017). New insights into the role of EMT in tumor immune escape.

Molecular Oncology, *11*(7), 824–846. https://doi.org/10.1002/1878-0261.12093

Théry, C., Boussac, M., Véron, P., Ricciardi-Castagnoli, P., Raposo, G., Garin, J., & Amigorena, S. (2001). Proteomic Analysis of Dendritic Cell-Derived Exosomes: A Secreted Subcellular Compartment Distinct from Apoptotic Vesicles. *The Journal of Immunology*, *166*(12), 7309–7318. https://doi.org/10.4049/jimmunol.166.12.7309

Thomas J Lynch, Daphne W Bell, Raffaella Sordella, Sarada Gurubhagavatula, Ross A Okimoto, Brian W Brannigan, Patricia L Harris, Sara M Haserlat, Jeffrey G Supko, Frank G Haluska, David N Louis, David C Christiani, Jeff Settleman, & Daniel A Haber. (2004). Activating mutations in the epidermal growth factor receptor underlying responsiveness of non-small-cell lung cancer to gefitinib. *The New England Journal of Medicine*, *350*(21), 2129–2139. https://doi.org/10.1056/NEJMoa040938

Thommen, D. S., Schreiner, J., Müller, P., Herzig, P., Roller, A., Belousov, A., Umana, P., Pisa, P., Klein, C., Bacac, M., Fischer, O. S., Moersig, W., Prince, S. S., Levitsky, V., Karanikas, V., Lardinois, D., & Zippelius, A. (2015). Progression of lung cancer is associated with increased dysfunction of T cells defined by coexpression of multiple inhibitory receptors. *Cancer Immunology Research*, *3*(12), 1344–1354. https://doi.org/10.1158/2326-6066.CIR-15-0097

Torres, S., González, Á., Cunquero Tomas, A. J., Calabuig Fariñas, S., Ferrero, M., Mirda, D., Sirera, R., Jantus-Lewintre, E., & Camps, C. (2020). A profile on cobas® EGFR Mutation Test v2 as companion diagnostic for first-line treatment of patients with non-small cell lung cancer. *Expert Review of Molecular Diagnostics*, *20*(6), 575–582. https://doi.org/10.1080/14737159.2020.1724094

Torres-Martínez, S., Calabuig-Fariñas, S., Gallach, S., Mosqueda, M., Munera-Maravilla, E., Sirera, R., Navarro, L., Blasco, A., Camps, C., & Jantus-Lewintre, E. (2023). Circulating Immune Proteins: Improving the Diagnosis and Clinical

Outcome in Advanced Non-Small Cell Lung Cancer. *International Journal of Molecular Sciences*, *24*(24), 17587. https://doi.org/10.3390/ijms242417587

Torres-Martínez, S., Calabuig-Fariñas, S., Moreno-Manuel, A., Bertolini, G., Herreros-Pomares, A., Escorihuela, E., Duréndez-Saéz, E., Guijarro, R., Blasco, A., Roz, L., Camps, C., & Jantus-Lewintre, E. (2023). Soluble galectin-3 as a microenvironment-relevant immunoregulator with prognostic and predictive value in lung adenocarcinoma. *Molecular Oncology*, *18*(1), 190–215. https://doi.org/10.1002/1878-0261.13505

Usó, M., Jantus-Lewintre, E., Bremnes, R. M., Calabuig, S., Blasco, A., Pastor, E., Borreda, I., Molina-Pinelo, S., Paz-Ares, L., Guijarro, R., Martorell, M., Forteza, J., Camps, C., & Sirera, R. (2016). Analysis of the immune microenvironment in resected non-small cell lung cancer: the prognostic value of different T lymphocyte markers. *Oncotarget*, *7*(33), 52849–52861. https://doi.org/10.18632/oncotarget.10811

Usó, M., Jantus-Lewintre, E., Calabuig-Fariñas, S., Blasco, A., Del Olmo, E., Guijarro, R., Martorell, M., Camps, C., & Sirer, R. (2017). Analysis of the prognostic role of an immune checkpoint score in resected non-small cell lung cancer patients. *OncoImmunology*, *6*(1), 1–9. https://doi.org/10.1080/2162402X.2016.1260214

Vandesompele, J., De Preter, K., Pattyn, F., Poppe, B., Van Roy, N., De Paepe, A., & Speleman, F. (2002). Accurate normalization of real-time quantitative RT-PCR data by geometric averaging of multiple internal control genes. *Genome Biology*, *3*(7), 1–12. https://doi.org/10.1186/gb-2002-3-7-research0034

Vigdorovich, V., Ramagopal, U. A., Lázár-Molnár, E., Sylvestre, E., Lee, J. S., Hofmeyer, K. A., Zang, X., Nathenson, S. G., & Almo, S. C. (2013). Structure and T Cell Inhibition Properties of B7 Family Member, B7-H3. *Structure*, *21*(5), 707–717. https://doi.org/10.1016/J.STR.2013.03.003

Visan, I. (2019). New ligand for LAG-3. *Nature Immunology*, *20*(2), 111–111. https://doi.org/10.1038/s41590-018-0307-8

Vuong, L., Kouverianou, E., Rooney, C. M., McHugh, B. J., Howie, S. E. M., Gregory, C. D., Forbes, S. J., Henderson, N. C., Zetterberg, F. R., Nilsson, U. J., Leffler, H., Ford, P., Pedersen, A., Gravelle, L., Tantawi, S., Schambye, H., Sethi, T., & MacKinnon, A. C. (2019). An orally active galectin-3 antagonist inhibits lung adenocarcinoma growth and augments response to PD-L1 blockade. *Cancer Research*, *79*(7), 1480–1492. https://doi.org/10.1158/0008-5472.CAN-18-2244

Wait, S., Alvarez-Rosete, A., Osama, T., Bancroft, D., Cornelissen, R., Marušić, A., Garrido, P., Adamek, M., van Meerbeeck, J., Snoeckx, A., Leleu, O., Hult, E. H., Couraud, S., & Baldwin, D. R. (2022). Implementing Lung Cancer Screening in Europe: Taking a Systems Approach. *JTO Clinical and Research Reports*, *3*(5), 100329. https://doi.org/10.1016/j.jtocrr.2022.100329

Wang, H., Zhou, F., Qiao, M., Li, X., Zhao, C., Cheng, L., Chen, X., & Zhou, C. (2021). The Role of Circulating Tumor DNA in Advanced Non-Small Cell Lung Cancer Patients Treated With Immune Checkpoint Inhibitors: A Systematic Review and Meta-Analysis. *Frontiers in Oncology*, *11*, 671874. https://doi.org/10.3389/FONC.2021.671874

Wang, J., Sanmamed, M. F., Datar, I., Su, T. T., Ji, L., Sun, J., Chen, L., Chen, Y., Zhu, G., Yin, W., Zheng, L., Zhou, T., Badri, T., Yao, S., Zhu, S., Boto, A., Sznol, M., Melero, I., Vignali, D. A. A., … Chen, L. (2019). Fibrinogen-like Protein 1 Is a Major Immune Inhibitory Ligand of LAG-3. *Cell*, *176*(1–2), 334-347.e12. https://doi.org/10.1016/j.cell.2018.11.010

Wang, M., Zhai, X., Li, J., Guan, J., Xu, S., Li, Y. Y., & Zhu, H. (2021). The Role of Cytokines in Predicting the Response and Adverse Events Related to Immune Checkpoint Inhibitors. *Frontiers in Immunology*, *12*, 670391. https://doi.org/10.3389/FIMMU.2021.670391

Wang, Y., Niu, X., Cheng, Y., Zhang, Y., Xia, L., Xia, W., & Lu, S. (2022). Exosomal PD-L1 predicts response with immunotherapy in NSCLC patients. *Clinical and Experimental Immunology*, *208*(3), 316–322. https://doi.org/10.1093/CEI/UXAC045

Wang, Y., Tong, Z., Zhang, W., Zhang, W., Buzdin, A., Mu, X., Yan, Q., Zhao, X., Chang, H. H., Duhon, M., Zhou, X., Zhao, G., Chen, H., & Li, X. (2021). FDA-Approved and Emerging Next Generation Predictive Biomarkers for Immune Checkpoint Inhibitors in Cancer Patients. *Frontiers in Oncology*, *11*, 683419. https://doi.org/10.3389/fonc.2021.683419

Warth, A., Körner, S., Penzel, R., Muley, T., Dienemann, H., Schirmacher, P., von Knebel-Doeberitz, M., Weichert, W., & Kloor, M. (2016). Microsatellite instability in pulmonary adenocarcinomas: a comprehensive study of 480 cases. *Virchows Archiv*, *468*(3), 313–319. https://doi.org/10.1007/S00428-015-1892-7

Weber, S., van der Leest, P., Donker, H. C., Schlange, T., Timens, W., Tamminga, M., Hasenleithner, S. O., Graf, R., Moser, T., Spiegl, B., Yaspo, M.-L., Terstappen, L. W. M. M., Sidorenkov, G., Hiltermann, T. Jeroen. N., Speicher, M. R., Schuuring, E., Heitzer, E., & Groen, H. J. M. (2021). Dynamic Changes of Circulating Tumor DNA Predict Clinical Outcome in Patients With Advanced Non-Small-Cell Lung Cancer Treated With Immune Checkpoint Inhibitors. *JCO Precision Oncology*, *5*(5), 1540–1553. https://doi.org/10.1200/PO.21.00182

Wei, X., Zhang, J., Gu, Q., Huang, M., Zhang, W., Guo, J., & Zhou, X. (2017). Reciprocal Expression of IL-35 and IL-10 Defines Two Distinct Effector Treg Subsets that Are Required for Maintenance of Immune Tolerance. *Cell Reports*, *21*(7), 1853–1869. https://doi.org/10.1016/j.celrep.2017.10.090

Welton, J. L., Khanna, S., Giles, P. J., Brennan, P., Brewis, I. A., Staffurth, J., Mason, M. D., & Clayton, A. (2010). Proteomics analysis of bladder cancer exosomes. *Molecular and Cellular Proteomics*, *9*(6), 1324–1338. https://doi.org/10.1074/mcp.M000063-MCP201

Westover, D., Zugazagoitia, J., Cho, B. C., & Lovly, C. M. (2018). Mechanisms of acquired resistance to first- and second-generation EGFR tyrosine kinase inhibitors. *Annals of Oncology*, *29*(Suppl_1), i10–i19. https://doi.org/10.1093/annonc/mdx703

Wischhusen, J., Waschbisch, A., & Wiendl, H. (2007). Immune-refractory cancers and their little helpers-An extended role for immunetolerogenic MHC molecules HLA-G and HLA-E? *Seminars in Cancer Biology*, *17*(6), 459–468. https://doi.org/10.1016/j.semcancer.2007.07.005

Wu, J. D., Higgins, L. M., Steinle, A., Cosman, D., Haugk, K., & Plymate, S. R. (2004). Prevalent expression of the immunostimulatory MHC class I chain-related molecule is counteracted by shadding in prostate cancer. *Journal of Clinical Investigation*, *114*(4), 560–568. https://doi.org/10.1172/JCI200422206

Wu, W., Haderk, F., & Bivona, T. G. (2017). Non-canonical thinking for targeting ALK-fusion onco-proteins in lung cancer. *Cancers*, *9*(12), 164. https://doi.org/10.3390/cancers9120164

Xie, L., Ni, W. K., Chen, X. D., Xiao, M. B., Chen, B. Y., He, S., Lu, C. H., Li, X. Y., Jiang, F., & Ni, R. Z. (2012). The expressions and clinical significances of tissue and serum galectin-3 in pancreatic carcinoma. *Journal of Cancer Research and Clinical Oncology*, *138*(6), 1035–1043. https://doi.org/10.1007/s00432-012-1178-2

Xing, S., & Ferrari de Andrade, L. (2020). NKG2D and MICA/B shedding: a 'tag game' between NK cells and malignant cells. *Clinical and Translational Immunology*, *9*(12), e1230. https://doi.org/10.1002/cti2.1230

xMAP® Technology – The World's Most Used Multiplexing Technology. (2023). https://www.luminexcorp.com/xmap-technology/#overview

Xu, F., Liu, J., Liu, D., Liu, B., Wang, M., Hu, Z., Du, X., Tang, L., & He, F. (2014). LSECtin expressed on melanoma cells promotes tumor progression by inhibiting antitumor T-cell responses. *Cancer Research*, *74*(13), 3418–3428. https://doi.org/10.1158/0008-5472.CAN-13-2690

Xue, J., Gao, X., Fu, C., Cong, Z., Jiang, H., Wang, W., Chen, T., Wei, Q., & Qin, C. (2013a). Regulation of galectin-3-induced apoptosis of Jurkat cells by both O-

glycans and N-glycans on CD45. *FEBS Letters*, *587*(24), 3986–3994. https://doi.org/10.1016/J.FEBSLET.2013.10.034

Xue, J., Gao, X., Fu, C., Cong, Z., Jiang, H., Wang, W., Chen, T., Wei, Q., & Qin, C. (2013b). Regulation of galectin-3-induced apoptosis of Jurkat cells by both O-glycans and N-glycans on CD45. *FEBS Letters*, *587*(24), 3986–3994. https://doi.org/10.1016/j.febslet.2013.10.034

Yamamoto, H., Shigematsu, H., Nomura, M., William, W., Sato, M., Okumura, N., Soh, J., Suzuki, M., Ignacio, I., Fong, K. M., Lee, H., Toyooka, S., Date, H., Lam, W. L., Minna, D., & Gazdar, A. F. (2010). PIK3CA Mutations and Copy Number Gains in Human Lung Cancers. *Cancer Research*, *68*(17), 6913–6921. https://doi.org/10.1158/0008-5472.CAN-07-5084.PIK3CA

Yang, C. Y., Yang, J. C. H., & Yang, P. C. (2020). Precision Management of Advanced Non-Small Cell Lung Cancer. *Annual Review of Medicine*, *71*, 117–136. https://doi.org/10.1146/annurev-med-051718-013524

Yang, Q., Guo, N., Zhou, Y., Chen, J., Wei, Q., & Han, M. (2020). The role of tumor-associated macrophages (TAMs) in tumor progression and relevant advance in targeted therapy. *Acta Pharmaceutica Sinica B*, *10*(11), 2516–2170. https://doi.org/10.1016/j.apsb.2020.04.004

Yang, R. Y., Hsu, D. K., & Liu, F. T. (1996). Expression of galectin-3 modulates T-cell growth and apoptosis. *Proceedings of the National Academy of Sciences of the United States of America*, *93*(13), 6737–6742. https://doi.org/10.1073/pnas.93.13.6737

Yang, Z., Guo, J., Weng, L., Tang, W., Jin, S., & Ma, W. (2020). Myeloid-derived suppressor cells-new and exciting players in lung cancer. *Journal of Hematology and Oncology*, *13*(1), 1–17. https://doi.org/10.1186/s13045-020-0843-1

Ye, J., Findeis-Hosey, J. J., Yang, Q., McMahon, L. A., Yao, J. L., Li, F., & Xu, H. (2011). Combination of napsin A and TTF-1 immunohistochemistry helps in differentiating primary lung adenocarcinoma from metastatic carcinoma in the

lung. *Applied Immunohistochemistry and Molecular Morphology*, *19*(4), 313–317. https://doi.org/10.1097/PAI.0b013e318205b059

Yilmaz, E., Karşidaı, T., Tatar, C., & Tüzün, S. (2015). Serum galectin-3: Diagnostic value for papillary thyroid carcinoma. *Turkish Journal of Surgery*, *31*(4), 192–196. https://doi.org/10.5152/UCD.2015.2928

Yoshida, Y., Murayama, T., Sato, Y., Suzuki, Y., Saito, H., & Nomura, Y. (2016). Gender Differences in Long-Term Survival after Surgery for Non-Small Cell Lung Cancer. *Thoracic and Cardiovascular Surgeon*, *64*(6), 507–514. https://doi.org/10.1055/s-0035-1558995

Yoshizawa, A., Motoi, N., Riely, G. J., Sima, C. S., Gerald, W. L., Kris, M. G., Park, B. J., Rusch, V. W., & Travis, W. D. (2011). Impact of proposed IASLC/ATS/ERS classification of lung adenocarcinoma: Prognostic subgroups and implications for further revision of staging based on analysis of 514 stage i cases. *Modern Pathology*, *24*(5), 653–664. https://doi.org/10.1038/modpathol.2010.232

Yun, J. K., Kwon, Y., Kim, J., Lee, G. D., Choi, S., Kim, H. R., Kim, Y. H., Kim, D. K., & Park, S. Il. (2023). Clinical impact of histologic type on survival and recurrence in patients with surgically resected stage II and III non-small cell lung cancer. *Lung Cancer*, *176*, 24–30. https://doi.org/10.1016/j.lungcan.2022.12.008

Zaleskis, G., Pasukoniene, V., Characiejus, D., & Urbonas, V. (2021). Do the benefits of being a smoker hint at the existence of PD-1/PD-L1 sensitizers for patients on single-agent immunotherapy? *Journal for ImmunoTherapy of Cancer*, *9*(8), 1–4. https://doi.org/10.1136/jitc-2021-003191

Zeng, Y., Chen, X., Larmonier, N., Larmonier, C., Li, G., Sepassi, M., Marron, M., Andreansky, S., & Katsanis, E. (2006). Natural killer cells play a key role in the antitumor immunity generated by chaperone-rich cell lysate vaccination. *International Journal of Cancer*, *119*(11), 2624–2631. https://doi.org/10.1002/ijc.22150

Zhang, C., & Hao, X. (2020). Prognostic significance of CD276 in non-small cell lung cancer. *Open Medicine*, *14*(1), 805–812. https://doi.org/10.1515/med-2019-0076

Zhang, J., Baran, J., Cros, A., Guberman, J. M., Haider, S., Hsu, J., Liang, Y., Rivkin, E., Wang, J., Whitty, B., Wong-Erasmus, M., Yao, L., & Kasprzyk, A. (2011). International cancer genome consortium data portal-a one-stop shop for cancer genomics data. *Database*, *2011*, bar026. https://doi.org/10.1093/database/bar026

Zhang, K., Cai, J., Lu, C., Zhu, Q., Zhan, C., Shen, Y., Gu, J., & Ge, D. (2021). Tumor size as a predictor for prognosis of patients with surgical IIIA-N2 non-small cell lung cancer after surgery. *Journal of Thoracic Disease*, *13*(7), 4114–4124. https://doi.org/10.21037/jtd-21-428

Zhang, Z., Wang, H., Ding, Q., Xing, Y., Xu, Z., Lu, C., Luo, D., Xu, L., Xia, W., Zhou, C., & Shi, M. (2018). Establishment of patient-derived tumor spheroids for non-small cell lung cancer. *PLoS ONE*, *13*(3), e0194016. https://doi.org/10.1371/JOURNAL.PONE.0194016

Zhao, J., Zhang, P., Wang, J., Xi, Q., Zhao, X., Ji, M., & Hu, G. (2017). Plasma levels of soluble programmed death ligand-1 may be associated with overall survival in nonsmall cell lung cancer patients receiving thoracic radiotherapy. *Medicine*, *96*(7), e6102. https://doi.org/10.1097/MD.0000000000006102

Zhao, W., Jiang, W., Wang, H., He, J., Su, C., & Yu, Q. (2021). Impact of Smoking History on Response to Immunotherapy in Non-Small-Cell Lung Cancer: A Systematic Review and Meta-Analysis. *Frontiers in Oncology*, 11, 703143. https://doi.org/10.3389/fonc.2021.703143

Zheng, M. (2016). Classification and Pathology of Lung Cancer. *Surgical Oncology Clinics of North America*, *25*(3), 447–468. https://doi.org/10.1016/j.soc.2016.02.003

Zhou, W., Chen, X., Hu, Q., Chen, X., Chen, Y., & Huang, L. (2018). Galectin-3 activates TLR4/NF-KB signaling to promote lung adenocarcinoma cell proliferation through activating lncRNA-NEAT1 expression. *BMC Cancer*, *18*(1), 1–14. https://doi.org/10.1186/s12885-018-4461-z

Zhu, C., Anderson, A. C., Schubart, A., Xiong, H., Imitola, J., Khoury, S. J., Zheng, X. X., Strom, T. B., & Kuchroo, V. K. (2005). The Tim-3 ligand galectin-9 negatively regulates T helper type 1 immunity. *Nature Immunology*, *6*(12), 1245–1252. https://doi.org/10.1038/ni1271

Zhu, H., Xie, D., Yu, Y., Yao, L., Xu, B., Huang, L., Wu, S., Li, F., Zheng, Y., Liu, X., Xie, W., Huang, M., Li, H., Zheng, S., Zhang, D., Qiao, G., Chan, L. W. C., & Zhou, H. (2021). KEAP1/NFE2L2 Mutations of Liquid Biopsy as Prognostic Biomarkers in Patients With Advanced Non-Small Cell Lung Cancer: Results From Two Multicenter, Randomized Clinical Trials. *Frontiers in Oncology*, *11*, 659200. https://doi.org/10.3389/fonc.2021.659200

Zhu, W. F., Li, J., Yu, L. C., Wu, Y., Tang, X. P., Hu, Y. M., & Chen, Y. C. (2014). Prognostic value of EpCAM/MUC1 mRNA-positive cells in non-small cell lung cancer patients. *Tumor Biology*, *35*(2), 1211–1219. https://doi.org/10.1007/s13277-013-1162-8

VII. APPENDICES

1. SUPPLEMENTARY MATERIAL

Supplementary Table 1. Efficiency results for the assays used in this study. The efficiency of each TaqMan® assay was evaluated by carrying out serial dilutions of a reference cDNA.

Gene	Slope	Efficiency	Percentage Efficiency
Immunoregulatory genes			
ACTB	-3.322	2	100
GUSB	-3.322	2	100
CDKN1A	-3.623	1.888	94
ICOSL	-3.733	1.853	93
CD276	-3.988	1.781	89
PDL1	-3.681	1.869	93
PDL2	-3.408	1.965	98
CD200	-3.783	1.847	92
CD40LG	-2.510	2.090	100
CD137L	-3.988	1.781	89
OX40L	-3.874	1.812	90
IL10	-3,348	1,989	99
IL6	-3.470	1.938	97
IL8	-3.481	1.938	97
IL12A	-3.523	1.922	96
IL12B	-4.346	1.699	85
IL17A	-3.322	2	100
IL13	-3.397	1.969	98
INFγ	-2.780	2.289	100
TGFβ	-3.617	1.890	94
LGALS3	-3.613	1.891	94
LGALS3BP	-3.322	2	100
LGALS9	-3.627	1.887	94
MICA	-3.536	1.918	96
MICB	-3.322	2	100
HLAG	-3.322	2	100
HLAE	-3.756	1.846	92
HLAF	-4.218	1.726	86
STAT3	-3.627	1,887	94
IDO1	-3.559	1.910	95
ACTB	-3.322	2	100
GUSB	-3.322	2	100
Genes related to macrophages polarization			
IL6	-3.470	1.938	97
CD206	-3.322	2	100
CD163	-3.322	2	100
IL10	-3,348	1.989	99
VEGFA	-3.322	2	100
IL12A	-3.523	1.922	96
NOS2	-3.322	2	100
ARG2	-3,348	1.989	99

Supplementary Table 2. Detailed clinicopathological characteristics of the advanced-stage NSCLC cohort.

ID	Age	Sex	Smoking status	Histology	Stage	PDL1 TPS[a]	Response[b]	DCB	PFS (months)	OS (months)
P1	52	F	Smoker	Other	IVB	90,00	PR	DCB	53.90	53,.90
P2	51	F	Smoker	Other	IVB	60,00	PD	Non-DCB	3.90	41.87
P3	76	F	Smoker	LUAD	IVB	60,00	PD	Non-DCB	2.03	29,70
P4	57	F	Smoker	LUSC	IVA	80,00	PD	Non-DCB	2.10	9.70
P5	55	M	Smoker	LUAD	IVA	60,00	SD	DCB	6.07	20.3
P6	58	F	Smoker	LUSC	IVB	NA	PD	Non-DCB	2.77	6.83
P7	80	F	Never Smoker	LUAD	IVA	90,00	PD	Non-DCB	1.47	2,17
P8	68	M	Smoker	LUAD	IVB	95,00	PR	DCB	29.73	29.80
P9	74	M	Former Smoker	LUSC	IVB	90,00	PR	DCB	48.67	48.67
P10	59	M	Smoker	LUSC	IVB	80,00	PR	DCB	10.53	3.27
P11	58	F	Smoker	LUAD	IVB	60,00	PD	Non-DCB	2.57	2.73
P12	62	M	Smoker	LUAD	IVA	60,00	PD	Non-DCB	5.33	19.60
P13	69	M	Smoker	LUSC	IVB	90,00	SD	DCB	8.87	15.60
P14	72	F	Never Smoker	LUSC	IVB	60,00	PR	DCB	11.37	13.40
P15	84	M	Former Smoker	LUSC	IIIB	70,00	PR	DCB	6.80	20.80
P16	57	M	Smoker	LUAD	IVB	70,00	CR	DCB	35.60	35.60
P17	87	M	Former Smoker	LUAD	IVA	80,00	PR	DCB	13.17	15.87
P18	67	M	Smoker	LUSC	IIIA	90,00	SD	DCB	8.03	9.07
P19	60	M	Smoker	LUAD	IVA	90,00	PD	Non-DCB	0.70	11.03
P20	85	M	Former Smoker	LUAD	IIIB	90,00	PD	Non-DCB	4.40	9.20
P21	63	F	Never Smoker	LUAD	IVB	80,00	PD	Non-DCB	0.60	15.80
P22	62	M	Smoker	LUAD	IVB	70,00	PD	Non-DCB	1.33	1.37
P23	59	M	Smoker	LUAD	IIIA	90,00	PD	Non-DCB	1.57	44.27
P24	68	M	Smoker	LUAD	IVA	70,00	SD	DCB	7.30	11.53
P25	52	M	Smoker	LUAD	IVB	90,00	PR	DCB	40.40	40.40
P26	67	F	Smoker	LUAD	IVB	60,00	CR	DCB	13.53	43.20
P27	69	M	Smoker	Other	IVB	90,00	PD	Non-DCB	4.77	4.90
P28	73	M	Smoker	LUAD	IVB	100,0	SD	DCB	6.53	12.50
P29	65	F	Smoker	LUAD	IVB	70,00	PR	DCB	18.60	28.00
P30	75	M	Smoker	LUSC	IIIB	60,00	SD	DCB	11.40	36.77
P31	61	M	Smoker	LUAD	IVA	70,00	SD	DCB	21.30	21.30
P32	63	M	Smoker	LUAD	IVA	60,00	CR	DCB	31.93	31.93
P33	69	M	Smoker	LUAD	IVB	90,00	PD	Non-DCB	2.60	40.23
P34	67	M	Smoker	LUAD	IIIB	95,00	SD	DCB	12.53	35.10
P35	75	M	Smoker	LUAD	IIIA	100,0	SD	DCB	15.03	25.50
P36	71	M	Smoker	LUSC	IIIA	90,00	PD	Non-DCB	1.40	3.90
P37	64	M	Smoker	LUAD	IVA	80,00	PR	DCB	42.17	42.17
P38	89	M	Former Smoker	LUAD	IIIA	80,00	PD	Non-DCB	2.43	2.43
P39	84	F	Never Smoker	Other	IVB	80,00	SD	DCB	42.97	42.97
P40	63	M	Smoker	LUAD	IVB	70,00	PD	Non-DCB	2.73	5.73
P41	55	M	Smoker	Other	IVB	100,0	CR	DCB	36.90	3.90
P42	82	M	Former Smoker	LUAD	IIIB	95,00	PR	DCB	16.53	16.53
P43	68	M	Former Smoker	LUAD	IVB	90,00	PD	Non-DCB	3.20	5.57
P44	59	F	Smoker	LUAD	IVB	90,00	PR	DCB	18.60	34.50
P45	74	M	Former Smoker	LUAD	IVA	70,00	PD	Non-DCB	3.17	6.30
P46	73	M	Former Smoker	LUSC	IIIB	60,00	PD	Non-DCB	1.37	3.03
P47	79	M	Former Smoker	LUAD	IVB	70,00	PR	DCB	18.90	22.60
P48	55	M	Smoker	LUAD	IVB	60,00	PR	DCB	31.80	31.80
P49	57	M	Smoker	LUSC	IIIB	60,00	PD	Non-DCB	1.60	3.50
P50	85	M	Smoker	LUAD	IVB	60,00	PD	Non-DCB	3.00	3.27
P51	74	M	Former Smoker	LUSC	IVA	80,00	PD	Non-DCB	3.47	3.47
P52	81	M	Smoker	LUAD	IVA	80,00	PR	DCB	17.23	17.23

[a]TPS: Tumor Proportion Score; F, female; M, male; LUAD, lung adenocarcinoma; LUSC, lung squamous carcinoma; PD, progression disease; PR, partial response; CR, complete response; SD, stable disease; DCB, durable clinical benefit; PFS, progression-free survival; OS, overall survival. [b]Recist Response at 6 months; ID, identification

Caracterization of cell lines and PDLCC cultures.

Regarding the adherent-cultured cells, PC471 cells exhibited a cubic shape, grew as a single layer, displayed strong cell-to-cell adhesion and filopodia showing a substantial presence of intracellular vesicles. PC435 showed also abundant cell-cell interaction in the form of filopodia. In contrast, PC301 grew as multilayers forming cell colonies. Adherent-cultured comercial cell lines cells H23, H520, H1993, A549, PC9, H1703 and SK-MES-1, exhibited limited interactions and grew independently, displaying distinct morphological characteristics. H23 cells displayed a circular shape with lamellipodia featuring large nuclei occupying most of the cell volume. Conversely, cells from H520 and H1993 featuring large nuclei, with some being giant, others having prominent nuclei and many showing filopodia and a high number of vesicles. A549 cells took on a triangular shape with a well-defined nuclear membrane, while PC9 and H1703 cells appeared elongated with less pronounced nucleic. SK-MES-1 exhibit a high number of vesicles and a triangular shape. H1395, HCC827, H1975, SW900, H2228, H358 and LUDLU-1 cells tended to form cell colonies. H1395 cells were small and circular, growing in multilayers. HCC827 and H1975 cells produced abundant filopodia and lamellipodia, but HCC827 cells had a polygonal shape with pronounced nuclei, in contrast to H1975 cells, which appeared more elongated with less conspicuous nuclei. H1650 cells exhibited mixed phenotype with abundant cell-cell interactions. In terms of shape, SW900 cells resembled H1975 cells, while H1650 cells resembled HCC827 cells, albeit smaller in both cases. Finally, some H2228 cells were giant, wedge-shaped, and inclined to form filopodia. Similarly, LUDLU-1 cells grow as large swollen aggregates, which will detach and eventually grow in suspension.

Regarding tumorspheres, tight spheroids were formed by HCC827, H1395, H23, H1650, H358, H2228 PC435, PC471 and PC301 whereas H1993, A549, PC9, H520, SK-MES-1 and H1703 formed loose and irregularly shaped, and SW900, LUDLU-1 and H1975 showed a mixed phenotype.

2. APPROVAL FROM THE INSTITUTONAL ETHICAL REVIEW BOARD

Consorcio Hospital General Universitario de Valencia

Comisión de Investigación

APROBACIÓN PROYECTO DE INVESTIGACIÓN

Esta Comisión tras evaluar en su reunión de   29 de Marzo de 2017   el Proyecto de Investigación:

Título:	Caracterización de la interacción entre célula madre tumoral y microambiente inmune en el cáncer de pulmón no microcítico		
I.P.:	Dr. Carlos Camps Herrero/ Susana Torres	Servicio/Unidad	Oncología

Acuerda respecto a esta documentación:

- Que cumple con los requisitos exigidos por esta Comisión para su realización, por tanto se decide su APROBACIÓN.

Los miembros que evaluaron esta documentación:

		Presente	Ausente	Disculpa
Presidente	Dr José Vte Bagan Sebastían	x		
	Dr. Carlos Camps Herrero	x		
	Dra. Goitzane Marcaída Benito			x
	Dr. Carlos Sánchez Juan	X		
	Dña. Anna Marti Monros	x		
	Dr. Emilio López Alcina	x		
	Dr. Rafael Paya Serrano	X		
	Dr. Miguel García del Toro	x		
	Dr. Jose Luis Sanchez Carazo	x		
	Dr. Francisco Ridocci Soriano	X		
	Dra. Empar Lurbe Ferrer			x
	Dª Amparo Muñoz Izquierdo	x		
	Dra. Amparo Esteban Reboll	x		
	Dr. Enrique Zapater Latorre	x		
Secretario	Dra. Dolores Lopez Alarcón	x		

Lo que comunico a efectos oportunos a jueves, 30 de marzo de 2017:

Fdo. Dr. Jose vte Bagan Sebastian
Presidente de la Comisión de Investigación:

1   CI-CHGUV

3. FUNDING

This thesis was supported by the following Spanish institutions:

- ❖ Centro de Investigación Biomédica en Red Cáncer.
  - Project CB16/12/00350.
- ❖ Fondo de Investigación Sanitaria-Fondo Europeo de Desarrollo Regional.
  - Projects PI15/00209, PI15/00753, PI18/00266 and IFEQ21/00194.
- ❖ Fundación Arnal Planelles.
- ❖ Generalitat Valenciana y Fondo Social Europeo
  - Project ACIF/2018/275
- ❖ ERA-NET EURONANOMED III
  - Project METASTARG JTC 2018-045

4. NATIONAL AND INTERNATIONAL CONGRESS COMUNICATIONS

- ❖ **S. Torres-Martínez**; Susana Torres-Martínez, Silvia Calabuig-Fariñas, Ester Munera-Maravilla, Giulia Bertolini, Eva Escorihuela, Marais Mosqueda, Rafel Sirera6 Ana Blasco, Luca Roz, Carlos Camps, Eloisa Jantus-Lewintre. ''Galectin-3 as a microenvironment-relevant immunoregulator through regulatory T cells in lung adenocarcinoma patients'' (Oral Communication). VI YOUNG RESEARCHERS MEETING. Málaga. 06-07 November 2023.

- ❖ **S. Torres-Martínez**; S. Calabuig-Fariñas; A. Moreno Manuel; M. Ferrero Gimeno; S. Gallach; M. Mosqueda; F. de Asís Aparisi; C. García; A. Blasco Cordellat; C. Camps; E. Jantus-Lewintre. ''Study of soluble markers as predictive and prognostic biomarkers to immunotherapy with pembrolizumab in first-line treatment of advanced Non-Small Cell Lung Cancer (NSCLC).'' (Oral Communication). VII Simposio de biopsia líquida. Virtual. 27-29 January 2022.

- ❖ **S. Torres-Martínez**; A. Moreno-Manuel; S. Calabuig-Fariñas; M. Ferrero Gimeno; J. Korsten; G. Bertolini; M. Mosqueda; E. Escorihuela; A. Blasco Cordellat; C. García; F. Aparisi; E. Del Olmo; Luca Roz; E. Jantus-Lewintre; C. Camps. ''Gal-3 as an immunosuppressive regulator in lung cancer stemness.

Prognostic and predictive implications in NSCLC.'' (Oral Communication). 14th Congress on Lung Cancer. Virtual. 10-12 November 2021.

❖ **S. Torres-Martínez**; A. Moreno-Manuel; S. Calabuig-Fariñas; Giulia Bertolini; M. Ferrero Gimeno; S. Gallach; M. Mosqueda; A. Blasco Cordellat; Ricardo Guijarro; M. Nuñez; F. Aparisi; Luca Roz; E. Jantus-Lewintre; C. Camps. '' Study of soluble markers as predictive and prognostic biomarkers to immunotherapy with pembrolizumab in advanced non-small cell lung cancer.'' (Oral Communication). 14th Congress on Lung Cancer. Virtual. 10-12 November 2021.

❖ **S. Torres-Martínez**; A. Moreno Manuel; S. Calabuig-Fariñas; M. Ferrero; S. Gallach; M. Mosqueda; A. Blasco-Cordellat; C. García; F. Aparisi; E. Jantus-Lewintre; C. Camps. ''Study of soluble markers as predictive and prognostic biomarkers to immunotherapy with pembrolizumab in first line treatment of advanced Non-Small Cell Lung Cancer (NSCLC).'' (Poster). III ISLB Annual virtual congress 2021. Virtual. 22 October.

❖ **S. Torres Martínez**; A. Moreno Manuel; S. Calabuig-Fariñas; G. Bertolini; M. Ferrero Gimeno; S. Gallach; M. Mosqueda; A. Blasco Cordellat; R. Guijarro; M. Nuñez; F. Aparisi; L. Roz; E. Jantus Lewintre; C. Camps. ''Analysis of plasma biomarkers as predictive and prognostic biomarkers to immunotherapy with first-line pembrolizumab advanced Non-small cell lung cancer.'' (Poster). 3rd ASEICA Educational Symposium. Virtual. 23-25 November 2021.

❖ **S. Torres Martínez**; A. Moreno Manuel; S. Calabuig-Fariñas; M. Ferrero Gimeno; J. Korsten; G. Bertolini; M. Mosqueda; E. Escorihuela; A. Blasco Cordellat; C. García; F. Aparisi; E. del Olmo; L. Roz; E. Jantus. ''Study of gal3 as an immunoregulator in lung cancer stemness. Prognostic and predictive implications in NSCLC.'' (Poster). 3rd ASEICA Educational Symposium. Virtual. 23-25 November 2021.

❖ **S. Torres-Martínez**; S. Calabuig-Fariñas; M. Ferrero; E. Duréndez; A. Moreno; M. Mosqueda; E. Escorihuela; S. Gallach-García; F. Aparisi; R. Guijarro; E. Jantus-Lewintre; C. Camps. ''Characterization of immunobiological properties of lung tumorspheres in NSCLC.'' (Poster). III Young Researchers Meeting from CIBERONC 2020. Virtual. 14-15 December 2020.

- **S. Torres-Martínez**; S. Calabuig-Fariñas; M. Ferrero; E. Duréndez; A. Moreno-Manuel; M. Mosqueda; E. Escorihuela; F. Aparisi; R. Guijarro; E. Jantus-Lewintre; C. Camps. ''Analysis of immunobiological properties of lung tumorspheres in NSCLC.'' (Poster). Educational Symposium of the spanish lung cancer group. Virtual. 25-27 November 2020.

- **S. Torres Martínez**; J. Garde-Noguera; S. Gallach; F. Aparisi; E. Escorihuela; J. Vidal-Martínez; R. Gisbert-Criado; A. Moreno; M. Ferrero- Gimeno; S. Calabuig-Fariñas; A. Blasco; B. Honrubia; J. García Sánchez; E. Jantus-Lewintre; C. Camps. ''Predictive and prognostic role of soluble biomarkers in advanced Non-Small Cell Lung Cancer (NSCL) patients treated with anti-PD1/PDL1 immunotherapy.'' (Poster). IASLC 2020 Hot Topic Meeting: Liquid Biopsy. Virtual. 28 August 2020.

- **S. Torres Martínez**; A. Herreros-Pomares; S. Calabuig-Fariñas; A. Moreno-Manuel; F. Aparisi; M. Mosqueda; E. Escorihuela; M. Meri; E. Jantus- Lewintre; C. Camps. ''Analysis of immunoregulatory factors produced by lung tumorspheres: Galectin-3 as immune modulator with prognostic value in NSCLC adenocarcinoma.'' (Poster). II Encuentro de Jóvenes Investigadores CIBERONC. Madrid. 27 November.

- **S. Torres Martínez**; A. Herreros-Pomares; S. Calabuig-Fariñas; A. Moreno-Manuel; M. Ferrero; F. Aparisi; M. Mosqueda; E. Escorihuela; E. Jantus-Lewintre; C. Camps. ''Analysis of immunoregulatory factors produced by lung tumorspheres: Galectin-3 as immune modulator with prognostic value in NSCLC adenocarcinoma.'' (Poster). ASEICA 2019. Madrid. 28-29 November 2019.

- **S. Torres Martínez**; A. Herreros-Pomares; S. Calabuig-Fariñas; A. Moreno-Manuel; M. Ferrero; F. Aparisi; M. Mosqueda; E. Escorihuela; E. Jantus-Lewintre; C. Camps. ''Analysis of immunoregulatory factors produced by lung tumorspheres: Galectin-3 as immune modulator with prognostic value in NSCLC adenocarcinoma.'' (Poster). 13th Congress on Lung Cancer. Valencia. 21-22 November 2019.

- **S. Torres-Martínez**; A. Herreros-Pomares; S. Calabuig-Fariñas; F. Zhang; M. Mosqueda; E. Escorihuela; A. Moreno-Manuel; S. Gallach; E. Jantus-Lewintre;

C. Camps. ''Análisis de factores inmunosupresores producidos por tumoresferas. Galectina-3 como modulador inmune con valor pronóstico en adenocarcinoma de pulmón.'' (Oral Communication). SEOM 2019. Pamplona. 22-25 October 2019.

❖ **S. Torres-Martínez**; A. Herreros-Pomares; F. Zhang; S. Calabuig-Fariñas; Á. González; R. Sirera; A. Moreno-Manuel; M. Mosqueda; E. Escorihuela; E. Duréndez; S. Gallach; J. Garde; E. Jantus-Lewintre; R. Guijarro; C. Camps. '' Analysis of immunosuppressive factors produced by tumorspheres in NSCLC. Prognostic value of Galectin-3 in adenocarcinoma.'' (Poster). ESMO Congress 2019. Barcelona. 27 September- 1 October 2019.

❖ **S. Torres-Martínez**; A. Herreros-Pomares; F. Zhang; S. Calabuig-Fariñas; R. Sirera; M. Mosqueda; E. Escorihuela; Á. González; N. Dong; S. Gallach; J. Garde; R. Guijarro; E. Jantus-Lewintre; C. Camps. ''Analysis of immunosuppressive factors produced by CSCs revealed Galectin-3 as immune modulator with prognostic value in NSCLC adenocarcinoma.'' (Poster). IALSC World Conference on Lung Cancer 2019. Barcelona. 07-10 September 2019.

❖ **S. Torres-Martínez**; S. Calabuig-Fariñas; A. Herreros-Pomares; C. Aguilar-Gallardo; M. Mosqueda; E. Escorihuela; E. Jantus-Lewintre; C. Camps. ''Characterization of immune microenvironment in cancer stem cells in non-small cell lung cancer. Analysis of immunosuppressive and immunoregulatory factors.'' (Poster). II Reunión general de ciberonc. Madrid. 02 February 2018.

❖ **S. Torres-Martínez**; S. Calabuig-Fariñas; R. Sirera; A. Herreros-Pomares; C. Aguilar-Gallardo; M. Mosqueda; A. Moreno; E. Esocrihuela; E. Jantus-Lewintre; C. Camps. ''Characterization of immune microenvironment in cancer stem cells in non-small cell lung cancer. Analysis of immunosuppressive and immunoregulator factors.'' (Poster). 1st ASEICA Educational Symposium. Madrid. 14-15 November 2017.

5. PUBLICATIONS

❖ ''Circulating Immune Proteins: Improving the Diagnosis and Clinical Outcome in Advanced Non-Small Cell Lung Cancer.'' **Susana Torres-Martínez,** Silvia Calabuig-Fariñas, Sandra Gallach, Marais Mosqueda, Ester Munera-Maravilla, Rafael Sirera, Lara Navarro, Ana Blasco, Carlos Camps, Eloisa Jantus-Lewintre. IJMS. 2023 Dec 18;24(24):17587.

❖ ''Soluble galectin-3 as a microenvironment-relevant immunoregulator with prognostic and predictive value in lung adenocarcinoma.'' **Susana Torres-Martínez**, Silvia Calabuig-Fariñas, Andrea Moreno-Manuel, Giulia Bertolini, Alejandro Herreros-Pomares, Eva Escorihuela, Elena Duréndez-Saéz, Ricardo Guijarro, Ana Blasco, Luca Roz, Carlos Camps, Eloisa Jantus-Lewintre. Molecular Oncology. 2024 Jan;18(1):190-215

❖ ''Analysis of Exosomal Cargo Provides Accurate Clinical, Histologic and Mutational Information in Non-Small Cell Lung Cancer.'' Elena Duréndez-Sáez, Silvia Calabuig-Fariñas, **Susana Torres-Martínez**, Andrea Moreno-Manuel, Alejandro Herreros-Pomares, Eva Escorihuela, Marais Mosqueda, Sandra Gallach, Ricardo Guijarro, Eva Serna, Cristian Suárez-Cabrera, Jesús M Paramio, Ana Blasco, Carlos Camps, Eloisa Jantus-Lewintre. Cancers. 2022 Jun 30;14(13):3216.

❖ ''Programmed Death-Ligand 1 (PD-L1) as Immunotherapy Biomarker in Breast Cancer.'' Martín Núñez Abad; Silvia Calabuig-Fariñas; Miriam Lobo de Mena; **Susana Torres-Martínez**; Clara García González; José Ángel García García; Vega Iranzo González-Cruz; Carlos Camps Herrero. Cancers. 2022 Jan 8;14(2):307.

❖ ''Cancer Epigenetic Biomarkers in Liquid Biopsy for High Incidence Malignancies.'' Cora Palanca-Ballester*, Aitor Rodriguez-Casanova*, **Susana Torres-Martínez***, Silvia Calabuig-Fariñas, Francisco Exposito, Diego Serrano, Esther Redin, Karmele Valencia, Eloisa Jantus-Lewintre, Angel Diaz-Lagares, Luis Montuenga, Juan Sandoval, Alfonso Calvo. *Equal Contribution. Cancers. 2021 Jun 16;13(12):3016.

❖ ''3D printing novel in vitro cancer cell culture model systems for lung cancer stem cell study.'' Alejandro Herreros-Pomares, Xuan Zhou, Silvia Calabuig-

Fariñas, Se-Jun Lee, **Susana Torres-Martínez**, Timothy Esworthy, Sung Yun Hann, Eloísa Jantus-Lewintre, Carlos Camps, Lijie Grace Zhang. Materials Science & Engineering C. 2021 Mar: 122: 111914.

❖ ''Update on systemic treatment in early triple negative breast cancer.'' Martín Núñez Abad, Silvia Calabuig-Fariñas, Miriam Lobo de Mena, María José Godes Sanz de Bremond, Clara García González, **Susana Torres Martínez**, José Ángel García-García, Vega Iranzo González-Cruz, Carlos Camps Herrero. Therapeutic Advances In Medical Oncology. 2021 Jan 31:13:1758835920986749.

❖ ''Exosomal microRNAs in non-small cell lung cancer.'' Elena Duréndez-Sáez; **Susana Torres-Martinez**; Silvia Calabuig-Fariñas; Marina Meri-Abad; Macarena Ferrero-Gimeno; Carlos Camps. Translational Cancer Research. 2021 Jun ;10(6):3128-3139.

❖ ''A profile on cobas® EGFR Mutation Test v2 as companion diagnostic with gefitinib in first-line treatment of patients with non-small cell lung cancer.'' **Susana Torres-Martínez**, Álvaro González, Alberto Jacobo Cunquero Tomas, Silvia Calabuig Fariñas, Macarena Ferrero, Danielle Mirda, Rafael Sirera, Eloisa Jantus-Lewintr, Carlos Camps. Expert Review of Molecular Diagnostics. 2020 Jun ;20(6):575-582.

❖ "Passenger mutations in cancer evolution". Aparisi F, Amado-Labrador H, Calabuig-Fariñas S, **Torres S**, Herreros-Pomares A, Jantus-Lewintre E, Blasco A, Iranzo V and Camps C. Cancer Rep Rev, 2019 Jun; 3:1-8.

6. AWARDS

- Oral Communication: Study of soluble markers as predictive and prognostic biomarkers to immunotherapy with pembrolizumab in advanced non-small cell lung cancer. 2º Premio XI Educational Symposium on Lung Cancer. November 2021

- Oral Communication: GAL3 as an immunosuppressive regulator in lung cancer stemness. prognostic and predictive implications in NSCLC. ACCÉSIT XI Educational Symposium on Lung Cancer. November 2021

- Oral Communication: Analysis of immunobiological properties of lung tumorspheres in NSCLC. ACCÉSIT X Educational Symposium on Lung Cancer. December 2021.